Triggers and outcomes in aquaporin-4 antibody-positive neuromyelitis optica spectrum disorder and MOG antibody-associated disease: The unanswered questions

Dr Anna Francis

Hilary Term 2026

Abstract

Aquaporin-4 antibody-positive neuromyelitis optica spectrum disorder (AQP4+ NMOSD) and myelin oligodendrocyte glycoprotein-associated disease (MOGAD) are antibody-mediated autoimmune inflammatory CNS syndromes (AICS). The precipitants of attacks are unknown. There is some evidence that infection or vaccination can trigger MOGAD.

Like multiple sclerosis, both can result in cerebral inflammation. Cognitive impairment in multiple sclerosis is well-documented, but whether it is a feature of NMOSD and MOGAD is debated. Studies attempting to resolve this question are flawed by small samples, inadequate control groups, erroneous statistical methods and, in the case of NMOSD, mixed seropositive and seronegative samples.

The large cohort of patients with AQP4+ NMOSD and MOGAD under the care of the John Radcliffe Hospital enabled an adequately powered study of cognitive outcomes in adults with these diseases. This is the first study to compare cognitive performance of patients with AQP4+ NMOSD and MOGAD to that of controls with a chronic autoimmune disease that spares the central nervous system.

This work confirms significantly poorer attention and processing speed in AQP4+ NMOSD compared with controls and identifies paediatric onset as a risk factor for impairment. The findings refute reports of cognitive impairment in MOGAD.

The SARS-CoV-2 pandemic delayed the study of cognition in adults with NMOSD and MOGAD. However, the mass SARS-CoV-2 vaccination programme afforded an unparalleled opportunity to research vaccine-related autoimmune phenomena.

This study used clinic-based observational, epidemiological and laboratory-based approaches to analyse associations between SARS-CoV-2 vaccination and onset of AICS, including AQP4 and MOGAD. The multimodal approach provides evidence that ChAdOx1S can trigger onset of MOGAD.

Research presented here highlights the importance of screening for cognitive impairment in young people with AQP4+ NMOSD and offering educational support if needed. It also demonstrates a role of vaccine-associated antigens and/or vaccine-induced immune pathways in development of MOGAD, which could provide the basis for further study of disease risk factors and, potentially, future treatments.

Acknowledgements

Many thanks to my supervisors, Prof. Jackie Palace and Prof Lars Fugger, for their guidance, inspiration and leadership.

Thanks also to Assoc. Prof Isabel Leite and Dr Kate Attfield for sharing their vast knowledge and for their moral support.

I thank both the NMO and CMS teams, who became my family.

I am hugely grateful to the team at the Oxford Centre for Neuroinflammation for their friendship and patience.

This work would not have been possible without Assoc Prof Paddy Waters, Dr Mark Woodhall and Dr Timothy Horvat, to whom I am indebted.

Equally important are those whose friendship I relied on so much during this DPhil- Matt, Sam, Rob and Jim- who were endlessly encouraging.

Thanks also to Gwil, Non and Teifi, for never failing to make me laugh when things got hard.

Most importantly, infinite thanks to the wonderful Helen Rees, who always believes in me.

Contents

Index of figures

Index of tables

Abbreviations

10/36 SPART: 10/36 Spatial Recall Test

ADEM: Acute disseminated encephalomyelitis

AEFI: Adverse event following immunisation

AIC: Akaike’s information criterion

AICS: Autoimmune inflammatory CNS syndrome(s)

ALFF: Amplitude of low-frequency fluctuations

APC: Antigen presenting cell

APRIL: A proliferation-inducing ligand

AQP4: Aquaporin-4

AQP4+ NMOSD: AQP4 antibody-positive neuromyelitis optica spectrum disorder

ARR: Annualised relapse rate

BAFF: B cell activating factor

BBB: Blood brain barrier

BDNF: Brain-derived neurotrophic factor

BICAMS: Brief International Cognitive Assessment for Multiple Sclerosis

BPI: Brief Pain Inventory

BRB-N: Brief Repeatable Battery of Neuropsychological tests

BVMT-R: Brief Visuospatial Memory Test-Revised

CBF: Cerebral blood flow

CI: Cognitive impairment/ cognitively impaired

CIS: Clinically isolated syndrome

CLOX: Executive Clock Drawing Task

CNS: Central nervous system

COWAT: Controlled Oral Word Association Test

CP: Cognitive preservation/ cognitively preserved

CSF: Cerebrospinal fluid

CVLT: California Verbal Learning Test

DC: Degree centrality

DoF: Degrees of freedom

DTI: Diffusion tensor imaging

DWI: Diffusion weighted imaging

EAAT: Excitatory amino acid transporter

EAE: Experimental autoimmune encephalomyelitis

EDSS: Expanded disability status scale

ELISA: Enzyme-linked immunosorbent assay

FA: Fractional anisotropy

FCS: Fully conditional specification

fMRI: Functional magnetic resonance imaging

FSS: Functional systems score

GBS: Guillain Barré syndrome

GDPR: General Data Protection Regulation

GFP: Green fluorescent protein

GP: General practice

GVDN: Global Vaccine Data Network

HADS: Hospital Anxiety and Depression Scale

HCs: Healthy controls

HLA: Human leucocyte antigen

IFNγ: Interferon gamma

IgG: Immunoglobulin class G

IgM: Immunoglobulin class M

IL-x: Interleukin-x

IST: Immunosuppressive therapy

ITP: Idiopathic thrombocytopaenic purpura

IVIg: Intravenous immunoglobulin

JCVI: Joint Committee on Vaccination and Immunisation

LEMS: Lambert Eaton myasthenic syndrome

LETM: Longitudinally extensive transverse myelitis

MAR: Missing at random

MBP: Myelin basic protein

MD: Mean diffusivity

MDEM: Multiphasic disseminated encephalomyelitis

MFIS: Modified Fatigue Impact Scale

MG: Myasthenia gravis

MHC: Major histocompatibility complex

MHRA: Medicines and Healthcare products Regulatory Agency

MICE: Multiple imputation with chained equations

MMSE: Mini Mental State Examination

MoCA: Montreal Cognitive Assessment

MOG: Myelin oligodendrocyte glycoprotein

MOGAD: MOG antibody-associated disease

MRI: Magnetic resonance imaging

MS: Multiple sclerosis

MSE: Mean squared error

MTR: Magnetisation transfer ratio

MuSK: Muscle specific kinase

nAChR: Nicotinic acetylcholine receptor

NAWM: Normal appearing white matter

NHS: National Health Service

NHSBT: National Health Service Blood and Transplant Division

NK cells: Natural killer cells

NMDAR: N-methyl D-aspartate receptor

NMODAS: NMO Diagnostic and Advisory Service

NMOSD: Neuromyelitis optica spectrum disorder

OCB: Oligoclonal bands

ON: Optic neuritis

OR: Odds ratio

pADS: Paediatric acquired demyelinating syndromes

PAMPs: Pathogen-associated molecular patterns

PASAT: Paced Auditory Serial Addition Test

PF4: Platelet factor 4

PIRA: Progression independent of relapse activity

PLEX: Plasma exchange

PLP: Proteolipid protein

PMM: Predictive mean matching

PRRs: Pattern recognition receptors

pwMOGAD: Person(s) with MOGAD

pwMS: Person(s) with MS

pwNMOSD: Person(s) with NMOSD

R^2: Coefficient of determination

REC: Research Ethics Committee

ReHo: Regional homogeneity

RIV: Relative increase in variance

RSE: Residual standard error

RSS: Residual sum of squares

S protein: SARS-CoV-2 spike protein

SD: Standard deviation

SDMT: Symbol Digit Modality Test

SE: Standard error

SIL: Supratentorial inflammatory lesion

SPART-DR: Spatial Recall Test- delayed recall

SPART-IR: Spatial Recall Test- immediate recall

SRT-CLTR: Selective Reminding Test- consistent long-term retrieval

SRT-DR: Selective Reminding Test- delayed recall

SRT-LTS: Selective Reminding Test- long term storage

SSE: Sum squared error

SSReg: Sum squared regression

SST: Total sum of squares

TfH: Follicular T helper cell

Th1/ Th2/ Th17: T helper type 1/ type 2/ type 17

TLR: Toll-like receptor

TM: Transverse myelitis

TMT: Trail Making Test

TNFα: Tumour necrosis factor alpha

Treg: Regulatory T cell

VGCC: Voltage gated calcium channel

VITT: Vaccine-induced thrombotic thrombocytopaenia

WAIS: Wechsler Adult Intelligence Scale

WCST: Wisconsin Card Sorting Test

wFCS: Weighted functional connectivity strength

WIAT: Wechsler Individual Achievement Test

WISC: Wechsler Intelligence Scale for Children

WHO: World Health Organisation

WLGT: Word List Generation Test

WMS-R: Wechsler Memory Scale Revised

Initials

EC: Ms Ellie Crispin

AF: Dr Anna Francis

TH: Dr Timotei Horvat

MM: Ms Madalina Miron

SM: Dr Sanjay Manohar

YS: Ms Yvonne Sharawakanda

PW: Assoc Prof Paddy Waters

Chapter 1

Introduction to neuromyelitis optica spectrum disorder and myelin oligodendrocyte glycoprotein-associated disease

a) Neuromyelitis optica spectrum disorder

The disease today known as neuromyelitis optica spectrum disorder (NMOSD) is an astrocytopathy that causes inflammation of the central nervous system, most commonly involving the optic nerves, spinal cord and periependymal brain regions. The *syndrome* of neuromyelitis optica (NMO), also known as Devic's disease, consists of simultaneous or rapidly sequential inflammation of the spinal cord (transverse myelitis; TM) and optic nerve(s) (optic neuritis; ON) of any aetiology (1). Cases of NMO were described as early as 1831 (2). Doubtless these early reports encompassed a range of aetiologies, including multiple sclerosis (MS), tertiary syphilis and other infectious, autoimmune, metabolic and toxic pathologies, as well as antibody-mediated diseases.

The association of ON and longitudinally extensive TM (LETM) with several recognised diseases and the inability to agree on strict criteria to define the syndrome led to much debate about the existence of a distinct pathology in NMO. For most of the late nineteenth and twentieth centuries, many physicians considered NMO to be a variant of MS. Others, like Allbutt, proposed NMO was separate entity (3) and, 24 years later, Devic coined the term "neuro-myélite optique" during his address to the Congrès Français de Médecin (4,5). He and his student, Gault,

asserted the pathological changes in biopsy specimens from NMO patients differed from those seen in MS (6).

Despite this evidence, the nosological debate continued and was summarised neatly by Stansbury, who wrote, “Until the etiologic agent in these diseases is discovered, clinical and pathologic characteristics constitute the only available basis for discussion” (7,8). In 1882, Dreschfeld hypothesised the cause of the disease was “some toxic agent circulating in the blood,” (9). In 2002, Cree *et al* wrote that vessel hyalanization and complement and immunoglobulin deposition in perivascular regions in cases of NMO implied antibody-mediated disease (10). It was not until 2004 that Lennon and colleagues identified an immunoglobulin present in 73% of patients with the NMO syndrome and in only 9% of patients with MS presenting with ON and TM[1] but not in patients with “typical” MS or miscellaneous neurological diseases (14). The target antigen was found to be AQP4, a tetrameric water channel found in the foot processes of astrocytes, particularly in the optic nerves, spinal cord and subpial or subependymal brain surfaces (15).

Refinement of diagnostic assays has improved sensitivity to up to 98.5% and specificity to 97.6% (16), enabling researchers to broaden the phenotype of AQP4 antibody-associated disease beyond NMO (1,17). Until the discovery of the antibody, diagnosis of NMO depended on presence of features that overlapped with other CNS diseases, required

[1] It is possible seropositive MS patients were misclassified, as both patients presented with optic neuritis and transverse myelitis but had MS-like cerebral lesions and we now realise that >50% patients have brain lesions at some time during the disease course (11,12) and 13 – 17.5% of patients fulfil Barkhof criteria for MS at disease onset (12,13).

both optic nerve and spinal cord inflammation, and most criteria excluded cases with lesions beyond the optic nerve and spinal cord (10). Diagnostic criteria have evolved over the last two centuries as our concept of the disease has changed (4,10,18,19). It is now recognised that AQP4 antibodies are also associated with brainstem syndromes (particularly area postrema syndrome) as well as diencephalitis and supratentorial parenchymal inflammation (13). Cerebral lesions are identified on MRI scans in 37- 57% of seropositive patients at some point in the disease course (12,20).

As a proportion of patients may not develop both ON and TM, neurologists adopted the term “NMO spectrum disorder” (NMOSD) when referring to seropositive patients, particularly without the typical combination of ON and LETM. Thus, the *syndrome* of NMO may have many aetiologies, while the *disease* NMOSD usually denotes presence of AQP4 antibodies in the context of appropriate CNS manifestations (1,21)[2].

Global prevalence of NMOSD is lower than MS, with prevalence estimates from 0.7 to 10 per 100,000, depending on definition and population studied (22,23). It is 9 times more common in females and relatively more frequent in Black and East-Asian populations (12,22–24). Age of onset is around a decade older than reported in relapsing-remitting MS (RRMS) (25,26) and is rare in children (27). The disease follows a relapsing course in around 90% patients (12,26). Long-term

[2] The existence of “seronegative NMOSD” is acknowledged (21) but as diseases are increasingly defined by detection of highly specific biomarkers, the definition may be redundant in the future.

disability is common and studies show up to 29% of patients are wheelchair-dependent and 18% have severe bilateral visual impairment after a median disease duration of 75 months (26). Unlike MS, there is no progressive phase and disability is accrued as a result of relapses (20,26,28).

b) MOG antibody-associated disease

Ten to fifty percent of AQP4 antibody negative NMO or NMO-like cases are associated with antibodies to myelin oligodendrocyte glycoprotein (MOG) (29–31). Like NMOSD, MOG antibody-associated disease (MOGAD) was thought be some to be a subtype of MS. This was supported by early studies identifying MOG antibodies more frequently in patients with MS compared with healthy controls, histological similarity between lesions in patients with MOG antibodies and type II MS lesions, and the encephalitogenic properties of MOG and MOG antibodies in experimental autoimmune encephalitis (EAE, an animal model of MS) (32,33). With the development of cell-based assays and the use of full length MOG protein in its native conformation, specificity of assays has improved to >98% (32–35). This has enabled identification of typical phenotypes, including ON, LETM, NMO, acute disseminated encephalomyelitis (ADEM), multiphasic disseminated encephalomyelitis (MDEM), cortical encephalitis and FLAIR hyperintense lesions in anti-MOG-associated encephalitis with seizures (FLAMES).

Presentation varies with age; ADEM is the commonest manifestation in children and ON is most common in adulthood (36–38).

In contrast to NMOSD, MOGAD is monophasic in 60-75% of cases (36,37,39) and does not show the same racial and gender bias (36,40,41). Disability outcomes are generally better (39,42,43). MOGAD more commonly affects children than NMOSD or MS (42,44,45).

Internationally agreed diagnostic criteria have been published, which include ADEM, cerebral monofocal or polyfocal deficits and cerebral cortical encephalitis among the core clinical features (46).

c) Cerebral involvement in AQP4+ NMOSD and MOGAD

The evidence above indicates cerebral involvement is not uncommon in NMOSD and MOGAD, particularly in children (27,36,47–52). The reasons for a preponderance of brain involvement in children are unclear, but susceptibility to cerebral lesions in children due to immaturity of myelin and immune responses have been proposed (53).

The long-term outcomes of TM and ON are well-documented (49,51,52,54) but the consequences of cerebral lesions are more difficult to assess. Outcomes are likely to depend on the location and size of lesions and the predilection for cerebral inflammation in childhood complicates the distinction between effects intracranial disease from effects of paediatric onset. Additionally, the majority of lesions in NMOSD are non-specific and thus their pathological relevance is debatable (48,55).

There is some evidence that brain involvement increases the risk of cognitive impairment (CI) in NMOSD (56–58) and MOGAD (59–61) but results are mixed. If this is the case, risk of CI in paediatric-onset AQP4+ NMOSD and MOGAD may be higher than in adults due to both increased incidence of cerebral lesions and non-specific effects of chronic disease during development (school absenteeism, fatigue and physical disability etc).

d) Immunological triggers of AQP4+ NMOSD and MOGAD

The evidence of an infectious trigger of NMOSD is mixed. Much of the evidence links acute infection to relapses, rather than onset attacks, and identifies increased rates of seropositivity to various organisms in established disease, rather than demonstrating seroconversion around disease onset (62). Given disability and immunosuppression following onset may predispose to certain infections, higher rates of antibodies to pathogens in affected individuals cannot be used as evidence of an initial infectious trigger. One paper reported higher incidence of antibodies to *H pylori* and *C pneumoniae* in patients with AQP4+ NMOSD compared with those with seronegative NMO or MS or in healthy controls (63). However, the study was underpowered, only tested antibodies to 4 pathogens, failed to account for important demographic differences between groups and was limited to a Japanese population. Another study reported a variety of different infections preceding AQP4+ NMOSD attacks (12) but no specific organism was identified,

cases were retrospective and the authors did not distinguish between onset events and relapses. One group reported a significantly higher proportion of patients with AQP4+ NMOSD had serological evidence of infection within a month of acute attacks than patients with non-inflammatory neurological diseases (64). This study was limited to 15 patients, included both onset and relapse attacks and 5 patients were immunosuppressed. Other studies have shown only 10% of children with NMOSD reported illness prior to onset attack (27) and AQP4+ TM is as likely to follow an infectious prodrome as seronegative TM (65).

Infectious prodromes are more common in MOGAD than NMOSD (66), preceding MOGAD onset in 20-67% of cases (67,68). Preceding infection is reported in 57% of children prior to first attack of MOGAD but only 10% of children before first clinical episode of MS (69). Both vaccination and infection are recognised triggers of childhood and adult ADEM (53,70,71), which is associated with MOG antibodies in up to 50% of cases (72,73). Vaccination precedes 5 – 10% of MOGAD diagnoses (67,74,75)

e) Linking triggers with cognitive outcomes

Paediatric MOGAD has a predilection for brain involvement (36,37,44,76) and children with NMOSD have a higher incidence of cerebral inflammation than adults (27,48,49). Children with MOGAD are more likely to experience infection or vaccination prior to disease onset than adults (77). It has been suggested that phenotype of NMOSD is

different in the presence or absence of a viral prodrome (64). A viral prodrome was reported in 65% of MOGAD patients with brainstem or cerebellar lesions (75) and infections are more commonly reported before ADEM than other presentations (66). Given children are more likely to be exposed to novel pathogenic antigens, either via contact with agents in the environment or vaccination, it is possible that an infectious trigger increases risk of intracranial inflammatory lesions. In this scenario, cerebral manifestations of disease would be less common in adults due to lower rates of exposure to novel pathogens but, when present in adults, would follow infection or vaccination as frequently as in children. This conjecture is supported by a report that found infection preceded first episode of MOG-associated ADEM in 77% of children and 83% of adults (71).

It is therefore conceivable that infectious triggers of MOGAD and possibly NMOSD give rise to cerebral inflammation and that this in turn gives rise to CI (fig 1).

Figure 1

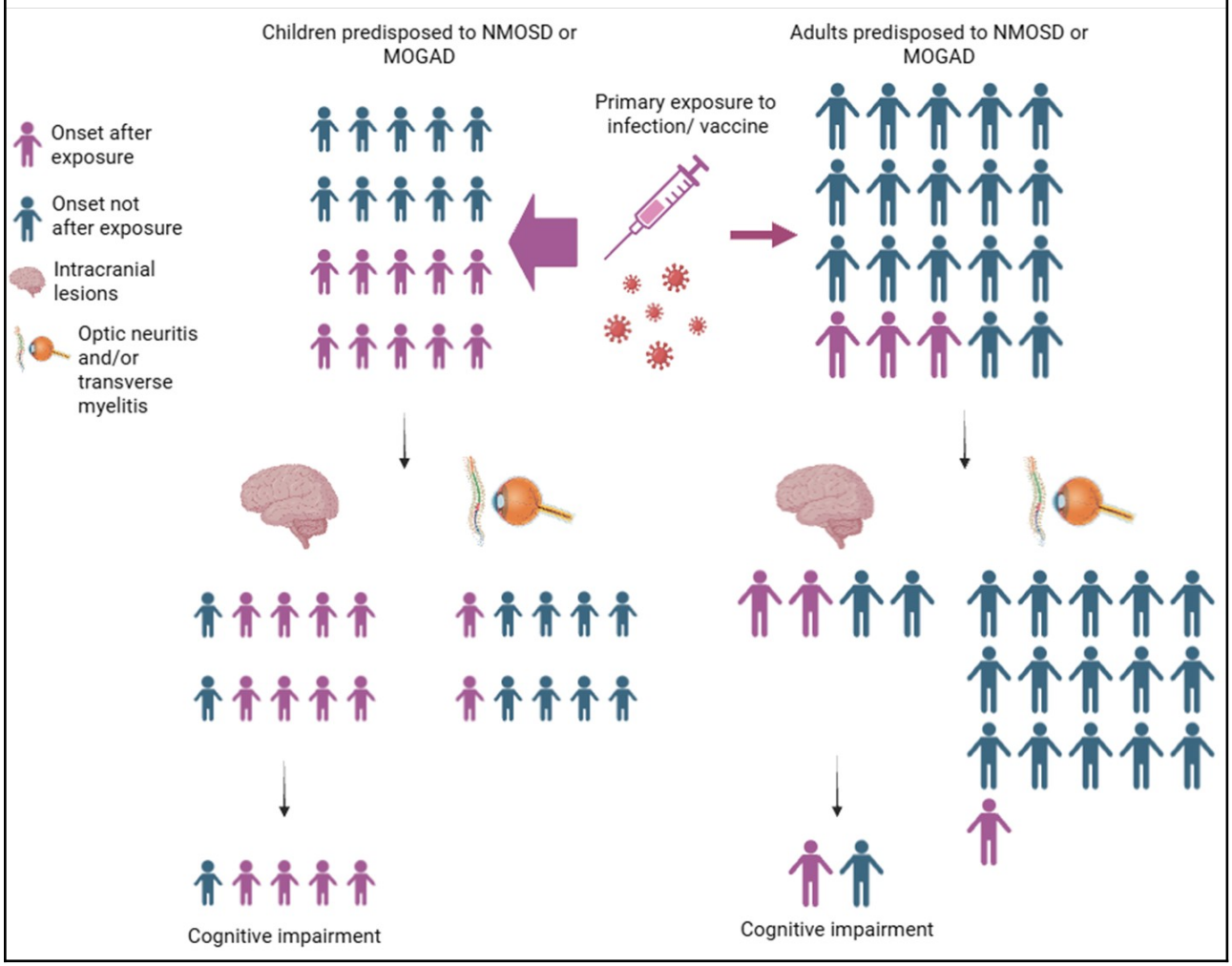

f) Evolution of the project

My original DPhil proposal was an investigation of cognitive outcomes in AQP4+ NMOSD and MOGAD. Disruption to clinics by the SARS-CoV-2 pandemic delayed data collection but presented the opportunity for another area of research when I recognised a number of patients with new acute inflammatory CNS syndromes (AICS) developed their first

symptoms within weeks of receiving a SARS-CoV-2 vaccine. The association was particularly marked for the MOGAD cohort.

Given the reports of infections and vaccines triggering MOGAD and NMOSD, the putative association between these triggers and increased risk of intracranial lesions (particularly in children), and the potential impact of cerebral inflammation on cognition, I undertook two simultaneous projects in an attempt to answer the following questions:

1) Is there evidence of CI in AQP4+ NMOSD and/or MOGAD and is this influenced by age at onset or the presence of cerebral inflammation?
2) Did vaccination against SARS-CoV-2 trigger onset of AQP4+ NMOSD and/or MOGAD? Were phenotypes of these diseases following SARS-CoV-2 vaccination different to those not preceded by vaccination?

If vaccination is associated with new AICS *and* predisposes to cerebral inflammation *and* cerebral inflammation is associated with CI, it may be inferred that cognitive outcomes are modulated by preceding immunological triggers.

g) <u>The Oxford NMO Diagnostic and Advisory Service</u>

The John Radcliffe Hospital in Oxford hosts one of two NHS England-commissioned Highly Specialised Services for the diagnosis and management of NMOSD and MOGAD (the Oxford NMO Diagnostic and

Advisory Service, NMODAS). It is one of the largest NMOSD and MOGAD centres worldwide, accepting referrals from the UK and the Republic of Ireland and conducts outreach clinics across the south of England[3].

Patients who use the service are asked if they wish to participate in the longitudinal study, “Tissue for the study of demyelinating conditions: clinical, genetic and immunological studies” (Oxford Research Ethics committee reference 16/SC/0224). This study involves real-time, prospective data collection regarding diagnosis and antibody status, attack dates and phenotypes, radiological changes, acute and long-term therapies and outcome measures (appendix 1).

Information from the study was originally stored in a Microsoft© Access™ Database Management System, hosted by an NHS server. In 2023, data were transferred to a Research Electronic Data Capture (REDCap) system. This GDPR-compliant, web-based data capture tool was pioneered specifically for use in clinical research informatics and has been used worldwide. The closed source code underlies an excellent security record (78).

I was part of a team responsible for shaping the data collection tools within REDCap, reviewing paper records and the Microsoft© Access archive to populate and update the database and transfer the information, as well as entering data in real time to ensure accurate contemporaneous data capture.

[3] Derriford Hospital in Plymouth, Gloucestershire Royal Hospital, Southampton Hospital, Kings College Hospital in London, St George’s Hospital in London, St Bartholomew’s Hospital in London, The Royal London Hospital, Princess Royal Hospital in Haywards Heath and the Royal Sussex County Hospital in Brighton

The following research was generously enabled by patients participating in this study and historical data were retrieved from REDCap and Microsoft© Access databases.

Chapter 2

Cognition in AQP4+ NMOSD and MOGAD, part 1 (MoCA)

2.1) Introduction: Cognition in AQP4+ NMOSD and MOGAD, part 1 (MoCA)

a) Substrates of cognitive impairment in neuroinflammatory disease

Multiple sclerosis is an inflammatory disease of the central nervous system (CNS) that causes demyelinating cerebral plaques in over 95% of patients (79). CI affects 43 – 70% of people with MS (80,81), predominantly impacting attention, processing speed and memory (80,82). The degree of impairment has been correlated with reductions in grey matter volumes (83), cortical thickness (84,85), thalamic volumes (83,86,87) and with higher lesion load (57,88,89). Reduced fractional anisotropy (FA) in different structures was associated with poorer performance on distinct cognitive tests (90). Progressive MS is more frequently associated with CI than relapsing-remitting forms and involves more domains (81,91).

NMOSD and MOGAD are also autoimmune disorders of the CNS that share some features with MS, but there are also distinct pathological, radiological and clinical characteristics (20,31,32,66,92–95). For example, a normal brain appearance on MRI is common in NMOSD but is very rare in MS (20,96,97). Compared with MS, lesion load is lower and lesions are often monofocal in NMOSD (20,97–100) and MOGAD

(92,101,102). “Black holes” on T1 weighted MRI, representing irreversible axonal loss, are less common in NMOSD and MOGAD (20,99). Inter-attack MRI scans detect clinically silent interval lesions frequently in MS but very rarely in NMOSD and MOGAD (102,103). Radiological cortical lesions are reported in up to 44.4% of MS cases but are absent in NMOSD and rare in MOGAD (88,97,98,104,105).

Volumetric studies also show differences between the diseases. Deep grey matter volumes are markedly and diffusely reduced in MS (96,98,101). Studies comparing NMOSD and MS confirm whole brain atrophy (106,107), atrophy of deep grey matter (56,108) and cortex (57,101,104,106) are milder in NMOSD. Head-to-head comparisons indicate total brain atrophy, grey matter volume loss and cortical atrophy are more marked in MS than MOGAD (101,102,109).

Microstructural damage of normal appearing white matter and grey matter revealed by FA measurements is common in MS but evidence in NMOSD and MOGAD is mixed (98,110–113). Direct comparisons demonstrate more severe microstructural disruption in MS than NMOSD (114,115). Microstructural changes in MOGAD are limited to patients with intracranial lesions (102) and are milder than those seen in MS (109).

In addition, a progressive course is exceedingly rare or absent in NMOSD and MOGAD (20,25,102,116) but primary progressive MS accounts for 15-20% of all cases and up to 90% of untreated patients

with relapsing-remitting forms transition to secondary progressive by 25 years (117).

Therefore, some of the clinical and radiological features associated with CI in MS are milder, rarer or absent in NMOSD and MOGAD. Anecdotally, clinicians report CI is less frequent in patients with NMOSD and MOGAD.

b) Literature regarding cognitive impairment in NMOSD

The outcomes of studies of CI in NMOSD are inconsistent and prevalence estimates vary from 29 to 67% (118). A meta-analysis including 273 people with NMOSD found evidence of impairments in processing speed, working memory, visual processing, verbal learning, verbal fluency and executive function, although samples were small and heterogeneous (119). The majority of studies have reported multidomain impairments in a substantial proportion of patients with NMOSD (supp table 1). However, one study found no impairments on the Mini Mental State Examination (MMSE), Frontal Assessment Panel or screen-based cognitive tests (120). Another found patients with NMOSD performed worse than healthy controls on a single test of attention but executive function, spatial processing and reaction times were intact (121).

Like MS, processing speed, attention and memory are the domains most frequently affected (118,119,122). The frank dementia sometimes observed in MS is not a feature of NMOSD and researchers have

attributed this to the absence of a progressive phase and lack of cortical lesions (122).

The differences in prevalence, severity, domains affected and correlates of CI reported in NMOSD are due to differences in testing protocols, variation in definitions of CI, small samples, inappropriate control groups and combining AQP4+ and seronegative NMO patients (supp table 1). Many studies employ parametric tests to interpret non-parametric data, compare groups without adjusting for important covariates and use simple correlational analyses to study complex multifactorial relationships.

c) Impact of age at onset on cognition in NMOSD

Regarding paediatric brain injury in general, the majority of studies show younger age of brain injury of any cause is associated with poorer cognitive and behavioural outcomes, possibly because younger children are forced to acquire even rudimentary skills with imperfect neural substrates (123). There is some evidence that cognitive deficits in paediatric MS are more severe than those acquired in adulthood (124) and that, within the paediatric MS cohort, cognitive outcomes worsen with younger age at onset (125,126).

Few studies have examined the influence of age at onset on cognition in NMOSD and the rarity of paediatric NMOSD means the impact on children is under-researched. A study of 67 children with NMOSD found younger onset age was associated with poorer cognitive outcomes (54).

Significant impairments in visuomotor integration, working memory, planning, attention and verbal fluency have been reported in children with NMOSD but no age correlation was performed (127). Conversely, increasing age at onset in adults with NMOSD is associated with worse cognitive outcomes (128–130).

d) Impact of supratentorial inflammatory lesions on cognition in NMOSD

Evidence of the impact of supratentorial inflammatory lesions (SILs) on cognition is inconclusive. Several studies have found no difference in cognitive test scores between patients with and without brain lesions (107,128,131–134) or that performance does not correlate with total lesion volume (107,111). In contrast, some groups have demonstrated increased risk of CI in the presence of brain lesions (58,135) and that lesion volume correlates with impairments in certain domains (56,57). A study of only 12 patients with NMOSD used rigorous and specific assessments to address this question and confirmed CI only in the single patient with a previously symptomatic SIL, while almost half the patients met criteria for CI using less specific tests (136). Inappropriate testing protocols, classification of brain lesions[4] and inclusion of brainstem lesions in analyses may be responsible for variation in outcomes between studies.

[4] "Non-specific" lesions are the most common lesion type in NMOSD and their aetiology and relevance are unknown (84,111,137), so their inclusion may dilute an effect of SILs

Children with NMOSD are more likely to present with SILs than adults (51,52,54), which can cause difficulty in distinguishing effects of SILs from effects of paediatric onset. It is possible that greater impact of disease onset in early childhood is mediated by the higher incidence of SILs in this group.

e) Literature regarding cognitive impairment in MOGAD

There are fewer studies of cognition in MOGAD and many focus on paediatric cases. Estimates of the prevalence of CI in MOGAD vary from 11 to 50% (59,61), with some studies reporting no significant impairments (138). Domains affected and correlations vary between studies (supp table 2). Studies are hampered by the same restrictions as those affecting studies of NMOSD, particularly sample sizes.

A multicentre study of 113 patients with MOGAD found significantly poorer performance on tests of semantic fluency and congruent visual processing speed, no significant impairments on tests of auditory processing speed or delayed recall and superiority on a test of immediate recall and a separate test of visual processing speed compared with healthy controls. Age, education and SILs predicted performance on some subtests (61).

f) Impact of age at onset and inflammatory brain lesions on cognition in MOGAD

Approximately half of children with ADEM have MOG antibodies (72,73). The most common MOGAD phenotype in children <12 years is ADEM (36–38,139,140). It is therefore often difficult to distinguish distinct contributions of SILs and age at onset to cognitive outcomes in MOGAD and SIL burden may mediate an effect of paediatric onset.

Up to 22% of children with ADEM develop CI (125) and onset age before 5 years predicted poorer outcomes in most measures (141). In children, higher age at onset is associated with better long-term language skills (142).

Focusing on MOGAD, 40% of children presenting with ADEM or MDEM were reported to develop cognitive difficulty, compared with 6.5% of those presenting with isolated ON or ON and TM (60). Onset age ≤10 years and lesions in the deep grey matter associated with increased risk of academic difficulty (139), although independent effects of these predictors were not assessed. ADEM was the presenting phenotype in 78.9% of children with MOGAD requiring special educational intervention and 41.3% of those without special educational needs (143). In a series of 116 children with MOGAD, 12 had residual cognitive problems and all were from the subgroup of 68 presenting with ADEM or non-ADEM encephalitis (144). A history of ADEM was found to significantly increase risk of CI in a study of 32 adults with MOGAD (145). Rare MOG antibody-associated leukodystrophies associated with

persistent cognitive and behavioural disorders have been described in young children (146,147).

Together, these studies suggest children with MOGAD are more likely to present with ADEM or encephalitis than adults, which increases risk of CI. Younger age at onset may contribute to cognitive outcome independently (148).

g) Hypotheses

Based on the observations above, the following hypotheses were proposed:

i) Primary hypothesis: Cognition in patients with NMOSD and MOGAD is poorer than cognition in control patients with a chronic CNS-sparing autoimmune disease.

ii) Secondary hypothesis: Cognition in patients with onset of NMOSD and MOGAD before optimal brain maturation is poorer than those with onset after. A cut-off of 30 years was selected, as essential processes such as hippocampal growth and cortical synaptic refinement continue to late adolescence and myelination, expansion of the corpus callosum and increases in grey matter density continue into the late twenties (149,150).

iii) Secondary hypothesis: Cognition in NMOSD and MOGAD patients with a history of SILs is poorer than in those without SILs.

2.2) Methods: Cognition in AQP4+ NMOSD and MOGAD, part 1 (MoCA)

a) Overview of study methods

a.i) Patient population

Patients were invited to participate if they met the following criteria:

1) Had a diagnosis of NMOSD according to published diagnostic criteria (151) or clinically definite diagnosis of MOGAD[5] *and* positive for either AQP4 or MOG antibodies using cell-based assays described by the Oxford Neuroimmunology Laboratory (16,35)[6].

   Controls required a diagnosis of myasthenia gravis (MG) with antibodies to the nicotinic acetylcholine receptor (nAChR) or muscle-specific kinase (MuSK) or a diagnosis of Lambert Eaton myasthenic syndrome (LEMS) with antibodies to the presynaptic voltage-gated calcium channel (VGCC).

2) Were under the care of the John Radcliffe Hospital NMODAS[7] and consented to enrolment in the umbrella study, Tissue for the Study of Demyelinating Conditions: Clinical, Genetic and

[5] No internationally agreed criteria for diagnosis of MOGAD was published until 2023 (46)
[6] Assay 2 in appendix 1 of Waters *et al*., 2016
[7] This includes patients with NMOSD and MOGAD reviewed at outreach clinics

Immunological Studies *or* under the care of the John Radcliffe Hospital Neuromuscular Disorders Team and consented to enrolment in the umbrella study, Tissue for the Study of Genetic and Autoimmune Disorders of the Neuromuscular Junction and Related Neuromuscular Disorders (Oxford Research Ethics Committee reference 21/SC/0018).

3) Aged between 25 and 65 years at time of testing.

The control group of patients with MG or LEMS (herein referred to as the MG group) were selected because, like AQP4+ NMOSD and MOGAD, they have chronic autoantibody-mediated disease with unpredictable relapses that often require steroids and/or immunosuppressant medications, variable physical disability and high levels of fatigue, anxiety and depression (152). As there is no CNS inflammation, differences in performance are more likely to be due to direct effects of AQP4+ NMOSD and MOGAD on the CNS than indirect effects of chronic autoimmune disease.

The lower age-limit of 25 was selected to ensure participants had completed their education and that optimal grey matter density and myelination had been achieved (149,150). The upper age limit of 65 years was selected based on a large study of the Montreal Cognitive Assessment (MoCA), demonstrating frequent impairment beyond 70 years of age in a representative population sample (153).

Participants were excluded if they had significant co-existent neurological or psychiatric disease[8] or if they relapsed within 4 weeks of assessment.

Patients meeting criteria and attending an appointment with the NMODAS or the myasthenia clinic in Oxford were invited to complete the MoCA opportunistically.

a.ii) Power calculation

Effect size was calculated in G*Power (v 3.1.9.7) (154) using values from Guo *et al.*, 2018 (155). With an estimated f value of 0.427, $\alpha = 0.05$ and power of 0.80, minimum group size was 19 (appendix 2).

a.iii) Neuroradiological assessment

All available brain MRI scans were reviewed for patients with AQP4+ NMOSD or MOGAD. The presence of SILs at any time during disease course was confirmed by an expert neuroradiologist (TH).

a.iv) Demographic and clinical variables

[8] The following were permitted as their presence was not felt to contribute significantly to scores: stable depression, anxiety or obsessive-compulsive disorder, history of viral meningitis without encephalitis, incidental small vessel disease or incidental small schwannoma detected on imaging. Seizures believed to be cerebral manifestations of NMOSD or MOGAD were permitted.

Demographic and clinical characteristics (e.g., age at disease onset, age at testing, sex) of NMOSD and MOGAD patients were extracted from the Microsoft© Access™ database prior to 2023 and from the REDCap database from 2023. Details of MG patients were extracted from medical records. Biological sex was recorded rather than gender, because biological sex influences cognitive test outcomes in MS (156). Expanded Disability Status Scale (EDSS) scores were measured the same day as cognitive tests were administered or taken from the most recent clinic appointment for those completing telephone assessments. Patients provided their native language (English versus not English) and years in education at the time of assessment.

b) Cognitive and psychosocial assessment

Cognition was assessed using the MoCA (appendix 3). This comprises 22 questions assessing domains of visuospatial function and executive function, naming, language (repetition and phonemic fluency), attention and working memory, verbal abstraction, orientation to time and place and short-term verbal recall. An additional point is added if participants completed less than 12 years of education. Scores of ≤25 (≤83.3%) are considered “impaired” (157).

Tests were administered by one of three staff members (AF, MM, YS) who completed the online training and certification (https://mocacognition.com/training-certification/).

The MoCA was chosen for its high test-retest reliability and discriminant validity (157). It is quick to administer and score, maximising the number of patients tested. It has been validated in MS (158) and has been used in research to assess cognition in NMOSD (128,130,133,159).

Patients unable to complete the full MoCA due to visual impairment or because the MoCA was administered by telephone were assessed using the MoCA-Blind (160), which excludes visual components (appendix 3). Because the maximum score using the MoCA Blind (22) is lower than the full MoCA, all scores were converted to percentages to allow comparison.

To control for psychosocial variables known to impact performance on cognitive tests (supp table 3), patients completed the Hospital Anxiety and Depression Scale (HADS), the Modified Fatigue Impact Scale (MFIS) and the Brief Pain Inventory (BPI). For details regarding questionnaire constructs and validation studies, see appendix 4.

Only those questionnaires completed within 2 weeks of MoCA were included.

c) Statistics

c.i) Comparisons of MoCA scores, demographic, clinical and psychosocial variables between diagnostic groups

Distributions of variables were assessed by visual inspection of frequency histograms and the Shapiro-Wilk test. Group means of

parametrically distributed continuous variables were compared with t-tests or one-way ANOVA with post-hoc Tukey-Kramer tests if omnibus tests were significant at p ≤0.10. Group differences in non-parametrically distributed data were assessed with the Mann-Whitney-U test or Kruskal-Wallis test of ranks followed by Dunn's procedure with Bonferroni correction if omnibus tests were significant at p ≤0.10.

Chi squared tests were used to compare differences in proportions between groups when expected cell count was >5 or Fisher's exact test of proportions if expected cell count was ≤5. Group differences significant at the p ≤0.10 level were explored with pairwise comparisons (multiple z-tests or Fisher's exact tests with Bonferroni correction).

c.ii) Univariable regression to identify predictors of %MoCA score

Univariable linear regression was used to investigate effects of diagnosis, age at onset and presence of SILs on MoCA scores. Other parameters with potential impact on MoCA scores were entered into univariable regressions to identify possible confounders.

Applicability of linear regression to data sets depends on distributions of, and relationships between, components of the data set (appendix 5). The linearity of relationships between independent variables and %MoCA scores was assessed by inspection of scatterplots. Distribution

of the residuals was assessed by inspection of QQ plots of standardised residuals and the Shapiro-Wilk test. Homoscedasticity of residuals was assessed with plots of standardised residuals against fitted values for continuous independent variables. Levene's test was used to assess equality of variance for categorical independent variables.

Outliers were defined as studentized residuals that fell ≥ 3 standard deviations from the predicted value (μ) in linear models. Cook's distances were considered significant if they exceeded 4/n.

c.iii) Normalising the distribution of %MoCA scores with data transforms

To overcome violations of the assumption of normality and homoscedasticity of the residuals, several transforms were applied to MoCA scores and models using each transform were assessed according to criteria in appendix 5. A square root reflect transform was selected:

$$Transformed\ MoCA\ score = \sqrt{101 - \%MoCA\ score}$$

Relevant data were back-transformed to response space to improve interpretability (appendix 6).

Values of the coefficient of determination (R^2) >0.15 were considered clinically significant (41).

c.iv) Multivariable regression with significant univariable and *a priori* predictors

To determine whether any effects of diagnosis were robust to other independent variables, simultaneous multivariable regressions were run with diagnosis as an independent variable. Significant predictors of the transformed %MoCA score at the p ≤0.10 level in univariable regressions were included, as well as the *a priori* predictor, onset age group.

Assumptions were as for univariable linear regression and the models were analysed with the same diagnostic procedures. Continuous variables were centred to avoid variance inflation.

Variance inflation factor (VIF) was used to assess multicollinearity. Variables with structural overlap (e.g., total MFIS score and MFIS cognitive subscore) were substituted into different models and the variable resulting in the most negative Akaike Information Criteria (AIC) value was included.

Backward elimination with serial drop-1 commands was applied to the best fitting model to allow further refinement and nested models were compared using AIC and sequential F tests (161).

C.V) Multiple imputation with chained equations

Because some participants did not complete psychosocial questionnaires, several variables were missing data points. To validate the conclusions using the incomplete data set, the pattern of missingness was analysed and variables with most data missing were

imputed using Multiple Imputation with Monte Carlo Markov Chain Equations (MICE) (162).

A feasibility study was undertaken to determine whether missing data were amenable to imputation and select the most accurate method (appendix 7). Multivariable regression models were applied to the imputed data sets and results were pooled to generate parameter estimates.

d) Effect of onset age group on %MoCA score in AQP4+ NMOSD and MOGAD

Clinical and demographic variables and MoCA scores were compared between groups with disease onset aged <30 years ≥30 years as described in 2.2.c.i.

Because groups were small, multivariable regression with many parameters may lack sensitivity to detect an effect of onset age group. After consultation with a medical statistician (SM), variables with significant between-group differences at the p ≤0.10 level and *a priori* predictors (diagnosis and SIL status) were entered into multivariable regressions in the form:

$$Transformed\ MoCA\ score \quad onset\ age\ group + covariate + onset\ age\ group * covariate$$

Model analysis and statistical testing were carried out as described in section 2.2.c.iv. As this was an exploratory analysis, no correction was made for multiple comparisons.

e) Effect of SILs on %MoCA score in AQP4+ NMOSD and MOGAD

Median MoCA scores between groups with and without SILs were examined using the statistical methods described in section 2.2.d. As the group with SILs was small, variables with significant between-group differences at the p ≤0.10 level and *a priori* predictors (diagnosis and SIL status) were entered into multivariable regressions as described in 2.2.d.

All statistical procedures other than power calculations were performed in R (v4.4.1) (163).

2.3) Results: Cognition in AQP4+ NMOSD and MOGAD, part 1 (MoCA)

a) Comparison of MoCA scores, demographic and psychosocial variables between diagnostic groups

Of the 136 patients who completed the MoCA, 35 (25.7%) had MG, 45 (33.1%) had AQP4+ NMOSD and 56 (41.2%) had MOGAD (table 1).

Table 1: Comparison of demographic and clinical variables according to diagnosis

	MG	NMOSD	MOGAD	Shapiro-Wilk	Test statistic	Statistic (p)
N (%)	35 (25.7)	45 (33.1)	56 (41.2)			
Median MoCA score (%) (range)**	90 (66.7-100)$_a$	83.3 (46.7-100)$_b$	86.7 (56.7-100)$_a$	W 0.91 p < 0.01	Kruskal-Wallis (H)	7.96 (0.019)
N impaired on MoCA (%)	12 (34.3)	24 (53.3)	20 (35.7)	NA	χ^2	4.12 (0.127)
Median age at onset (years) (range)*	35 (1-64)	38 (23 – 61)	34 (6-65)	W 0.97, p = 0.01	Kruskal-Wallis (H)	5.10 (0.078)
N onset age group <30 years (%)	11 (33.3)	9 (20.0)	14 (25.5)	N/A	χ^2	1.78 (0.411)
Median age at testing (years) (range)**	50 (27-64)$_a$	51 (28-65)$_a$	41 (25-64)$_b$	W 0.96, p <0.01	Kruskal-Wallis (H)	15.23 (<0.001)
Median disease duration (months) (range)**	85 (1-593)$_a$	90 (5-308)$_a$	38 (3-498)$_b$	W 0.79, p <0.01	Kruskal-Wallis (H)	12.96 (0.002)
N female (%)**	21 (60.0)$_a$	39 (86.7)$_b$	36 (64.3)$_{ab}$	NA	χ^2	8.57 (0.014)
Median years in education (range)	13 (7-21)	15 (10-21)	15 (9-21)	W 0.97, p <0.01	Kruskal-Wallis (H)	2.78 (0.250)
N English as first language (%)	29 (82.9)	32 (71.1)	46 (82.1)	NA	χ^2	2.30 (0.317)
Median HADS-A score (range)*	9 (2-15)$_a$	5 (0-19)$_b$	5 (0-19)$_b$	W 0.95, p <0.01	Kruskal-Wallis (H)	5.11 (0.078)
Median HADS-D score (range)**	7 (1-17)$_a$	6 (0-15)$_{ab}$	2.5 (0-18)$_b$	W 0.90, p <0.01	Kruskal-Wallis (H)	8.20 (0.016)
Median MFIS score (range)**	43.5 (0-72)$_a$	34.5 (0-83)$_{ab}$	22 (0-75)$_b$	W 0.95, p <0.01	Kruskal-Wallis (H)	8.25 (0.016)
Median MFIS cognitive subscore (range)*	16 (0-30)$_a$	12.5 (0-39)$_{ab}$	8.5 (0-36)$_b$	W 0.93, p <0.01	Kruskal-Wallis (H)	5.25 (0.073)
Median BPI score (range)	33 (0-98)	19 (0-92)	12 (0-99)	W 0.84, p <0.01	Kruskal-Wallis (H)	1.98 (0.372)

*p ≤0.10; **p ≤0.05
Subscript a and b indicate groups that are significantly different in pairwise comparisons

There was a significant group difference in median %MoCA scores, with highest median score observed in the MG group (90%) and lowest in the AQP4+ NMOSD group (83.3%). *Post hoc* analysis confirmed significant differences in scores between the AQP4+ NMOSD group and both the MG group (z = -2.64, p = 0.021) and the MOGAD group (z = -2.41, p = 0.024) (fig 2). More patients met criteria for CI in the AQP4+ NMOSD group (53.3%) than either other group but this did not reach statistical significance (table 1).

Figure 2. Boxplot of %MoCA scores by diagnosis

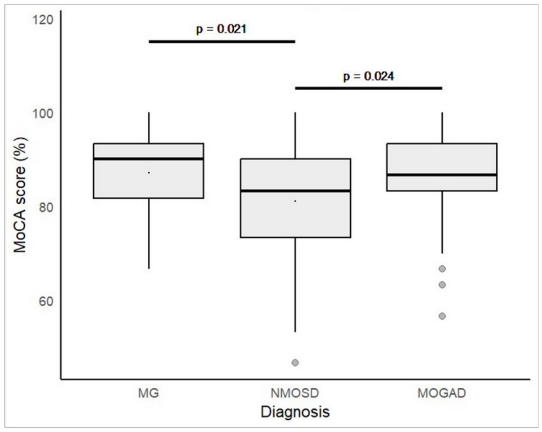

Median age at testing and median disease duration were significantly lower in the MOGAD group compared with either other group. A significantly greater proportion of the AQP4+ NMOSD group was female compared with the MG group. Pairwise comparisons confirmed median HADS-A score was significantly higher in the MG group than either other group. HADS-D, total MFIS, and MFIS cognitive scores were significantly higher in the MG group compared with the MOGAD group. BPI scores

were also highest in the MG group but did not reach statistical significance (table 1; supp table 4; supp fig 1 – 9). There were no significant differences in the proportions of patients with onset aged <30 years.

b) Univariable linear regression prior to data transform

Analysis of the residuals for each of the univariable regressions confirmed data did not meet assumptions of linear regression (appendix 5).

No published work has addressed the issue of non-parametric data in regression models of cognition in neuroinflammatory disease and it is likely some published results were the result of injudicious use of simple linear regression.

c) Transforming the %MoCA score

A variety of transforms was applied to %MoCA scores to compel the residuals to approximate a normal distribution without compromising linearity.

A square root reflect transform resolved heteroscedasticity, compelled the residuals to a normal distribution and removed outliers (appendix 6)

d) Univariable regression of transformed %MoCA score

Univariable regression was used to quantify the relationship between each predictor and transformed %MoCA scores and estimate its contribution to variance in scores. Results are summarised in table 2.

Table 2. Univariable regressions of √(101-%MoCA score)

Independent variable	β (SE)	T statistic	P (β)	R^2	F statistic (DoF)
Diagnosis				0.063	4.504 (2, 133)
AQP4+ NMOSD*	0.700 (0.277)	2.532	0.013		
MOGAD	0.049 (0.265)	0.186	0.853		
Age at onset	0.012 (0.008)	1.457	0.147	0.016	2.124 (1, 131)
Onset age group≥30*	0.455 (0.248)	1.833	0.069	0.025	3.362 (1, 131)
Age at testing	0.014 (0.010)	1.404	0.163	0.015	1.972 (1, 134)
Disease duration	-0.001 (0.001)	-0.783	0.435	0.005	0.614 (1, 131)
Sex	0.318 (0.236)	1.344	0.182	0.013	1.806 (1, 134)
Education (years)*	-0.088 (0.035)	-2.489	0.014	0.046	6.198 (1, 129)
Language (not English)*	0.860 (0.254)	3.383	<0.001	0.079	11.450 (1, 131)
HADS-A score*	0.051 (0.025)	2.009	0.047	0.038	4.035 (1, 101)
HADS-D score*	0.073 (0.025)	2.894	0.005	0.079	8.377 (1, 97)
Total MFIS score*	0.015 (0.005)	3.155	0.002	0.093	9.957 (1, 97)
MFIS cognitive score*	0.033 (0.010)	3.258	0.002	0.097	10.610 (1, 99)
BPI score*	0.019 (0.004)	5.535	<0.001	0.250	30.630 (1, 92)

*p ≤0.10

Predicted %MoCA score in the AQP4+NMOSD group was 4.48% lower than in the MG group (p = 0.013) (appendix 6; supp table 5; supp fig 10). There was no significant difference in predicted transformed %MoCA score between the MOGAD group and the MG group. Diagnosis explained 6.3% of the variance beyond the mean model (R^2 = 0.063). This is considered low (41).

Other statistically significant predictors of transformed %MoCA scores are listed in table 3 (supp table 6 – 13; supp fig 11 – 18). Contrary to

expectation, onset age <30 years predicted scores 3.34% higher than onset age ≥30 years. Environmental factors (language, education) and psychosocial factors (anxiety, depression, and fatigue) were significant predictors, with pain scores explaining most variance (R^2 = 0.250).

Table 3. Effects of significant predictors of transformed %MoCA score in univariable regressions

Variable	Effect of each 1 unit increase in continuous variables/ effect of categorical variable vs comparator	R^2	p
Diagnosis AQP4+ NMOSD	$\%MoCA_{MG} - 4.48\%$	0.063 (low)	0.013
Onset age group (≥30)	$\%MoCA_{<30\ years} - 3.34\%$	0.025 (low)	0.069
Education	+0.888 – 0.016(current years of education)	0.046 (low)	0.014
First language	$\%MoCA_{English} - 6.96\%$	0.079 (low)	<0.001
HADS-A score	-0.356 – 0.005(current HADS-A score)	0.038 (low)	0.047
HADS-D score	-0.511 – 0.011(current HADS-D score)	0.079 (low)	0.005
$MFIS_{total}$	-0.098 – 0.000(current $MFIS_{total}$ score)	0.093 (low)	0.002
$MFIS_{cognitive}$	-0.221 – 0.002(current $MFIS_{cognitive}$ score)	0.097 (low)	0.002
BPI score	-0.122 – 0.001(current BPI score)	0.250 (moderate)	<0.001

e) Multivariable regression with significant univariable and *a priori* predictors

To determine whether diagnosis was a significant predictor of cognitive performance after adjustment for *a priori* variables (onset age group) and significant predictors in univariable models, multivariable regressions were performed.

Interaction terms between diagnosis and other variables were not statistically significant so were not included in multivariable models.

Model 1: Independent variables were diagnosis (MG, MOGAD and AQP4+ NMOSD), onset age group, years in education, first language

(not English), HADS-A score, HADS-D score, total MFIS score and BPI score (supp table 14; supp fig 19).

Diagnosis of AQP4+ NMOSD remained a statistically significant predictor of transformed MoCA score. Years of education and first language were also significant after adjusting for the other variables (table 4a).

The model explained 31.7% of the variance beyond the mean model, which is statistically and clinically significant (table 4b).

Table 4a & b: Multivariable regression, model 1

a. Values of regression coefficients

		β (SE)	T statistic	p
Diagnosis				
	AQP4+ NMOSD*	0.801 (0.303)	2.640	0.010
	MOGAD	0.334 (0.296)	1.129	0.263
Onset age group≥30		0.236 (0.278)	0.846	0.400
Education*		-0.099 (0.040)	-2.451	0.017
Language (not English)*		0.757 (0.285)	2.655	0.010
HADS-A		0.033 (0.035)	0.925	0.358
HADS-D		-0.019 (0.051)	-0.373	0.711
Total MFIS		0.003 (0.010)	0.275	0.784
BPI		0.009 (0.006)	1.569	0.121

Reference variable for diagnosis = MG
* p ≤0.05

b. Assessment of model 1

Adj R^2	RSE (DoF)	F statistic (DoF)	P (F statistic)	AIC (eDoF)
0.317	0.94 (74)	5.281 (9, 74)	<0.001	-0.79 (10)

Model 2: Independent variables were the same as model 1 but MFIS cognitive subscore replaced total MFIS score (supp table 15; supp fig 20).

Diagnosis of AQP4+ NMOSD remained a statistically significant predictor of transformed MoCA score, as did years of education and first language. BPI score approached statistical significance (table 5a).

The model explained 33.2% of the variance beyond the mean model, which is statistically and clinically significant (table 5b).

Table 5a & b: Multivariable regression, model 2

a. Values of regression coefficients

		β (SE)	T statistic	p
Diagnosis				
	AQP4+ NMOSD*	0.742 (0.302)	2.452	0.017
	MOGAD	0.342 (0.286)	1.196	0.236
Onset age group≥30		0.269 (0.272)	0.988	0.326
Education*		-0.095 (0.040)	-2.398	0.019
Language (not English)*		0.763 (0.276)	2.765	0.007
HADS-A		0.023 (0.035)	0.656	0.514
HADS-D		-0.044 (0.046)	-0.970	0.335
MFIS cognitive		0.022 (0.016)	1.392	0.168
BPI		0.010 (0.005)	1.915	0.059

Reference variable for diagnosis = MG
* p ≤0.05

b. Assessment of model 2

Adj R^2	RSE (DoF)	F statistic (DoF)	P (F statistic)	AIC (eDoF)
0.332	0.93 (75)	5.644 (9, 75)	<0.001	-3.25 (10)

A drop-one method was applied to the best fitting model (model 2) (supp table 16).

Model 3: Backwards elimination was used to determine whether diagnosis remained a predictor in an optimised predictive model. The third drop1 command generated model 3, which was the optimal model (table 6a & b; supp table 17; supp fig 21). Independent variables were diagnosis, years of education, first language, MFIS cognitive subscore and BPI score. AQP4+ NMOSD predicted significantly lower %MoCA score than MG

This model had the highest R^2, explaining 34.5% of the variance beyond the mean model.

Table 6a & b: Multivariable regression, model 3

a. Values of regression coefficients

		β (SE)	T statistic	p
Diagnosis				
	AQP4+ NMOSD*	0.825 (0.284)	2.909	0.005
	MOGAD	0.413 (0.276)	1.499	0.138
Education*		-0.104 (0.039)	-2.681	0.009
Language (not English)*		0.736 (0.272)	2.702	0.008
MFIS cognitive		0.016 (0.011)	1.404	0.164
BPI		0.008 (0.005)	1.898	0.061

Reference variable for diagnosis = MG
* Statistically significant variable

b. Assessment of model 3

Adj R^2	RSE (DoF)	F statistic (DoF)	P (F statistic)	AIC (eDoF)
0.345	0.92 (78)	8.388 (6, 78)	<0.001	-7.61 (7)

f) Multiple imputation with chained equations: Study data (whole cohort)

Because some predictors in regressions were missing values, multiple imputation was used to increase the power of the models. For descriptions and explanations of the MICE feasibility study and model selection, see appendices 7 & 8.

Results of applying model 3 to the imputed data sets were similar to those obtained with the original, incomplete data set, confirming AQP4+ NMOSD predicted significantly lower MoCA scores than MG (table 7; supp table 18).

Table 7. Comparison of regression model 3 applied to original and imputed data

		Raw data		Imputed data	
N		84		131	
F statistic (p)		8.388 (<0.001)		5.711 (<0.001)	
R^2		0.345		0.245	
		β (SE)	p	β (SE)	p
Diagnosis					
	AQP4+ NMOSD	0.825 (0.284)	0.005*	0.613 (0.261)	0.020*
	MOGAD	0.413 (0.276)	0.138	0.247 (0.247)	0.320
Education		-0.104 (0.039)	0.009*	-0.069 (0.034)	0.045*
Language (not English)		0.736 (0.272)	0.008*	0.618 (0.250)	0.015*
MFIS cognitive		0.016 (0.011)	0.164	0.010 (0.014)	0.513
BPI		0.008 (0.005)	0.061	0.010 (0.004)	0.043*

*p <0.05

g) Comparison of AQP4+ NMOSD and MOGAD groups

Pairwise comparisons indicated %MoCA scores of patients with AQP4+ NMOSD were significantly lower than those of patients with MOGAD. This was explored with univariable regression excluding the MG cohort. Restricting analyses to these groups also permitted investigation of effects of SIL status.

When transformed %MoCA score was regressed against diagnosis (AQP4+ NMOSD versus MOGAD), there was a significant effect of diagnosis (β_{MOGAD} = -0.651, p = 0.011). This indicates MOGAD predicts higher *raw* %MoCA scores than AQP4+ NMOSD. Effects of other predictors on the combined AQP4+ NMOSD and MOGAD groups are displayed in table 8 (supp fig 22 – 35; supp table 19 - 32).

Table 8. Univariable regression of transformed %MoCA scores (AQP4+ NMOSD and MOGAD only)

Independent variable	β (SE)	T statistic	P (β)	R^2	F statistic
Diagnosis MOGAD*	-0.651	-2.591	0.011	0.064	6.715 (1, 99)
Onset age group≥30	0.213	0.690	0.492	0.005	0.476 (1, 98)
Age at testing	0.010	0.844	0.401	0.007	0.712 (1, 99)
Disease duration	0.000	0.062	0.951	0.000	0.004 (1, 98)
Sex	0.269	0.917	0.362	0.008	0.840 (1, 99)
Education (years)*	-0.095	-2.153	0.034	0.047	4.634 (1, 95)
Language (not English)*	0.910	3.097	0.003	0.088	9.590 (1, 99)
HADS-A score*	0.054	1.936	0.056	0.044	3.749 (1, 81)
HADS-D score*	0.072	2.499	0.015	0.075	6.245 (1, 77)
Total MFIS score*	0.016	3.019	0.003	0.103	9.113 (1, 79)
MFIS cognitive score*	0.031	2.777	0.007	0.088	7.714 (1, 80)
BPI score*	0.019	4.654	<0.001	0.229	21.662 (1, 73)
EDSS*	0.184	2.888	0.005	0.080	8.341 (1, 96)
SIL status	0.362	0.877	0.383	0.008	0.769 (1, 96)

*p ≤0.05

Model 4: Multivariable regression was used to determine whether diagnosis of MOGAD predicted significantly higher %MoCA scores than AQP4+ NMOSD after adjusting for *a priori* predictors (onset age group and SIL status) and covariates that were significant in univariable regressions (diagnosis, education, first language, and scores for HADS-A, HADS-D, MFIS cognitive, BPI and EDSS).

None of the independent variables were statistically significant predictors of transformed %MoCA score (at the p ≤0.05 level) in multivariable regression (table 9; supp table 33; supp fig 36).

Table 9a & b: Multivariable regression, model 4

a. Values of regression coefficients

		β (SE)	T statistic	p
Diagnosis MOGAD		-0.368 (0.315)	-1.169	0.247
Onset age group ≥30		0.084 (0.369)	0.227	0.821
Education		-0.092 (0.053)	-1.723	0.090
Language		0.661 (0.358)	1.848	0.070
HADS-A		0.034 (0.050)	0.687	0.495
HADS-D		-0.086 (0.069)	-1.256	0.214
MFIS cognitive		0.021 (0.021)	1.014	0.315
BPI		0.014 (0.007)	1.930	0.059
EDSS		0.022 (0.102)	0.214	0.832
SIL status		-0.114 (0.490)	-0.233	0.817

Reference variable for diagnosis = AQP4+ NMOSD
* p ≤0.05

b. Assessment of model 4

Adj R^2	RSE (DoF)	F statistic (DoF)	P (F statistic)	AIC (eDoF)
0.232	1.03 (55)	2.960 (10, 55)	0.005	13.19 (11)

Model 5: Backward elimination was applied to model 4 to see whether exclusion of extraneous variables revealed a significant effect of diagnosis on transformed %MoCA score (supp table 34). Predictors in the final model (model 5) included diagnosis, education, first language and BPI score. Diagnosis was not a predictor of transformed %MoCA score in this optimised model, but education and BPI scores were (table 10a & b; supp table 35; supp fig 37).

Table 10a & b: Multivariable regression, model 5

a. Values of regression coefficients

		β (SE)	T statistic	p
Diagnosis MOGAD		0.426 (0.263)	-1.620	0.114
Education*		-0.103 (0.049)	-2.085	0.041
Language		0.605 (0.331)	1.826	0.073
BPI score*		0.013 (0.005)	2.483	0.016

Reference variable for diagnosis = AQP4+ NMOSD
* p ≤0.05

b. Assessment of model 5

Adj R^2	RSE (DoF)	F statistic (DoF)	P (F statistic)	AIC (eDoF)
0.277	0.99 (61)	7.219 (4, 61)	<0.001	4.03 (5)

Data from the combined cohort of AQP4+ NMOSD and MOGAD were not amenable to imputation with MICE (appendix 8).

h) Effect of onset age group on %MoCA score in combined AQP4+ NMOSD and MOGAD groups

Those with disease onset aged <30 years (86.7%) had similar median %MoCA scores to those with onset at ≥30 years (86.4%) (table 11, fig 3a). Univariable regression did not reveal a significant effect of onset age group on transformed %MoCA score in this cohort (table 8)

Figure 3. Boxplot of %MoCA scores according to onset age group (a) and SIL status (b) (AQP4+ NMOSD and MOGAD only)

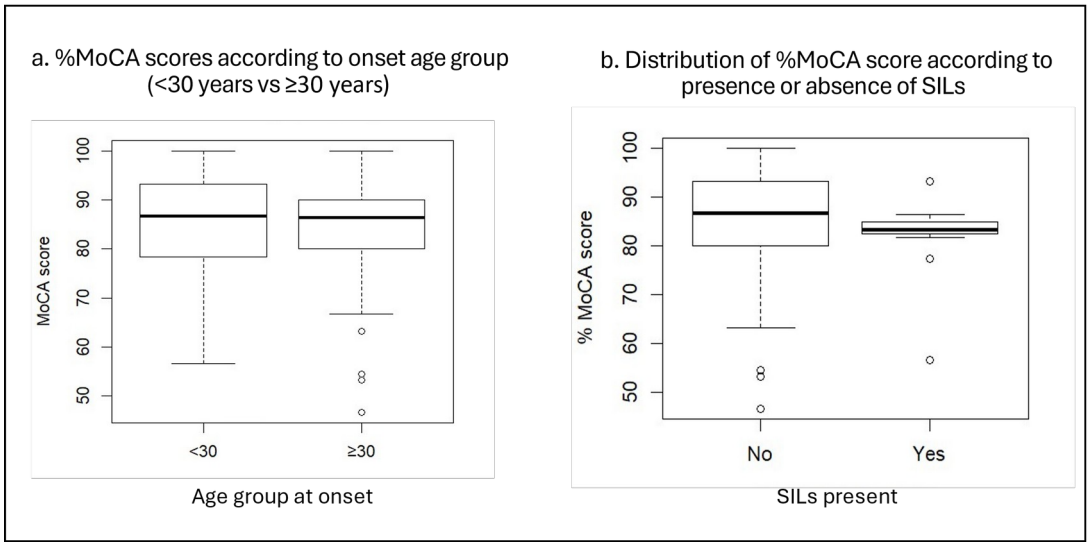

Table 11: Comparison of demographic and clinical variables according to onset age group (<30 years vs ≥30 years) (AQP4+ NMOSD and MOGAD only)

	Age at onset < 30 years (N = 23)	Age at onset ≥ 30 years (N = 77)	Test statistic (p)
Median % MoCA (range)	86.7 (56.7 – 100)	86.4 (46.7 - 100)	U = 962 (0.534)
Median age at testing (range)*	34 (25 – 51)	49 (28 – 65)	U = 317 (<0.001)
Median disease duration (months) (range)*	118 (4 – 498)	47 (3 – 308)	U = 1180 (0.016)
N sex at birth female (%)	18 (78.3%)	56 (72.7%)	χ^2 = 0.068 (0.795)
Median education duration (years) (range)*	17 (9 – 21)	14 (10 – 21)	U = 1114 (0.018)
N first language not English (%)	6 (26.1%)	17 (22.1%)	χ^2 = 0.014 (0.906)
Median HADS-A score (range)	5.5 (1 – 15)	5 (0 -19)	U = 611 (0.781)
Median HADS-D score (range)	3 (0 – 9)	3 (0 – 18)	U = 468 (0.663)
Median total MFIS score (range)	29 (1 – 66)	26.5 (0 – 83)	U = 547 (0.977)
Median MFIS cognitive subscore (range)	11.5 (0 – 34)	10.5 (0 – 39)	U = 626 (0.577)
Median BPI score (range)	0 (0 – 61)	17 (0 – 99)	U = 332 (0.111)
Median EDSS score (range)	1 (0 – 6)	1.5 (0 – 7)	U = 756 (0.547)
SILs present (%)†	4 (17.4%)	7 (9.1%)	OR = 0.48 (0.271)

*p ≤0.10; † Fisher's exact test

To determine whether onset age group was a significant predictor of %MoCA score after adjusting for relevant predictors, variables that were significantly different between onset age groups and *a priori* predictors were incorporated into multivariable regressions with interaction terms, which allowed detection of discrete effects of variables on different age groups.

Age at testing, disease duration and years of education were significantly different between onset age groups (table 11). Adjusting for these variables did not reveal any significant main effect of onset age group on transformed %MoCA score, nor any significant interactions. Adjusting for *a priori* predictors diagnosis and SIL status did not produce statistically significant main effects or interactions (supp table 36 - 40).

i) <u>Effect of SILs on %MoCA score in combined AQP4+ NMOSD and MOGAD groups</u>

Only 11 patients had SILs (4 with AQP4+ NMOSD and 7 with MOGAD). There was no significant difference in median %MoCA score between patients with (83.3%) and without SILs (86.7%) (fig 3b, table 12). Univariable regression did not reveal an effect of SILs on %MoCA score (table 8).

A significantly greater proportion of patients with brain lesions spoke English as a first language (table 12). No adjustment could be made

because all patients with supratentorial lesions spoke English as a first language. There were no other significant differences between groups.

Table 12: Comparison of demographic and clinical variables according to presence or absence of supratentorial inflammatory lesions

	No lesions (N = 90)	Lesions (N = 11)	Test statistic (p)
Median % MoCA (range)	86.7 (46.7 – 100)	83.3 (56.7 – 93.3)	U = -3496 (0.255)
N diagnosis AQP4+ NMOSD (%)	41 (45.6)	4 (36.4)	Fisher's p (0.750)
Median age at onset	36 (6 – 65)	31 (19 – 53)	U = -3376 (0.123)
N onset age group ≥30 (%)	70 (77.8)	7 (63.6)	Fisher's p (0.286)
Median age at testing (range)	44 (27 – 65)	35 (25 – 65)	U = -3496 (0.257)
Median disease duration (months) (range)	51 (3 – 498)	90 (8 – 325)	U = -3608 (0.308)
N sex at birth female (%)	67 (74.4)	8 (72.7)	Fisher's p (~1.000)
Median education duration (years) (range)	15 (9 – 21)	16 (11 – 17)	U = -3292 (0.788)
N first language not English (%)*	23 (25.6)	0	Fisher's p (0.065)
Median HADS-A score (range)	5 (0 – 19)	5.5 (4 – 11)	U = -2571(0.750)
Median HADS-D score (range)	3 (0 – 18)	6 (0 – 8)	U = -2346 (0.835)
Median total MFIS score (range)	27 (0 – 83)	32 (1 – 55)	U = -2418 (0.893)
Median MFIS cognitive subscore (range)	10 (0 – 39)	13 (0 – 26)	U = -2480 (0.988)
Median BPI score (range)	16 (0 – 99)	13 (0 – 60)	U = -2091 (0.745)
Median EDSS score (range)	1.0 (0 – 7.0)	2.0 (0 – 6.5)	U = -3530(0.521)

*p ≤0.10

After adjusting for the effect of SIL status, diagnosis of MOGAD remained a significant predictor of transformed %MoCA score (β = -0.723, p = 0.646) (supp table 41; supp fig 38). This indicates that, in the absence of SILs, MOGAD predicted a significantly higher raw MoCA score than AQP4+ NMOSD and the presence of SILs did not significantly alter the relationship. There was no significant main effect of SILs or interaction.

The interaction between SIL status and onset age group was explored in section 2.3.h.

j) Neuropsychometric evaluation

Twenty-two of the 66 patients scoring below the threshold for diagnosis of CI accepted referral for formal neuropsychometric evaluation. Two patients did not attend the assessments, 7 patients were awaiting assessment or outcome is unknown at time of writing, 1 patient died and 1 patient did not qualify for neurocognitive assessment with local services but scored on the MoCA 93.3% a year later.

Of the 11 patients assessed, 6 had no evidence of impairment, 4 had below-expected performance in one or more domains that was attributed to attentional fluctuations caused by stress, anxiety or fatigue and 1 scored poorly due to language difficulties, cultural factors, limited education and grief. No patient was found to have significant organic CI.

2.4) Discussion: Cognition in AQP4+ NMOSD and MOGAD, part 1 (MoCA)

a) Poorer cognitive performance in AQP4+ NMOSD compared with disease controls

In line with other studies, the current work confirmed patients with AQP4+ NMOSD perform significantly worse on the MoCA than controls.

This study improves upon earlier work in several ways.

i) Statistical evaluation revealed raw MoCA scores were not suitable for analysis using methods that depend on parametric distribution. Most studies have used such methods to analyse MoCA scores (128,130,133,155,159), potentially resulting in spurious associations (supp table 1). The current study confirms a diagnosis of AQP4+ NMOSD is associated with poorer MoCA performance compared with controls when greater statistical rigour is applied to the data.

ii) The effects of potential confounders and mediators were examined and incorporated into multivariable models. Although previous studies have identified correlations between demographic and clinical variables and cognitive performance in NMOSD, few have adjusted for these in models (supp table 1).

Regressions were used to identify and exclude potential confounders in the current study, rather than to design a

predictive model. Nevertheless, the significant impact of covariates like education and pain highlights the need to adjust for these factors. This is the first study to examine the influence of native language on cognitive test performance in NMOSD and has implications for patient selection in future work.

Neuropathic pain is a common consequence of TM in AQP4+ NMOSD and may contribute to poorer performance in this group (164,165). A larger study using multivariable regression to examine effects of variables on MoCA scores in NMOSD identified significant effects of education and race and a borderline effect of pain (133). If race is a proxy for language, the results presented here are remarkably similar and confirm the protective effects of education on cognitive performance in NMOSD (58,128,130,132,166), as well as the detrimental effects of pain (88).

iii) Some studies fail to report the proportion of seronegative cases in their cohorts, and seronegative patients even dominate in some (supp table 1) (130,167–169). Seronegative NMOSD is likely to reflect heterogeneous pathologies with disparate effects on cognition. If serostatus impacts cognitive performance (130,135), the inclusion of only seropositive patients means the effects of diagnosis can be estimated with more certainty.

iv) Most research has compared performance of disease groups with that of healthy controls. Significant confounders such as depression, anxiety, fatigue, pain and physical disability are often ignored or cannot be accounted for. Unadjusted comparisons with healthy controls cannot determine whether CI is organic or the result of the challenges facing individuals with a chronic, relapsing autoimmune disease.

By using a control group of patients with MG, who experience similar psychosocial impact but no CNS inflammation, it was possible to distinguish an effect of the cerebral inflammatory milieu from indirect effects of chronic disease. Indeed, MoCA scores were higher in the MG group than the AQP4+ NMOSD group, despite higher levels of depression, anxiety, fatigue and pain- features that correlate negatively with cognitive performance (supp table 3) (80,170–175).

v) The majority of previous studies of cognition in NMOSD and MOGAD were retrospective. The current study was prospective, reducing risk of selection bias, optimising data capture and minimising variability in test administration.

b) <u>MoCA performance in patients with MOGAD is not statistically different to that of controls</u>

Few studies have examined the effects of MOGAD on adult cognition (supp table 2) and only one compared MoCA scores of adults with MOGAD to those of healthy controls (112). Median score was significantly lower than that of controls but only 13 MOGAD patients completed the MoCA and scores were not adjusted for important demographic and clinical variables.

In the current study, although 35.7% of MOGAD patients in the current cohort met criteria for CI, this was a similar proportion to the control group. Diagnosis of MOGAD had no significant effect on MoCA score relative to controls after adjusting for relevant covariates. Therefore, poor test scores are likely to reflect indirect effects of chronic relapsing disease.

c) MoCA performance in AQP4+ NMOSD versus MOGAD

Both pairwise comparisons and univariable regression indicated patients with AQP4+ NMOSD scored significantly lower on the MoCA than patients with MOGAD. The effect of diagnosis did not survive multivariable regression, probably due to a combination of true re-attribution of variance but also due to the reduced power of multivariable models caused by lower residual degrees of freedom. It is possible that the independent effect of diagnosis would have survived if groups were larger.

Practically, if the study sample is representative of the population, patients with AQP4+ NMOSD are predicted to perform worse on cognitive testing than those with MOGAD, regardless of the underlying drivers. This should be considered in service delivery and resource allocation for patients.

d) Aetiology of impaired MoCA scores in AQP4+ NMOSD

Poorer test scores of the AQP4+ NMOSD group compared with the MG group cannot be explained by the psychosocial variables tested. The MG group had higher median scores on questionnaires that predicted worse performance in univariable regression and no significant predictor x diagnosis interaction was found to account for the differences. Furthermore, diagnosis of AQP4+ NMOSD remained a predictor of poor performance after adjusting for variables that were statistically significant in univariable regressions. Potential explanations are discussed in chapter 5.

Differences may also reflect lack of specificity of the test itself. The high incidence of CI among control patients and the absence of organic impairment in patients referred for formal psychometric cognitive assessment suggest the MoCA may be measuring a separate construct with greater impact in NMOSD than in MOGAD and MG. This construct may be attention.

Formal psychometric testing noted impaired attention and concentration among patients referred for poor MoCA performance. It is arguable that “fluctuating attention”, to which poor scores were attributed, is itself a cognitive impairment. I propose that impaired attention, which has been reported widely in NMOSD, underpins the significantly worse MoCA scores in this group.

The MoCA was designed for detection of mild CI (157) and while it has been validated in MS (176), the positive predictive value is only 66% (158). Other groups have used the MoCA in studies of NMOSD (112,128,130,155,167,168), but results show intraindividual instability in patients (133).

e) Effects of onset age group and SILs on MoCA scores in mixed AQP4+ NMOSD and MOGAD groups

The current study did not confirm an effect of onset age group on cognitive outcomes in AQP4+ NMOSD and MOGAD.

While onset age group may not have an effect on MoCA performance, it is possible that cognitive ramifications are more severe at very young ages, when brain insults disrupt acquisition of rudimentary skills, and at older ages, when cerebral reserve has started to decline. Discrepant effects would not be detected with binary age groups used here. Lack of effect may also be due to underpowering.

Median scores were not significantly lower in patients with SILs than those without and univariable regression did not demonstrate an effect of SILs. The lack of statistical significance may be an effect of underpowering. Additionally, all patients with SILs spoke English as a first language, which may have counteracted effects of SILs on MoCA scores.

In conclusion, the results demonstrate MoCA performance of patients with AQP4+ NMOSD but not MOGAD is significantly poorer than performance of the control group, and this was independent of relevant covariates. However, the MoCA may lack specificity for organic CNS pathology.

f) Amendments to the protocol based on current data

i) The Rao Brief Repeatable Battery of Neuropsychological tests (Rao BRB-N) was selected for future testing. Although more time-consuming to administer and score, it was designed for use in MS, rather than mild CI, and includes tests of attention and processing speed, which are reportedly affected in NMOSD (84,128,132,177,178). It has been used in NMOSD (88,134,166,179) and MOGAD (59,180). The Rao BRB-N provides greater detail regarding cognitive domains affected and specificity

of up to 94% has been recorded (181). The Stroop Colour-Word Test was added to assess executive function.

ii) The current study was underpowered to detect effects of SILs and young-onset disease. Because age at testing and age at onset were correlated, many patients with young-onset disease were ineligible for inclusion as they were <25 years old at the time of the study. In subsequent phases, the minimum age of participants was reduced to 20 years. Patients with brain lesions and/or disease onset in childhood were identified for cognitive assessment.

iii) Only patients with English as a first language were offered cognitive assessment with the Rao BRB-N.

Chapter 3

Cognition in AQP4+ NMOSD and MOGAD, part 2 (Rao BRB-N)

3.1) Methods: Cognition in AQP4+ NMOSD and MOGAD, part 2 (Rao BRB-N)

a) Testing protocol

Patients were tested in a quiet room by a single examiner (AF). Tests were administered in the established order (156) (appendix 9).

The Selective Reminding Test (SRT) was used to examine verbal long-term storage (LTS), consistent long-term retrieval (CLTR) and delayed recall (DR). Immediate and delayed visuospatial recall was assessed with the Spatial Recall Test (SPART). Auditory attention and processing speed was tested using the Symbol Digit Modalities Test (SDMT) and visuospatial attention with the Paced Auditory Serial Additions Test (PASAT, 3-second version). Phonological verbal fluency was assessed with the Word List Generation Test (WLGT). The Stroop Colour-Word Test was used to assess executive function. Interference scores (Stroop-IS) are calculated such that more negative scores indicate poorer ability to inhibit automatic responses (182).

b) Statistics

b.i) General methods

Methods to assess distributions of demographic and clinical variables and statistics to compare variables between categories were applied as described in section 2.2.c.i.

Univariable regressions were performed for each test of the Rao BRB-N and Stroop test and linearity of the relationship between independent variable and score, homoscedasticity of residuals and distribution of the residuals were assessed as described in section 2.2.c.ii. Results of tests violating the assumptions of linear regression were transformed. Significant outliers, significant Cook's distances and clinically significant values of R^2 are defined in section 2.2.c.ii.

b.ii) Multivariable regressions

For each sub-test, variables that were significant in univariable regressions (unadjusted $p \leq 0.10$) were entered into multivariable regressions with *a priori* predictors (diagnosis and onset age group). As the primary hypothesis was that diagnosis affects performance on any of 9 different tests, false discovery rate corrections for effect of diagnosis were made using the Benjamin-Hochberg procedure. Initial analyses were performed for the 3 diagnostic categories (MG, AQP4+ NMOSD and MOGAD).

Models were optimised by backward elimination with serial drop-1 procedures, as described in section 2.2.c.iv.

This process was repeated for AQP4+ NMOSD and MOGAD groups only to identify significant differences in Rao BRB-N and Stroop interference scores between these groups. Multivariable models included presence of SILs as an *a priori* predictor.

Studies using the Rao BRB-N detected differences between patients with AQP4+ NMOSD and healthy controls using samples of 22 (135). Therefore, a minimum group size of 25 was adopted for the current study.

b.iii) Multiple imputation with chained equations (MICE)

MICE was used to impute missing values for multivariable regressions as described in section 2.2.c.v (appendix 7). This included testing feasibility and optimising performance with a test dataset. Independent variables most frequently lacking data points were identified and regression models that included these variables as predictors were re-run after imputation.

b.iv) Effect of onset age group on test scores in AQP4+ NMOSD and MOGAD

Differences in demographic and clinical variables between groups with onset aged <30 years and onset aged ≥30 years were compared as described in section 2.2.d. Covariates significantly different between onset age groups at the p ≤0.10 level and *a priori* predictors were entered into multivariable regressions.

b.v) Effect of SILs on test scores in AQP4+ NMOSD and MOGAD

The effects of SIL status on test scores were examined as described in section 2.2.e. Briefly, covariates that were significantly different between groups with and without SILs at the p ≤0.10 level and *a priori* predictors were included in multivariable regressions with SIL status.

3.2) Results: Cognition in AQP4+ NMOSD and MOGAD, part 2 (Rao BRB-N)

a) Effect of diagnosis on Rao BRB-N and Stroop interference scores

a.i) Comparison of demographic and clinical variables, BRB-N and Stroop scores between all diagnostic groups

A total of 125 patients consented to testing with the Rao BRB-N and Stroop test (table 13). Omnibus tests confirmed statistically significant differences in age at testing ($H = 4.72$, $p = 0.094$) and proportion of females ($\chi^2 = 5.67$, $p = 0.059$) at the $p \leq 0.10$ level but pairwise comparisons did not reach statistical significance (supp table 42).

In contrast to patterns observed in section 2.3, anxiety, depression, fatigue and pain scores were highest in the AQP4+ NMOSD group, although this only reached statistical significance for BPI score in pairwise comparisons (supp table 42).

Table 13. Comparison of demographic and clinical variables according to diagnosis

Feature	MG	AQP4+ NMOSD	MOGAD	Shapiro-Wilk	Test statistic	Statistic (p)
N (%)	50 (40)	27 (21.6)	48 (38.4)	N/A	N/A	N/A
Median age onset (years) (range)	34.5 (3 – 62)	37 (10 – 61)	33 (4 – 62)	0.976 (0.002)	Kruskal-Wallis (H)	0.66 (0.718)
N aged <30 at onset (%)	22 (44.9)	10 (37.0)	16 (33.3)	N/A	χ^2	1.21 (0.547)
Median age testing (years) (range)*	49.5 (22 - 65)$_a$	49 (23 – 65)$_a$	40 (20 – 64)$_a$	0.957 (<0.001)	Kruskal-Wallis (H)	4.72 (0.094)
Median disease duration (months) (range)	92 (11 – 610)	95 (22 – 371)	69 (6 – 418)	0.811 (<0.001)	Kruskal-Wallis (H)	3.68 (0.159)
N female (%)*	33 (66.0)$_a$	24 (88.9)$_a$	31 (64.6)$_a$	N/A	χ^2	5.67 (0.059)
Median years in education (range)	14 (10 – 20)	15 (10 – 21)	14 (11 – 21)	0.960 (0.001)	Kruskal-Wallis (H)	1.24 (0.537)
Median HADS-A score (range)	7 (0 – 17)	8 (1 – 15)	6 (0 – 17)	0.972 (0.035)	Kruskal-Wallis (H)	0.75 (0.687)
Median HADS-D score (range)*	3.5 (0 – 11)$_a$	6 (0 – 14)$_a$	4 (0 – 15)$_a$	0.932 (<0.001)	Kruskal-Wallis (H)	5.50 (0.064)
Median MFIS total score (range)*	33 (0 – 74)$_a$	42 (0 – 71)$_a$	37 (0 – 73)$_a$	0.957 (0.003)	Kruskal-Wallis (H)	5.05 (0.080)
Median MFIS cognitive subscore (range)*	14 (0 – 34)$_a$	18 (0 – 36)$_a$	12.5 (0 – 40)$_a$	0.961 (0.006)	Kruskal-Wallis (H)	4.77 (0.092)
Median BPI score (range)**	11 (0 – 86)$_a$	44 (0 – 92)$_b$	14 (0 – 79)$_a$	0.855 (<0.001)	Kruskal-Wallis (H)	11.1 (0.004)

*p ≤0.10; **p ≤0.05
Subscript a and b indicate groups that are significantly different in pairwise comparisons

Patients with AQP4+ NMOSD had the lowest mean or median scores on all tests other than the SRT-LTS and SRT-CLTR. Pairwise comparisons confirmed the AQP4+ NMOSD group had significantly lower mean scores than the MG group on the PASAT (z = -3.23, p = 0.004). Scores on the Stroop test (mean diff. = -6.72, p = 0.045), SDMT (mean diff. = -9.65, p <0.001) and PASAT (z = -4.10, p <0.001) were also significantly lower in the AQP4+ NMOSD group compared with the MOGAD group, and the difference in SPART-IR score approached statistical significance (mean diff. = -2.95, p = 0.076) (table 14; supp table 43; fig 4).

Table 14. Comparison of Rao-BRB-N and Stroop test scores according to diagnosis

	MG	AQP4+ NMOSD	MOGAD	Shapiro-Wilk (p)	Test statistic	Statistic (p)
n	50	27	48	N/A	N/A	N/A
Median SRT-LTS (range)	41.5 (12 – 69)	46 (12 – 65)	49 (10 – 66)	0.968 (0.005)	Kruskal-Wallis (U)	1.04 (0.596)
Mean SRT-CLTR (SD)	31.5 (14.9)	32 (16.9)	35.5 (14.0)	0.987 (0.281)	ANOVA (F 2,122)	0.85 (0.431)
Median SRT-DR (range)	9 (3 – 12)	7.5 (0 – 12)	9 (3 – 12)	0.930 (<0.001)	Kruskal-Wallis (U)	1.00 (0.605)
Mean SPART-IR (range)*	20.2 $(5.5)_a$	17.7 $(5.9)_a$	20.6 $(5.4)_a$	0.982 (0.09)	ANOVA (F 2, 120)	2.47 (0.089)
Median SPART-DR (range)	6.5 (2 – 10)	6.5 (0 – 10)	8 (2 – 10)	0.928 (<0.001)	Kruskal-Wallis (U)	2.88 (0.237)
Mean SDMT (range)**	46.8 $(9.5)_{ab}$	42.1 $(10.8)_b$	51.7 $(10.6)_a$	0.985 (0.204)	ANOVA (F 2, 119)	7.79 (0.001)
Median PASAT (range)**	48 $(20 – 60)_a$	35 $(16 – 56)_b$	49 $(29 – 60)_a$	0.930 (<0.001)	Kruskal-Wallis (U)	17.4 (<0.001)
Mean WLG (range)	32.0 (10.4)	29.3 (9.8)	31.7 (7.8)	0.989 (0.464)	ANOVA (F 2, 122)	0.71 (0.496)
Mean Stroop interference score*	2.87 $(9.6)_{ab}$	-1.41 $(9.9)_a$	5.31 $(9.2)_b$	0.982 (0.223)	ANOVA (F 2, 92)	2.97 (0.057)

*p ≤0.10; **p ≤0.05
Subscript a and b indicate groups that are significantly different in pairwise comparisons

Figure 4. Rao BRB-N and Stroop interference scores according to diagnosis

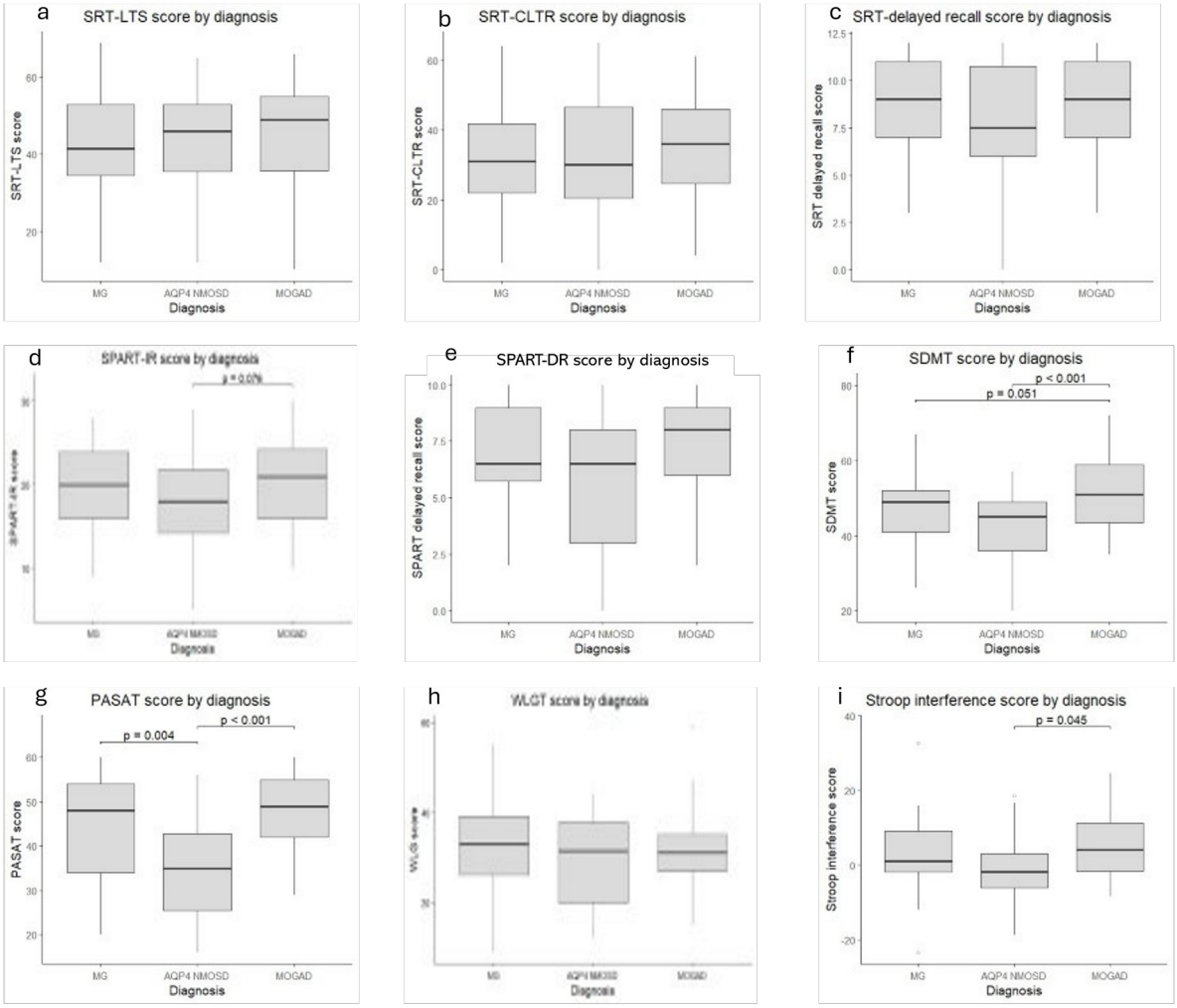

a.ii) Univariable regression of Rao BRB-N and Stroop test scores for whole cohort

For model assessment and transforms, see appendix 10. A square root reflect transform was applied to SRT-LTS, SRT-DR, SPART-DR and PASAT scores prior to regression.

Significant predictors of each test in univariable regression are presented in table 15 (supp table 44 - 52).

Table 15. Results of univariable regressions

Test	Variables significant at α ≤ 0.10	Variables not significant at α ≤ 0.10
Transformed SRT-LTS	Sex at birth, education	Diagnosis, onset age group, age at testing, disease duration, HADS-A score, HADS-D score, total MFIS score, MFIS cognitive subscore, BPI score
SRT-CLTR	Sex at birth, education	Diagnosis, onset age group, age at testing, disease duration, HADS-A score, HADS-D score, total MFIS score, MFIS cognitive subscore, BPI score
Transformed SRT-DR	Sex at birth, education	Diagnosis, onset age group, age at testing, disease duration, HADS-A score, HADS-D score, total MFIS score, MFIS cognitive subscore, BPI score
SPART-IR	**Diagnosis**, HADS-D score, BPI score	Age at testing, onset age group, disease duration, sex at birth, education, HADS-A score, total MFIS score, MFIS cognitive subscore
Transformed SPART-DR	Nil	Diagnosis, onset age group, age at testing, disease duration, sex at birth, education, HADS-A score, HADS-D score, total MFIS score, MFIS cognitive subscore, BPI score
SDMT	**Diagnosis**, sex at birth, education, HADS-D score, total MFIS score, MFIS cognitive subscore, BPI score	Onset age group, age at testing, disease duration, HADS-A score
Transformed PASAT	**Diagnosis,** HADS-D score, total MFIS score, MFIS cognitive subscore, BPI score	Onset age group, age at testing, disease duration, sex at birth, HADS-A score
WLGT	Disease duration, education, HADS-D score, total MFIS score, MFIS cognitive subscore, BPI score	Diagnosis, onset age group, age at testing, sex at birth, HADS-A score
Stroop IS	Age at testing, onset age group, HADS-D score, total MFIS score, MFIS cognitive subscore	Diagnosis, disease duration, sex at birth, education, HADS-A score, BPI score

Diagnosis of AQP4+ NMOSD predicted significantly lower SPART-IR (β = -2.287, p = 0.091) and SDMT score (β = -4.719, p = 0.059) and higher transformed PASAT score (i.e., lower raw PASAT score; β = 1.242, p = 0.001) compared with MG. Diagnosis of MOGAD predicted significantly higher SDMT score compared with MG (β = 4.927, p = 0.020) (supp table 47, 49 & 50).

The effect of a diagnosis of AQP4+ NMOSD on PASAT score survived adjustment for multiple comparisons (supp table 50). Effects of

diagnoses on SPART-IR and SDMT scores did not survive adjustment for multiple comparisons (supp table 47 & 49).

a.iii) Multivariable regression of Rao BRB-N and Stroop test scores for whole cohort

Test scores were regressed against multivariable models that included significant predictors in univariable regressions and *a priori* predictors (onset age group and diagnosis). For test scores that were predicted by diagnosis in univariable regression, multivariable regression was used to determine whether the effect was robust to relevant covariates. For test scores not significantly predicted by diagnosis, an effect may be revealed after adjusting for covariates that behave as negative confounders.

In multivariable regressions, diagnosis of AQP4+ NMOSD predicted significantly lower scores on the SDMT ($\beta = -6.564$, $p = 0.018$) and PASAT ($\beta = 0.972$, $p = 0.034$) compared with MG (table 16 - 19). The effect persisted after optimisation. The effect of diagnosis on SPART-IR scores was no longer statistically significant ($\beta_{AQP4+\ NMOSD} = -2.614$, $p = 0.127$) and was not reinstated by optimisation of the model. Diagnosis of MOGAD did not predict SDMT scores after adjusting for relevant variables (table 16 & 17).

Table 16a & b. Multivariable regression of SDMT score, full model

a. Values of regression coefficients for model 1

		β (SE)	T statistic	p	p_{adj}
Diagnosis					
	AQP4+ NMOSD*	-6.564 (2.721)	-2.412	0.018	0.306
	MOGAD	2.600 (2.039)	1.275	0.206	0.961
Onset age group ≥30		0.735 (1.935)	0.380	0.705	N/A
Sex at birth*		-8.063 (2.150)	-3.750	<0.001	N/A
Education		0.400 (0.399)	1.002	0.320	N/A
HADS-D score		-0.111 (0.380)	-0.293	0.771	N/A
Total MFIS score		-0.111 (0.076)	-1.455	0.150	N/A
BPI score		-0.027 (0.052)	-0.514	0.608	N/A

b. Assessment of full model

Adj R^2	RSE (DoF)	F statistic (DoF)	P (F statistic)	AIC (eDoF)
0.284	8.49 (80)	5.363 (8, 80)	<0.001	389.25 (9)

Reference variable for diagnosis MG. *p ≤0.05

Table 17a & b. Multivariable regression of SDMT score, optimal model

a. Values of regression coefficients for optimal model

		β (SE)	T statistic	p
Diagnosis				
	AQP4+ NMOSD*	-6.613 (2.582)	-2.562	0.012
	MOGAD	2.655 (1.994)	1.332	0.187
Sex at birth*		-8.121 (2.075)	-3.913	<0.001
Total MFIS score*		-0.169 (0.045)	-3.739	<0.001

b. Assessment of optimal model

Adj R^2	RSE (DoF)	F statistic (DoF)	P (F statistic)	AIC (eDoF)
0.302	8.38 (84)	10.520 (4, 84)	<0.001	383.32 (5)

Reference variable for diagnosis MG. *p ≤0.05

Table 18a & b. Multivariable regression of PASAT score,full model

a. Values of regression coefficients for model 1

		β (SE)	T statistic	p	p_{adj}
Diagnosis					
	AQP4+ NMOSD*	0.972 (0.451)	2.155	0.034	0.315
	MOGAD	-0.056 (0.345)	-0.162	0.872	0.961
Onset age group≥30		-0.047 (0.322)	-0.147	0.883	N/A
HADS-D score		-0.036 (0.064)	-0.567	0.572	N/A
Total MFIS score		0.024 (0.013)	1.836	0.070	N/A
BPI score		0.005 (0.008)	0.538	0.592	N/A

b. Assessment of full model

Adj R^2	RSE (DoF)	F statistic (DoF)	P (F statistic)	AIC (eDoF)
0.159	1.40 (77)	3.623 (6, 77)	0.003	63.68 (7)

Reference variable for diagnosis MG. *p ≤0.05

Table 19a & b. Multivariable regression of PASAT score, optimal model

a. Values of regression coefficients for optimal model

		β (SE)	T statistic	p
Diagnosis				
	AQP4+ NMOSD*	1.019 (0.428)	2.377	0.020
	MOGAD	-0.050 (0.338)	-0.149	0.882
Total MFIS score*		0.023 (0.008)	2.987	0.004

b. Assessment of optimal model

Adj R^2	RSE (DoF)	F statistic (DoF)	P (F statistic)	AIC (eDoF)
0.816	1.38 (80)	7.312 (3, 80)	<0.001	58.21 (4)

Reference variable for diagnosis MG. *p ≤0.05

There was no effect of diagnosis on any other test (supp table 53 - 66).

a.iv) Multiple imputation with chained equations: study data (whole cohort)

For explanations of, and data from, the MICE feasibility study, see appendix 11.

Multivariable regression models for SPART-IR, SDMT, PASAT, WLGT and Stroop interference scores included variables with missing data and were re-run with imputed data.

Most models were not altered substantially beyond expected increases in R^2 and the F statistic (appendix 11 table a11.ii – a11.vii). The most notable change was reinstatement of MOGAD as a significant predictor of SDMT score ($\beta = 5.705$, $p = 0.010$), whereas the effect of AQP4+ NMOSD only approached statistical significance ($\beta = -4.412$, $p = 0.074$). AQP4+ NMOSD remained a predictor of poorer PASAT performance after imputation ($\beta = 1.007$, $p = 0.009$).

a.v) Regression of Rao BRB-N and Stroop interference scores (AQP4+ NMOSD and MOGAD)

Significant differences between AQP4+ NMOSD and MOGAD groups in pairwise comparisons prompted analysis restricted to these cohorts. This also permitted exploration of the effects of SIL status and EDSS score.

Univariable regression confirmed AQP4+ NMOSD predicted significantly lower scores on the SPART-IR (β = -2.934, p = 0.033), SDMT (β = -9.646, p <0.001) and Stroop test (β = -6.721, p = 0.032) and higher transformed scores (lower raw scores) on the SPART-DR (β = 1.417, p = 0.032) and PASAT (β = 1.567, p <0.018) compared with a diagnosis of MOGAD (table 20a; supp table 67 - 75). All survived adjustment for multiple comparisons at the p ≤0.10 level.

Multivariable regressions confirmed AQP4+ NMOSD predicted significantly lower SPART-IR (β = -3.336, p = 0.017) and SDMT (β = -8.901, p = 0.007) scores and higher transformed (lower raw) SPART-DR (β = 0.470, p = 0.005) and PASAT scores (β = 1.179, p = 0.012) compared with MOGAD after accounting for relevant variables (table 20b, supp table 76 - 84). The significant effects of diagnosis survived adjustment for multiple comparisons.

Table 20a & b. Tests in which diagnosis predicted significantly different scores in AQP4+ NMOSD and MOGAD groups

a. Univariable regressions (unadjusted p≤ 0.10)

Test outcome	$\beta_{AQP4+\ NMOSD}$ (SE)	T statistic	P	R^2
SPART-IR	-2.954 (1.358)	-2.174	0.033	0.102
Transformed SPART-DR	0.319 (0.160)	2.001	0.049	0.054
SDMT	-9.646 (2.609)	-3.698	<0.001	0.162
Transformed PASAT	1.567 (0.313)	5.012	<0.001	0.273
Stroop interference	-6.721 (2.747)	-2.446	0.018	0.102

b. Multivariable regressions (unadjusted p≤ 0.05)

Test outcome	$\beta_{AQP4+\ NMOSD}$	T statistic	P
SPART-IR	-3.484 (1.368)	-2.547	0.013
Transformed SPART-DR	0.505 (0.164)	3.076	0.004
SDMT	-9.087 (3.176)	-2.861	0.006
Transformed PASAT	1.197 (0.449)	2.666	0.011

a.vi) Multiple imputation with chained equations: study data (AQP4+ NMOSD and MOGAD)

Data from the MICE feasibility study are available in appendix 11.

Multivariable regression models for SDMT, PASAT, WLGT and Stroop interference scores included variables with missing data and were re-run with imputed data. The relationships between diagnosis and test scores were similar to those in the absence of imputation (appendix 11, table a11.ix – a11.xii). Specifically, AQP4+ NMOSD was a significant predictor of lower PASAT score but not WLGT and Stroop interference scores. The effect on SDMT score approached statistical significance.

b) Effect of age at onset on Rao BRB-N and Stroop test scores (AQP4+ NMOSD and MOGAD)

Median age at testing was significantly older ($p < 0.001$) and disease duration was shorter ($p < 0.001$) in patients with onset ≥30 years. Median HADS-A score was significantly lower in the group with onset ≥30 years ($p = 0.007$). The proportion of participants with SILs was significantly smaller in the group with onset ≥30 years ($p = 0.002$) (table 21; supp fig 39 & 40).

Table 21: Comparison of demographic and clinical variables according toonset age group (<30 years vs ≥30 years) (AQP4+ NMOSD and MOGAD)

	Age at onset < 30 years (N = 26)	Age at onset ≥ 30 years (N = 49)	Test statistic (p)
% AQP4+ NMOSD	38.5	34.7	χ^2 = 0.105 (0.746)
Median age at testing (range)*	32 (20 – 45)	49 (31 – 65)	U = -234.5 (<0.001)
Median disease duration (months) (range)*	133.5 (6 – 418)	45 (7 – 371)	U = 619.5 (<0.001)
N sex at birth female (%)	73.1	73.5	χ^2 = 0.001 (0.971)
Median education duration (years) (range)	14 (10 – 19)	14.75 (10 – 21)	U = 272 (0.977)
Median HADS-A score (range)*	11 (2 – 17)	6 (0 – 16)	U = 374.5 (0.007)
Median HADS-D score (range)	5 (0 – 15)	5 (0 – 14)	U = 232.5 (0.604)
Median total MFIS score (range)	42 (2 – 73)	39 (0 – 73)	U = 248.0 (0.445)
Median MFIS cognitive subscore (range)	15 (2 – 34)	13.5 (0 – 40)	U = 294.0 (0.188)
Median BPI score (range)	26(0 – 92)	18.5 (0 – 92)	U = 229.5 (0.497)
Median EDSS score (range)	1 (0 – 6)	2.75 (0 – 7.5)	U = 318.5 (0.722)
N SILs present (%)*	53.8	19.1	χ^2 = 9.34 (0.002)

*p ≤ 0.10

Age at onset was not a significant predictor of any test score in univariable regressions, whether considered as a binary or continuous variable (table 22; supp table 85) and was not a predictor of any score in multivariable regressions designed to assess effect of diagnosis

(section 3.2.a.v).

Table 22. Univariable regression of test scores against onset age group (AQP4+ NMOSD and MOGAD)

Test	B_{age} (SE)	T statistic	P	F	R^2
Transformed SRT-LTS	0.027 (0.309)	0.089	0.930	0.008 (1, 73)	0.000
SRT-CLTR	-1.897 (3.668)	-0.517	0.607	0.268 (1, 73)	0.004
Transformed SRT-DR	0.134 (0.171)	0.788	0.433	0.621 (1, 72)	0.009
SPART-IR	0.375 (1.415)	0.265	0.792	0.070 (1, 72)	0.001
Transformed SPART-DR	0.043 (0.166)	0.257	0.798	0.066 (1, 70)	0.001
SDMT	0.924 (2.873)	0.322	0.749	0.104 (1, 71)	0.001
Transformed PASAT	-0.119 (0.363)	-0.328	0.744	0.107 (1, 67)	0.002
WLGT	2.589 (2.132)	1.214	0.229	1.475 (1, 71)	0.020
Stroop interference	-1.435 (2.942)	-0.488	0.628	0.238 (1, 53)	0.004

After adjusting for relevant covariates and their interactions, there was no main effect of onset age group on any test (supp table 86 – 130). The only significant interactions with onset age group were HADS-A score (β = -1.699, p = 0.029) and presence of SILs (β = 16.114, p = 0.011) on Stroop test scores. There was no main effect of onset age group when the interaction terms were omitted to reduce variance inflation.

Although most interactions were not statistically significant, examination of the interaction plots revealed differential effects of some variables on selected tests according to onset age group (fig 5 - 13):

i) SRT-LTS, SRT-CLTR, SRT-DR, SDMT and PASAT scores improved with increasing age at testing in those with onset aged <30 years and declined with age at testing in those with onset aged ≥30 years. The interaction approached statistical significance for SDMT score (β = -0.687, p = 0.054).

ii) Scores on the SRT-LTS, SRT-CLTR, SRT-DR, SPART-IR and SPART-DR declined with increasing disease duration in those with onset aged <30 years and improved in those with onset at ≥30 years. The interaction approached statistical significance for transformed SRT-DR score (β = -0.004, p = 0.054).

Figure 5a - e: Interaction plots of onset age group and other variable on transformed SRT-LTS score

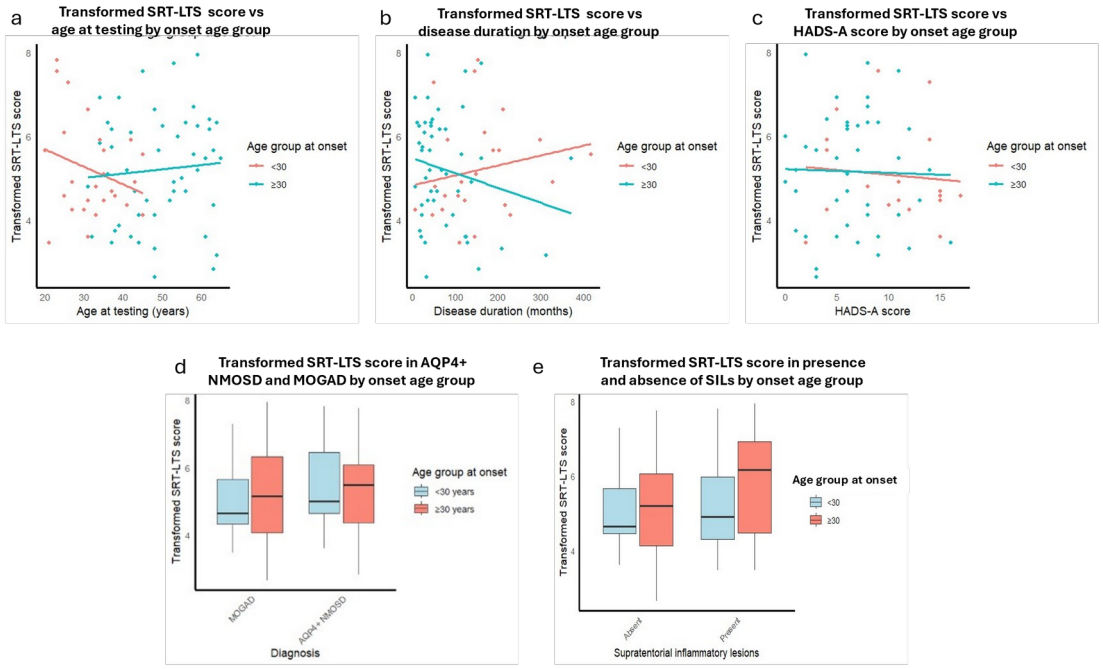

Figure 6a - e: Interaction plots of onset age group and other variable on SRT-CLTR score

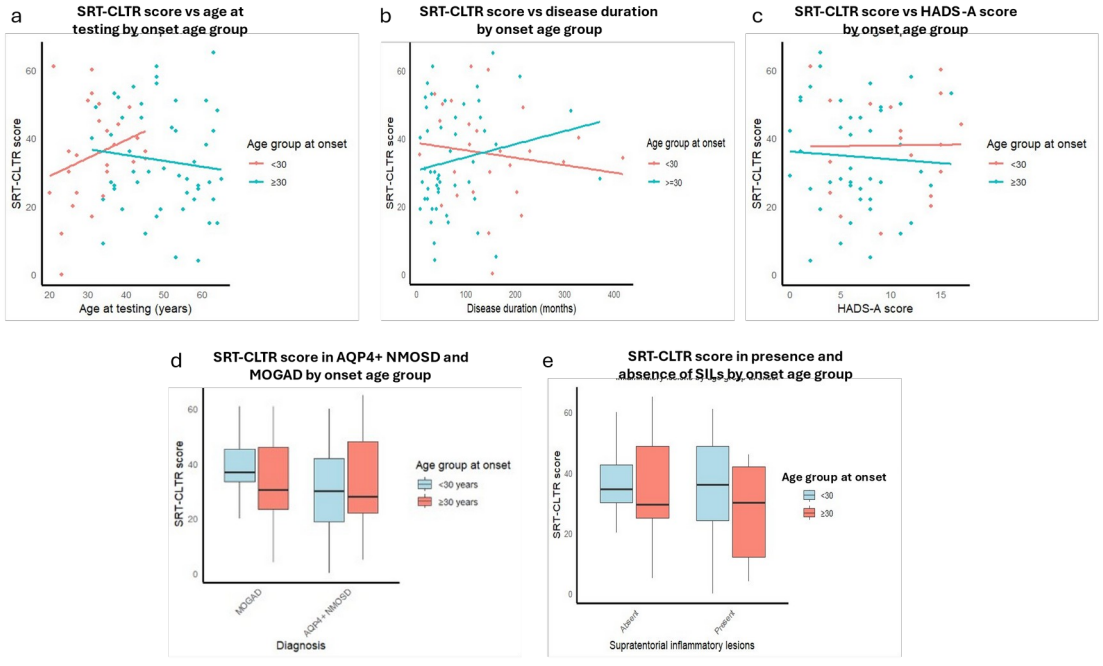

Figure 7a - e: Interaction plots of onset age group and other variable on transformed SRT-DR score

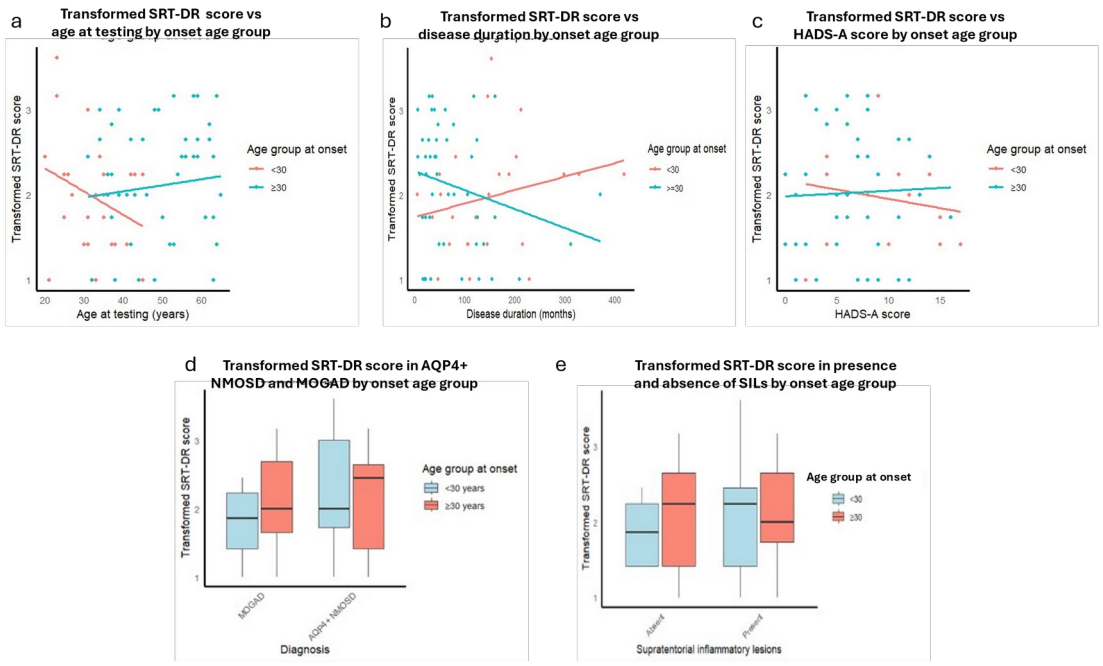

Figure 8a - e: Interaction plots of onset age group and other variable on SPART-IR score

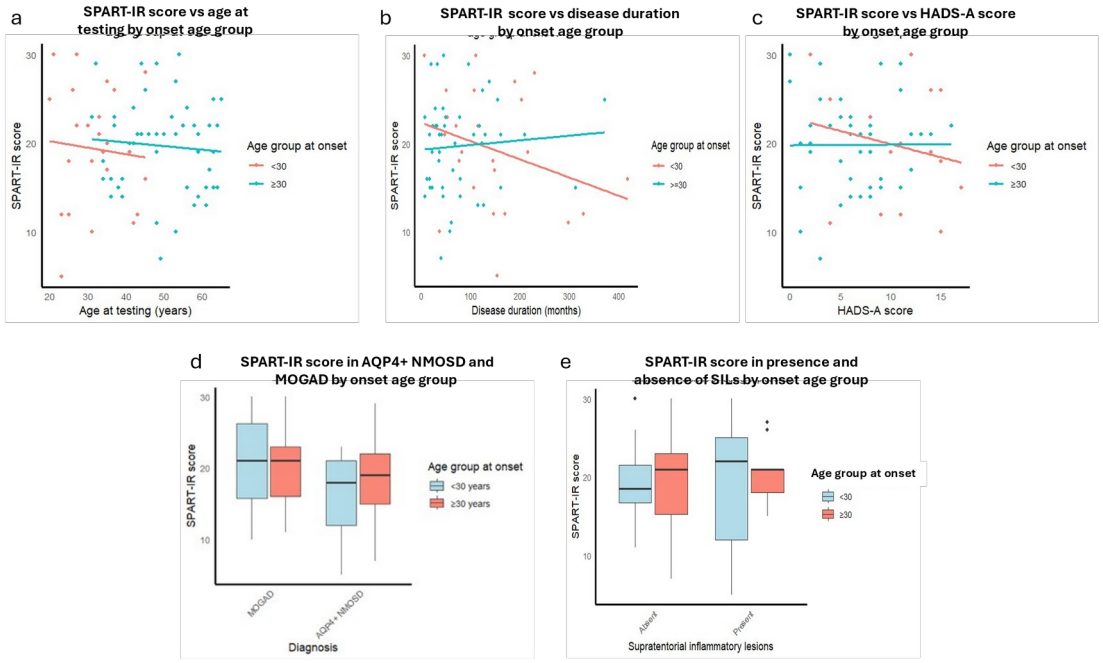

Figure 9a - e: Interaction plots of onset age group and other variable on transformed SPART-DR score

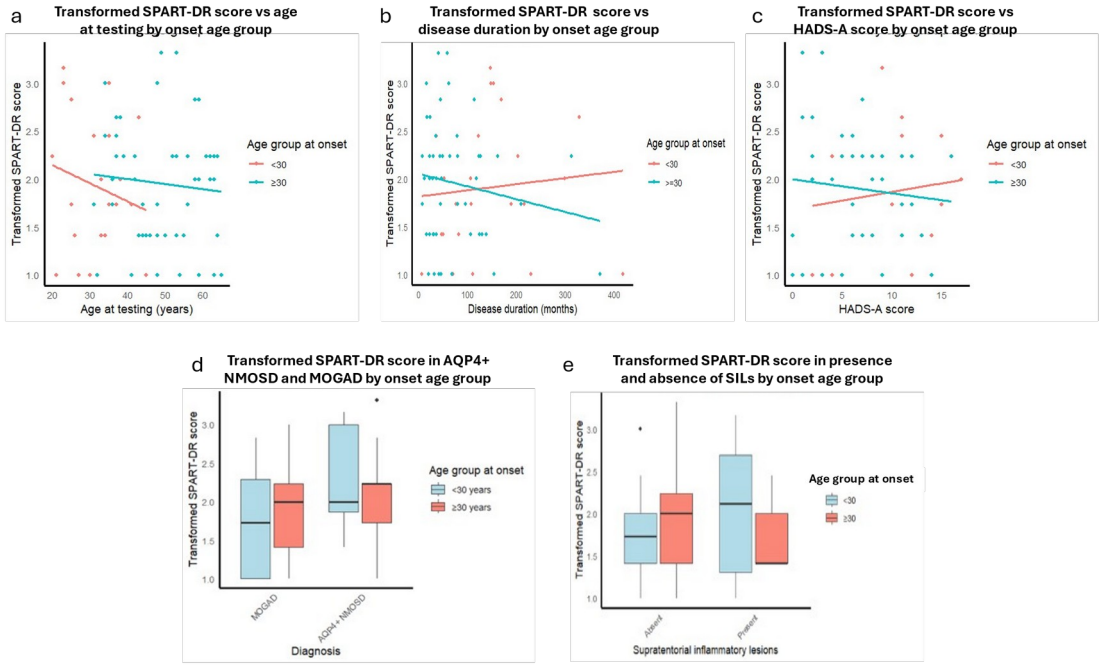

Figure 10a - e: Interaction plots of onset age group and other variable on SDMT score

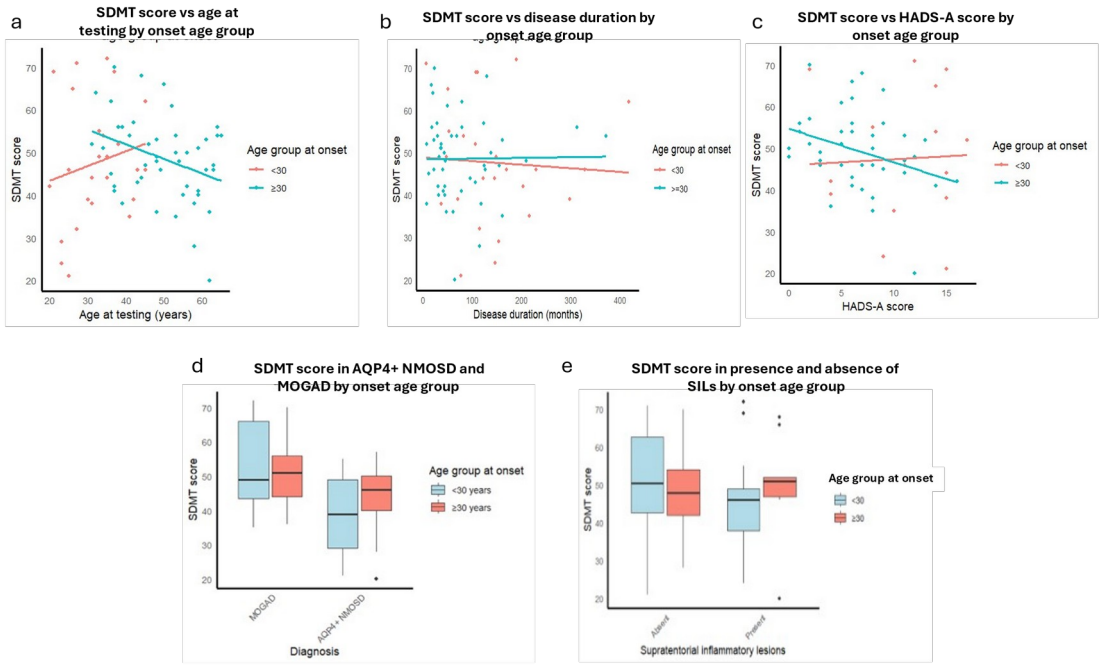

Figure 11a - e: Interaction plots of onset age group and other variable on transformed PASAT score

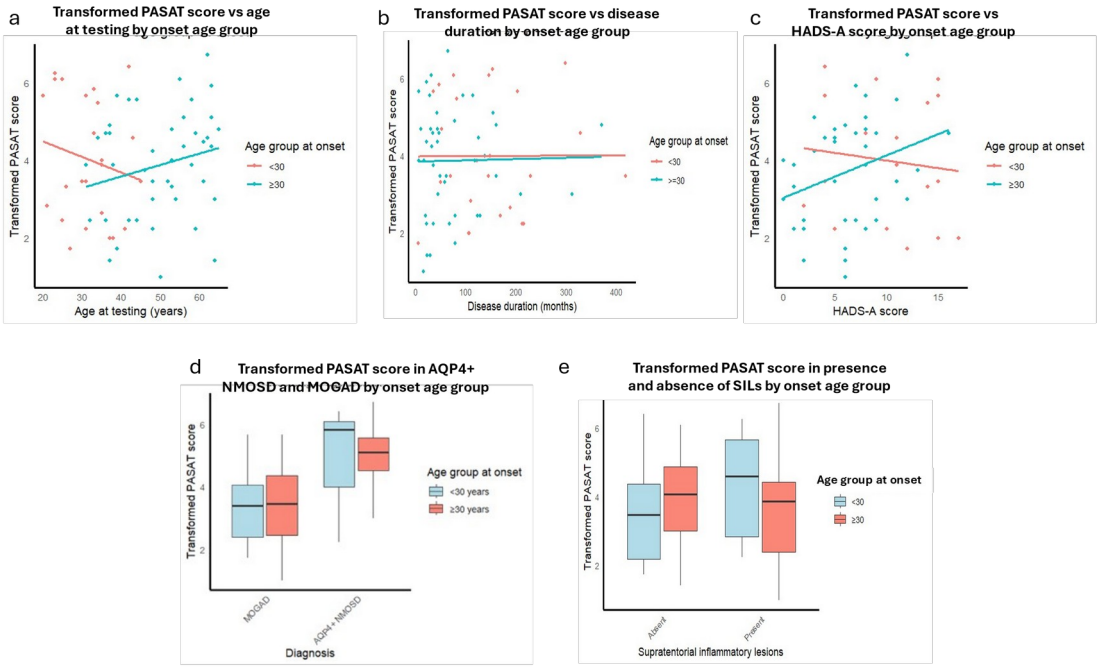

Figure 12a - e: Interaction plots of onset age group and other variable on WLGT score

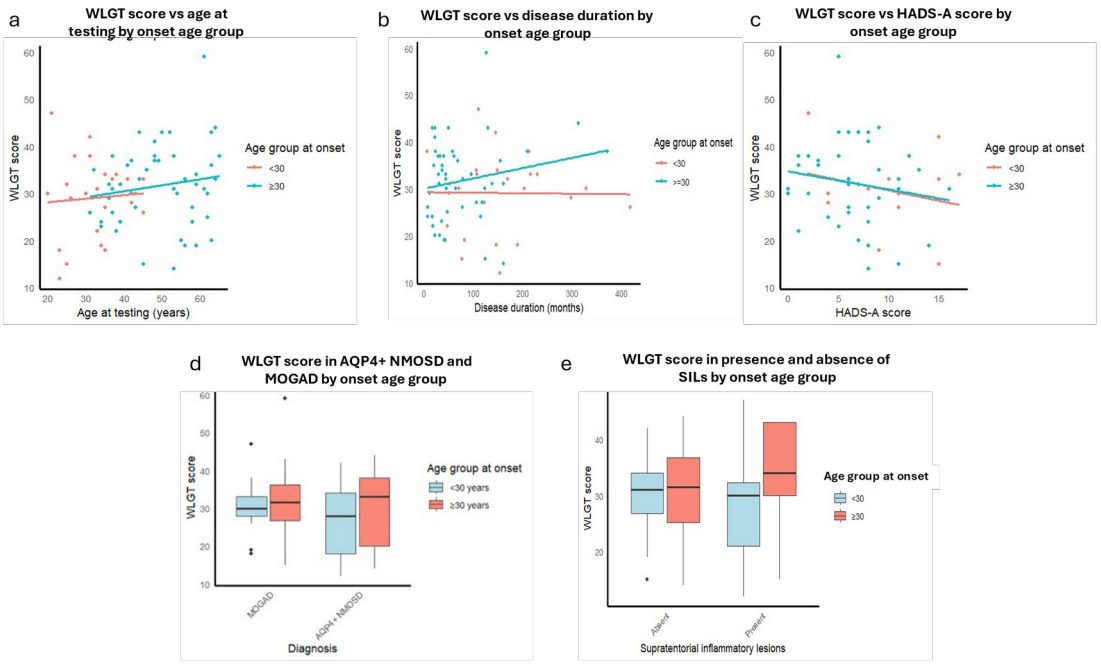

Figure 13a - e: Interaction plots of onset age group and other variable on Stroop interference score

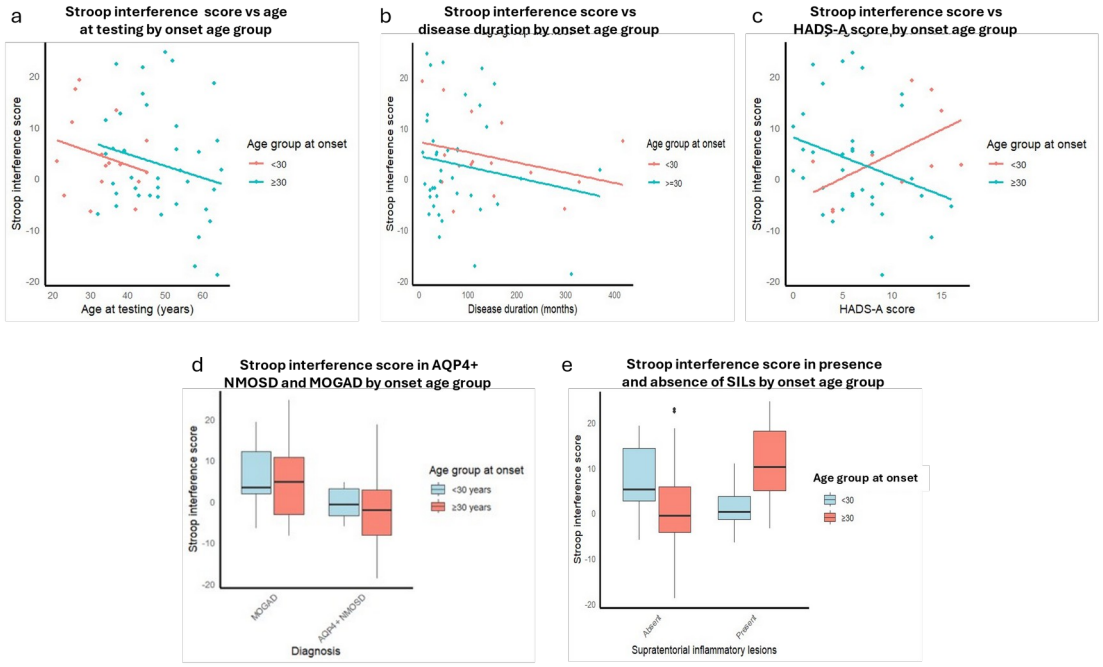

SRT subtest scores increased with increasing age at testing in the group with onset aged <30 years and decreased with higher age at testing in the group with onset aged ≥30 years. Conversely, scores decreased with increasing disease duration in the group with onset aged <30 years and increased with disease duration in the group with onset aged ≥30 years. Disease duration is the difference between age at onset and age at testing and therefore correlates positively with age at testing and negatively with age at onset (supp fig 41a & b). In addition, age at onset correlated closely with age at testing (r = 0.86, supp fig 42).

c) Effect of SILs on Rao BRB-N and Stroop interference scores (AQP4+ NMOSD and MOGAD)

Patients with SILs were significantly younger at testing (p = 0.018), with a higher proportion of participants with onset aged <30 years (p = 0.004) compared with those without SILs (table 23). There were no other significant differences in demographic and clinical features.

Univariable regression confirmed no main effect of SILs on any tests (table 24). Presence of SILs was not a predictor of any test score in multivariable regressions looking for a main effect of diagnosis (section 3.2.a.v).

Table 23: Comparison of demographic and clinical variables in presence and absence of SILs

	Lesions absent (N = 50)	Lesions present (N = 23)	Test statistic (p)
% AQP4+ NMOSD	38.0	34.8	χ^2 = 0.070 (0.791)
N onset age group ≥30 years (%)*	38 (76.0)	9 (39.1)	Fisher p = 0.004
Median age at testing (range)*	42.5 (25 – 65)	34 (20 – 63)	U = -500.5 (0.018)
Median disease duration (months) (range)	63 (6 – 418)	114 (16 – 328)	U = -833.5 (0.114)
N sex at birth female (%)	78.0	65.2	χ^2 = 1.337 (0.248)
Median education duration (years) (range)	14 (10 – 21)	14.5 (10 – 19)	U = -684 (0.985)
Median HADS-A score (range)	8 (0 – 17)	7 (0 – 15)	U = -516 (0.621)
Median HADS-D score (range)	5 (0 – 14)	5 (0 – 15)	U = -488 (0.954)
Median total MFIS score (range)	39 (0 – 73)	42 (2 – 70)	U = -580 (0.575)
Median MFIS cognitive subscore (range)	14 (0 – 40)	17.5 (2 – 35)	U = -581 (0.370)
Median BPI score (range)	20 (0 – 92)	27 (0 – 81)	U = -520.5 (0.829)
Median EDSS score (range)	1 (0 – 7.5)	2 (0 – 6.5)	U = -702 (0.623)

*p ≤ 0.10

Table 24. Univariable regression of test scores against SIL status

Test	$B_{lesions}$ (SE)	T statistic	p	F	R^2
Transformed SRT-LTS	0.431 (0.315)	1.369	0.175	1.873	0.003
SRT-CLTR	-4.603 (3.762)	-1.224	0.225	1.497	0.021
Transformed SRT-DR	0.079 (0.178)	0.441	0.660	0.195	0.003
SPART-IR	-0.133 (1.456)	-0.091	0.928	0.008	0.000
Transformed SPART-DR	-0.001 (0.170)	-0.039	0.969	0.002	0.000
SDMT	-1.900 (3.000)	-0.633	0.529	0.401	0.006
Transformed PASAT	0.183 (0.387)	0.472	0.638	0.223	0.003
WLGT	0.001 (2.091)	0.000	~1	0.000	0.000
Stroop interference	3.207 (2.988)	1.073	0.288	1.152	0.022

There was no effect of SIL status in multivariable regression of test scores against onset age group, SIL status and their interaction (section 3.2.b).

Regressions of scores against SIL status, diagnosis and an SIL x diagnosis interaction revealed no significant effects of SIL status and no significant interaction term, although diagnosis remained a significant predictor of SDMT (β = -8.042, p = 0.012), transformed PASAT (β = 1.569, p <0.001) and Stroop interference scores (β = -6.650, p = 0.041), and a borderline predictor of SPART-IR score (β = -2.745, p = 0.092) (supp table 131 - 148).

After adjusting for diagnosis, onset age group and age at testing, there was no significant main effect of SIL status on any Rao BRB-N subtest score (supp table 131 – 148; fig 14 – 22). There was a significant interaction between SIL status and age at testing on Stroop interference score (β = 0.623, p = 0.018) (fig 22b; supp table 148).

Figure 14a & b. Effects of interactions between SIL status and a) diagnosis and b) age at testing on transformed SRT-LTS score

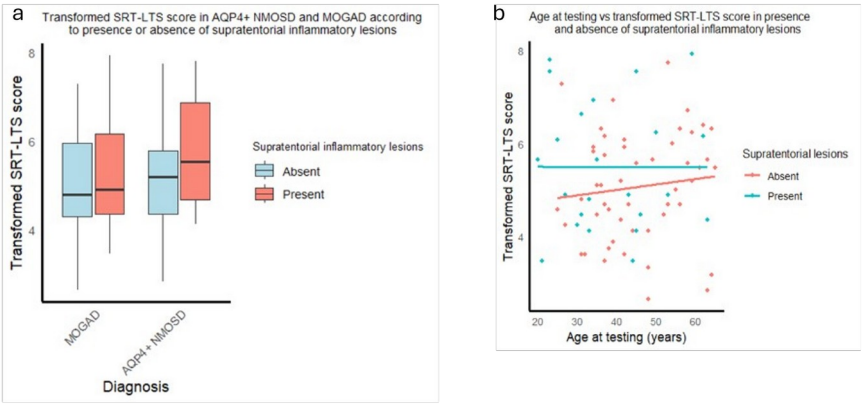

Figure 15a & b. Effects of interactions between SIL status and a) diagnosis and b) age at testing on SRT-CLTR score

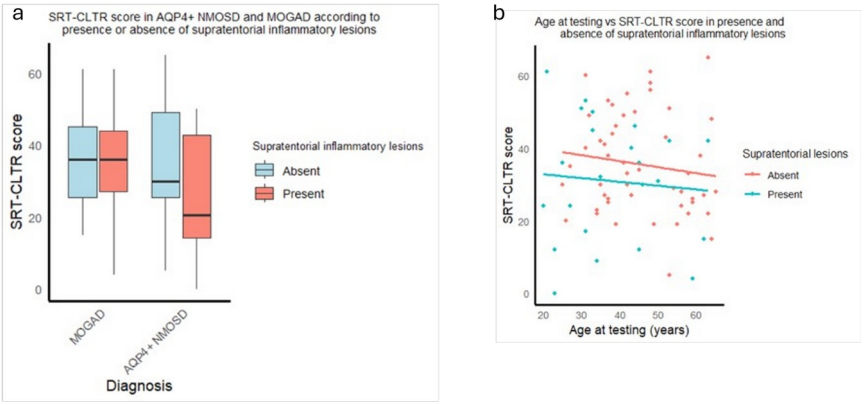

Figure 16 a & b. Effects of interactions between SIL status and a) diagnosis and b) age at testing on transformed SRT-DR score

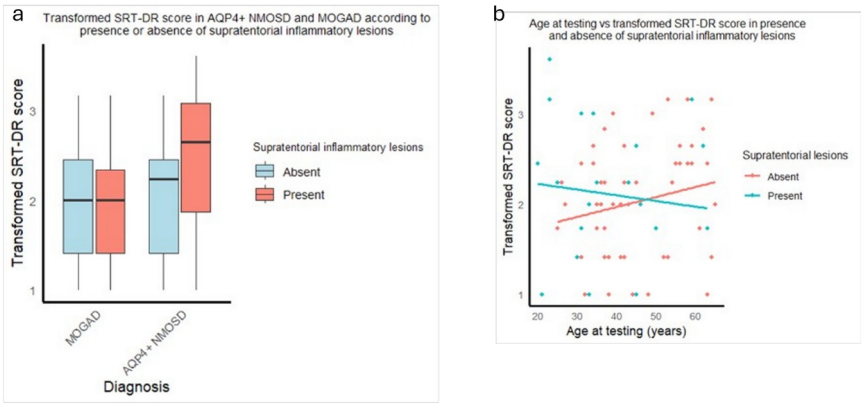

Figure 17a & b. Effects of interactions between SIL status and a) diagnosis and b) age at testing on SPART-IR score

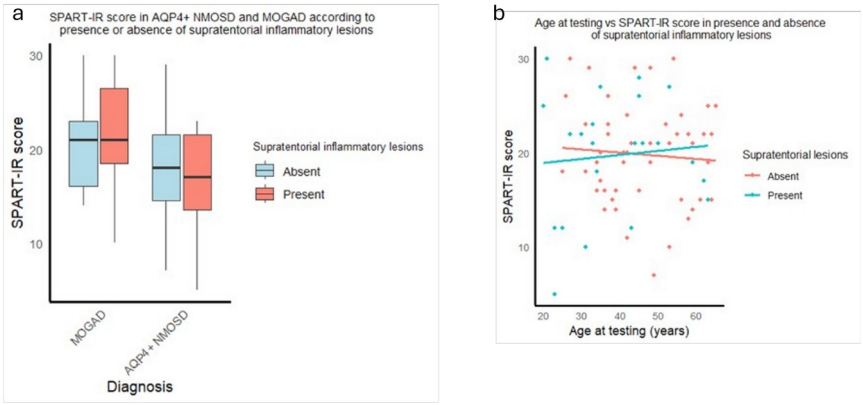

Figure 18a & b. Effects of interactions between SIL status and a) diagnosis and b) age at testing on transformed SPART-DR score

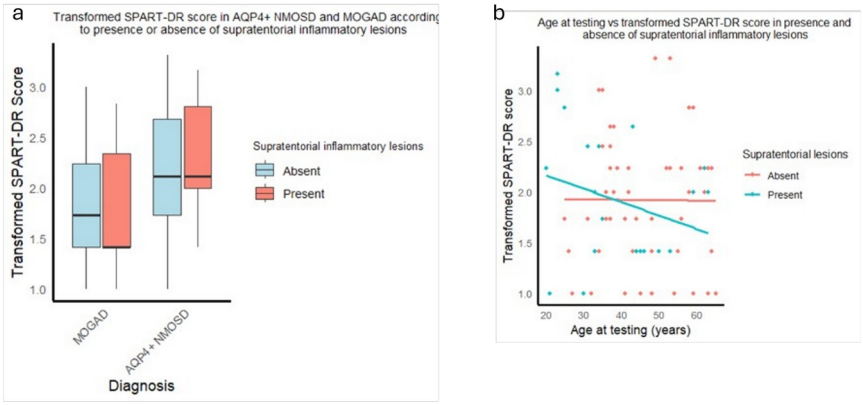

Figure 19a & b. Effects of interactions between SIL status and a) diagnosis and b) age at testing on SDMT score

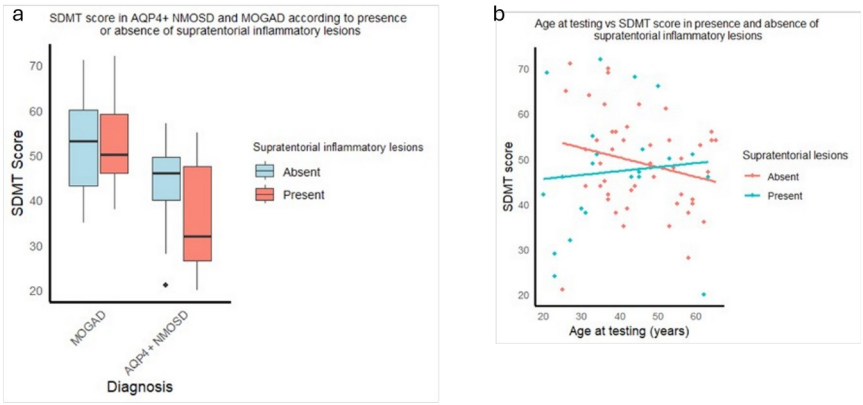

Figure 20a & b. Effects of interactions between SIL status and a) diagnosis and b) age at testing on transformed PASAT score

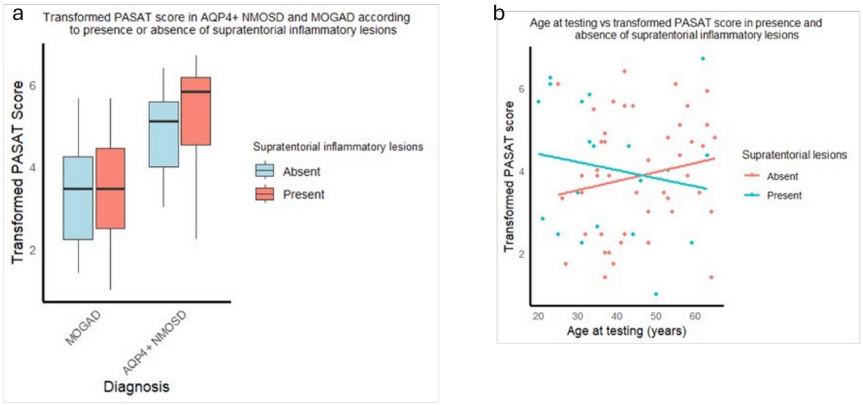

Figure 21a & b. Effects of interactions between SIL status and a) diagnosis and b) age at testing on WLGT score

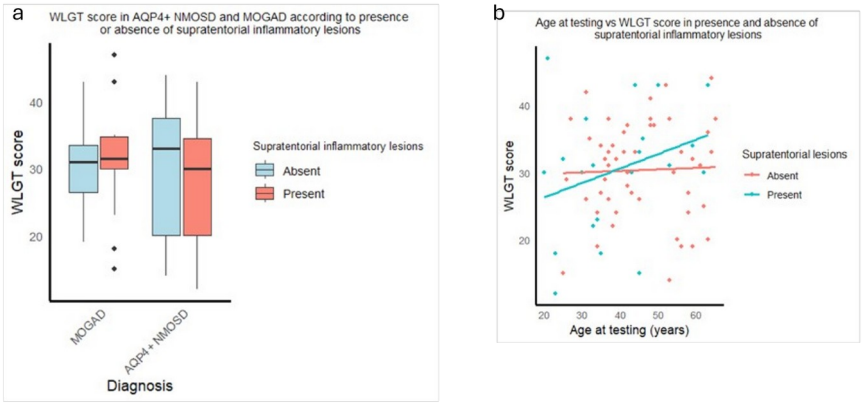

Figure 22a & b. Effects of interactions between SIL status and a) diagnosis and b) age at testing on Stroop interference score

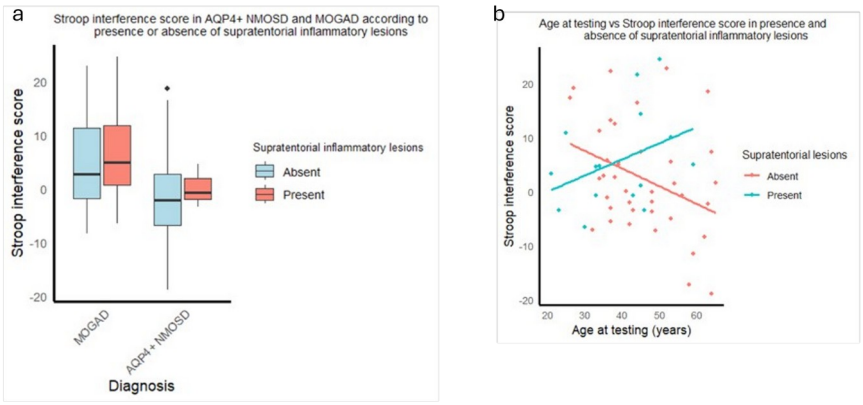

In addition to the statistically significant interaction between age at testing and SIL status on Stroop score, interaction plots suggested non-statistically significant interactions between age at testing and SIL status on SRT-DR, SPART-DR, SDMT, PASAT and WLGT scores. In general, patients with SILs performed better as age at testing increased, whereas patients without SILs tended to perform worse with increasing age at testing.

VIF for each model was low, so bivariable regressions without interaction terms were omitted.

3.3) Discussion: Cognition in AQP4+ NMOSD and MOGAD, part 2 (Rao BRB-N)

The data contain several interesting observations:

a) Patients with AQP4+ NMOSD obtained lower scores than patients with MG on most tests of the Rao BRB-N and the Stroop test in pairwise comparisons. Univariable regressions confirmed AQP4+ NMOSD predicted statistically significant lower scores on SPART-IR, SDMT and PASAT scores compared with MG in univariable regressions and the effect persisted for SDMT and PASAT scores after adjusting for relevant covariates, before correction for multiple comparisons.

b) Patients with AQP4+ NMOSD performed significantly worse than patients with MOGAD on several components of the Rao BRB-N in pairwise comparisons and univariable regressions. The effect of diagnosis on SPART-IR, SPART-DR SDMT and PASAT scores survived multivariable regression correction for multiple comparisons.

These results indicate patients with AQP4+ NMOSD perform significantly worse than controls *and* patients with another chronic inflammatory CNS disease on tests of attention and processing speed and visuospatial memory.

c) Although there was no main effect of onset age group, regression plots revealed non-statistically significant interactions between

onset age group and age at testing for SRT-subtests, SDMT and PASAT scores. Apparent interactions may be a consequence of the wide variance in both onset age groups unduly influencing the fitted regression lines, but the consistency of the interaction across multiple tests suggests a potential real effect worth further exploration.

The disparate effects of age at testing on scores depending on onset age group could be due to the existence of an optimal response age, at which point the advantages of structural and functional brain maturity are balanced by the cognitive deterioration caused by an ageing brain. Assuming an optimum age at testing of around 30, all patients with onset ≥30 years were tested during the theoretical age range of declining performance. Declining Rao BRB-N scores with increasing age at testing have been reported in health as well as in MS and NMOSD (88,156,183,184). The majority of patients with onset <30 years were tested before 30 years of age, during the theoretical upward performance trajectory.

If this were the explanation, the interactions between onset age group and disease duration should mimic the interactions between onset age group and age at testing, as age at testing is positively correlated with disease duration. However, the relationship is complicated by the high correlation between age at onset and age at testing.

One unifying explanation for the apparent paradoxical effects of age at testing and disease duration on SRT scores is that the close correlation between the two variables means age at testing could be a proxy of age at onset. This implies patients with onset in early childhood were tested at younger ages and, independent of direct effects of age at testing, were at risk of poorer scores on the SRT, SDMT and PASAT and that scores improved with onset in later childhood to twenties. In the group with onset aged ≥30, increasing age at onset is associated with declining scores on the same tests, independent of the effect of age at testing. As disease duration is negatively correlated with age at onset, the effect of disease duration would thus appear the reverse of the effect of age at testing on these tests.

Although age at testing is partly dependent on age at onset and the two variables are correlated, for many biological processes the effects of age at the start of the process are distinct from the effects of age when the process is assessed. Therefore, attempts should be made to distinguish between effects of age at onset and age at testing, if possible, as this would dictate the populations more likely to benefit from intervention.

~~d)~~ Regression plots showed a significant interaction between SIL status and age at testing for Stroop interference score and non-significant interactions between SIL status and age at testing for SRT-DR, SPART-DR, SDMT, PASAT, and WLGT scores. The

consistency across multiple tests suggests a real effect obscured by high standard errors.

Interpretation of interactions between age at testing and onset age group and between age at testing and SIL status require consideration. First, it should be remembered that no interaction between onset age group and age at testing reached threshold for statistical significance and the only significant interaction between SIL status and age at testing was for Stroop interference score. Examination of the interaction plots confirms test scores displayed large variance within and considerable overlap between groups. Any theories are speculative and based on the premise the interactions are real if consistent across multiple tests.

Second, interpretation is complicated by the interplay between factors. For example, patients with onset <30 years were more likely to have SILs (structural confounding). Close correlations (e.g., between age at onset and age at testing) can lead to confounding. Both can lead to spurious attribution of variance and large standard errors, which reduces power of regression models.

Two further questions emerged from the work above:

1) Are the (non-significant) effects of age at testing within onset age groups independent of the effects of age at onset within

onset age groups, or are apparent interactions with age at testing due to confounding by age at onset?

2) Given the significant effect of a diagnosis of AQP4+ NMOSD compared with MOGAD on several elements of the Rao BRB-N and Stroop test, what are the predictors of test scores among this group alone?

Chapter 4

Cognition in AQP4+ NMOSD and MOGAD, part 3 (Rao BRB-N)

4.1) Methods: Cognition in AQP4+ NMOSD and MOGAD, part 3 (Rao BRB-N)

a) Effects of age at onset

a.i) Are effects of age at testing within onset age groups independent of effects of age at onset within onset age groups

To determine whether the interaction between age at onset as a continuous variable[9] and onset age group could confound the apparent interaction between age at testing and onset age group, test scores were plotted against age at onset as a continuous variable for each onset age group and compared with equivalent plots of scores against age at testing.

The interactions were assessed formally using multivariable regressions in the form:

$$Test\ score \quad onset\ age\ group + age\ at\ onset + onset\ age\ group * age\ at\ onset$$

In the event that interaction plots between age at onset and onset age group resembled those for age at testing and onset age group, effects of age at onset and age at testing were distinguished by centring each

[9] Herein referred to as age at onset, distinct from the binary variable, onset age group

continuous variable and regressing scores against onset age group, age at onset, age at testing and interactions in the form:

$$Test\ score \quad onset\ age\ group + age\ at\ onset + age\ at\ testing + onset\ age\ group * age\ at\ onset + onset\ age\ group * a$$

To verify the effect of age at onset within group was a biological phenomenon and not caused by imposing artificial thresholds, restricted cubic splines were applied to model curvature in the data (appendix 12).

a.ii) Effects of paediatric onset

Test scores were regressed against paediatric onset (age at onset ≤18 years) as a binary variable in univariable regressions. Variables that were significantly different between patients with paediatric and adult onset and *a priori* predictors (diagnosis and SIL status) were incorporated in multivariable regression models with interaction terms.

b) Predictors of test scores in AQP4+ NMOSD

Results of all Rao BRB-N tests and Stroop interference scores were regressed against each of the independent variables for the AQP4+ NMOSD group, as described in section 2.2.c.ii. Multivariable models included the *a priori* predictor, SIL status, and variables significant in univariable regressions at the p ≤0.10 level, as described in section 2.2.c.iv.

4.2) Results: Cognition in AQP4+ NMOSD and MOGAD, part 3 (Rao BRB-N)

a) Effects of age at onset

a.i) Are effects of age at testing within onset age groups independent of effects of age at onset within onset age groups

The effect of age at onset within onset age groups mimicked the effect of age at testing on SRT subtests, SDMT, PASAT and WLGT scores (fig 23). As age at onset increased, scores on all tests but the WLGT demonstrated an improvement in the group with onset <30 years and a deterioration in the group with onset ≥30 years. Unlike the interactions between onset age group and age at testing, interactions between age at onset and onset age group were observed for SPART-IR, SPART-DR and Stroop tests. Whereas interactions between age at testing and onset age group reversed direction for SPART-IR, WLGT and Stroop tests, interactions between age at onset and onset age group showed a consistent pattern on all but the WLGT.

Figure 23. Effect of age at onset on test scores according to onset age group

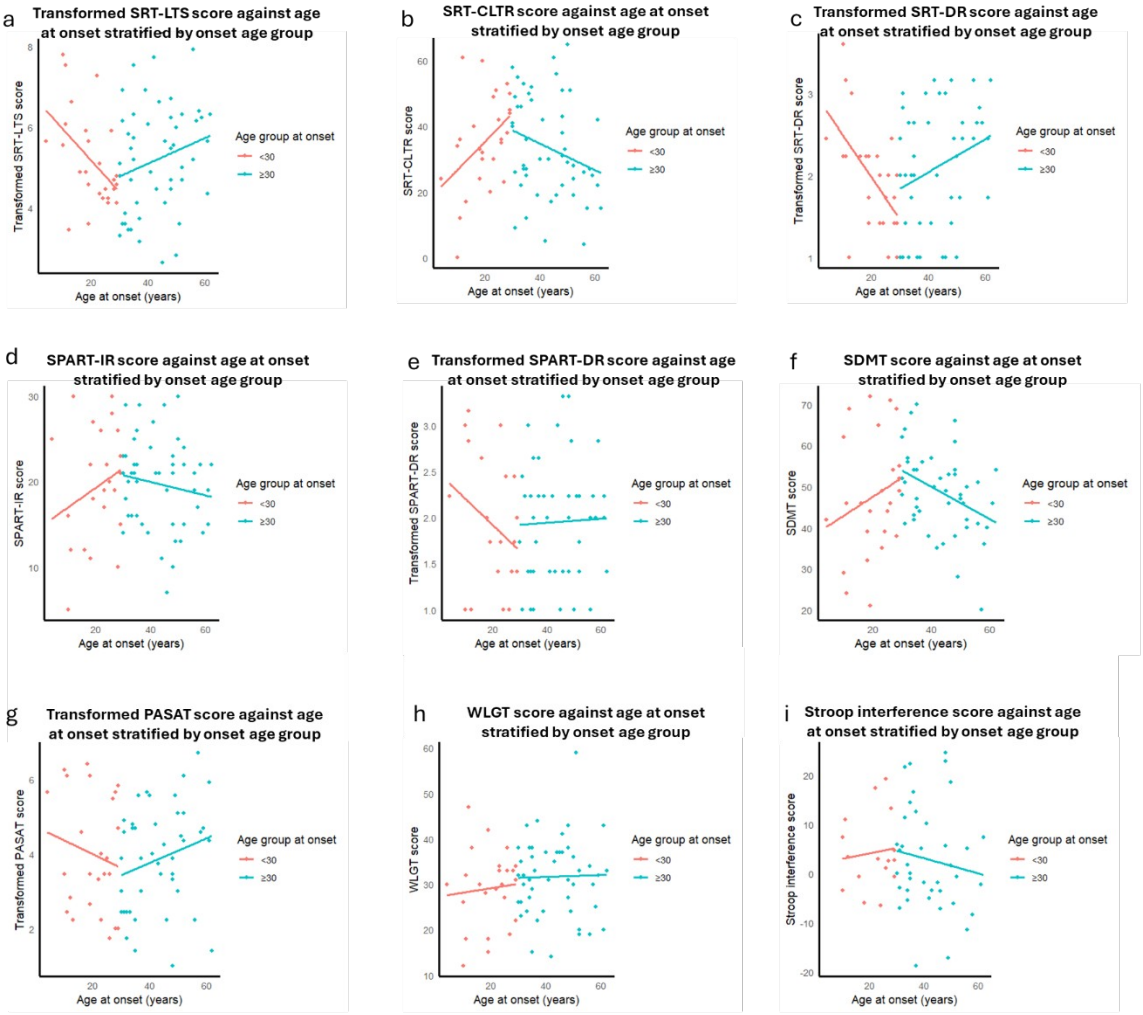

There were no significant statistically significant main effects of age at testing and no significant age at testing x onset age group interactions (section 3.2.b).

Before adjusting for age at testing, multivariable regressions of age at onset x onset age group demonstrated significant main effects of age at onset for transformed SRT-LTS (β = -0.079, p = 0.024), SRT-CLTR (β = 0.863, p = 0.034) and transformed SRT-DR scores (β = -0.051, p = 0.006). Statistically significant interactions between age at onset and

onset age group were found for transformed SRT-LTS (β = 0.109, p = 0.005), SRT-CLTR (β = -1.269, p = 0.007), transformed SRT-DR (β = 0.079, p <0.001) and SDMT scores (β = -0.854, p = 0.019) (table 25, supp table 149 – 157).

After adjusting for effects of age at testing and onset age group x age at testing interactions, significant main effects of age at onset (β = -0.048, p = 0.019) and onset age group β = 0.766, p = 0.026) on transformed SRT-DR score persisted. There were statistically significant interactions between age at onset and onset age group for transformed SRT-LTS (β = 0.138, p = 0.005), SRT-CLTR (β = -1.519, p = 0.009) and transformed SRT-DR scores (β = 0.088, p = 0.021). Main effects of age at onset on transformed SRT-LTS (β = -0.073, p = 0.052) and SRT-CLTR (β = 0.774, p = 0.082) and age at onset x onset age group interactions for SPART-IR scores (β = -0.439, p = 0.057) approached statistical significance (table 26; supp table 158 - 166). High VIF values resulting from inclusion of interaction terms and collinearity between age at onset and age at testing may have negated the significance of age at onset x onset age group interactions on other Rao BRB-N tests.

Table 25. Statistically significant main effects and interactions of age at onset and onset age group on test scores

Test	$\beta_{age\ at\ onset}$ (SE)	T statistic	P ($\beta_{age\ at\ onset}$)	$B_{onset\ age\ group}$ (SE)	T statistic	P ($\beta_{onset\ age\ group}$)	$\beta_{age\ group*age\ at\ onset}$ (SE)	T statistic	P ($\beta_{age\ group*onset}$)	F statistic	R^2 model	P model
Transformed SRT-LTS†*	-0.078 (0.034)	-2.134	0.024	0.957 (0.608)	1.572	0.120	0.109 (0.038)	2.870	0.005	2.821	0.069	0.045
SRT-CLTR†*	0.863 (0.400)	2.156	0.034	-11.736 (-7.230)	-1.623	0.109	-1.269 (0.453)	-2.799	0.007	2.858	0.070	0.043
Transformed SRT-DR†‡*	-0.051 (0.018)	-2.851	0.006	0.744 (0.323)	2.300	0.024	0.071 (0.020)	3.513	<0.001	4.446	0.124	0.006
SDMT*	0.463 (0.315)	1.469	0.146	-2.751 (5.625)	-0.489	0.626	-0.854 (0.357)	-2.395	0.019	1.594	0.062	0.060

Table 26. Statistically significant main effects and interactions of age at onset, onset age group and interactions on test scores after adjusting for age at testing and interactions

Test	$\beta_{age\ at\ onset}$ (SE)	T statistic	P ($\beta_{age\ at\ onset}$)	$B_{onset\ age\ group}$ (SE)	T statistic	P ($\beta_{onset\ age\ group}$)	$\beta_{age\ group*age\ at\ onset}$ (SE)	T statistic	P ($\beta_{age\ group*onset}$)	F statistic	R^2 model	P model
Transformed SRT-LTS*	-0.073 (0.037)	-1.973	0.052	0.990 (0.635)	1.559	0.124	0.138 (0.048)	2.899	0.005	2.107	0.070	0.075
SRT-CLTR*	0.774 (0.439)	1.764	0.082	-12.517 (7.575)	-1.652	0.103	-1.519 (0.568)	-2.767	0.009	2.030	0.065	0.085
Transformed SRT-DR†‡*	-0.048 (0.019)	-2.453	0.017	0.766 (0.336)	2.279	0.026	0.088 (0.025)	4.359	<0.001	3.221	0.132	0.011

†Significant main effect of age at onset ‡ Significant main effect of onset age group * Significant interaction

Adjusting for age at onset and age at onset x onset age group interactions did not reveal significant main effects of age at testing, nor interactions between age at testing and onset age group. The contrasting effects can be seen in plots showing clear age at onset x onset age group interactions after adjusting for age at testing (supp fig 43) but attenuation or elimination of age at onset x age at testing interactions after adjusting for age at onset (supp fig 44).

Statistical significance of interactions between age at onset and onset age group, homogeneity of the interactions of onset age group with age at onset across tests (not observed in interactions between onset age group and age at testing) and persistence after accounting for age at testing indicates a true, independent interaction between age at onset and onset age group.

Modelling non-linear effects with splines resulted in a statistically significant effect of age at onset for SRT-DR score ($p = 0.011$) and near-significant effects of age at onset on SRT-LTS ($p = 0.054$), SRT-CLTR ($p = 0.058$) and SDMT scores ($p = 0.088$) (supp table 167 – 175), i.e., those tests that demonstrated statistically significant interactions between age at onset and onset age group.

Crucially, predicted scores of SRT subtests, SPART-IR, SDMT, PASAT and Stroop tests assumed a quadratic function and the optimum predicted scores for each test corresponded with an onset of around 30 years, justifying a single cut-point of 30 years in linear regressions (fig 24).

Figure 24. Modelling the relationship between test scores and age at onset with restricted cubic splines

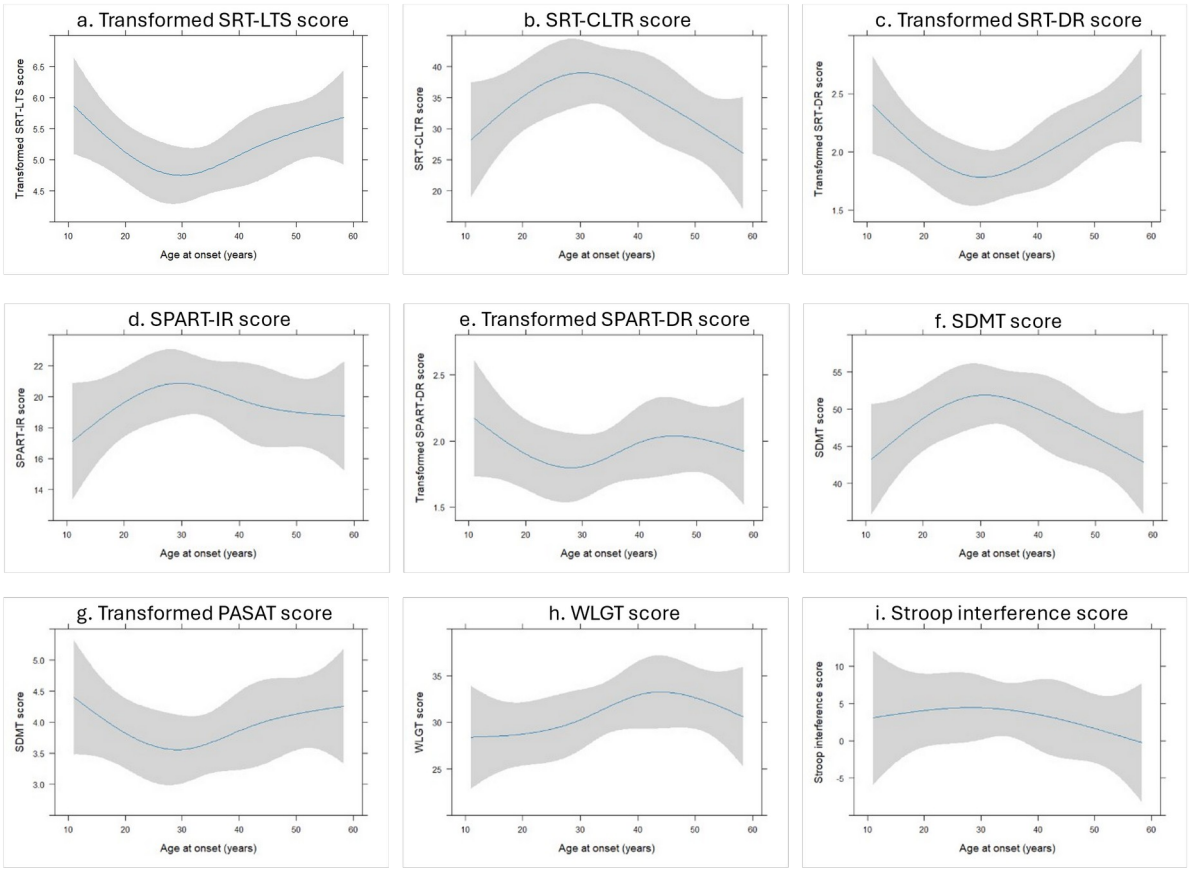

Exploration of the interactions between age at onset, age at testing and SIL status is available in appendix 13. There was no convincing evidence of either age parameter dominating putative interactions with SIL status.

Exploration of interactions between age at onset, onset age group and SIL status is available in appendix 14. Although there was weak evidence that interactions between age at onset and onset age group were not mediated by an interaction between age at onset and SIL status for most tests, it was impossible to elucidate the precise

interactions between predictors. Stroop test scores demonstrated the most convincing interactions between age parameters and SIL status.

a.ii) Effects of paediatric onset

The scarcity of patients with paediatric onset and biological evidence of peak brain maturation in the third decade meant analysis to this point focused on onset age groups <30 and ≥30 years. The interaction between age at onset and onset age group was suggestive of an effect of paediatric onset on test scores.

Box plots revealed lower scores among combined AQP4+ NMOSD and MOGAD patients with paediatric onset on most tests (fig 25). Univariable regression confirmed paediatric onset was associated with statistically significantly lower scores on the SRT-LTS (β = 0.748, p = 0.082), SRT-DR (β = 0.455, p = 0.065) and SPART-IR (β = -3.981, p = 0.050) (table 27).

Patients with paediatric disease onset were significantly younger at testing (p < 0.001), had shorter disease durations (p <0.001) and were more likely to have SILs (p = 0.001) (table 28).

Figure 25: Effect of paediatric onset on test scores in AQP4+ NMOSD and MOGAD

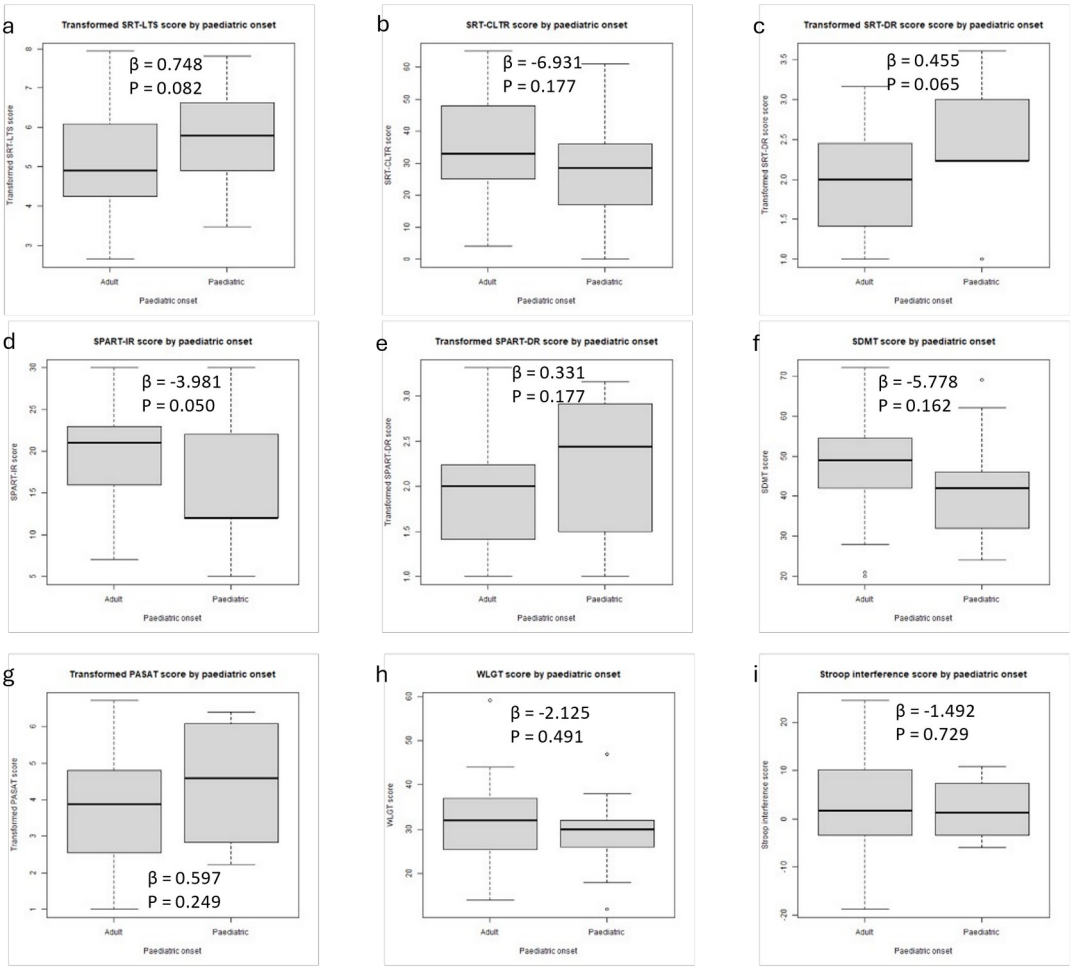

Table 27: Univariable regression of test scores against paediatric-onset disease (AQP4+ NMOSD and MOGAD)

Test	$\beta_{paediatric}$ (SE)	T statistic	P (β)	F (df)	R^2
Transformed SRT-LTS*	0.748 (0.424)	1.766	0.082	3.119 (1, 73)	0.041
SRT-CLTR	-6.931 (5.080)	-1.364	0.177	1.862 (1, 73)	0.025
Transformed SRT-DR*	0.455 (0.242)	1.877	0.065	3.522 (1, 72)	0.047
SPART-IR*	-3.981 (1.994)	-1.997	0.050	3.988 (1, 72)	0.052
Transformed SPART-DR	0.331 (0.243)	1.364	0.177	1.861 (1, 70)	0.026
SDMT	-5.778 (4.092)	-1.412	0.162	1.993 (1, 71)	0.027
Transformed PASAT	0.597 (0.513)	1.163	0.249	1.353 (1, 67)	0.020
WLGT	-2.125 (3.068)	-0.693	0.491	0.480 (1, 71)	0.007
Stroop interference	-1.492 (4.291)	-0.348	0.729	0.121 (1, 53)	0.002

p ≤0.10

Table 28. Comparison of demographic and clinical variables in paediatric- and adult-onset disease (AQP4+ NMOSD and MOGAD only)

	Paediatric-onset (n = 10)	Adult-onset (n = 65)	Statistic (p)
Diagnosis AQP4+ NMOSD (%)	5 (50)	22 (33.8)	Fisher's exact (0.480)
Median age onset (years) (range)*	11.5 (4 – 18)	35.0 (19 – 62)	U = -1495.0 (<0.001)
Median age testing (years) (range)*	26.0 (20 – 45)	44.0 (25 – 65)	U = -1579.0 (<0.001)
Median disease duration (months) (range)*	58 (110 - 418)	186 (6 – 371)	U = -2070.5 (<0.001)
N female (%)	7 (70)	48 (73.8)	Fisher's exact (~1)
Median years in education (range)	15.0 (10 – 19)	14.3 (10 – 21)	-U = 1837.0 (0.452)
Median HADS-A score (range)	4.5 (2 - 11)	8.0 (0 - 17)	U = -1280.0 (0.294)
Median HADS-D score (range)	5.5 (0 – 10)	5.0 (0 – 15)	U = -1306.5 (0.692)
Median MFIS total score (range)	30.5 (2 – 66)	39.5 (0 – 73)	U = -1296.5 (0.522)
Median MFIS cognitive subscore (range)	12.0 (2 – 27)	15.0 (0 – 40)	U = -1356.5 (0.663)
Median BPI score (range)	20.5 (0 – 69)	24.5 (0 – 92)	U = -1192.5 (0.454)
Median EDSS (range)	2.25 (0 – 5.5)	1.0 (0 – 7.5)	U = -1744.0 (0.488)
N SILs (%)*	8 (80)	15 (23.1)	Fisher's exact (0.001)

p ≤0.10

In multivariable regression, the most notable effects were observed when test scores were regressed against paediatric onset, diagnosis and the interaction term. Not only did paediatric onset remain a significant predictor of transformed SRT-LTS (β = 1.571, p = 0.012), transformed SRT-DR (β = 0.999, p = 0.008) and SPART-IR scores (β = -6.136, p = 0.043), adjusting for diagnosis also exposed significant main effects of paediatric onset on SRT-CLTR (β = 018.209, p = 0.014) and SDMT scores (β = -13.091, p = 0.024) (table 29; supp table 176 - 211).

Statistically significant interactions between paediatric onset and diagnosis were found for SRT-CLTR (β = 22.342, p = 0.028) and transformed SRT-DR scores (-0.978, p = 0.046), and the interaction term approached statistical significance for SRT-LTS and SDMT scores. Interaction plots confirmed more marked differences between paediatric

and adult onset cases in AQP4+ NMOSD on all tests (fig 26; table 29; supp tables 176 - 211).

Table 29: Main effects and interactions of paediatric disease onset and diagnosis (AQP4+ NMOSD and MOGAD only)

	$B_{diagnosis}$ (SE)	T statistic	P	$B_{paediatric\ onset}$ (SE)	T statistic	P	$B_{paediatric\ onset * diagnosis}$ (SE)	T statistic	P
Transformed SRT-LTS	0.164 (0.323)	0.508	0.613	1.571 (0.611)*	2.570	0.012	-1.592 (0.845)	-1.885	0.064
SRT-CLTR	-0.572 (3.867)	-0.149	0.882	-18.209 (7.233)*	-2.518	0.014	22.372 (9.995)*	2.238	0.028
Transformed SRT-DR	0.008 (0.175)	0.046	0.963	0.999 (0.264)*	2.747	0.008	-0.978 (0.482)*	-2.029	0.046
SPART-IR	2.201 (1.435)	1.534	0.130	-6.136 (2.976)*	-2.062	0.043	4.299 (3.943)	1.090	0.279
Transformed SPART-DR	-0.251 (0.169)	-1.485	0.142	0.650 (0.391)	1.659	0.102	-0.528 (0.493)	-1.071	0.288
SDMT	7.481 (2.744)*	2.727	0.008	-13.091 (5.666)*	-2.310	0.024	14.519 (7.512)	1.933	0.057
Transformed PASAT	-1.560 (0.342)*	-4.568	<0.001	0.360 (0.683)	0.527	0.600	0.115 (0.904)	0.127	0.899
WLGT	1.299 (2.256)	0.576	0.567	-6.273 (4.659)	-1.346	0.183	7.701 (6.176)	1.247	0.217
Stroop test	6.290 (2.967)*	2.120	0.039	-3.755 (7.206)	-0.521	0.605	3.650 (8.805)	0.415	0.680

*p ≤0.05

Main effects of diagnosis on SDMT, PASAT and Stroop interference scores survived adjustment for paediatric onset and diagnosis x paediatric onset interactions (i.e., there were significant effects of diagnosis, independent of paediatric versus adult onset), but main effects of diagnosis on SPART-IR and SPART-DR did not. This may be due to loss of statistical power after stratification, structural overlap or because the effect of diagnosis on visuospatial memory was partially dependent on non-statistically significant effects of paediatric onset within diagnostic groups.

For detailed analyses, see appendix 15.

Figure 26. Effects of interaction between diagnosis and paediatric onset on test scores

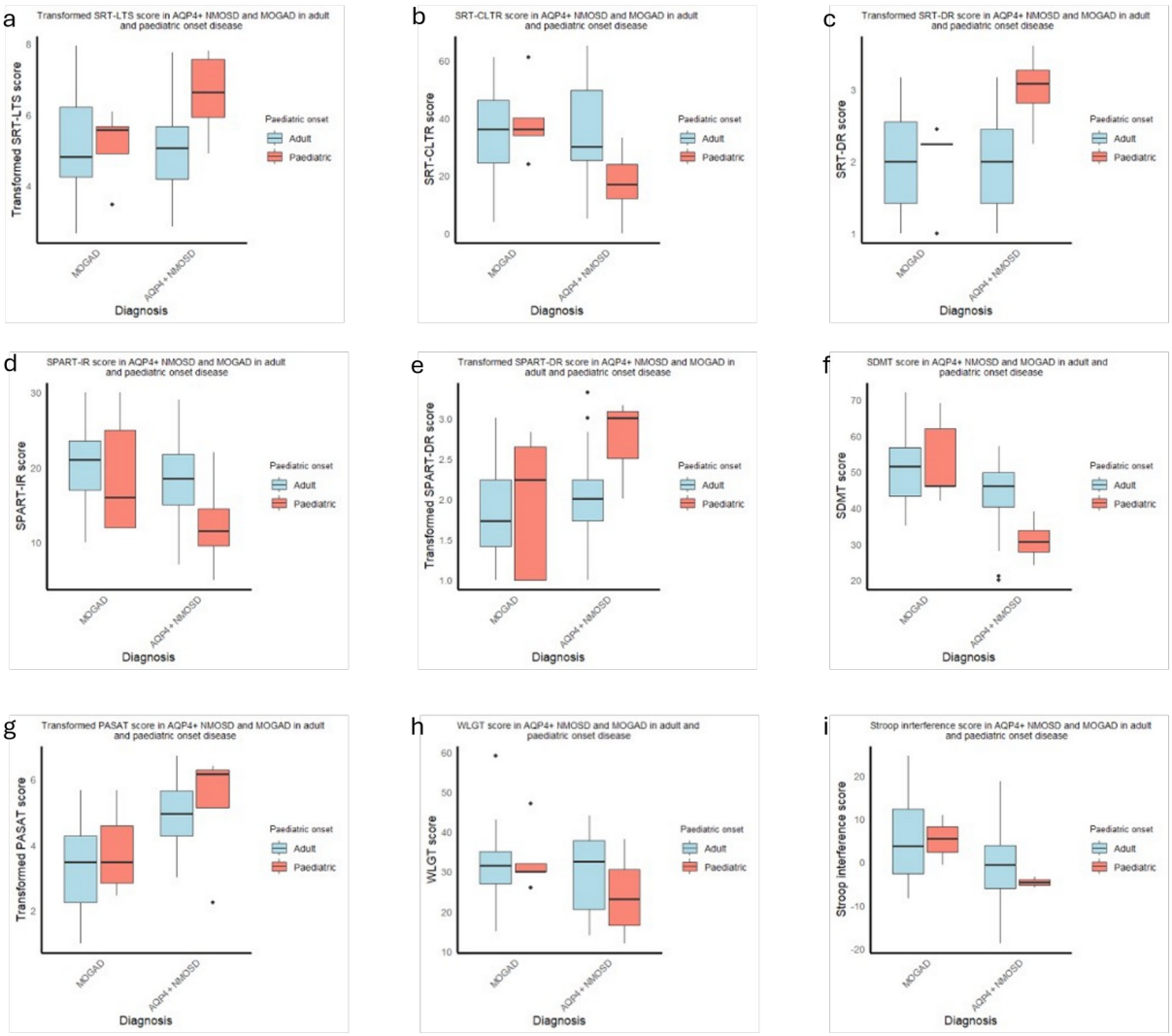

There was no significant effect of paediatric onset on scores among patients with MG (supp fig 45).

b) Predictors of test scores in AQP4+ NMOSD

Data from 27 patients were included (table 1). Univariable regressions revealed paediatric onset was the most common predictor across tests, reaching statistical and clinical significance for SRT-LTS, -CLTR, -DR, SPART-IR and SDMT scores (table 30, fig 27, supp table 212 - 220), i.e., those tests for which an effect of paediatric onset was retained after stratifying by diagnosis (table 29). Paediatric onset was the only significant predictor of transformed SRT-LTS and SPART-IR scores.

Figure 27. Effect of paediatric onset on test scores in the AQP4+ NMOSD group

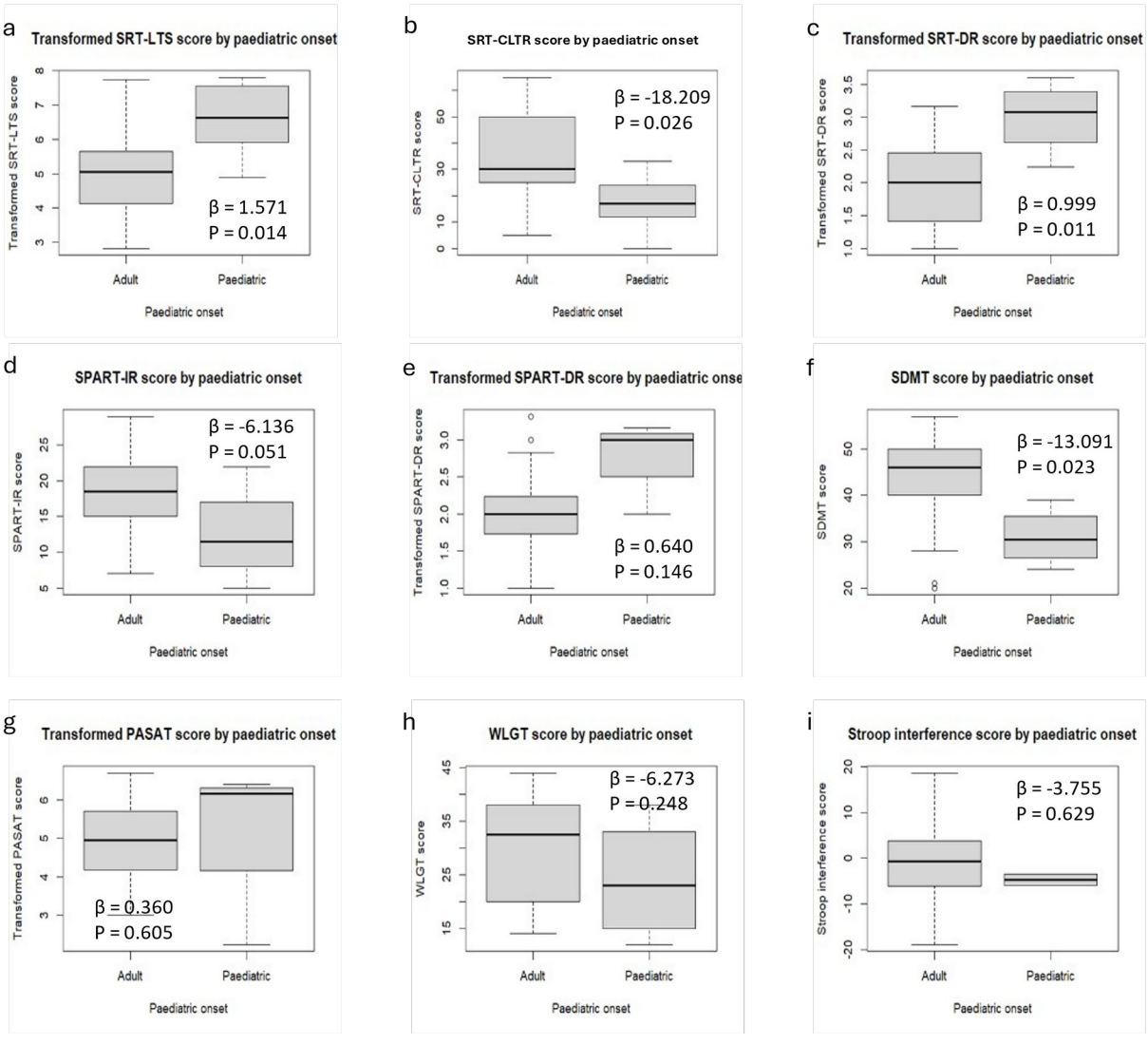

Table 30: Independent variables significant in univariable regressions restricted to patients with AQP4+ NMOSD

Test	Variables significant at α ≤ 0.10	Variables not significant at α ≤ 0.10
Transformed SRT-LTS	Paediatric onset	Age at onset, age at testing, disease duration, sex at birth, education, HADS-A score, HADS-D score, total MFIS score, MFIS cognitive subscore, BPI score, EDSS, SILs
SRT-CLTR	Paediatric onset, education, EDSS score	Age at onset, age at testing, disease duration, sex at birth, HADS-A score, HADS-D score, total MFIS score, MFIS cognitive subscore, BPI score, SILs
Transformed SRT-DR	Paediatric onset, education, EDSS score	Age at onset, age at testing, disease duration, sex at birth, HADS-A score, HADS-D score, total MFIS score, MFIS cognitive subscore, BPI score, SILs
SPART-IR	Paediatric onset	Age at testing, age at onset, disease duration, sex at birth, education, HADS-A score, HADS-D score, total MFIS score, MFIS cognitive subscore, BPI score. EDSS, SILs
Transformed SPART-DR	Nil	Age at onset, age at testing, disease duration, paediatric onset, sex at birth, education, HADS-A score, HADS-D score, total MFIS score, MFIS cognitive subscore, BPI score, EDSS, SILs
SDMT	Paediatric onset, HADS-A score, HADS-D score, total MFIS score, MFIS cognitive subscore, BPI score, EDSS score	Age at onset, age at testing, disease duration, sex at birth, education, SILs
Transformed PASAT	Nil	Age at onset, age at testing, disease duration, paediatric onset, HADS-A score, HADS-D score, total MFIS score, MFIS cognitive subscore, BPI score, EDSS, SILs
WLGT	HADS-D score	Diagnosis, age at onset, age at testing, disease duration, paediatric onset, sex at birth, education, HADS-A score, total MFIS score, MFIS cognitive subscore, EDSS, SILs
Stroop IS	Education	Age at onset, age at testing, disease duration, paediatric onset, sex at birth, HADS-A score, HADS-D score, total MFIS score, MFIS cognitive subscore, BPI score, EDSS, SILs

The effect of paediatric onset on SRT-LTS survived multivariable regression but effects on SRT-CLTR, SRT-DR and SDMT scores did not (supp table 221-227)[10]. However, in addition to the small population of patients with paediatric onset AQP4+ NMOSD, regressions were limited by small numbers of AQP4+ NMOSD patients with complete data and, in larger models, by inclusion of more predictors, both of which reduce residual degrees of freedom and limit power of regressions to detect

[10] Multiple regression could not be applied to tests with no predictor significant at the p ≤0.10 level (SPART-DR, PASAT)

effects. Nevertheless, effects of education on SRT-CLTR, transformed SRT-DR and Stroop interference scores survived multivariable regression.

SILs were more common among AQP4+ NMOSD patients with paediatric onset than those with adult onset (OR = 15.51, p = 0.017; supp table 228). Scatter plots suggested little effect of SIL status in adult-onset disease but the single case of paediatric-onset AQP4+ NMOSD without supratentorial lesions obtained the highest scores on the SRT-CLTR, SRT-DR, SPART-DR and SDMT (supp fig 46 - 54). As paediatric onset predicted significantly lower scores in three of these tests, it is possible some of the effect of paediatric onset was mediated by an interaction with SILs. However, only 1 of 5 paediatric-onset patients had no SILs, so structural overlap and small subgroups meant there was insufficient data to distinguish the independent effects of paediatric onset and SILs in patients with AQP4+ NMOSD.

4.3) Discussion: Cognition in AQP4+ NMOSD and MOGAD, part 3 (Rao BRB-N)

Plots of scores for all Rao BRB-N subtests demonstrated improvements with increasing age at onset in patients with AQP4+ NMOSD and MOGAD and onset aged <30 years. Scores declined with increasing age at onset in those with onset aged ≥30 years for all but the WLGT. Using splines to model effects of age at onset on test scores confirmed this pattern. Interactions were largely independent of age at testing, suggesting the decline in scores with increasing age at onset observed in the group with onset aged ≥30 years was not caused purely by collinearity with age at testing. Papers reporting a decline in cognitive performance with increasing age at testing have not examined independent effects of age at onset and their conclusions regarding the driver of deterioration may be erroneous.

Interactions between age at onset and onset age group suggested patients with onset of AQP4+ NMOSD or MOGAD in childhood may be more impaired than those with onset in young adulthood on most Rao BRB-N subtests. Box plots showed lower scores among the paediatric cohort for all tests other than the WLGT and Stroop test, and univariable regression confirmed paediatric onset was a statistically significant predictor of lower raw SRT-LTS, SRT-DR and SPART-IR scores.

The effects of diagnosis on SRT subtests and SDMT were more marked in, or limited to, those with paediatric onset and the small cohort with

paediatric onset was not sufficient to cause a main effect of diagnosis on SRT subscores in univariable regression. Diagnosis of AQP4+ NMOSD predicted significantly lower SDMT, PASAT and Stroop interference scores and possibly SPART subscores, independent of paediatric onset.

Paediatric onset was the most frequent predictor of test scores within the AQP4+ NMOSD group. Education was a significant predictor of three subtests in univariable and multivariable regressions. Education and paediatric onset were predictors of SRT-CLTR and SRT-DR scores in univariable regressions but only education survived multivariable regression. Within the AQP4+ NMOSD group, it is possible effects of paediatric onset on some subscores were mediated by education.

Chapter 5

Discussion of cognition in AQP4+ NMOSD and MOGAD

The central finding of this research is that patients with AQP4+ NMOSD demonstrate worse cognitive performance than disease controls using two assessment methods- the MoCA and the Rao BRB-N with Stroop test. Not only were scores among patients with AQP4+ NMOSD poorer than those with MG on tests of attention and processing speed, this study is the first to show poorer performance associated with AQP4+ NMOSD compared with MOGAD in tests of visuospatial memory, attention and processing speed and executive function. This work also indicates an impact of paediatric onset on cognitive outcomes in AQP4+ NMOSD.

a) Patients with AQP4+ NMOSD showed a trend towards lower scores on tests of attention and processing speed than patients with MG and significantly lower scores than patients with MOGAD

Multivariable linear regressions revealed AQP4+ NMOSD predicted poorer performance than MG on the MoCA, SDMT and PASAT[11]. This is in accordance with other studies from myriad countries showing attention

[11] The significant effect of AQP4+ NMOSD on scores compared with the control group did not survive adjustment for multiple comparisons, so only a trend towards lower scores in the AQP4+ NMOSD group can be inferred. The significant effect of AQP4+ NMOSD on scores compared with a diagnosis of MOGAD survived adjustment for multiple comparisons

and processing speed are the most commonly impaired domains in NMOSD (88,107,118,128,132,134,137,167, 179,185-189).

SILs are present in some cases of AQP4+ NMOSD but are not a feature of MG. It is tempting to attribute differences in scores between these groups to the effects of inflammatory CNS lesions in AQP4+ NMOSD. Several lines of evidence indicate this is not the case.

First, the AQP4+ NMOSD cohort scored significantly lower than the MOGAD cohort on the same tests, despite similar incidence of SILs in both diseases.

Second, head-to-head comparisons of test scores in combined AQP4+ NMOSD and MOGAD patient groups with and without SILs showed no significant differences.

These observations could be explained by different pathological changes associated with lesions in both diseases, including greater astrocyte loss and complement deposition in NMOSD, as well as rarefication and cavitation that are not reported in MOGAD (190–192). If this were the case, presence of SILs may have greater impact in AQP4+ NMOSD than in MOGAD.

Third, univariable regressions of test scores against SIL status revealed no effect of SILs and multivariable regression identified main effects of diagnosis but no significant effect of SIL status or diagnosis x SIL interactions in combined AQP4+ NMOSD and MOGAD groups. SIL status was not a predictor of scores in the AQP4+ NMOSD group. This suggests

the effect of diagnosis on scores was not due to more severe pathological changes within lesions in NMOSD.

Alternative explanations for these deficits are needed.

Cerebral biochemical changes may be responsible for lower scores in the AQP4+ NMOSD group. Magnetic resonance spectroscopy identified altered neurotransmitter ratios in the cingulate cortex of patients with AQP4+ NMOSD compared with healthy controls that correlated negatively with scores on a trail-making task (193). It has been suggested antibody binding leads to AQP4 internalisation, triggering a downstream cascade that culminates in reduced excitatory amino acid transporter (EAAT) expression by astrocytes and increased extracellular levels of excitotoxic glutamate with subsequent changes in cerebral glucose metabolism (193,194). Binding of MOG antibodies to oligodendrocytes would not have the same excitotoxic effect.

Poorer performance in the AQP4+ NMOSD group may also be attributable to subtle structural changes not detected by clinical grade scans.

i) **Atrophy:** A pathological study demonstrate neuronal loss in cortical layers II-IV beyond the corticospinal and optic pathways in AQP4+ NMOSD (88). Some imaging studies report significant and widespread cortical thinning in patients, independent of cerebral lesions (84,112). Others report only regionally restricted cortical thinning (101,104,112).

Deep grey matter volumes are not significantly different from those of healthy controls according to some groups (101,109,110,195,196), while others show atrophy limited to the thalami (104,108) or widespread deep grey matter loss (112,137,189). Regional atrophy has been correlated with poorer processing speed and attention. For example, volumes of the thalamus (137), nucleus accumbens (113) and various white matter pathways (169) in NMOSD correlate negatively with PASAT score. Volumes of the thalamus, caudate, putamen and nucleus accumbens (113) and frontal white matter regions (169) correlate negatively with SDMT performance.

Although atrophy may explain poorer attention and processing speed in AQP4+ NMOSD compared with MG, whether this could account for cognitive deficits compared with the MOGAD group is unclear. A volumetric study showed similar cortical thicknesses in both diseases (195). Others report cortical and deep grey matter volumes are reduced in MOGAD compared with healthy controls and NMOSD patients (101,109,195,197) and predict performance on the MoCA, SDMT and PASAT (145,198), while another showed deep grey matter volumes were normal in MOGAD and reduced in NMOSD (196). As the bulk of the evidence suggests the degree of atrophy in MOGAD is at least equivalent to that in NMOSD, it seems this is unlikely to explain contrasting cognitive performance between the two diseases, but differences in location of atrophy and ratio of neuronal to glial loss may contribute.

ii) **Microstructural changes**: Diffusion weighted imaging has identified increased white matter radial diffusivity and reduced global and regional tract fractional anisotropy in NMOSD, which correlates with performance on several cognitive tests, including the PASAT (111,113,185). Visual attention and processing speed correlates with microstructural integrity of white matter pathways largely involving visual processing areas, as well as strength of global connectivity (132). Magnetisation transfer ratio in normal appearing white matter was lower in patients with NMOSD compared with healthy controls (115). These microstructural changes exist in the absence of lesions on conventional scans (199). Such changes may explain poorer scores compared with the MG group, independent of SILs.

Changes in microstructural integrity may also explain differences in test performances in AQP4+ NMOSD and MOGAD. Although one study reported microstructural axonal damage in MOGAD but not AQP4+ NMOSD (196), others have found no differences in MOGAD compared with controls (109,195) and milder and anatomically limited changes in diffusion metrics compared with NMOSD (198).

iii) **Functional changes:** Resting state functional MRI in NMOSD has shown regional changes in activity compared with healthy controls (200). Alterations in resting state connectivity of visual and dorsal attentional networks in NMOSD are reported by three separate groups (137,159,179) and correlate with BRB-N

performance (179). Resting state connectivity within default mode, working memory and executive networks predicts attention and processing speed in NMOSD (137).

Few studies have examined functional connectivity in MOGAD. One study reported distinct patterns of altered connectivity in NMOSD and MOGAD, but the effect of these changes on cognitive performance was not explored (198).

iv) **Cellular changes:** AQP4 knockout mice display impaired long-term hippocampal long-term potentiation and altered long-term depression *in vivo* and *in vitro* (201,202), believed to underlie impaired long-term learning on spatial memory tests (194,201). In addition to altered EAAT expression, mechanisms posited to induce changes in plasticity include reduced expression of p75 neurotrophin receptors (201), deranged N-methyl D-aspartate receptor (NMDAR) function and increased extracellular potassium altering the neuronal membrane potential (202). As these changes are specific to astrocyte function and astrocyte-neuron interactions, similar changes would not be anticipated to result from MG or MOG antibodies

iv) **Psychosocial factors:** Depression, anxiety, fatigue and pain scores were highest in the AQP4+ NMOSD group in part 2 of this study and significantly predicted SPART-IR, SPART-DR, SDMT and PASAT scores (i.e., test scores that were predicted by diagnosis of AQP4+ NMOSD versus MOGAD). Although diagnosis survived adjustment for these factors, they may summatively contribute to

poorer cognitive performance directly or through use of medications. This would not explain poorer performance on MoCA tests, as patients with MG reported the highest levels of depression, anxiety, fatigue and pain in that part of the study.

Normal cognitive performance of the MOGAD group contrasts with the few available studies of cognition in adults with MOGAD, which show impairments on a range of tests (supp table 2). Differences in outcomes could be due to the use of multiple regression to adjust for relevant variables, different assessment paradigms and use of a more appropriate control group.

b) Paediatric onset of AQP4+ NMOSD is associated with poor verbal memory and attention/ processing speed

The original hypothesis predicted poorer cognitive performance in patients with AQP4+ NMOSD and MOGAD with onset age <30 years. There was no main effect of onset age group but performance improved in those with onset aged <30 years as age at onset increased and declined with increasing age in those with onset aged ≥30 years on all but the WLGT. Using splines to model the data non-linearly confirmed the pattern. The opposing effects of increasing age at onset within each onset age group explains why linear regression detected no main effect in the absence of the interaction term.

Other groups have demonstrated declining cognition with increasing testing age in health and in NMOSD but have not adjusted for age at onset (88,123,183). The current work shows detrimental effects of increasing age at onset in combined NMOSD and MOGAD groups if onset is ≥30 years, which persisted after adjusting for age at testing. Results are similar to those in adult-onset MS, where age at onset correlates negatively with processing speed, visual and verbal memory, and late-onset disease is associated with poorer performance after adjusting for age at testing (203). The authors hypothesised this to be due to decreased cognitive reserve at disease onset.

Lower scores at younger age at onset in those with onset aged <30 years suggested a deleterious effect of paediatric-onset disease. Univariable regression confirmed paediatric onset was associated with lower scores on all tests in combined AQP4+ NMOSD and MOGAD groups, including statistically significant effects on SRT and SPART-IR scores.

Subsequent analysis showed onset of AQP4+ NMOSD in childhood was associated with poorer performance on tests of verbal memory and visual attention and processing speed than onset in adulthood or a diagnosis of MOGAD. Diagnosis of AQP4+ NMOSD was an independent predictor of visual and auditory attention and processing speed and executive function.

The effects of paediatric onset on cognitive performance within the AQP4+ NMOSD group support the work of others demonstrating poorer

outcomes with younger onset ages in paediatric demyelinating diseases (123,125,126,141), including AQP4+ NMOSD (54).

There was no evidence of an effect of paediatric onset in the MOGAD group. The literature regarding an effect of age at onset of MOGAD is mixed, with some studies showing no effect of onset age within paediatric cohorts (138,143) while another reported lower scores associated with younger onset in MOGAD (139).

Several factors could explain lower scores associated with paediatric onset. Paediatric demyelinating diseases are associated with high levels of school absenteeism (204,205) and hospital admission before age 5 was associated with poor reading ability, even when the reason for hospital admission was non-neurological (206)[12]. Expectations of teachers and parents may be lower for children with physical disability, leading to low motivation in the child and/or less academic opportunity. Physical disabilities, such as visual impairment, may impede learning. These psychosocial issues may explain why children with isolated TM show impairments on cognitive tests (207). This would not explain deteriorating scores with increasing age at onset in adulthood.

A unifying model for the interaction between diagnosis and age at onset with respect to memory, attention and processing speed is that binding of AQP4 IgG to astrocytes triggers cellular and microstructural changes (see above) that disrupt the plasticity and connectivity required for skill acquisition. Cellular changes in older childhood and young adulthood do

[12] This study used data from paediatric hospital admissions in 1946 and the reasons for and experience of hospitalisation and long-term effects are likely to have changed in the intervening time. In addition, the direction of cause and effect is unclear

not have the same effects because skills are already achieved and there is sufficient cognitive reserve to withstand microstructural insult (123,125). As age at onset increases beyond early adulthood, cognitive reserve declines and test performance deteriorates due to failure to compensate for cellular and microstructural changes in existing circuits.

c) SIL status does not predict cognitive performance in AQP4+ NMOSD and MOGAD

Some studies have demonstrated lower cognitive scores in NMOSD in the presence of SILs (56,58), while others failed to show an effect (131–134,208). Most studies of cognition in MOGAD have focused on children and the majority conclude presence of SILs/ADEM predicts CI (60,61,139,143,145). As paediatric cases of both diseases are associated with higher incidence of SILs (36,37,209), it was important to determine whether SILs affected cognitive performance, whether the interaction between age at onset and SIL status mediated the interaction between age at onset and onset age group, and if SILs mediated the effect of paediatric onset in AQP4+ NMOSD.

The current study found no main effect of SILs on any test score in combined AQP4+ NMOSD and MOGAD groups, nor in the AQP4+ NMOSD group alone. There was no evidence that interactions between age at onset and onset age group were caused by an underlying interaction

between age at onset and SIL status on any test other than the Stroop test.

Within the AQP4+ NMOSD group, it was impossible to reliably separate the effects of SIL status from paediatric onset. It is possible that SIL status mediated or modulated the effect of paediatric onset in this group.

The current study demonstrates no main effect of SILs on cognitive outcome in mixed AQP4+ NMOSD and MOGAD patients and in AQP4+ NMOSD patients alone. Larger groups are needed to definitively exclude interactions with onset age and effects within the AQP4+ NMOSD paediatric-onset subgroup.

d) Limitations

i) Although the cohort was relatively large compared with other studies, individual subgroups were small. This limited power, particularly in multivariable regressions, where limited subgroups led to unstable estimates of regression coefficients with large standard errors.

Usable data was further limited by missing values, as many patients declined to complete psychosocial questionnaires. Although attempts were made to compensate for this with multiple imputation, this is never perfect.

ii) Multicollinearity between some variables (e.g., age at onset and age at testing) and structural overlap between others (e.g., paediatric onset and SIL status) led to unstable estimates of coefficients with large standard errors. This was a particular issue when trying to separate the effects of paediatric onset and SILs among patients with AQP4+ NMOSD.

iii) Because much of the work in the current study was exploratory, most outcomes were not adjusted for multiple comparisons. Statistically significant effects and interactions of onset age group, age at onset and SIL status should be interpreted cautiously.

Conditioning on a function (onset age group) of an independent variable (age at onset) can lead to multicollinearity (as evidenced by moderately high VIF values in multivariable regressions) and means the binary groups have different covariance structures that may not reflect the natural relationships between age at onset and scores. This was a particular consideration in 3-way interactions, when this issue was compounded by smaller group sizes, making estimates less accurate.

The problem of different covariance structures was addressed by permitting natural curvature of the predicted scores with cubic splines, which demonstrated the natural fit of the data resembled a quadratic function with a peak at 30 years for all but two tests, indicating that modelling age at onset within onset age groups

with a cut point at 30 years was appropriate to the data and interactions were not a product of imposing arbitrary thresholds. Further work is needed to ensure accurate modelling of SPART-DR and WLGT scores.

v) The age at which SILs were detected was not accounted for. The absence of interactions between SIL status and onset age group or paediatric onset on tests other than the Stroop test may be because the subgroup with young onset and SILs included patients whose childhood attacks did not involve SILs but whose adult relapses did. If adults with SILs are less susceptible to their effects than children, an interaction may have been missed. Examining effects of SILs that occurred in paediatric subgroups would have restricted group size to a prohibitive degree.

vi) Patients with AQP4+ NMOSD and MOGAD have relatively high probabilities of bilateral ON, leading to impaired colour vision. Patients with reduced colour perception were exempt from Stroop testing, reducing the power of the test to detect effects of variables. Even those with subjectively retained colour perception may have subclinical colour desaturation that impaired performance. Although many studies of NMOSD have also used the Stroop test to assess executive function, future work should focus on assessment methods that do not rely on intact colour vision or high visual acuity.

vii) Finally, the control group was selected to permit comparison of cognitive scores between patients with AQP4+ NMOSD or MOGAD with a group of patients with similar psychological and social burdens of chronic autoimmune disease but without the direct effects of CNS inflammation. However, there is controversial evidence of cognitive deficits in MG. For example, one group reported significantly lower scores on multiple cognitive tests compared with healthy controls (210). Two small studies reported significantly poorer performance on tests of memory and spatial orientation compared with healthy controls (211,212). However, no study adjusted for anxiety, depression and fatigue, samples were as small as 11 (212), and all failed to correct for multiple comparisons, even though up to 50 cognitive subtests were compared across groups.

Others have found no convincing evidence of CI in MG, with one group concluding, “evidence of cognitive and memory deficits [in MG] was notably lacking” (213). One study found no deficits in sustained attention and auditory processing speed (214), while another reported performance was equivalent or superior to standardized population norms on tests of verbal and visual learning and recall (215). Keesey found no significant differences in attention, memory and language between 25 people with MG and healthy controls, concluding that evidence of direct effects of MG antibodies on CNS function was, “remarkably unconvincing” (152).

In summary, there is mixed evidence of non-specific cognitive changes in MG that are likely the result of depression, anxiety, fatigue and medications. Therefore, the choice of this group to control for common sequelae of chronic disease was appropriate.

e) Conclusions

Patients with AQP4+ NMOSD are at risk of deficits in visual memory, attention and processing speed and executive function, independent of the presence of SILs. Those with onset in childhood are at higher risk of deficits in verbal memory and visual processing speed and attention. Cognitive performance was poorest in patients with onset in childhood or older adulthood, justifying cognitive screening of patients with disease onset at extremes of age. Patients with MOGAD are not impaired in any cognitive domain compared with controls.

Chapter 6

Introduction to post-SARS-CoV-2 vaccine acute inflammatory CNS syndromes

a) Background

At the time of starting this DPhil in 2021, the SARS-CoV-2 pandemic remained a huge global threat. Vast efforts were put into development of vaccines, including novel methods utilising mRNA and viral-vectored platforms (for reviews, see 216 & 217).

Due to the necessity for rapid vaccine development, clinical trials were shorter than is normal practice, with some approved before completion of phase 3 studies and several approved within a year of announcement of a pandemic (216). This prompted concerns among researchers about the safety of licenced SARS-CoV-2 vaccines (218).

It was in this context that I recognised a number of patients attending the Oxford NMODAS clinic developed their first symptoms within weeks of receiving a SARS-CoV-2 vaccine. The association was particularly marked for the MOGAD cohort.

I undertook a systematic approach to determine whether there was evidence of an association between new-onset autoimmune inflammatory CNS diseases, particularly MOGAD, and preceding SARS-CoV-2 vaccination.

b) What is known about the causes of MOGAD?

In contrast to AQP4+ NMOSD, no genetic risk factor for MOGAD has been identified (219,220) and there is no significant gender or racial bias (37,40,93,94). However, as discussed in section 1d, there is evidence that clinical onset of MOGAD may be triggered by infection or vaccination. One study identified an infectious prodrome in 22% of new-onset MOGAD cases (67), while another found 67% of patients had preceding infection (221). A review found infectious prodromes preceded up to 70% of MOGAD attacks and were more frequently associated with ADEM than other phenotypes (66).

c) Autoimmune disease after vaccination

The theory that infection and vaccination may precipitate autoimmune disease is well-established (222–225), although confirmed instances are rare (226,227). Causality is more likely when the association is frequent, reported by multiple countries, the outcome has a low background incidence, the outcome recurs on re-exposure and is replicable in animal models (227,228).

In the absence of a proven mechanism by which a vaccine drives an autoimmune response, the most reliable methodology for detecting

associations are large-scale epidemiological studies, although these may fail to detect very rare sequelae. Most epidemiological studies have failed to find consistent associations between a variety of autoimmune diseases and the vaccines to which they were attributed in case reports and series (224,226,227). Nevertheless, statistically robust epidemiological studies have identified convincing links between Guillain-Barré syndrome (GBS) and the 1976 American H1N1 influenza vaccine, (224,226,229). Epidemiological studies also confirmed an association between ITP and the MMR vaccine (226,230,231).

The risk of a vaccine triggering autoimmunity is likely to depend on the antigen(s) in the vaccine, the presence and type of adjuvants, method of vaccine production (70), the presence of contaminants as well as genetic and environmental influences on the host's immune system.

d) Demyelination and ADEM can follow infection and vaccination

ADEM is an inflammatory CNS disease of presumed autoimmune aetiology, characterised by multifocal demyelination (232,233). CNS demyelination and ADEM are among the most commonly reported adverse events following immunisation (AEFIs); a review of 71 instances of CNS demyelination following vaccination included 29 cases of ADEM, 9 of TM and 8 of ON (234). The frequency of CNS involvement in post-vaccine autoimmunity may be due to "immunological ignorance", i.e., failure to develop tolerogenic mechanisms controlling potentially self-reactive lymphocytes if the adaptive immune system does not

encounter the antigen in development, as may occur if self-antigens are only expressed in the immunoprivileged CNS and not the thymus.

ADEM has been reported following multiple vaccine types (70,235–237). Between 5 and 18% of ADEM cases occur within 1 month of vaccination, with incidences between 1 in 50,000 and 1 in 10 million vaccine doses, (53,235).

ADEM is more frequent in children than adults, regardless of vaccine status (235,236). This is believed to be due to a combination of age-related differences in CNS structure and immune responses (53).

e) MOGAD commonly presents with ADEM or ADEM-like disease in children

Between 37 and 50% of paediatric patients with ADEM were found to have MOG antibodies in the serum (72,73). ADEM is the most common manifestation of MOGAD in children aged ≤ 12 years (33,36,37) and 67% of children with MOGAD have brain lesions during attacks, even without clinical encephalitis (76). In contrast, ON is the most frequent syndrome in adults with MOGAD and brainstem and cerebral manifestations are rarer (37,238).

Many reports of post-vaccine ADEM cited above predate readily available MOG antibody testing and it is likely that some cases were associated with MOG antibodies. This is more likely for post-vaccine

cases followed by relapses with typical MOGAD features, such as bilateral ON and TM (235,236).

f) MOGAD following vaccination

Given the relatively high incidence of infection before MOGAD attacks (235), the association between vaccination and ADEM and the significant proportion of ADEM cases associated with MOG antibodies, it is unsurprising that vaccination has been reported to precede MOGAD onset. In a case series from Japan, 4 of 54 (7.4%) children with MOGAD received a vaccine before onset, although the intervals between events were not reported (74). A series from a single centre in America reported vaccination within 4 weeks of onset in 2 of 28 (7%) paediatric cases of MOGAD (69).

Post-vaccine MOGAD cases seem to present more frequently with ADEM and/or multifocal CNS involvement. MOGAD presenting with LETM and multifocal intracranial lesions was reported following a combination of tetanus, MMR and varicella vaccines (237). Another study identified diphtheria, tetanus and pertussis vaccination preceding 2 of 50 onset MOGAD attacks (67), including a case presenting with LETM and a cerebral lesion. Vaccination preceded onset of MOGAD in 4 of 37 (10.8%) patients with symptomatic brainstem or cerebellar lesions (75). Review articles have also noted the high incidence of infection and vaccination prior to MOG antibody-associated ADEM (66).

The association between vaccination and ADEM-like or multifocal presentations of MOGAD may be driven by the fact children are exposed to vaccines more frequently than adults and developmental differences in CNS structures and immune systems render them susceptible to intracranial lesions, i.e., age is a confounder. An alternative explanation is that children with MOGAD present with brain lesions because they are more likely to be exposed to novel infections or vaccines and the trigger dictates the phenotype.

g) Autoimmune disease following ChAdOx1S vaccination

During the SARS-CoV-2 pandemic, countries rapidly licenced several vaccines that were distributed rapidly and at scale. The vaccination programme in the UK commenced the first week of December 2020 and by December 30th 2021, 88% of the adult population had received two doses of SARS-CoV-2 vaccine (239).

Among those licenced in the UK were AstraZeneca's ChAdOx1S (Vaxzevria; Covishield), Pfizer-BioNTech's BNT-162b2 (Cominarty) and Moderna's mRNA-1273. These vaccines used novel approaches to introduce antigen to the host.

ChAdOx1S is a DNA vaccine that is created by inserting DNA encoding the SARS-CoV-2 spike (S) protein into the DNA of a chimpanzee

adenovirus. Modified adenoviral vectors replicate in HEK-293 cells, which are then lysed and transgenic viral particles are retrieved and combined with excipients in the vaccine. Infection of host cells by recombinant adenoviral particles is followed by nuclear translocation of adenoviral DNA, transcription of the S gene and subsequent translation and expression of the S protein on the host cell surface, triggering B and T cell-mediated immunity (216–218)[13].

In contrast, BNT162b2 and mRNA-1273 are mRNA-based vaccines, meaning DNA encoding the S protein is inserted into plasmid DNA, amplified in bacterial cells and transcribed *in vitro*. mRNA molecules are complexed with lipid nanoparticles, which allows entry to host cells for mRNA translation into the S protein (217).

Rapid vaccine uptake in a short period permits detection of rare AEFIs that would be missed if uptake was lower or dispersed in time. Causality is difficult to prove if events are rare but some AEFIs associated with SARS-CoV-2 vaccines are confirmed or highly likely. Most prominent is vaccine-induced thrombotic thrombocytopaenia (VITT), which has an incidence of between 1:26,500 and 1:127,300 doses (240). Despite its rarity, the link with viral vectored vaccines was enabled by the large volume of vaccines administered over a short period and the Yellow

[13] Specifically, the Early E1 gene, which is critical for viral replication, and the E3 gene are removed from the adenoviral DNA, which renders it replication incompetent. A shuttle vector carrying the DNA sequence encoding the SARS-CoV-2 spike (S) protein is inserted into the previous E1 locus using recombinant DNA technology. Adenoviral particles infect the immortalised HEK-293 cell line, which are engineered to express E1, permitting adenoviral replication. HEK-293 cells are lysed, recombinant adenoviral particles collected and packaged into vaccines. Adenoviral particles infect host cells and use the host nuclear machinery for DNA transcription, including of the S protein. The S protein transcript is then translated into protein and expressed on host cells.

Card reporting scheme. Epidemiological and biological research has confirmed that ChAdOx1S can trigger VITT (241–243).

Neurological diseases, particularly those of autoimmune origin, are among the most commonly reported SARS-CoV-2 vaccine-associated AEFIs and have been reported following a range of vaccine subtypes (244–246). Early case series and observational studies were often underpowered, associations were inconsistent and most failed to account for background disease rates. Subsequent work has debunked many of these findings.

However, some neurological sequelae are reported more consistently and have been substantiated in epidemiological studies, such as GBS and Bell's palsy following ChAdOx1S and haemorrhagic stroke following BNT162b2 (247,248). The Medicines & Healthcare Products Regulatory Agency (MHRA) now lists Bell's palsy, GBS and TM as rare sequelae of ChAdOx1S (249). Guidelines for vaccination for UK healthcare professionals list VITT, GBS and TM as rare side effects of the ChAdOx1S vaccine (250) but not of BNT162b2 (251). The Global COVID Vaccine Safety Network prospectively collected information on almost 250,000,000 doses of ChadOx1S, BNT16b2 and mRNA-1273 across 8 countries and identified significantly increased risks of GBS and cerebral venous sinus thrombosis following first-dose ChADOx1S, with weaker signals for TM and cardiac and haematological complications. BNT162b2 was associated with a significantly increased risk of myocarditis but not of inflammatory CNS disease (252).

In summary, there is reasonable evidence that vaccination can trigger some autoimmune diseases, including ADEM. We also know many cases of ADEM are associated with MOG antibodies and there is evidence that MOGAD can follow vaccination. SARS-CoV-2 vaccines have been linked with autoimmune diseases, including some targeting neurological antigens.

Chapter 7

Post-SARS-CoV-2 vaccine acute inflammatory CNS syndromes part 1: Observational study of post-vaccine new-onset inflammatory CNS disease

7.i) Methods: Observational study of post-vaccine new-onset inflammatory CNS disease

a) Full cohort description

The UK hosts two NHS-commissioned Highly Specialised Services for NMOSD and MOGAD in the UK, one in Oxford and one in Liverpool. Patients under the care of either centre with new AICS presenting between 1st December 2020 and 26th January 2022 were screened for exposure to SARS-CoV-2 vaccination in the 8 weeks prior to symptom onset.

The Oxford NMODAS cohort was screened prospectively during clinic appointments and retrospectively. Retrospective screening was performed by extracting all patients with disease onset between 1st December 2020 and 26th January 2022 from the Oxford NMODAS REDCap and Microsoft Access™ databases. These capture attack dates as well as details of vaccination and infection in the weeks prior to disease onset. In addition, referral letters, clinic notes and NHS Spine vaccination records were checked for every patient with disease onset between these dates.

Details of cases from the Liverpool Highly Specialised Service for NMOSD and MOGAD were sent to Oxford for inclusion in the study.

Inclusion criteria:

1) New onset AICS clinically consistent with NMOSD or MOGAD (i.e., CNS inflammation in the presence of antibodies to AQP4 or MOG OR TM and/or ON with or without supratentorial or brainstem involvement). Patients did not have to fulfil diagnostic criteria for NMOSD (151) or MOGAD (46) to be included.

2) Age 18 years or older at onset.

3) Symptom onset between 1st December 2020 and 26th January 2022[14].

4) Referral to one of the two Highly Specialised Services for NMOSD and MOGAD in the UK before September 2024.

For inclusion within the post-vaccine new-onset AICS cohort:

5) Symptom onset within 8 weeks of SARS-CoV-2 vaccination

Exclusion criteria:

[14] I.e., onset from day 1 of possible exposure to 8 weeks after last date of possible exposure, defined by study criteria

1) Known historical CNS inflammatory disease or clinical review revealed previous clinical episodes compatible with CNS inflammation.

2) Alternative diagnosis made by time of review.

The selected exposure period from December 2020 to December 2021 corresponded with the time most first-dose vaccines were administered in the UK (239).

Many studies have defined the window for diagnosing AEFIs as up to 6 weeks from vaccine (248,252,253). As the risk period for AEFIs varies according to the adverse event of interest, vaccine administered and population exposed (254) and AEFIs are considered feasible up to 12 weeks after vaccination (228), an 8-week post-vaccination risk window was chosen to optimise case detection.

For each patient, vaccine date and type were verified using the NHS Spine vaccination record and/or general practitioner records.

Demographic characteristics were extracted from the REDCap and Microsoft Access™ databases and NHS records. Sex was defined as biological sex at birth. Race was defined according to self-description by patients.

Attack date, clinical phenotype and EDSS at nadir were established from patient report, contemporary hospital documentation and referral letters.

Radiological phenotype was assessed by a neuroradiologist with a special interest in inflammatory CNS disease (TH) who reviewed initial and subsequent scans for each patient. LETM was defined as inflammatory signal change extending 3 or more vertebral segments.

Results of CSF and serum testing were requested from the referring hospital or traced using the Electronic Patient Record if patients were diagnosed in the John Radcliffe Hospital.

Serostatus was determined using live cell-based assays for both MOG and AQP4 antibodies as described (16,35). Only seropositive patients were included in the NMOSD group to ensure specificity of diagnosis. Seronegative patients meeting the IPND criteria for diagnosis of NMOSD (151) were included in the seronegative group.

Outcome was assessed by clinical review during routine appointments. EDSS and visual acuities were assessed by trained neurologists and/or ophthalmologists in Oxford and Liverpool. Because the EDSS fails to capture the impact of visual and sphincter disturbance that are common sequelae of NMOSD and MOGAD, clinical outcome was also graded according to the following criteria:

Good- full recovery, minor sensory symptoms not interfering with normal function and/ or visual acuity at least 6/7.5 in both eyes.

Moderate- residual motor deficit but mobile with or without unilateral assistance, sensory disturbance significantly disrupting normal function, sphincter disturbance (need for catheterisation, incontinence requiring

pads, enemata or manual methods required for bowel management), significant erectile dysfunction or visual acuity better than 6/36 but poorer than 6/7.5 in one or both eyes.

Poor- requiring bilateral assistance to mobilise or wheelchair user, plegic in one or more limbs or visual acuity equal to or poorer than 6/36 in one or both eyes.

Data were analysed by vaccine type (ai) and serostatus (aii).

The cohort description is purely descriptive as groups were too small to make meaningful statistical inferences.

b) Proportion of new-onset AICS occurring within 8 weeks of SARS-CoV-2 vaccination (John Radcliffe Hospital cohort)

To determine what proportion of patients with new-onset AICS between 1st December 2020 and 26th January 2022 occurred within 8 weeks of vaccination, analyses were restricted to patients seen at the John Radcliffe Hospital NMODAS[15]. Patients with new onset AICS within 8 weeks of SARS-CoV-2 vaccination are referred to as the *post-vaccine AICS group*.

[15] I.e., excluding Liverpool NMODAS cases, cases seen in outreach clinics and one patient who died during the acute episode. Inclusion of these patients would inflate the proportion of vaccine-associated cases, as it is possible patients with onset of disease after vaccination were more likely to be referred to specialised outreach clinics than those without a recognised trigger and because the denominator (total number of patients with new-onset AICS between 1st December 2020 and 26th January 2022 in outreach hospitals and Liverpool NMODAS) is unknown.

Post-vaccine AICS cases seen at the John Radcliffe Hospital were identified as described in section 8.1.a. Records of all patients seen by the Oxford NMODAS at the John Radcliffe Hospital with disease onset between 1st December 2020 and 26th January 2022 were reviewed and those meeting criteria 1-3 (section 8.1.a) were included as the denominator. NHS Spine and GP records were checked to verify dates and types of SARS-CoV-2 vaccinations.

The proportion of patients with onset within 8 weeks of vaccination was calculated:

$$\frac{No.\ new\ AICS\ cases\ between\ 1st\ Dec\ 2020 \wedge 26th\ Jan\ 2022\ with\ SARS\ CoV\ 2\ vaccine \in preceding\ 8\ weeks}{Total\ no.\ new\ AICS\ cases\ between\ 1st\ Dec\ 2020 \wedge 26th\ Jan\ 2022}$$

The procedure was repeated separately for cases of MOGAD, seronegative AICS and AQP4+ NMOSD.

c) Distribution of vaccine types in post-vaccine and non-post-vaccine AICS and index dose analysis (John Radcliffe Hospital cohort)

Total AICS cases were identified as described in section 8.1.b. Patients with AICS during the observation period who had received a SARS-CoV-2 vaccination at any point *prior* to disease onset were included in index dose analyses.

Index dose analysis was used to compare the proportions of vaccines received by the post-vaccine AICS group in the 8 weeks prior to disease onset with the proportions of vaccines administered most recently to

patients with onset of new AICS more than 8 weeks after vaccination. The results are expressed as odds ratios (ORs). Statistical significance was calculated using Fisher's exact test.

The procedure was repeated separately for cases of MOGAD (ii) and seronegative AICS (iii). The post-vaccine AQP4+ NMOSD group was too small for analysis.

d) Relapse on revaccination (John Radcliffe Hospital cohort)

Vaccination records of patients with AICS after first SARS-CoV-2 vaccine were checked to determine whether repeat vaccination triggered relapses. Recurrent events on rechallenge would suggest causality.

7.2) Results: Observational study of post-vaccine new-onset inflammatory CNS disease

a) Full cohort description

Thirty-eight patients with new post-SARS-CoV-2-vaccine AICS (*post-vaccine AICS*) arising between 1st December 2020 and January 26th 2022 were referred to Oxford (34) and Liverpool (4) NMODAS. This includes one patient referred to Oxford following onset of ADEM with LETM who but died before they were assessed.

a.i) Analysis by vaccine type

Of the 38 post-vaccine AICS patients, the majority (27; 71.1%) presented following receipt of ChAdOx1S and around a quarter (11; 28.9%) presented after receiving BNT162b2. No post-vaccine AICS patient received Moderna's mRNA-1273 (Spikevax) or Janssen's Ad26.COV2.S (Jcovden) vaccines (fig 28 & 29).

Figure 28. Numbers and diagnoses of post-vaccine AICS referrals to Oxford and Liverpool NMODAS (whole cohort)

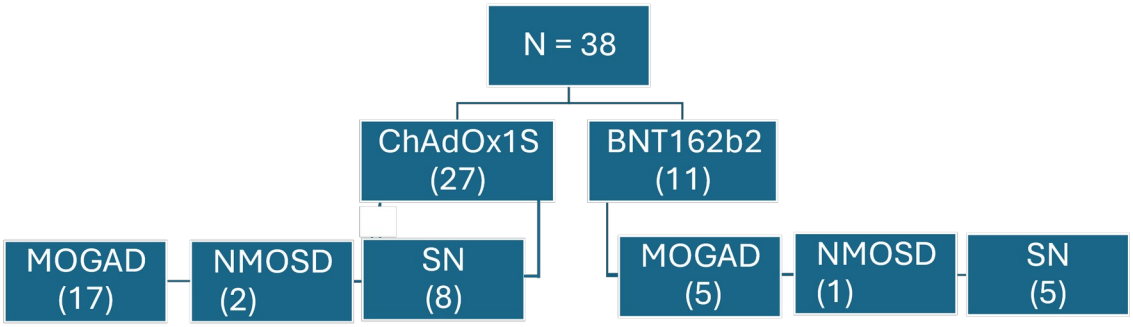

SN seronegative

Figure 29: Proportions of post-vaccine AICS cases receiving each vaccine

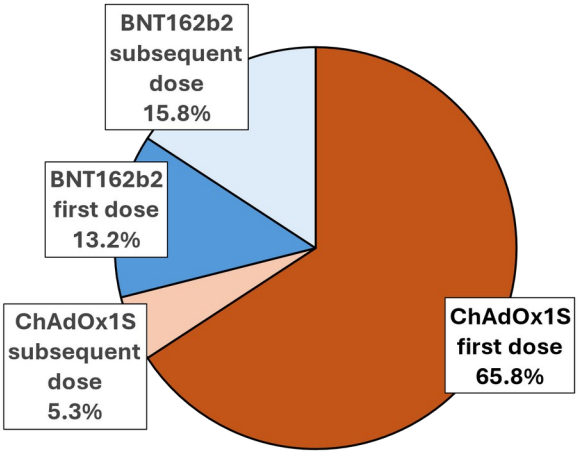

Demographics: There was a lower proportion of females in the ChAdOx1S group compared with the BNT162b2 group (51.9% and 72.7%, respectively) and median age of onset was higher (49 and 27 years, respectively), reflecting the advice of the Joint Committee on Vaccination and Immunisation (JCVI) issued in May 2021 that ChAdOx1S

should be avoided in the under-forties (255,256). Median interval between vaccination and symptom onset was shorter among ChAdOx1S recipients (15 days) than BNT162b2 recipients (22 days). Onset after first dose was more common among ChAdOx1S recipients (25/27; 92.6%) than those who received BNT162b2 (5/11; 45.5%) (table 31, fig 29).

Table 31. Characteristics of post-vaccine AICS cases according to vaccine type

		ChAdOx1S	BNT162b2
N (%)		27 (71.1)	11 (28.9)
N presenting after first dose (%)		25 (92.6)	5 (45.5)
N MOGAD (%)		17 (63.0)	5 (45.5)
N AQP4+ NMOSD (%)		2 (7.4)	1 (9.1)
N seronegative (%)		8 (29.6)	5 (45.5)
N female (%)		14 (51.9)	8 (72.7)
Median age at onset (yrs) (range)		49 (28 – 76)	27 (18 – 50)
Median time to symptom onset (days) (range)		15 (1 – 52)	22 (7 – 55)
Clinical syndrome			
	ON alone (%)	7 (25.9)	7 (63.6)
	TM alone (%)	10 (37.0)	3 (27.3)
	ON + TM (%)	2 (7.4)	1 (9.1)
	Brain/ brainstem alone (%)	1 (3.7)	0
	Brain/brainstem + TM and/or ON (%)*	7 (25.9)	0
Any TM		17 (63.0)	4 (36.4)
Inflammatory brain lesions present on MRI*		15 (55.6)	1 (9.1)

*This does not include 3 cases of clinical and radiological facial nerve involvement

Diagnosis: A greater proportion of ChAdOx1S recipients developed MOGAD (17/27; 63.0%) than BNT162b2 recipients (5/11; 45.5%). Conversely, BNT162b2 recipients were more likely to be seronegative (5/11; 45.5%) than ChAdOx1S recipients (8/27; 29.6%) (table 31, fig 30).

The odds of a post-vaccine MOGAD case having received ChAdOx1S were 3.4:1. The odds of a post-vaccine AQP4+ NMOSD patient having received ChAdOx1S were 2:1 and the odds of a post-vaccine seronegative patient having received ChAdOx1S were 1.6:1.

Figure 30: Proportion of post-vaccine AICS cases with each diagnosis according to vaccine type

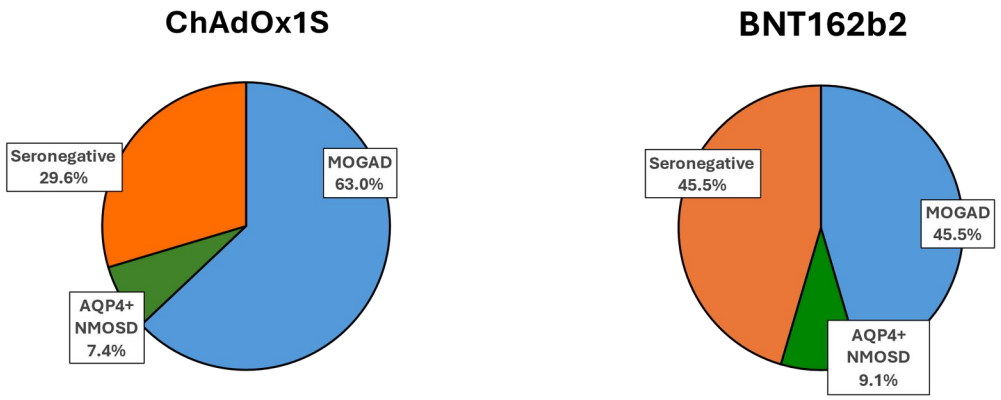

Phenotype: Clinical manifestations of supratentorial and/or brainstem involvement were common among ChAdOx1S recipients, affecting 8/27 (29.6%), often in conjunction with TM and/or ON (7/27; 25.9%). Lower motor neuron facial palsy was a feature of 3 post-ChAdOx1S cases, bringing the total number of ChAdOx1S recipients with any intracranial involvement to 11 (40.7%). In contrast, no patients in the BNT162b2 group presented with clinical manifestations of intracranial involvement. Similarly, radiological supratentorial and/or brainstem involvement affected a higher proportion of ChAdOx1S recipients (15/27; 55.6%) than BNT162b2 recipients (1/11; 9.1%) (table 31).

Isolated ON affected only 7/28 (25.9%) of ChAdOx1s recipients, whereas isolated ON was the most common presentation among BNT162b2 recipients, affecting 7/11 (63.6%) (7/11; 63.6%) (table 31, fig 32). TM, alone or in combination, affected 17/27 (63.0%) of the ChAdOx1S group, compared with 4/11 (36.4%) of the BNT162b2 group.

In summary, ChAdOx1S recipients comprised the largest subgroup of the post-vaccine cohort, were more likely to present after first dose and to present with clinical and/or radiological manifestations of brain involvement. TM was common following ChAdOx1S, often as part of a multifocal CNS inflammatory process. MOGAD was more common amongst ChAdOx1S recipients than BNT162b2 recipients. The majority of BNT162b2 recipients were seronegative, brain involvement was rare and isolated ON was common.

a.ii) Analysis by diagnosis (full cohort): Post-vaccine MOGAD

Demographics and phenotype (see table 32 & 33)

MOGAD patients comprised the majority of post-vaccine AICS cases (22/38; 57.9%). Twelve (54.5%) MOGAD patients were female, reflecting the ratio in the general population but the median age at onset (49.5 years) was older than is reported in demographic studies (40). Two patients presented between 43 and 56 days after vaccination.

Over three quarters of post-vaccine MOGAD cases followed ChAdOx1s (17/22; 77.3%) and 15 of these (88.2%) experienced their onset attack after the first dose of vaccine, whereas 2/5 (40%) BNT162b2 recipients experienced onset after the first dose. The median age of ChAdOx1S recipients with new-onset MOGAD was higher than BNT162b2 recipients (52 and 25 years, respectively), likely due to JCVI guidance issued in May 2021 (255,256).

One patient had a history of HLA-B27-associated recurrent scleritis. No other patient had historical neurological or autoimmune disease.

The distribution of phenotypes among BNT162b2 recipients reflected those of sporadic MOGAD (37,39), whereas phenotypes of ChAdOx1S recipients were less typical. Over half ChAdOx1S recipients (11/17; 64.7%) experienced TM as part of their first attack, compared with only 1/5 (20.0%) BNT162b2 recipients. Conversely, 5/17 (29.4%) ChAdOx1S recipients presented with isolated ON, compared with 4/5 (80%) BNT162b2 recipients. Four (23.5%) ChAdOx1S recipients presented with clinical supratentorial/ brainstem involvement, compared with none of the BNT162b2 recipients (fig 31).

Median EDSS score at nadir was higher among MOGAD patients following ChAdOx1S (5.5, range 2.0 – 8.0) than BNT162b2 (3.0, range 2.0 – 7.0), reflecting the higher incidence of TM among ChAdOx1S recipients.

Table 32. Characteristics of post-vaccine AICS cases according to diagnosis

	AQP4+ NMOSD	MOGAD	Seronegative
ChAdOx1S: BNT162b2	2:1	17:5	8:5
Median interval from vaccination to onset (range) (days)	25 (1 – 55)	15 (6 – 52)	15 (6 – 42)
Median age at onset (range) (years)	46 (28-50)	49.5 (22 – 76)	40 (18 – 58)
N female	3 (100)	12 (54.5)	7 (53.8)
Clinical syndrome:			
ON alone (%)	1 (33.3)	9 (40.9)	4 (30.8)
TM alone (%)	0	8 (36.4)	5 (38.5)
ON + TM (%)	0	1 (4.5)	2 (15.4)
Brain/ brainstem alone (%)	0	1 (4.5)	0
Brain/brainstem + TM and/or ON (%)*	2 (33.3)	3 (13.6)	2 (15.4)
Symptomatic ON (%)	2 (66.7)	12 (54.5)	7 (53.8)
Symptomatic TM (%)	1 (33.3)	11 (50.0)	9 (69.2)
Symptomatic brain/brainstem (%)*	2 (66.7)	4 (18.2)	2 (15.4)
Radiological brain/ brainstem*	2 (66.7)	9 (40.9)	6 (46.2)
Median CSF protein (range) (g/L)†	0.37 (0.30 – 0.43)	0.60 (0.33 – 2.25)	0.65 (0.23 – 6.81)
Median CSF leucocyte count (range) (/μL)†	23 (5 – 41)	36 (0 – 248)	3 (0 – 489)
N unmatched CSF oligoclonal bands (%)††	0	0	2 (15.4)
Median EDSS at nadir (range)§	2.0	3.5 (2.0 – 8.0)	3.75 (2.5 – 10)
Median antibody titre at onset (range)‡	1:225 (1:50 – 1:400)	1:1600 (300 – 6400)	N/A
N acute treatment (%)	3 (100)	19 (86.4)	13 (100)
N IV or PO steroids (%)	3 (100)	19 (86.4)	12 (92.3)
N IVIg (%)	0	2 (9.1)	3 (23.1)
N PLEX (%)	1 (33.3)	3 (13.6)	6 (46.2)
N oral steroid taper > 1 month	2 (66.7)	18 (81.8)	8 (61.5)
Median follow up (range) (months)	39 (36 – 41)	31 (13 – 43)	38.5 (5 – 44)
Median EDSS at last follow-up (range)	2.0 (0 – 4.0)	1.0 (0 – 6.5)	2.0 (0 – 10)
N with good outcome (%)	1 (33.3)	14 (63.4)	6 (46.2)
N with moderate outcome (%)	2 (66.7)	6 (27.3)	5 (38.5)
N with poor outcome (%)	0	2 (9.1)	2 (15.4)
N relapsers (%)	2 (66.7)	6 (27.3)	1 (7.7)
N seroreverted (%)	1 (33.3)	5 (22.7)	N/A
N on IST/DMT at last encounter (%)$	3 (100)	5 (22.7)	3 (23.1)

Legend for table 32
* This does not include the 3 patients with lower motor neuron facial weakness
**N AQP4+ NMOSD = 2; N MOGAD = 13; N seronegative = 13
† N AQP4+ NMOSD= 2; N MOGAD = 13; N seronegative = 14
†† N AQP4+ NMOSD = 2; N MOGAD = 13; N seronegative = 13
§ Two AQP4+ NMOSD patients with nadir EDSS available scored 2.0
‡ Titres measured by serial dilutions. Median value is not numerical median. N AQP4+ NMOSD = 2; N MOGAD = 21
$ IST includes prednisolone ≥10mg daily
CSF cerebrospinal fluid; IV intravenous; IVIg intravenous immunoglobulins; OCB oligoclonal bands; PLEX plasma exchange

Sixteen (94.1%) ChAdOx1S recipients and 3 (60%) BNT162b2 recipients received acute steroid treatment, reflecting higher incidence of TM and greater disability in ChAdOx1S recipients, although proportions of patients requiring treatment escalation were similar (17.6% and 20%, respectively). Three (13.6%) patients with isolated ON did not receive acute treatment. The majority of patients (18/22; 81.8%) were prescribed a tapering course of oral prednisolone.

Figure 31. Proportions of clinical phenotypes among postvaccine MOGAD patients by vaccine type

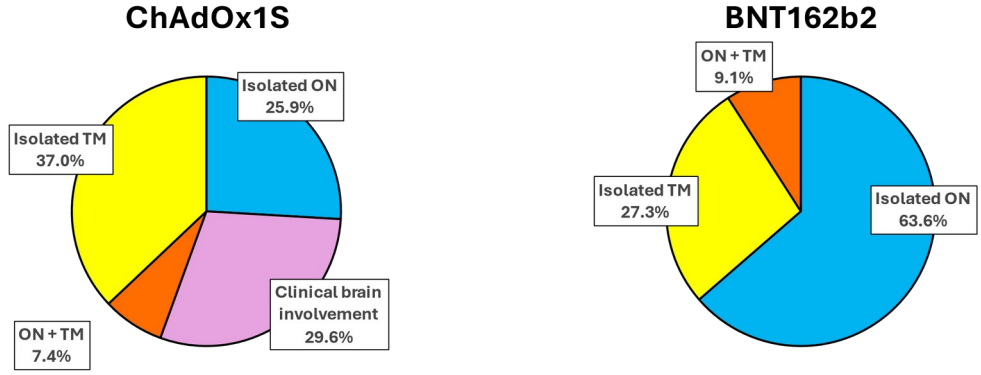

Table 33. Characteristics of post-vaccine MOGAD cases according to vaccine type

		ChAdOx1S	BNT162b2
N (%)		17 (77.3)	5 (22.7)
N female (%)		9 (40.9)	3 (60)
Median age (range) (years)		52 (28 – 76)	25 (22 – 50)
Median interval (range) (days)		15 (6 – 52)	14 (10 – 42)
Onset after first vaccine (%)		15 (88.2)	2 (40)
Clinical phenotype			
	ON alone (%)	5 (29.4)	4 (80.0)
	TM alone (%)	7 (41.2)	1 (20.0)
	ON + TM (%)	1 (5.9)	0
	Brain/ brainstem alone (%)	1 (5.9)	0
	Brain/brainstem + TM and/or ON (%)	3 (17.6)	0
Any TM (%)		11 (64.7)	1 (20.0)
Radiological brain/ brainstem (%)		9 (52.9)	0
Median EDSS at nadir (range)		5.5 (2.0 – 8.0)	3.0 (2.0 – 7.0)
Median MOG ab titre when first tested (range)‡		1600 (400 – 3200)	1000 (300 – 2400)
Median CSF leucocyte count (cells/µL) (range)**		36 (0 – 248)	NA
Median CSF protein (g/L)†		0.60 (0.33 – 2.25)	0.65
Patients with unmatched CSF OCBs (%)††		0	0
N acute treatment (%)		16 (94.1)	3 (60.0)
	N PO or IV steroid (%)	16 (94.1)	3 (60.0)
	N IVIg (%)	1 (5.9)	1 (20.0)
	N PLEX (%)	2 (11.8)	1 (20.0)
N oral steroid taper > 1 month		15 (88.2)	3 (60.0)
Median follow up time (range) (months)		35 (13 – 43)	27 (20 – 35)
Median EDSS at last review (range)		1.0 (0 – 6.5)	1.0 (0 – 3.0)
N with good outcome (%)		11 (64.7)	3 (60.0)
N with moderate outcome (%)		5 (29.4)	1 (20.0)
N with poor outcome (%)		1 (5.9)	1 (20.0)
N relapsers (%)		6 (35.3)	0
N seroreverted (%)		2 (11.8)	3 (60.0)

** N ChAdOx1S = 13; N BNT162b2 = 0
† N ChAdOx1S = 13; N BNT162b2 = 1
†† N ChAdOx1S = 12; N BNT162b2 = 0
‡ Titres measured by serial dilutions. Median value is not numerical median.

Paraclinical data (see table 32 & 33)

As most patients presented initially to their local hospitals rather than the John Radcliffe Hospital, investigations varied between patients.

One patient presenting with unilateral ON had received treatment for a latent syphilis infection two weeks prior to onset. As this patient recovered without intervention, subsequently relapsed twice and MOG antibodies were persistently positive, his presentation was felt to be due to MOGAD rather than tertiary syphilis.

Another patient with TM was found to have Borrelia IgG in CSF and serum as well as Borrelia IgM in the serum. They received intravenous methylprednisolone and recovered significantly prior to treatment with ceftriaxone. Classic radiological features of MOGAD (LETM with a lesion in the conus), the rapid response to steroids before antibiotic treatment and persistently high MOG antibody titres were more consistent with MOGAD than neuroborreliosis.

No other patient was found to have coexistent infection or autoimmunity explaining their presentation.

Four patients were tested for SARS-CoV-2 N antibodies after a median of 7 months from symptom onset. One patient had equivocal results and the remainder were negative.

Radiological supratentorial and/or brainstem inflammatory lesions were observed in over half ChAdOx1S recipients (9/17; 52.9%) and none of the BNT162b2 recipients. Lesions were typically multifocal, fluffy T2 hyperintensities (fig 32 - 35)[16].

Of 11 ChAdOx1S recipients with TM, 6 (54.5%) had radiologically confirmed LETM (fig 32 - 34). The one BNT162b2 recipient with TM had multiple short cord lesions (fig 36).

Figure 32a-c. MRI brain and spinal cord of a 52-year-old post-ChAdOx1S MOGAD patient presenting with rhomboencephalitis, ON and TM

a) Axial T2 weighted brain MRI. Bilateral T2 hyperintensities within the middle cerebellar peduncles characteristic of MOGAD (arrows)

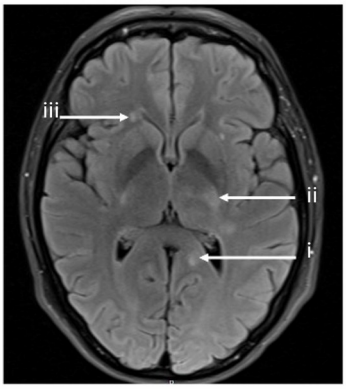

b) Axial T2 -weighted FLAIR MRI. Multifocal hyperintensities involving the left trigone (i), posterior limb of the left internal capsule (ii) and frontal horn of the right lateral ventricle (iii). These are not typical of MOGAD presenting in adulthood

c) Sagittal T2 -weighted cervical spine MRI. Longitudinally extensive transverse myelitis extending between the levels of C3 and T1 (arrows)

[16] Image 32 was published in Francis, Elhadd, Camera *et al*., Acute inflammatory diseases of the central nervous system after SARS-CoV-2 vaccination. Neurol Neuroimmunol Neuroinflamm 2022;10(1):e20063

Figure 33a-c. MRI brain and spinal cord of a 28-year-old post-ChAdOx1S MOGAD patient presenting with paraparesis and urinary retention

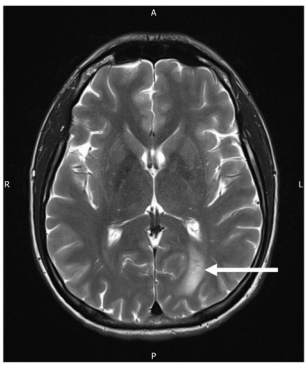

a) Axial T2 weighted brain MRI. Ill-defined large left occipital T2 hyperintensity (arrow)

b) Sagittal T2 weighted whole spine MRI. T2 hyperintensity and oedema extending from the level of C2 to the conus

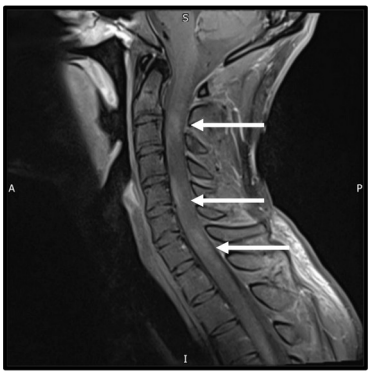

c) Sagittal post-gadolinium T1 weighted cervical spine MRI. Patchy enhancement of transverse myelitis (arrows)

Figure 34a-c. MRI brain and spinal cord of 38-year-old post-ChAdOx1S MOGAD patient presenting with fever, confusion, paraparesis and urinary retention

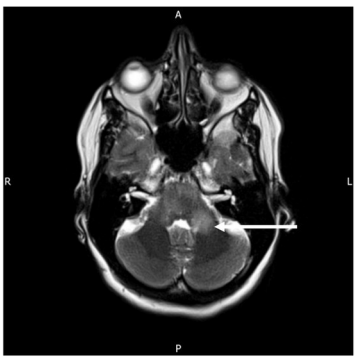

a) Axial T2 weighted brain MRI. Diffuse, fluffy hyperintensities in the pons and left middle cerebellar peduncle (arrow)

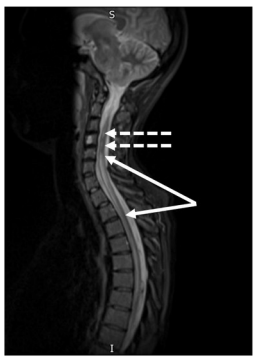

b) Sagittal T2 weighted cervicothoracic spine MRI. Mixed short (dashed arrows) and long (solid arrows) lesions

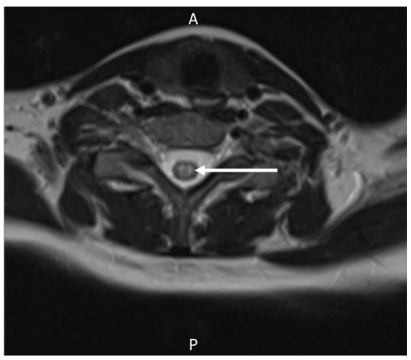

c) Axial T2 weighted cervical spine MRI. Symmetrical grey matter T2 hyperintensity (arrow)

Figure 35a-d. MRI brain and spinal cord of a 58-year-old post-ChAdOx1S MOGAD patient presenting with urinary retention and lower limb dysaesthesia

a) Axial T2 weighted brain MRI. Bilateral T2 hyperintensities within the middle cerebellar peduncles, more marked on the right (arrows)

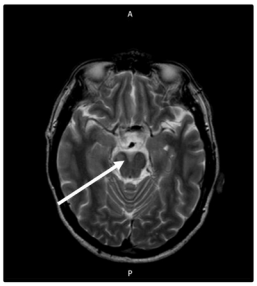

b) Axial T2 weighted brain MRI. Fluffy T2 hyperintensity in the right cerebral peduncle (arrow)

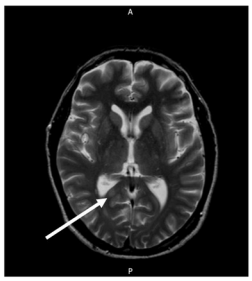

c) Axial T2 weighted brain MRI. Fluffy T2 hyperintensity in the right trigone (arrow)

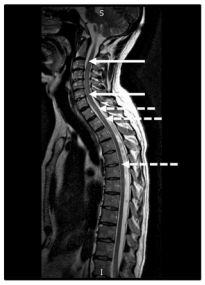

d) Sagittal T2 weighted cervicothoracic spine MRI. Borderline longitudinally extensive transverse myelitis extending between levels of C2 and C4 (solid arrows). Multiple poorly –defined short cord lesions (dashed arrows)

Figure 36a & b. MRI spinal cord of 31-year-old post-BNT162b2 MOGAD patient presenting with lower limb dysaesthesia, paraparesis and urinary retention

a) Sagittal T2 weighted thoracic spine MRI. Short T2 hyperintensity with localised oedema (arrow). Other short lesions were observed throughout the thoracic cord

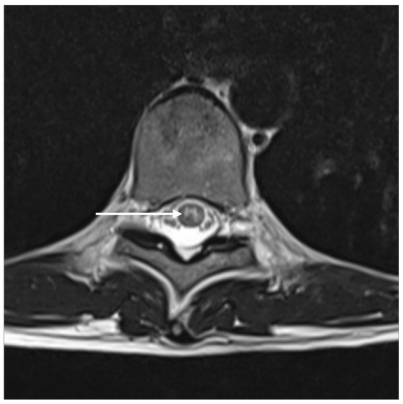

b) Axial T2 weighted thoracic spine MRI. T2 hyperintensity affecting the grey matter, producing “H” sign described in MOGAD (arrow)

Fourteen (82.4%) ChAdOx1S patients underwent CSF examination compared with only 2 (40%) BNT162b2 recipients. CSF leucocyte count was only recorded for ChAdOx1S recipients and was moderately elevated (median 36/μL). Median CSF protein concentration in ChAdOx1S recipients was slightly elevated (0.60 g/L) but 2 patients had concentrations greater than 1g/L. As only one BNT162b2 recipient had

CSF protein concentration recorded, comparison was not possible. None of the patients tested had unmatched oligoclonal bands in the CSF.

Longitudinal outcomes (see table 32 & 33)

Over a median follow-up period of 31 months, 6/22 (27.3%) MOGAD patients relapsed, all of whom received ChAdOx1S. Four patients had 5 episodes of isolated ON, one had ON and a new cerebral lesion on MRI and another had a brainstem relapse.

Median EDSS score at last follow-up was 1.0, which was the same among ChAdOx1S recipients (range 0 – 6.5) and BNT162b2 recipients (range 0 – 3.0).

Outcomes were similar across the two vaccines. Of the 17 ChAdOx1S recipients, 11 (64.7%) achieved a good outcome, 5 (22.7%) had a moderate outcome and 1 (4.5%) achieved a poor outcome because they required bilateral walking aids. Of the 5 BNT162b2 recipients, 3 (60%) had a good outcome, 1 (20%) had a moderate outcome and 1 (20%) had a poor outcome due to persistent visual impairment. Five patients with moderate outcome had residual sphincter dysfunction.

Four (18.2%) patients were on long-term immunosuppressant medications at last review. All had received ChAdOx1S, all had experienced at least 1 relapse and all remained MOG antibody seropositive on latest testing.

After a median interval of 24.5 months between initial and latest antibody testing, MOG antibodies were below the diagnostic threshold in 2/17 (11.8%) ChAdOx1S recipients and 3/5 (60%) BNT162b2 recipients.

In summary, post-vaccine MOGAD patients were more likely to have received ChAdOx1S than BNT162b2. ChAdOx1S recipients were more likely to present with TM, often in conjunction with symptomatic or asymptomatic brain lesions. This is in contradistinction to the BNT162b2 recipients, who largely presented with ON and in whom inflammatory brain lesions were not seen. MOGAD patients that received ChAdOx1S were more likely to relapse and less likely to serorevert than BNT162b2 recipients.

aii) Analysis by diagnosis (full cohort): Post-vaccine seronegative AICS

Demographics and phenotypes (see table 32 & 34)

Thirteen patients developed AICS in the absence of MOG or AQP4 antibodies within 8 weeks of SARS-CoV-2 vaccination. Eight (61.5%) developed symptoms after receiving ChAdOx1S and 5 (38.5%) developed symptoms following vaccination with BNT162b2. All 8 ChAdOx1S recipients and 3/5 (60%) BNT162b2 recipients had onset after the first dose of vaccine.

Table 34. Characteristics of post-vaccine seronegative cases according to vaccine type

		ChAdOx1S	BNT162b2
N (%)		8	5
N female (%)		3 (37.5)	4 (80.0)
Median age (range) (years)		42.5 (35 – 58)	27 (18 – 36)
Median interval (range) (days)		11 (6 – 23)	32 (7 - 42)
Onset after first vaccine (%)		8 (100)	3 (60.0)
Clinical phenotype			
	ON alone (%)	2 (25.0)	2 (40.0)
	TM alone (%)	3 (37.5)	2 (40.0)
	ON + TM (%)	1 (12.5)	1 (20.0)
	Brain/ brainstem alone*	0	0
	Brain/brainstem + TM and/or ON (%)*	2 (25.0)	0
Any TM (%)		6 (75.0)	3 (60.0)
Radiological brain/ brainstem (%)*		5 (62.5)	1 (20.0)
Median EDSS at nadir (range)§		4.0 (3.0 – 10.0)	3.5 (2.5 – 8.5)
Median CSF leucocyte count (cells/µL) (range)		4.5 (0 – 489)	1 (0 – 19)
Median CSF protein (g/L)†		1.13 (0.37 – 6.81)	0.32 (0.23 – 0.91)
Patients with unmatched CSF OCBs (%)††		0	2 (50.0)
N acute treatment (%)		8 (100)	5 (100)
	N PO or IV steroid (%)	7 (87.5)	5 (100)
	N IVIg (%)	3 (37.5)	0
	N PLEX (%)	6 (66.7)	1 (20)
N oral steroid taper > 1 month		4 (50)	4 (80.0)
Median follow up time (range) (months)		38 (17 – 44)	42 (5 – 44)
Median EDSS at last review (range)§		3.0 (0 – 10.0)	2.0 (1.0 – 3.0)
N with good outcome (%)		2 (25.0)	2 (40.0)
N with moderate outcome (%)		3 (37.5)	3 (60.0)
N with poor outcome (%)		3 (37.5)	0
N relapsers (%)		1 (12.5)	0
N with final diagnosis MS (%)		0	2 (40)

*This does not This does not include the 3 patients with lower motor neuron facial weakness
§ N ChAdOx1S = 8, including 1 patient who died. Excluding this patient reduces median EDSS at nadir to 3.5 and median EDSS at follow-up to 2.5; N BNT162b2 = 4
†N ChAdOx1S = 7; N BNT162b2 = 5 (CSF protein concentration of 6.81 g/L was verified. Patient had concomitant demyelinating polyradiculoneuropathy)
†† N ChAdOx1S = 7; N BNT162b2 = 5

ChAdOx1S recipients were older than BNT162b2 recipients (median ages 42.5 years and 27 years, respectively), reflecting JCVI guidance (255,256). Median interval between vaccination and disease onset was

shorter among ChAdOx1S recipients (11 days) than BNT162b2 recipients (32 days) and all patients presented within 42 days of vaccination.

One ChAdOx1S recipient had a history of psoriatic arthritis and another had IgA glomerulonephropathy and cerebral palsy. One BNT162b2 recipient had type 1 diabetes mellitus and another had urticaria and idiopathic angioedema.

As observed in the post-vaccine MOGAD cohort, TM was more common among ChAdOx1S recipients (6/8; 75%) than BNT162b2 recipients (3/5; 60%). Symptomatic brain lesions accounted for 2/8 (25%) of post-ChAdOx1S presentations and none of the post-BNT162b2 presentations. ON was more common after BNT162b2, affecting 3/8 (37.5%) ChAdOx1S recipients but 3/5 (60.0%) BNT162b2 recipients (fig 37).

Figure 37. Proportions of clinical phenotypes among post-vaccine seronegative AICS patients by vaccine type

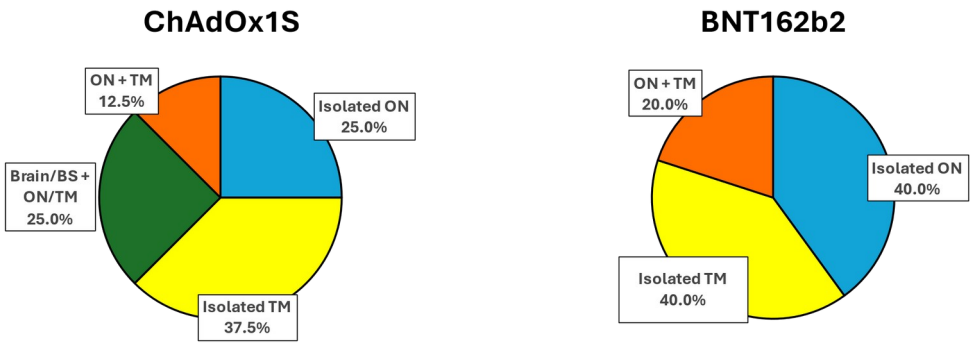

Of the 12 patients with data available, median EDSS score at nadir was 3.75 and was similar in both vaccine groups (4.0 after ChAdOx1S and 3.5 after BNT162b2). The highest EDSS score among ChAdOx1S

recipients was 10 (death due to disease), which occurred in a 44-year-old man with IgA glomerulonephropathy and cerebral palsy.

All patients received rescue therapy, 12 (92.3%) with intravenous or oral steroid and 1 (7.7%) with IVIg for presumed GBS. Six (75.0%) ChAdOx1S recipients required treatment escalation. Only 1 (20%) BNT162b2 required treatment escalation, reflecting the greater incidences of TM and brain lesions among ChAdOx1S recipients.

An unusual phenotype amongst seronegative ChAdOx1S recipients

Simultaneous focal or generalised neuropathies and AICS were diagnosed in 5/13 (38.5%) of the post-ChAdOx1S seronegative cohort, all after the first dose. The combination of acute CNS and PNS pathology was not observed in the post-BNT162b2 cohort.

The first patient developed a rapidly progressive ADEM-like disease with dramatic brain and spinal cord lesions (fig 38). Nerve conduction studies revealed a widespread sensorimotor neuropathy with axonal and demyelinating features. CSF protein was 4.48 g/L and GBS was considered. No causative antibody was detected. This patient died of ADEM 31 days after vaccination.

The second case presented with bilateral ON and facial diplegia 11 days after their first ChAdOx1S vaccine. An MRI confirmed bilateral T2 hyperintensity and gadolinium enhancement of the geniculate ganglia

and facial nerves (fig 39). CSF protein concentration was elevated at 1.13 g/L.

The third patient presented 8 days after vaccination with back pain and leg paraesthesia followed by facial diplegia, headache, meningism and Lhermitte’s phenomenon. An MRI of the spinal cord at onset was unremarkable, nerve conduction studies confirmed patchy peripheral demyelination and CSF analysis revealed a markedly elevated protein concentration of 6.81 g/L with pleiocytosis. A repeat MRI scan of the spinal cord 5 months after symptom onset confirmed a short thoracic cord lesion.

The fourth patient presented 19 days after the ChAdOx1S vaccine with left lower motor neuron facial weakness, distal paraesthesia, leg weakness and urinary urgency. An MRI confirmed TM (fig 40) and enhancement of the left facial nerve in the internal acoustic meatus.

The final patient presented with confusion, somnolence, seizures and flaccid paraparesis 16 days after vaccination. Nerve conduction studies were not undertaken. CSF protein concentration was elevated at 3.30 g/L. An MRI of the brain and spinal cord revealed multifocal ADEM-like lesions affecting white and grey matter and LETM (fig 41). This patient tested positive for acute Hepatitis E virus.

Figure 38a-d. MRI brain and spinal cord of a 44-year-old post-ChAdOx1S seronegative patient presenting with ophthalmoplegia, flaccid paraparesis,rhomboencephalitis and ventilatory failure

a) Sagittal T2 weighted FLAIR brain MRI. Multifocal hyperintensities throughout the white matter and deep grey matter

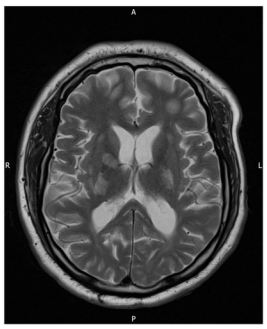

b) Axial T2 weighted brain MRI. Multifocal ill-defined hyperintensities affecting the white matter, basal ganglia and thalami

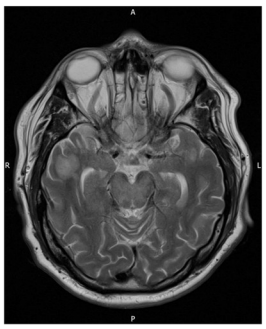

c) Axial T2 weighted brain MRI. Multifocal hyperintensities including within the right inferior temporal lobe and midbrain

d) Sagittal T2 weighted MRI spinal cord. LETM extending from the cervicomedullary junction to the lower thoracic cord

Figure 39a & b. MRI brain of a 50-year-old post-ChAdOx1S seronegative patient presenting with seronegative optic neuritis and facial diplegia

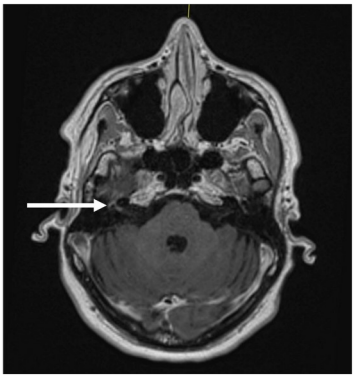

a) Axial post-gadolinium T1 weighted MRI brain. Contrast enhancement of the right facial nerve and geniculate ganglion

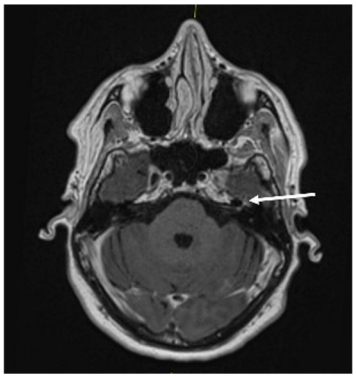

b) Axial post-gadolinium T1 weighted MRI brain. Contrast enhancement of the left facial nerve and geniculate ganglion

Figure 40a & b. MRI spinal cord of a 41-year-old post-ChAdOx1S seronegative patient presenting with transverse myelitis and unilateral facial palsy

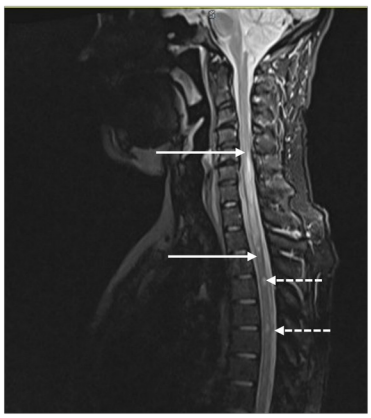

a) Sagittal T2 weighted spinal cord MRI. Long central cord lesion with oedema extending from the level of C5 to T3 (solid arrows) with shorter cord lesions in thoracic cord

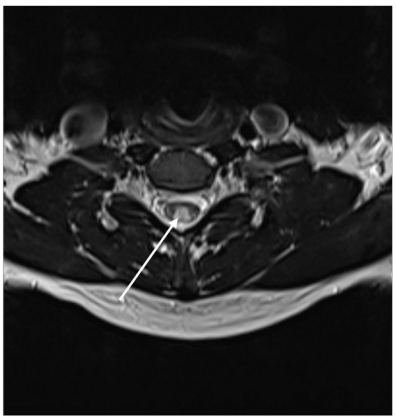

b) Axial T2 weighted cervical cord MRI. Hyperintensity predominantly affecting the central and dorsal spinal cord (arrow)

Figure 41a & b. MRI brain and spinal cord of a 40-year-old post-ChAdOx1S seronegative patient presenting with confusion, seizures and flaccid paraparesis

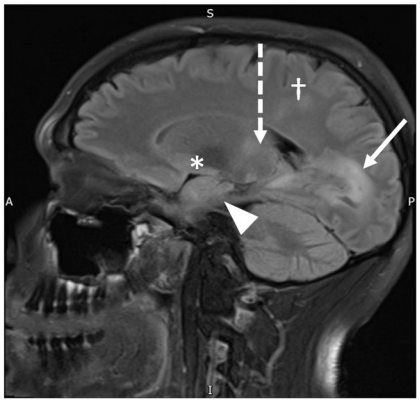

a) Sagittal T2 weighted FLAIR brain MRI. Multifocal lesions within occipital lobe (solid arrow), thalamus (dashed arrow), hypothalamus (asterisk), midbrain (arrowhead) and cerebral white matter (†)

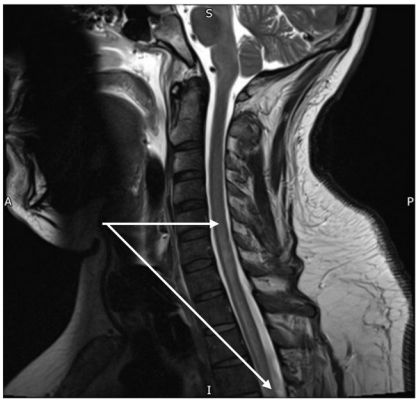

b) Sagittal T2 weighted cervical spine MRI. Longitudinally extensive lesion from mid-cervical to upper thoracic cord (arrow, lower boundary not captured here)

Paraclinical data (see table 32 & 34)

Investigations varied between patients. One ChAdOx1S recipient tested positive for Hepatitis E virus (see above). One patient’s serum tested positive for Borrelia IgM but they died before further tests were undertaken (see above). Their presentation was not consistent with Lyme disease. Antinuclear antibodies were detected in one patient. No other patient had an infectious or autoimmune cause of their symptoms found.

Two patients were tested for SARS-CoV-2 anti-N antibodies. One was positive, the other negative at 12 months after symptom onset.

Inflammatory parenchymal brain lesions were observed in 5/8 (62.5%) ChAdOx1S recipients (fig 38, 41 & 42). Facial nerve hyperintensity and enhancement were seen on MRI scans of a further 3 ChAdOx1S recipients. In contrast, only 1/5 (20%) BNT162b2 recipients had intracranial lesions. These consisted of multiple well-circumscribed periventricular and juxtacortical cerebral lesions, consistent with a diagnosis of MS (fig 43).

Four (50.0%) ChAdOx1S recipients had LETM (fig 38, 40 – 42) and 2 (25.0%) had short cord lesions. Only 1 (20.0%) BNT162b2 recipient had LETM. Two (40.0%) had short cord lesions, including the patient with other radiological features of MS (fig 43).

Figure 42a-c. MRI brain and spinal cord of a 35-year-old post-ChAdOx1S seronegative patient presenting with back pain and tetraparesis

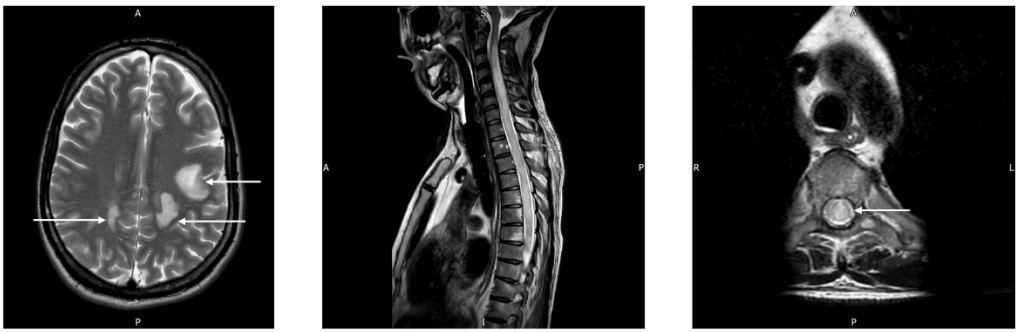

a) Axial T2 weighted brain MRI. Well-defined biparietal white matter T2 hyperintensities (arrows)

b) Sagittal T2 weighted cervicothoracic spinal cord MRI. Hyperintensity and oedema from the cervicothoracic junction to the conus

c) Axial T2 weighted thoracic spinal cord MRI. Hyperintensity and swelling affecting the whole diameter of the cord (arrow)

Figure 43a-c: MRI brain and spinal cord of an 18-year-old post-BNT162b2 seronegative patient presenting with paraparesis and urinary incontinence

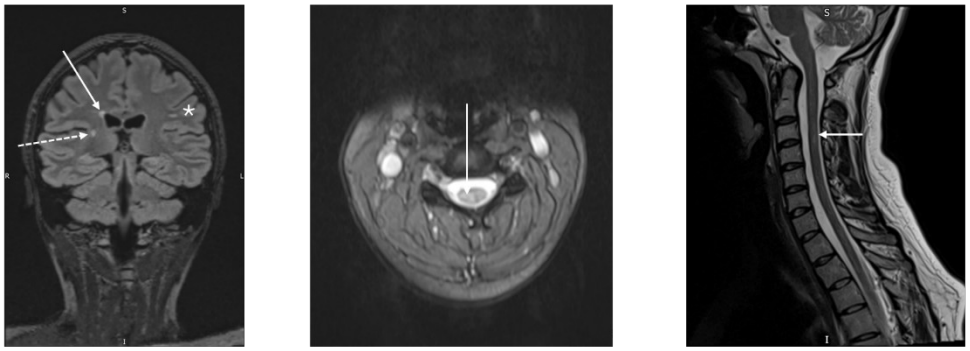

a) Coronal T2 weighted FLAIR MRI brain. Well-defined periventricular (solid arrow), juxtacortical (dashed arrow) and deep white matter (asterisk) lesions, typical of MS

b) Axial T2 weighted cervical spinal cord MRI. T2 hyperintensity involving right hemicord (arrow)

c) Sagittal T2 weighted cervicothoracic spinal cord MRI. Short cervical spine hyperintensity (arrow)

All seronegative patients underwent CSF analysis. Median CSF leucocyte count was within normal range in the post-ChAdOx1S and post-BNT162b2 groups (4.5/μL and 1/μL, respectively), although two patients in the ChAdOx1S group had CSF leucocyte counts of >50/μL. Median protein was elevated in the ChAdOx1S recipients (1.13 g/L) but not the BNT162b2 recipients (0.32 g/L). Four ChAdOx1S recipients had CSF

protein concentrations >1 g/L, all had focal or generalised neuropathies and 2 had ADEM.

Unpaired oligoclonal bands were detected in none of the CSF samples from ChAdOx1S recipients and in 2/5 (40%) of CSF samples from BNT162b2 recipients, including one patient with multiple MS-like lesions on MRI.

Post-mortem brain and spinal cord biopsies were available from one seronegative ChAdOx1S recipient. The cortex and white matter were grossly oedematous. Histological examination of the cerebrum and brainstem showed demyelination with relative axonal sparing and perivascular infiltrates of foamy macrophages and T lymphocytes (fig 44). These features are characteristic of ADEM.

Figure 44a-c. Post-mortem biopsy specimens taken from a post-ChAdOx1S seronegative patient with ADEM and flaccidtetraparesis

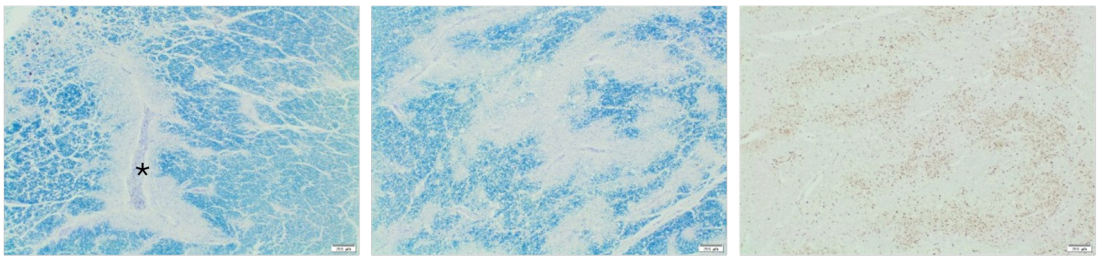

a) Luxol fast blue staining of section through cerebral peduncle. Asterisk represents a blood vessel with surrounding pallor caused by demyelination

b) Luxol fast blue staining of section through cerebral peduncle with patchy demyelination (white)

c) CD68 (macrophage) staining of region of cerebral peduncle adjacent to b. Densest macrophage infiltration (brown) corresponds with areas of demyelination in b

Images courtesy of Dr Monika Hofer

Longitudinal outcomes (see table 32 & 34)

Median follow-up time was similar- 38 months for the ChAdOx1S cohort and 42 for the BNT162b2 cohort. One ChAdOx1S recipient relapsed with ON and commenced azathioprine. None of the BNT162b2 recipients had

further clinical events. However, both BNT162b2 recipients with CSF-restricted oligoclonal bands developed silent intracranial lesions on serial imaging and both have been diagnosed with MS and commenced disease modifying therapies.

Median EDSS score at last follow-up was 2.0 (range 1.0 – 10)[17]. Although median final EDSS scores were similar, 2/7 (28.6%) surviving ChAdOx1S recipients had final EDSS scores > 6.0, whereas the maximum EDSS score among BNT162b2 recipients was 3.0.

Four patients (30.8%) had good outcomes, 6 (46.2%) had moderate outcomes and 3 (23.1%) had poor outcomes. All patients with poor outcomes received ChAdOx1S.

In summary, like post-ChAdOx1S MOGAD patients, post-ChAdOx1S seronegative AICS cases typically presented with TM, sometimes in conjunction with intracerebral lesions. Five (62.5%) ChAdOx1S recipients presented with generalised or facial neuropathies, often with hyperproteinorrachia.

Relapses were rare in the seronegative cohort. Outcomes were generally poorer among ChAdOx1S recipients, reflecting the higher incidence of ADEM and LETM. Two of the BNT162b2 recipients have been diagnosed with MS.

[17] If the patient who died is excluded, median EDSS score remains 2.0 (range 1.0 – 8.0).

aii) Analysis by diagnosis (full cohort): Post-vaccine AQP4+ NMOSD

Only 3 cases of new-onset AQP4+ NMOSD presented within 8 weeks of SARS-CoV-2 vaccination. Two occurred following first-dose ChAdOx1S and one followed the second BNT162b2 vaccine.

Due to small numbers, comparison of clinical and paraclinical features between vaccine types was not performed. All patients were female and all identified as Afro-Caribbean. None had pre-existing autoimmune or neurological disease. Each case is outlined below and information is summarised in table 32.

One 28-year-old presented with symptoms of brainstem and spinal cord inflammation the day following her first ChAdOx1S vaccination. An MRI confirmed cervical LETM, a discrete pontine lesion and periependymal enhancement, typical of AQP4+ NMOSD (fig 45). CSF confirmed a lymphocytosis (41 cells/μL) with normal protein concentration (0.3 g/L) and no oligoclonal bands. An autoimmune screen detected antibodies to nuclear antigens, DNA and Ro. There were no clinical features of systemic lupus erythematosus or sicca syndrome. She received IV methylprednisolone acutely followed by an oral prednisolone taper. Due to personal preferences, the patient remained on only prednisolone for over a year before relapsing with TM. She subsequently commenced ciclosporin. Thirty-six months after onset her EDSS score was 0 and her outcome was good.

Figure 45a-c. MRI brain and spinal cord of 28-year-old post-ChAdOx1S AQP4+ NMOSD patient presenting with unilateral neck and facial pain, diplopia and hand paraesthesia and weakness

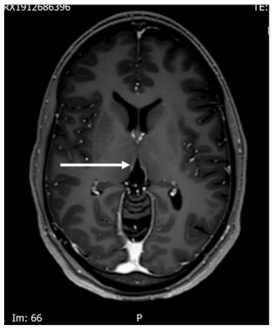

a) Axial post -gadolinium T1 weighted MRI brain. Subtle periependymal contrast enhancement (arrow), described in AQP4+ NMOSD

b) Axial T2 weighted cervical spinal cord MRI. Bright spotty lesions (arrow), described in AQP4+ NMOSD

c) Sagittal T2 weighted cervical spine MRI. Cervical LETM (arrows)

Another patient presented at age 50 years with reduced visual acuity, area postrema syndrome and diplopia 25 days after her first ChAdOx1S vaccine. She had a history of Hepatitis B infection but her viral load was undetectable at onset of neurological symptoms. An MRI revealed T2 hyperintensities in the periaqueductal grey typical of area postrema syndrome with additional lesions in the brainstem and cervical cord, despite absence of myelopathic signs or symptoms (fig 46). CSF analysis was unremarkable (lymphocyte count 5/μL, protein concentration 0.43g/L, no unmatched oligoclonal bands). An autoimmune screen detected antibodies to nuclear antigens, DNA and smooth muscle but there were no features of systemic lupus erythematosus or autoimmune hepatitis. She received IV methylprednisolone and plasma exchange (PLEX), followed by mycophenolate mofetil and long-term prednisolone. AQP4 antibodies were below the threshold of detection 18 months after her attack. At 41

months after onset there were no relapses, outcome was moderate and EDSS score at last follow-up was 2.0.

Figure 46a-c. MRI brain and spinal cord of a 50-year-old post-ChAdOx1S AQP4+ NMOSD patient presenting with area postrema syndrome, diplopia and unilateral optic neuritis

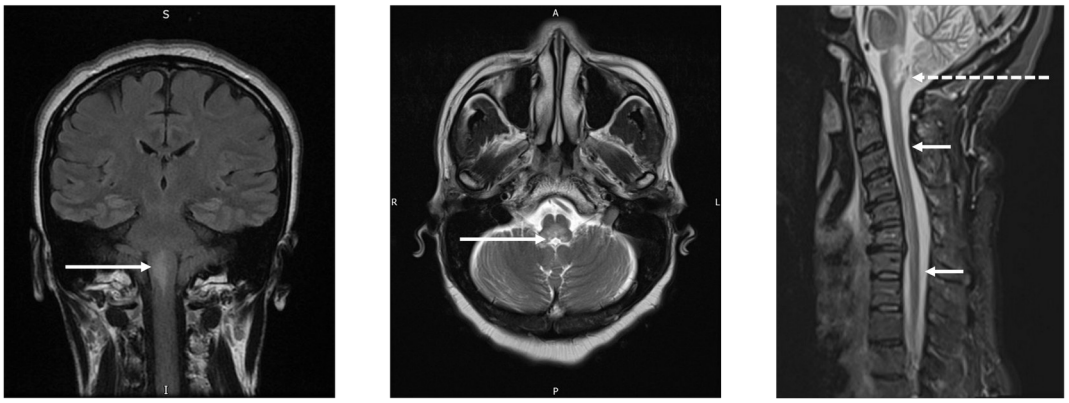

a) Coronal T2 weighted FLAIR MRI brain. Poorly-defined medullary lesion (arrow)

b) Axial T2 weighted MRI brain. Poorly-defined lesion abutting fourth ventricle (arrow)

c) Sagittal T2 weighted cervical MRI spine. Asymptomatic central cord lesion (solid arrows) and posterior medullary lesion (dashed arrow)

The final patient presented at age 46 years with reduced visual acuity in the left eye 55 days after her second BNT162b2 vaccine. She had a history of type 2 diabetes mellitus. An MRI of the brain was normal but no dedicated orbital imaging was obtained and CSF was not sampled. An autoimmune screen detected antibodies to nuclear antigens, DNA and Ro but there were no symptoms or signs of systemic lupus erythematosus or sicca syndrome. She received a 5-day course of oral methylprednisolone but no tapering course of steroid. AQP4 antibodies were not checked at the time of presentation. The patient relapsed with TM the following year. AQP4 antibodies were assayed approximately 2 years after her initial presentation. She started oral prednisolone but

relapsed again with TM, after which rituximab infusions were commenced. After a follow-up of 39 months, outcome was moderate and EDSS score was 4.0.

In summary, 3 patients presented with a first attack of AQP4+ NMOSD within 8 weeks of SARS-CoV-2 vaccination, including one who developed symptoms within 24 hours of vaccination and one who developed symptoms 55 days later. Demographic, clinical and radiological features were largely typical of AQP4+ NMOSD. All had evidence of immune dysregulation with antibodies to nuclear antigens and DNA, which are often present in patients with AQP4+ NMOSD.

b) Proportion of new-onset AICS occurring within 8 weeks of SARS-CoV-2 vaccination (John Radcliffe Hospital cohort)

By September 2024, Oxford NMODAS had reviewed 57 adult patients with first episode AICS in the 60 weeks from 1st December 2020 to 26th January 2022 at the John Radcliffe Hospital (fig 47). Of these, over half (29; 50.9%) occurred within 8 weeks of a SARS-CoV-2 vaccination.

Figure 47. Patients with new AICS between 1st December 2020 and 26th January 2022 reviewed by Oxford NMODAS at the John Radcliffe Hospital

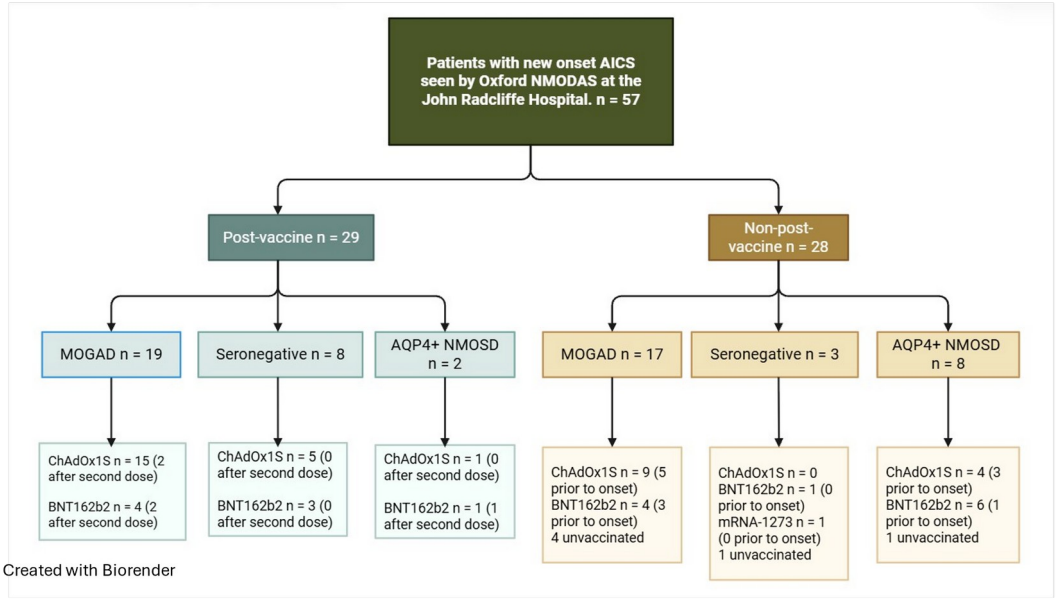

2 AQP4+ NMOSD patients received both ChAdOx1S and BNT162b2 between 1st December 2000 and 1st December 2021. Vaccines listed for post-vaccine patients are vaccines received within 8 weeks prior to disease onset. In all non-post-vaccine diagnostic categories, most vaccinated patients received multiple doses of the same vaccine during the period of interest.

There were 36 instances of new-onset MOGAD over the 60-week observation period, of which 19 (52.8%) occurred in the 8 weeks following vaccination (15 after ChAdOx1S, 4 after BNT162b2).

Eleven patients had seronegative AICS. Eight (72.7%) occurred within 8 weeks of SARS-CoV-2 vaccination, (5 after ChAdOx1S and 3 after BNT162b2).

Ten patients had new onset AQP4+ NMOSD. Two (20%) occurred within 8 weeks of SARS-CoV-2 vaccination, 1 after ChAdOx1S vaccination and 1 after BNT162b2.

c) Index dose analysis (John Radcliffe Hospital cohort)

c.i) Index dose analysis for all AICS

Twenty-one (72.4%) of the post-vaccine cases seen at the John Radcliffe Hospital followed ChAdOx1S and 8 (27.6%) followed BNT162b2.

Of the 28 non-post-vaccine AICS patients, 6 (21.4%) received no SARS-CoV-2 vaccines between December 2020 and December 2021 and 10 received a first SARS-CoV-2 vaccine after disease onset (fig 47).

The remaining 12 non-post-vaccine cases with disease onset after vaccination were included in index dose analyses. Eight had received ChAdOx1S and 4 had received BNT162b2 most recently.

The OR of a post-vaccine patient having received ChAdOx1S versus alternative compared with a non-post-vaccine case prior to onset was 1.30 ($p = 0.72$).

c.ii) Index dose analysis for MOGAD

Of the 19 post-vaccine MOGAD cases, 15 (78.9%) followed ChAdOx1S and 4 (21.1%) followed BNT162b2.

Of the 17 non-post-vaccine MOGAD patients, 8 received at least one SARS-CoV-2 vaccine prior to symptom onset. Five had received ChAdOx1S most recently and 3 had received BNT162b2 most recently. The OR of a post-vaccine MOGAD patient having received ChAdOx1S versus alternative compared with a non-post-vaccine case was 2.18 ($p = 0.63$).

c.iii) Index dose analysis for seronegative AICS

Of the 8 post-vaccine seronegative AICS cases, 5 (62.5%) experienced symptom onset after ChAdOx1S and 3 (37.5%) experienced symptom onset after BNT162b2.

All 3 non-post-vaccine seronegative cases were unvaccinated prior to onset so index dose analysis was not possible.

d) Relapse on revaccination

Of the post-ChAdOx1S AICS cases, 11/21 (52.4%) were not vaccinated against SARS-CoV-2 again, 4 (19.0%) received at least one further ChAdOx1S vaccine and 6 (28.6%) received at least one further alternative. Of the post-BNT162b2 cases, 5/8 (62.5%) were not revaccinated and 3 (37.5%) had at least one further dose of BNT162b2.

None of the 13 patients who were revaccinated after their first attack had a relapse within 8 weeks of revaccination.

Summary: New instances of MOGAD and seronegative NMOSD seen by the Oxford NMODAS between December 2020 and January 2021 clustered in the 8 weeks after patients received their SARS-CoV-2 vaccinations. The majority of cases followed ChAdOx1S. Post-vaccine MOGAD patients were twice as likely to have received ChAdOx1S prior to onset as non-post-vaccine vaccinated patients, but this did not reach statistical significance.

Chapter 8

Post-SARS-CoV-2 vaccine acute inflammatory CNS syndromes part 2: Epidemiological and statistical analyses (focus on MOGAD)

8.1) Methods: Epidemiological and statistical analyses

The data presented in chapter 7 suggested an association between the ChAdOx1S vaccine and AICS, particularly with MOGAD. The following analyses focus on this potential relationship.

a) Conditional odds ratios of receiving ChAdOx1S versus alternative in the post-vaccine AICS, MOGAD and seronegative AICS cohorts compared with the English population

Because vaccine dominance in the post-vaccine AICS group and subgroups could reflect national patterns of vaccination, the proportions were compared with the patterns of vaccination observed in the English population.

Odds of a post-first-dose AICS patient receiving ChAdOx1S versus alternative SARS-CoV-2 vaccine prior to onset were calculated as described in appendix 16. For the remainder of the text, the post-first-SARS-CoV-2 vaccine-onset AICS, MOGAD and seronegative groups will be referred to as the *post-first-dose AICS group*, the *post-first-dose MOGAD group* and the *post-first-dose-seronegative group*, respectively.

Upon request, the MHRA provided vaccine records that included the number of vaccines administered each week in England between 7th December 2020 and 5th December 2022, sorted by brand, dose number and age.

The conditional odds of receiving a first dose of ChAdOx1S in the adult English population were calculated as described in appendix 16.

Conditional ORs were calculated as the odds of a post-first-dose AICS patient receiving a first dose ChAdOx1S vaccine versus alternative compared with the odds of a first-dose vaccine recipient in the English population receiving ChAdOx1S.

Following the publication of guidance by the JCVI in May 2021 recommending avoidance of ChAdOx1S in people under 40 years old (255,256), there was a shift in the age-specific proportions of people receiving ChAdOx1S. To account for this, data were stratified according to date of vaccination (7th December 2020 to 2nd May 2021 versus 3rd May 2021 to 5th December 2021) and age at vaccination (18 – 39 years versus ≥ 40 years).

ORs were calculated for the whole post-vaccine AICS, MOGAD and seronegative cohorts.

It was important to determine whether any significant ORs were limited to comparisons between the post-vaccine AICS and MOGAD groups with the English population or whether the same pattern was observed in non-post-first-dose cases. The latter would indicate some shared

demographic variable amongst people with MOGAD that increased risk of receiving a certain vaccine, rather than a certain vaccine increasing risk of MOGAD (reverse causality).

To exclude this, analysis was repeated for the post-first-dose AICS cases seen at the John Radcliffe Hospital *and* for new-onset AICS cases who received at least one dose of SARS-CoV-2 vaccine between 1st December 2020 and 31st November 2021 but experienced symptom onset outside the 8-week post-exposure period (the "non-post-first-dose AICS" cohort). In this way, it was possible to directly compare the conditional ORs of post-first-dose AICS and non-post-first-dose AICS. Similar ORs in both groups would suggest a common risk factor for exposure to ChAdOx1S and to AICS, rather than causality (appendix 16). Limiting analyses to the John Radcliffe Hospital populations also permitted comparison of the conditional odds of receiving a first dose of ChAdOx1S in the post-first-dose AICS group and the non-post-first-dose AICS group.

b) Self-controlled case series (John Radcliffe Hospital cohort)

The self-controlled case series (SCCS) is a method of modelling the incidence rate ratio or hazard ratio following an exposure. Like a cohort study, the incidence or hazard of an event in the presence of an exposure is compared with the incidence or hazard in the absence of an exposure. Unlike a cohort study, comparison is not between exposed and unexposed groups, but rather between exposed and unexposed

periods in the same individual (230). This means time-invariant influences on incidence rate (race, socioeconomic status etc) that would need to be controlled for in cohort or case-control studies can be ignored (230,257).

The SCCS also has features of a case-control study, in that cases are identified and times of exposures sought retrospectively, meaning the event of interest can be rare (258).

The SCCS models the *conditional* likelihood of the distribution of the events observed. It does not address the question, “what is the risk of an event after an exposure?”, but rather, “given an event occurs, how much more likely is it to occur following an exposure compared with a period outside the post-exposure window?” (257). The statistic of interest is the *change* in incidence rate between exposed and unexposed periods, i.e., the incidence rate ratio (IRR). This is useful when the population at risk of the event and population/ baseline incidence rate are unknown (230).

The SCCS method has been used in multiple studies of vaccines (257,259,260), including SARS-CoV-2 vaccines (247,248,261).

For a more detailed explanation of the rationale, see appendix 17.

The populations of interest were patients with new-onset AICS, MOGAD and seronegative AICS cases seen by the NMODAS at the John Radcliffe Hospital[18]. The events of interest were first attack of AICS, MOGAD or seronegative AICS and the exposure was first dose of ChAdOx1S

[18] By definition, only those exposed to ChAdOx1S were included in the analyses

vaccine. The risk period was an 8-week interval starting on the day of vaccination (appendix 17).

The SCCS package available via the CRAN website (262) was used to calculate the incidence rate ratio using R (v4.4.1) (163). Codes were adapted from those published by Farrington and colleagues (257).

For the combined AICS group, the MOGAD group and seronegative AICS group, model 1 examined the IRR of onset of all first attacks during the 8-week window after the first ChAdOx1S vaccine. Sensitivity analysis was conducted by reducing the post-exposure risk period to 6 weeks in model 2.

c) Seasonality of MOGAD attacks, focusing on onset attacks (John Radcliffe Hospital cohort)

Another epidemiological method of identifying associations between a potential environmental exposure and disease is to compare the timings of the peak of exposure with the peak of disease incidence. If exposure is a trigger, the peak of the population exposures should coincide with or slightly precede the peak in disease incidence. It is important to identify seasonal peaks in the absence of an exposure.

Other studies have used temporal trends to identify AEFIs. For example, the association between the Pandemrix influenza vaccine and a 17-fold increased risk of narcolepsy in Finland was identified because the peak

incidence closely followed the highest vaccine administration rates (260,263).

The Oxford NMODAS REDCap and Microsoft Access™ databases were interrogated for all MOGAD onset attacks and relapses occurring in adults between 1st January 2010 and 31st December 2021. Only patients meeting Banwell criteria for diagnosis of MOGAD were included (46). If there was uncertainty regarding the date, veracity or phenotype of the attack, the patient's electronic and paper records were checked and the local consultant was contacted for clarification. Attacks without sufficient data or attacks occurring within 1 month of a preceding attack were excluded.

Seasonality analysis was performed for total attacks, onset attacks and relapses. Attacks between 2010 and 2020 were combined to improve the power of the analyses to detect seasonal fluctuations. Data from 2021 were analysed separately to determine whether seasonal patterns of attacks during the vaccine roll-out differed to those of preceding years.

Seasonality was assessed using Edwards' test with Roger's modification (appendix 18). The primary outcomes were seasonality of total attacks and seasonality of onset attacks. The significance threshold was set at $\alpha \leq 0.05$.

Statistical analysis was performed using the DESCRIBE package within WINPEPI, version 3.18 (264). This automatically adjusts for length of month.

8.2) Results: Epidemiological and statistical analyses

a) Conditional odds ratios of receiving ChAdOx1S versus alternative in the post-vaccine AICS cohort and subgroups compared with the English population

For English population and AICS cohort figures for SARS-CoV-2 vaccination statistics, see table 35a-e.

a.i) Conditional odds ratio of receiving ChAdOx1S versus alternative in the post-first-dose AICS cohort compared with the English population (whole cohort)

Post-first-dose AICS patients had statistically significantly higher odds of receiving a first dose of ChAdOx1S versus alternative than the rest of the vaccinated English population (OR 4.82, $p < 0.001$) (table 35a & 36). This was also true when analyses were limited to post-first-dose patients vaccinated between 7th December 2020 and 2nd May 2021 (OR 11.49, $p <0.001$), patients vaccinated at ages 18 – 39 years (OR 5.42, $p = 0.005$) and patients vaccinated at age ≥40 years (OR 9.92, $p = 0.003$). The odds of a post-first-dose AICS patient vaccinated between 3rd May 2021 and 5th December 2021 receiving ChAdOx1S were higher than those of the English population receiving a first dose vaccine during the same period (OR 3.73) but this did not reach statistical significance (tables 35a – e & 36).

a.ii) Conditional odds ratios of receiving a first dose of ChAdOx1S versus alternative in the post-first-dose and non-post-first-dose AICS group (John Radcliffe Hospital cohort)

The conditional odds of post-first-dose AICS patients seen at the John Radcliffe Hospital receiving a first vaccination with ChAdOx1S versus alternative compared with the English population were similar to those of the overall post-first-dose AICS cohort (OR 3.66, p = 0.007). ORs in the John Radcliffe post-first-dose AICS group after stratifying by age and date of vaccination were similar to results from the whole post-first-dose AICS cohort (table 36).

Post-first-dose AICS patients seen at the John Radcliffe Hospital were over 3 times more likely to have received a first dose of ChAdOx1S versus alternative than non-post-first dose AICS patients (OR 3.22, p = 0.080).

The conditional odds of a non-post-first-dose AICS patient see at the John Radcliffe Hospital having received a first dose ChAdOx1S versus alternative compared with the conditional odds in the English population was 1.11 (p = 0.851), i.e., lower than the significant OR of 3.66 in post-first-dose AICS cases.

After stratifying by date and age at vaccination, the conditional odds of a non-post-vaccine AICS case receiving a first dose of ChAdOx1S were not significantly greater than the odds in the English population. This is

in contrast to the results for post-first-dose AICS cases seen at the John Radcliffe, which demonstrated significantly higher conditional odds of vaccination with ChAdOx1S than the English population for all subgroups other than the group vaccinated between 3rd May and 5th December 2021 (table 36).

Table 35: Numbers of first-dose vaccine recipients aged ≥ 18 years in English population and post-first-dose AICS cohorts

a. English population and AICS cohort, 7th December 2020 - 5th December 2021

	English population*	Post-first-dose AICS (whole cohort)	Post-first-dose AICS (Oxford)	Non-post-first-dose AICS (Oxford)	Post-first-dose MOGAD (whole cohort)	Post-first-dose MOGAD (Oxford)	Non-post-first dose MOGAD (Oxford)	Post-first-dose seronegative AICS
ChAdOx1S	20,592,816	25	19	15	15	13	11	5
Alternative	19,864,445	5	5	13	2	2	6	3

b. English population and AICS cohort, 7th December 2020 – 2nd May 2021

	English population*	Post-first-dose AICS (whole cohort)	Post-first-dose AICS (Oxford cohort)	Non-post-first-dose AICS (Oxford)	Post-first-dose MOGAD (whole cohort)	Post-first-dose MOGAD (Oxford)	Non-post-first dose MOGAD (Oxford)	Post-first-dose seronegative AICS
ChAdOx1S	19,216,314	23	17	14	14	12	10	4
Alternative	9,600,527	1	1	2	0	0	0	1

c. English population and AICS cohort,3rd May 2021 – 5th December 2021

	English population*	Post-first-dose AICS (whole cohort)	Post-first-dose AICS (Oxford cohort)	Non-post-first-dose AICS (Oxford)	Post-first-dose MOGAD (whole cohort)	Post-first-dose MOGAD (Oxford)	Non-post-first dose MOGAD (Oxford)	Post-first-dose seronegative AICS
ChAdOx1S	1,376,502	2	2	1	1	1	1	1
Alternative	10,263,918	4	4	11	2	2	6	2

d. English population and AICS cohort aged 18 - 39 years, 7th December 2020 – 5th December 2021

	English population*	Post-first-dose AICS (whole cohort)	Post-first-dose AICS (Oxford cohort)	Non-post-first-dose AICS (Oxford)	Post-first-dose MOGAD (whole cohort)	Post-first-dose MOGAD (Oxford)	Non-post-first dose MOGAD (Oxford)	Post-first-dose seronegative AICS
ChAdOx1S	2,722,975	7	5	5	5	4	5	0
Alternative	10,532,761	5	5	10	2	2	6	3

e. English population and AICS cohort aged≥ 40 years, 7th December 2021 – 5th December 2021

	English population*	Post-first-dose AICS (whole cohort)	Post-first-dose AICS (Oxford cohort)	Non-post-first-dose AICS (Oxford)	Post-first-dose MOGAD (whole cohort)	Post-first-dose MOGAD (Oxford)	Non-post-first dose MOGAD (Oxford)	Post-first-dose seronegative AICS
ChAdOx1S	17,869,841	18	14	10	10	9	6	5
Alternative	9,331,684	0	0	3	0	0	0	0

Data courtesy of MHRA

Table 36: ORs of receiving first-dose ChAdOx1S vs alternative in the post-first-dose AICS cohort compared with thevaccinated adult English population

	Post-first-dose AICS (whole cohort)	Post-first-dose AICS (Oxford)	Non-post-first-dose AICS (Oxford)	Post-first-dose MOGAD (whole cohort)	Post-first-dose MOGAD (Oxford)	Non-post-first-dose MOGAD (Oxford)	Post-first-dose seronegative AICS
OR all dates, all ages	4.82 (1.81 – 16.13)**	3.66 (1.32 – 12.57)**	1.11 (0.49 – 2.54)	7.23 (1.68 - 65.27)**	6.27 (1.42 - 57.16)**	1.77 (0.60 – 5.83)	1.61 (0.31 – 10.36)
OR 7th Dec 2020 – 2nd May 2021, all ages	11.49 (1.87 – 472.43)**	8.49 (1.33 - 354.44)**	3.50 (0.80 – 31.70)	7.49 (1.15-315.08)*	6.50 (0.98 - 275.71)*	5.50 (0.80 - 236.33)	2.00 (0.20 – 98.38)
OR 3rd May 2021 – 5th Dec 2021, all ages	3.73 (0.34 – 26.02)	3.73 (0.34 –26.02)	0.68 (0.02 – 4.66)	3.73 (0.06 – 71.77)	3.73 (0.06 – 71.77)	1.24 (0.03 – 10.24)	3.72 (0.06 – 71.77)
OR age 18 – 39 years, all dates	5.42 (1.48– 21.64)**	3.87 (0.89 – 16.82)*	1.93 (0.52 – 6.21)	9.67 (1.58 – 101.58)**	7.73 (1.11 – 85.70)*	3.22 (0.78 – 12.68)	1.86 (0.04 – 18.84)
OR age ≥ 40 years, all dates	9.92 (1.58 – 411.56)**	7.83 (1.21 -329.31)*	1.74 (0.45 - 9.84)	5.74 (0.83 – 247.01)	5.22 (0.74 – 226.42)	3.66 (0.47 - 164.64)	3.13 (0.38 – 144.04)

Data presented are ORs (95% confidence intervals); *p ≤ 0.05; **p ≤ 0.01

a.iii) Conditional odds ratios of receiving ChAdOx1S versus alternative in the post-first-dose MOGAD cohort compared with the English population (whole cohort)

Post-first-dose MOGAD patients had statistically significantly higher odds of receiving ChAdOx1S than the rest of the vaccinated English population (OR 7.23, p = 0.002) (table 35a & 36). The odds of post-first dose MOGAD patients receiving ChADOx1S versus alternative were significantly higher than the vaccinated English population when analyses were restricted to patients vaccinated between 7th December 2020 and 2nd May 2021 (OR 7.49, p = 0.030) and patients vaccinated at age 18 - 39 years (OR 9.76, p = 0.005). Among patients aged ≥40 years at vaccination, the OR approached statistical significance (OR 5.74, p = 0.069). The odds of a post-first-dose MOGAD patient vaccinated between 3rd May 2021 and 5th December 2021 receiving ChAdOx1S versus alternative were higher than the odds in the English population

receiving a first dose vaccine in this period but it did not reach statistical significance (OR 3.73, p = 0.314) (table 35a – e & 36).

a.iv) Conditional odds ratios of receiving ChAdOx1S versus alternative in the post-first dose and non-post-first-dose MOGAD cohort compared with the vaccinated English population (John Radcliffe Hospital cohort)

Post-first-dose MOGAD patients seen at the John Radcliffe Hospital were 6.27 times more likely to have received a first vaccination with ChAdOx1S versus alternative compared with the vaccinated English population (p = 0.008).

Post-first-dose MOGAD cases seen at the John Radcliffe Hospital were more likely to have received a first dose of ChAdOx1S than non-post-first dose MOGAD cases that were vaccinated, although this did not reach statistical significance (OR 3.41, p = 0.229).

The odds of a non-post-first-dose MOGAD patient seen at the John Radcliffe Hospital receiving a first dose of ChAdOx1S were not significantly higher than for the rest of the vaccinated English population (OR 1.77, p = 0.334) (table 35a & 36). Among stratified non-post-first-dose MOGAD subgroups, none had statistically significant higher conditional odds of receiving ChAdOx1S than the rest of the English population. This is distinct from the post-first-dose MOGAD cohort, for whom significant ORs were found for the total group (OR 6.27, p = 0.007), the group vaccinated between 7th December 2020 and

5th May 2021 (OR 6.50, p = 0.045) and the group aged 18-39 years at onset (OR 7.73, p = 0.019; table 35a – e & 36; fig 48).

a.v) Conditional odds ratios of receiving ChAdOx1S versus alternative in the post-first-dose seronegative cohort compared with the English population (whole cohort)

The odds of a post-first-dose seronegative patient receiving a first dose of ChAdOx1S versus alternative compared with the vaccinated English population were 1.61 (p = 0.727).

Although the odds of receiving ChAdOx1S in the post-vaccine seronegative AICS cohort were greater than those of the vaccinated English population after stratifying by date and age, no OR reached statistical significance (table 35a – e, table 36). ORs were not calculated for non-post-vaccine seronegative cases as only 2 vaccinated cases were identified.

Figure 48. Proportion of first dose vaccine brands among post-first-dose MOGAD cases (a) and among vaccinated non-post-vaccine MOGAD cases (b) seen at Oxford NMODAS with onset between 1st December 2020 and 26th January 2022

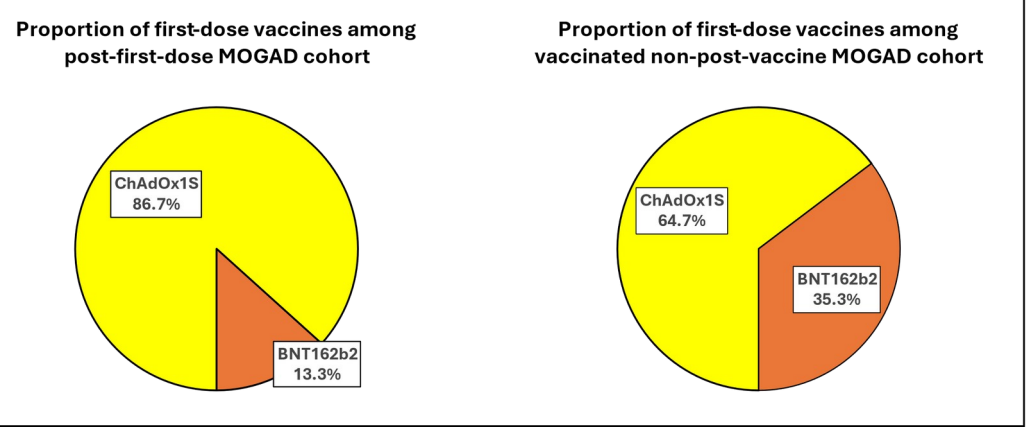

b) Self-controlled case series (John Radcliffe Hospital cohort only)

b.i) Self-controlled case series for all AICS

Thirty-four events contributed to the calculation of IRR.

There was a statistically significant effect of ChAdOx1S exposure on the incidence rate of new onset AICS when the post-exposure risk period was 56 days (IRR 10.52, p <0.001). A similar effect was observed when the risk window was reduced to 42 days (IRR 12.93, p <0.001) (table 37).

Table 37. Incidence rate ratio of first episode of AICS associated with first dose ChAdOx1S exposure

Model	IRR (95% CI)	P
Model 1 (56-day post-exposure risk period)	10.52 (5.41 – 20.44)	<0.001
Model 2 (42-day post-exposure risk period)	12.93 (6.71 – 24.92)	<0.001

b.ii) Self-controlled case series for MOGAD

Twenty-four events contributed to the calculation of IRR.

There was a statistically significant effect of ChAdOx1S exposure on the incidence rate of new onset MOGAD when the post-exposure risk window was 56 days (IRR 8.27, p <0.001). A similar effect was observed when the risk window was reduced to 42 days (IRR 9.55, p <0.001) (table 38).

Table 38. Incidence rate ratio of first episode of MOGAD associated with first dose ChAdOx1S exposure

Model	IRR (95% CI)	P
Model 1 (56-day post-exposure risk period)	8.27 (3.62 – 18.85)	<0.001
Model 2 (42-day post-exposure risk period)	9.55 (4.21 – 24.64)	<0.001

b.iii) Self-controlled case series for seronegative AICS

The model did not converge due to low numbers (n = 5).

c) Seasonality of MOGAD attacks

There were 311 confirmed attacks in 173 adults between 2010 and 2020. There was no effect of season on total attack incidence (χ^2 = 1.12 (2DoF); p = 0.571) (fig 49).

Figure 49a & b. Seasonal analysis of total MOGAD attacks 2010- 2020

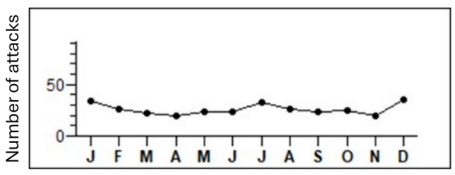

a. Total MOGAD attacks in adults by month, 2010 – 2020.
χ^2 = 1.12 (2DoF); p = 0.571

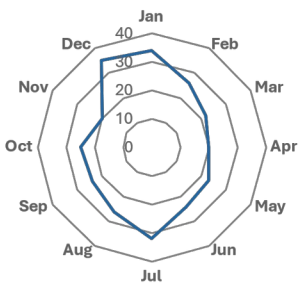

b. Radar plot of all MOGAD attacks in adults by month, 2010 - 2020

There were 54 attacks in 52 adults in 2021. There was no statistically significant seasonal effect with Edwards's test (χ^2 = 4.04 (2DoF); p = 0.133). However, inspection of the radar plot suggested a cluster of attacks between March and May (fig 50).

Figure 50a & b. Seasonal analysis of total MOGAD attacks 2021

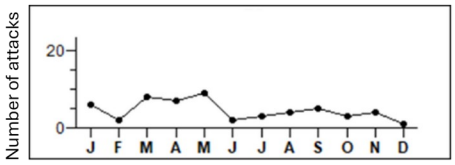

a. Total MOGAD attacks in adults by month, 2021
χ^2 = 4.04 (2DoF); p = 0.133

b. Radar plot of all MOGAD attacks in adults by month, 2021

There were 139 onset MOGAD attacks in adults between 2010 and 2020. There was no significant seasonal effect on incidence during this period (χ^2 = 0.56 (2DoF); p = 0.757) (fig 51).

Figure 51a & b. Seasonal analysis of onset MOGAD attacks 2010- 2020

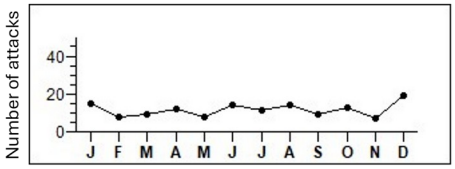

a. Onset MOGAD attacks in adults by month, 2010 – 2020.
χ^2 = 0.56 (2DoF); p = 0.757

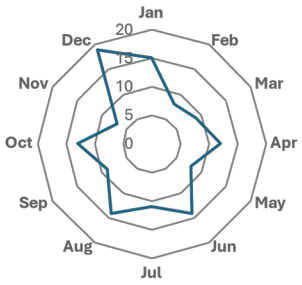

b. Radar plot of onset MOGAD attacks in adults by month, 2010 - 2020

There were 35 onset MOGAD attacks in 2021. Edward's test approached statistical significance (χ^2 = 5.26 (2DF); p = 0.072). The radar plot demonstrates a clear peak in cases between March and May (fig 52).

Figure 52a & b. Seasonal analysis of onset MOGAD attacks 2021

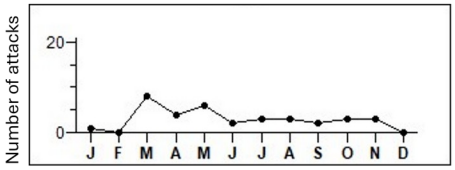

a. Onset MOGAD attacks in adults by month, 2021
χ^2 = 5.26 (2DF); p = 0.072

b. Radar plot of onset MOGAD attacks in adults by month, 2021

There was no evidence of seasonality of relapses between 2010 and 2020 (fig 53) or in 2021 (fig 54).

Figure 53a & b. Seasonal analysis of MOGAD relapses 2010- 2020

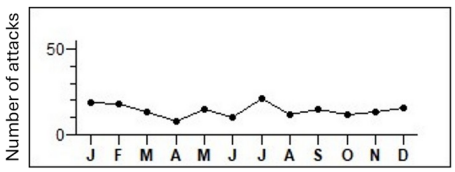

a. MOGAD relapses in adults by month, 2010 -2020
χ^2 = 0.66 (DF = 2); p = 0.718

b. Radar plot of MOGAD relapses in adults by month, 2010 – 2020

Figure 54a & b. Seasonal analysis of MOGAD relapses 2021

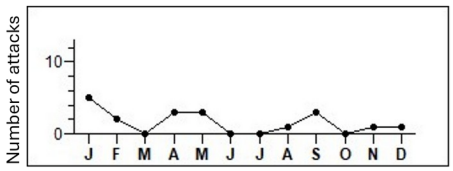

a. MOGAD relapses in adults by month, 2021
$\chi^2 = 2.36$ (DF = 2); p = 0.317

b. Radar plot of MOGAD relapses in adults by month, 2021

Summary: The post-first-dose AICS group as a whole was significantly more likely to have received a first dose of ChAdOx1S than the rest of the vaccinated English population, which persisted after stratifying by date and age of vaccination. Results were similar for the post-first-dose MOGAD cohort, with ORs > 3.0 for all subgroup comparisons. Although the odds of receiving ChAdOx1S versus alternative vaccine were higher in some non-post-vaccine MOGAD groups than the English vaccinated population, they were not statistically significant and ORs were smaller than those of the post-first-dose MOGAD group.

SCCS confirmed exposure to ChAdOx1S was associated with an increased incidence rate of AICS and of MOGAD in particular. A peak in MOGAD onset cases between March and May 2021 was

observed, coinciding with peak vaccine uptake, but it did not reach statistical significance.

Chapter 9

Post-SARS-CoV-2 vaccine acute inflammatory CNS syndromes part 3: Laboratory studies of association between ChAdOx1S and new-onset MOGAD

9.1) Methods: Laboratory studies of association between ChAdOx1S and new-onset MOGAD

a) Testing pre-vaccine MOG antibody status in post-vaccine MOGAD patients

The National Health Service Blood and Transplant service (NHSBT) stores 1ml of plasma for 3 years after each blood donation.

All participants in the post-vaccine MOGAD cohort were contacted to determine if any had donated blood in the preceding 3 years *and* prior to onset of MOGAD. Patients consented for their NHS numbers to be shared with NHSBT and those with available samples were contacted directly by NHSBT to confirm their consent to retrospective testing for MOG antibodies.

Received plasma was kept chilled prior to testing, which was carried out the day after receipt. MOG antibodies were tested by the Oxford laboratory as described by Waters *et al* (35).

b) Testing sera of healthy pre- and post-ChAdOx1S vaccine recipients for MOG antibodies

As part of the phase I/II clinical trial of ChAdOx1S (ClinicalTrials.gov ID NCT04324606), 1,077 healthy individuals aged 18-55 were randomised to receive ChAdOx1S or the meningococcal conjugate vaccine (MenACWY). Serum was sampled on days 0 and 28 of vaccination. Patients gave consent for use of their samples in affiliated studies (South Central Berkshire Research Ethics Committee reference 20/SC/0145).

To determine whether ChAdOx1S was capable of inducing *de novo* MOG antibody synthesis, the rates of seroconversion in healthy participants in the active arm of the above trial were determined.

To test whether seroconversion was specific to the vaccine, rates of seroconversion among BNT162b2 recipients would have been measured using serum of donors involved in the Protective Immunity from T Cells in Healthcare Workers (PITCH) study (study reference MR/X009297/1) (265). The PITCH consortium stored serum samples of participants from day 0 and day 28 of vaccination, aligning with those of the ChAdOx1S recipient samples used in the first part of the study.

The background rates of combined symptomatic and asymptomatic MOG antibody seroconversion are not known so power calculations were not possible. The number of samples tested was decided on pragmatic

grounds. The Oxford Neuroimmunology Laboratory (PW) kindly agreed to test 400 paired pre- and post- ChAdOx1S samples, based on their capacity to process research samples while offering a clinical service.

MOG antibody detection was carried out as described (35), with the modification that sera were screened with secondary antibodies to human Fc, rather than IgG1, to increase sensitivity. Tertiary antibodies were coupled to an Alexafluor reporter and fluorescence was measured semi-quantitatively on a scale of 0 (no fluorescence) to 4 (strong fluorescence). Plates were read independently by 2 investigators (EC & PW). In case of disparity, PW reviewed the coverslip and assigned a fluorescence score. Any sample with a fluorescence scale score ≥ 2 was re-tested with more specific secondary antibodies to IgG1.

Concordance between raters was assessed with Cohen's quadratic weighted kappa (κ_w).

The primary outcome was number and proportion of samples converting from MOG IgG1 negative (fluorescence scores <2) to positive (fluorescence scores ≥ 2). Secondary outcomes were the proportion of samples converting from scores <2 to scores ≥ 2 using the less specific anti-human-Fc secondary antibody and the median change in fluorescence scores between day 0 and day 28 of ChAdOx1S vaccine using the anti-human-Fc secondary antibody.

9.2) Results: Laboratory studies of association between ChAdOx1S and new-onset MOGAD

a) Testing pre-vaccine MOG antibody status in post-vaccine MOGAD patients

Of 4 blood donors among the post-vaccine MOGAD cohort, NHSBT had a stored sample for one patient- a white male with disease onset aged 49 years. The plasma was obtained 30 days prior to his first dose of ChAdOx1S. MOG antibodies were not detected in this sample.

This patient developed symptoms of TM 28 days after receipt of the first ChAdOx1S vaccine. The first sample tested for MOG antibodies was taken 12 months after onset and was strongly positive (titre 1:4,000).

b) Testing sera of healthy pre- and post-ChAdOx1S vaccine recipients for MOG antibodies

The Oxford Vaccine Group provided 387 pairs of serum samples drawn at day 0 and day 28 of ChAdOx1S vaccination.

Concordance of fluorescence grading was high (κ_w= 0.839, 95% CI 0.810 – 0.869). Concordance of median change in fluorescence (Δfluorescence) was adequate (κ_w= 0.565, 95% CI 0.407 – 0.722).

No samples tested positive using the highly specific anti-human-IgG1 secondary antibody.

Across 387 paired samples, the median Δfluorescence was + 0.025, i.e., a minimal change between day 0 and day 28 after ChAdOx1S.

Samples from 17 participants had fluorescence scores of 2 or more at any stage using the less-specific anti-human-Fc antibody. None showed the pattern of antibody binding typical of MOGAD (PW, personal communication).

Samples from 14 participants scored ≥2 at both time points, i.e., fluorescence did not increase significantly after vaccination.

Samples from 1 participant had a fluorescence score of 2 prior to ChAdOx1S vaccination and a post-vaccine fluorescence score of 1.5. This is of doubtful significance.

Samples from 2 participants had fluorescence scores of <2 prior to ChAdOx1S vaccination and scores of ≥2 twenty-eight days after

vaccination. Fluorescence scores from one participant increased from a baseline of 0 to a post-vaccine score of 2.5. Fluorescence scores of the other increased from a baseline of 0 to a post-vaccine score of 2.0.

Summary: The pre-disease plasma sample of a post-vaccine MOGAD patient did not contain MOG IgG1 28 days prior to ChAdOx1S vaccination. They developed ON 30 days after vaccination, suggesting seroconversion must have occurred within the narrow 58-day window. Of 387 paired serum samples from healthy ChAdOx1S recipients, none converted to MOG IgG1 positive within 28 days of vaccination but two developed new antibodies that reacted with MOG.

Chapter 10

Discussion of post-SARS-CoV-2 vaccine acute inflammatory CNS syndromes

10.1) Study outcomes

The aim of this study was to determine whether there was evidence of a causal association between any SARS-CoV-2 vaccine and new AICS. As evidence of an association between MOGAD and ChAdOx1S emerged, this became the focus of the study.

a) I have provided evidence of an association between SARS-CoV-2 vaccination and new AICS

a.i) **Onset AICS attacks were overrepresented within 8 weeks of SARS-CoV-2 vaccination.** Over half new AICS cases reviewed by the John Radcliffe Hospital occurred within 8 weeks of SARS-CoV-2 vaccination. In addition, SCCS confirmed the incidence rate of onset AICS attacks in the 8 weeks following first-dose ChAdOx1S vaccination was 7.2 times greater during the 8-week post-vaccination period compared with during the unexposed period.

a.ii) **Most cases of post- vaccine AICS occurred after the first dose**. Almost 80% of patients with post-vaccine AICS presented after the first dose of vaccine. If some cases were not

triggered by vaccination, the proportion occurring after a first dose should be approximately equal to the number of cases occurring after the second dose, as most of the UK received two doses of SARS-CoV-2 vaccines in 2021 (239).

a.iii) **Post-SARS-2-CoV-2 vaccine AICS has been reported elsewhere.** There are many case reports and case series documenting new-onset AICS following SARS-CoV-2 vaccination.

E.g., A case series from Korea reported 3 new cases of MOGAD and 3 cases of new undefined CNS demyelination occurring within 1 month of SARS-CoV-2 vaccination (244). Four cases of TM following SARS-CoV-2 vaccination were reported in Mexico (246). Cases of seronegative ON with TM (266) and ADEM with multifocal lesions (267–270) are reminiscent of the current cohort.

b) I have provided evidence that there is a stronger association between ChAdOx1S and AICS than between BNT162b2 and AICS

b.i) **ChAdOx1S was overrepresented among patients presenting with post-SARS-CoV-2 vaccine AICS.** Patients with post-vaccine AICS between 1st December 2020 and 26th January 2022 were more likely to have received ChAdOx1S (71.1%) than BNT162b2 (28.9%) within 8 weeks prior to symptom onset.

This was not merely a reflection of population vaccine patterns. The odds of a post-first-dose AICS patient having received ChAdOx1S versus alternative were 4.82 times higher than the odds of a vaccinated person in the English population. This is unlikely to be solely due to demographic differences between AICS cases and the English population because non-post-first-dose AICS cases did not have significantly higher odds of receiving ChAdOx1S versus alternative compared with the English population, even after stratifying by date and age.

b.ii) **Over 90% of post-ChAdOx1S AICS occurred after the first dose, compared with less than 50% of BNT162b2 recipients.** If the temporal association was coincidental rather than causal, similar numbers of new-onset cases would be expected to occur after first and subsequent doses during 2021, when most people received at least 2 SARS-CoV-2 vaccinations.

b.iii) **A distinct post-ChAdOx1S AICS phenotype with TM, multifocal lesions and brain involvement was not seen among BNT162b2 recipients.** The presentation was similar in seronegative and MOG antibody cases, which may reflect a common pathophysiology.

b.iv) **Post-ChAdOx1S vaccine-associated autoimmunity has been reported elsewhere.** VITT is of particular interest because constituents of ChAdOx1S have been shown *mechanistically* to

cause disease by altering the conformation of platelet factor 4 (PF4), leading to exposure of an immunogenic epitope with subsequent B-cell secretion of anti-PF4 IgG (240,241,271). Evidence of associations between ChAdOx1S and GBS and facial palsy is discussed below.

b.v) **Post ChAdOx1S vaccine-associated AICS has been reported elsewhere.** Three cases of TM were reported during the clinical trials of ChAdOx1S, one of which was potentially related to the vaccine (272). Case reports of multifocal CNS inflammatory disease following ChAdOx1S include a case from Brazil characterised by bilateral ON and LETM 3 days after receiving the first dose of ChAdOx1S (266) and two from Australia, including onset ON with multifocal brain lesions following first dose ChADOx1S (267) and a fatal case of ADEM presenting 12 days after the first ChAdOx1S vaccine (268).

Cases of LETM and multifocal lesions following first dose of ChAdOx1S resemble the post-vaccine cohort reported in the current study.

Since we first reported an association between ChAdOx1S and AICS (273,274), several case series and epidemiological studies have published similar results. A centre in India reported 29 cases of new-onset AICS within 42 days of SARS-COV-2 vaccination (253). All but two cases followed ChAdOx1S. A literature review identified 31 instances of seronegative TM within 42 days of

SARS-CoV-2 vaccination, most commonly following ChAdOx1S (275).

More compelling is epidemiological evidence of links between ChAdOx1S and new AICS. A prospective multinational study of 99 million vaccine recipients by the Global Vaccine Data Network found an association between first dose ChAdOx1S and both ADEM and TM (252). A large UK study identified a trend towards an increased risk of encephalitis, meningitis and TM (IRR 1.32, CI 0.99 – 1.76), which includes diagnoses of ADEM, post-immunisation ADEM, and unspecified myelitis, among others[19].

Although there are case reports of AICS following other SARS-CoV-2 vaccines (269,275), these are less common, the phenotype is less stereotyped and they may originate from countries where mRNA-based vaccines predominated (e.g., 244).

c) I have provided evidence of a specific association between ChAdOx1S and new-onset MOGAD

C.i) **ChAdOx1S was overrepresented among post-vaccine MOGAD patients in the current study.** Overall, post-vaccine

[19] This study may have underestimated the risk of AICS after SARS-CoV-2 vaccination, as outcomes of interest were coded according to ICD-10 criteria and were therefore dependent on clinician coding. Outcomes of interest included “acute CNS demyelinating events” and “encephalitis, meningitis and myelitis”. Syndromes such as ADEM and transverse myelitis could have fulfilled criteria for either outcome and division between the two could have diminished their statistical significance.

MOGAD followed vaccination with ChAdOx1S in over three quarters of cases.

This was not solely due to higher rates of ChAdOx1S uptake in the English population; post-first-dose MOGAD patients were 7.23 times more likely to have received ChAdOx1S versus alternative than the rest of the vaccinated English population. The higher odds of receiving ChAdOx1S among post-first-dose MOGAD cases was not solely due to demographic features predisposing to disease and increasing risk of exposure to ChAdOx1S as post-first-dose MOGAD patients were more than 3 times more likely to have received ChAdOx1S than non-post-first-dose MOGAD cases.

It is of note that ORs of ChAdOx1S in the post-vaccine MOGAD sample were large and statistically significant among patients aged 18-39 years at vaccination, because this was also the age-group at highest risk of VITT (240). It is possible that patients who developed either disease after vaccination had an underlying predisposition that was unmasked by some component of ChAdOx1S and that older adults with the predisposition had generally already experienced the first event by the time they received the vaccine. Alternatively, immune senescence may limit the risk of autoimmunity in older adults.

The high OR was supported by the results of the SCCS, which estimated the incidence rate of new onset MOGAD occurring

during the post-ChAdOx1S exposure window increased by 8.27 times.

The high odds of receiving ChAdOx1S among post-vaccine MOGAD patients was also remarked on by Jarius *et al*., who stated, "… most documented cases [of post-SARS-CoV-2 vaccine MOGAD] occurred after previous vaccination with the vector-based Oxford/ AstraZeneca vaccine ChAdOx1-S/ChAdOx1 nCoV-19 (18/20 patients, 90%), despite the fact that vastly more patients have been immunized with other vaccines worldwide, suggesting some sort of a causal relationship" (276)[20].

C.ii) **Almost 90% of patients with post-ChAdOx1S vaccine MOGAD presented after the first dose of vaccine.** In contrast, only 40% of post-BNT162b2 MOGAD patients presented after the first dose.

The literature also suggests risk of MOGAD is greatest after first dose (277,278). For example, of 10 cases of post-SARS-CoV-2 vaccine MOGAD, all occurred after ChAdOx1S, 9 after the first dose (253). A literature review found almost 90% of post-ChAdOx1S MOGAD cases occurred after the first dose (276). The same phenomenon was observed in VITT, with almost 90% of cases following the first dose of adenoviral SARS-CoV-2 vaccine (240).

[20] This review included 4 cases published by the Oxford NMODAS (274)

C.iii) **The post-ChAdOx1S vaccine MOGAD phenotype was distinct from the typical presentation.** Isolated ON is the most common MOGAD phenotype in adults, accounting for around 50% of initial presentations, with TM comprising approximately 25% and brain manifestations 12.5% (37,39). ON comprised 80% of onset attacks in post-BNT162b2 MOGAD patients. Less than a third of post-ChAdOx1S MOGAD patients presented with this isolated ON but almost 60% presented with TM, which is atypical (fig 55).

Figure 55. MOGAD phenotypes reported by Satukijchai*et al.* compared with phenotypes in post-ChAdOx1S cohort

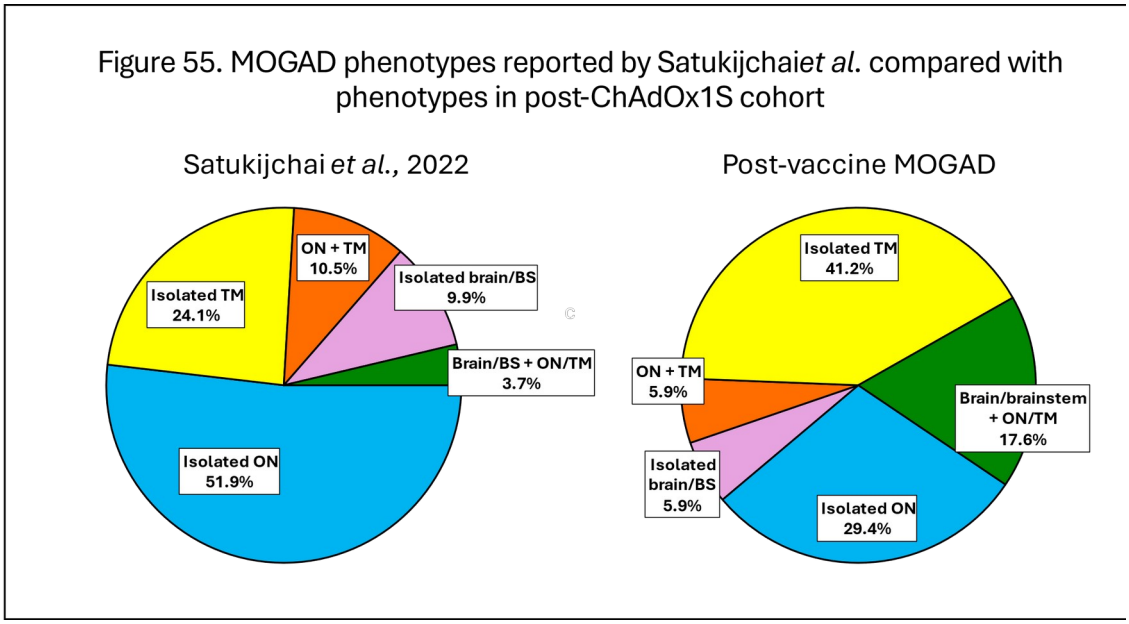

BS- brainstem

Clinical supratentorial or brainstem involvement was observed in 23.5% of ChAdOx1S recipients and none of the BNT162b2 recipients. Studies estimate clinical brain involvement affects 9.1% – 13.0% of adults with MOGAD during their first attack (37,238) and is more common among children.

Radiological brain involvement was observed in 52.9% of ChAdOx1S recipients and none of the BNT162b2 recipients. Incidental brain lesions are reported in up to 45% of MOGAD-associated attacks of ON and TM (39). However, imaging abnormalities are often small and non-specific, whereas the lesions in the post-ChAdOx1S cohort were large, fluffy and multifocal, reminiscent of ADEM. In our experience this is unusual and their absence from the post-BNT162b2 MOGAD cohort suggests distinct pathogenic processes underlie disease in these two groups.

Similar post-ChAdOx1S MOGAD phenotypes to those reported here have been reported in the scientific literature. LETM and/or brain lesions have been reported by separate groups in Germany (277,279,280), India (253,278), the UK (274) and Italy (281). Multiaxial involvement was reported in 8/10 post-ChAdOx1S MOGAD cases, 7 of which involved the brain (253). An international literature review reported TM was part of the onset phenotype in 88.2% of post-ChAdOx1S cases, often associated with brain lesions (276). The high prevalence of symptomatic brain lesions following ChAdOx1S vaccination is consistent with high rates of ADEM in cases of MOGAD occurring after vaccination or infection, discussed in section 6f.

Case reports of MOGAD following BNT162b2 and mRNA-1273 are sparse and phenotypes are more typical of “idiopathic” MOGAD,

with patients most commonly presenting with ON and not always after the first dose (244,276,282).

This atypical and stereotyped MOGAD presentation, almost always following first dose ChAdOx1S, suggests a causal relationship.

c.iv) **The identification of a seasonal peak in onset MOGAD cases in 2021, despite not reaching statistical significance, is further evidence of an association with ChAdOx1S.**

According to MHRA data, the highest concentration of first ChAdOx1S vaccinations in adults was in the week commencing 15th March 2021. The highest concentration of first BNT162b2 vaccinations given to adults was in the week commencing 7th June 2021. The peak in MOGAD onset cases closely followed the peak in ChAdOx1S administration and predated the peak in BNT162b2 uptake.

c.v) Strong evidence of a temporal link between ChAdOx1S and MOGAD onset was provided by a case of antibody seroconversion following administration of the vaccine.

Seroconversion must have occurred within the short window between sampling and symptom onset, although whether it occurred before or after vaccination cannot be proven.

d) Evidence of SARS-CoV-2 vaccine-associated seronegative AICS

In addition to the association between ChAdOx1S and MOGAD, I also found evidence that ChAdOx1S may increase the risk of seronegative AICS. This association is more difficult to quantify, largely because seronegative AICS is likely to comprise multiple pathologies.

d.i) **Almost three quarters of new-onset AICS cases seen in the John Radcliffe Hospital by Oxford NMODAS arose within 8 weeks of SARS-CoV-2 vaccination**

d.ii) **Over 60% of seronegative post-SARS-CoV-2 AICS patients had received ChAdOx1S.** This increased to 72.7% when only post-first-dose vaccine cases were considered. Post-vaccine seronegative patients were 1.61 times more likely to receive ChAdOx1S than the vaccinated English population.

In addition, two BNT162b2 recipients were diagnosed subsequently with relapsing-remitting MS, one of whom had radiological evidence of pre-existing disease. Therefore, the number of true *de novo* AICS cases following BNT162b2 was lower than the number of patients with new neurological *symptoms* following BNT162b2. This increases the predominance of ChAdOx1S among the new-onset seronegative AICS cohort.

d.iii) **A distinct seronegative AICS phenotype was observed following ChAdOx1S, similar to that seen in post-ChAdOx1S MOGAD cases.** Multifocal CNS involvement was common, with brain involvement observed in three quarters of

ChAdOx1S recipients**.** This is consistent with case reports of ADEM or ADEM-like presentations following ChADOx1S (267,268) and with epidemiological studies (252). Intracranial parenchymal lesions were see in only 1 BNT162b2 recipient who was later diagnosed with MS.

LETM was confirmed on MRI scans of 4/8 seronegative ChAdOx1S recipients but only 1 BNT162b2 recipient. In addition to case reports of seronegative LETM following first-dose ChAdOx1S (283,284), a literature review identified 12 cases of post-ChAdOx1S TM, all occurring after the first dose. Cases occurring after mRNA-1273 or BNT162b2 were rarer and some followed second doses (275).

d.iv) **A unique combination of peripheral and central nervous system dysfunction was identified in 5/8 post-ChAdOx1S seronegative AICS patients.** Hyperproteinorrachia and nerve conduction studies showing demyelinating or mixed demyelinating and axonal patterns suggest a possible autoimmune neuronopathy, although no causative antibodies were detected in any patient tested.

Case reports and large-scale epidemiological studies support an association between ChAdOx1S and GBS and facial palsy. A case series from India documented 7 cases of GBS arising within 14 days of ChAdOx1S (285). Interestingly, all had facial diplegia, mirroring the high incidence of facial nerve involvement in our

cohort. An epidemiological study marrying vaccine records from the English National Immunisation Database with hospital admission and mortality data for over 32,500,000 individuals confirmed a significantly increased risk of GBS and facial palsy following the first dose of ChAdOx1S (247), a finding replicated in SCCS (248). Following a review of the evidence by the MHRA (249), the risk of GBS was added to the product literature for CHAdOx1S (250).

Very rare cases of simultaneous central and peripheral demyelination have been reported following infection or vaccination prior to the SARS-CoV-2 pandemic (236,286). More recently, there have been several reports of the phenomenon following SARS-CoV-2 vaccination. AlKofat *et al.* describe a patient presenting with GBS and multifocal brain and cord lesions 10 days after their first ChAdOx1S vaccine (287). An instance of TM and demyelinating sensorimotor peripheral neuropathy occurring 3 weeks after the first ChAdOx1S vaccine was reported in Lisbon (288). A Canadian paper describes polyradiculoneuropathy with facial diplegia 11 days after the first ChAdOx1S vaccine, followed by ON and multifocal brain lesions (289). A similar case has been reported following Janssen/ Johnson & Johnson’s adenoviral vector-based (Ad26.COV2.S) vaccine (290). There are no reports of BNT162b2 vaccination preceding this syndrome.

The specificity of this very rare presentation following adenoviral-vectored vaccines suggests they may be triggers. It is possible ChAdOx1S is associated with autoreactive lymphocyte responses to an antigen expressed in both central and peripheral nervous compartments.

e) <u>No evidence of association between SARS-CoV-2 vaccination and AQP4+ NMOSD</u>

There is no evidence that ChAdOx1S is associated with development of AQP4+ NMOSD. The ratio of post-vaccine AQP4+ NMOSD: MOGAD cases was 1:7. The ratio of non-post-vaccine AQP4+ NMOSD: MOGAD was around 1:2 and epidemiological studies predict a ratio of around 1:4 (22,24,40). This suggests a disproportionate increase in post-vaccine MOGAD referrals, not matched by post-vaccine cases of AQP4+ NMOSD.

One patient with AQP4+ NMOSD presented within 24 hours of vaccination and *de novo* immunological responses would be expected to evolve over a longer period (228). Another post-vaccine AQP4+ NMOSD patient presented at the upper limit of the post-exposure risk window following the second BNT162b2 vaccination, while most suspected SARS-CoV-2 vaccine-associated immunological diseases have followed the first dose (247,252,276).

There have been occasional case reports of new onset AQP4+ NMOSD following SARS-CoV-2 vaccination. Unlike the literature on post-SARS-

CoV-2 vaccine MOGAD, there is no dominant vaccine associated with AQP4+ NMOSD and cases can follow vaccination with Sputnik V (291), mRNA-1273 and ChAdOx1S (244).

f) Post-SARS-CoV-2 vaccine MOGAD cases follow a typical trajectory after onset

Although the initial radiological and phenotypic presentation of post-ChAdOx1S MOGAD cases was atypical, subsequent disease trajectory was not.

Recovery following initial attack was generally good, even following profound disability at nadir. Five patients had residual bowel dysfunction and/or ongoing catheterisation. These results are consistent with the literature, which reports complete or near-complete recovery from initial attack in 62 – 78% of patients but that long-term bladder dysfunction affects 24 - 28% of patients with MOGAD (36,67,292).

Twenty-seven percent of post-vaccine MOGAD patients relapsed over a median follow-up of 30.5 months, which is similar to the 25.1% - 43.1% reported in incidence cohorts (36,37,238). Most relapses comprised isolated ON, even after brain and spinal cord involvement during the initial attack. This is the most common manifestation of MOGAD relapses in adults (36,37,67).

All relapses occurred in ChAdOx1S recipients. It is unclear if this simply reflects a difference in group size and follow-up times or if it is due to an

underlying difference in the pathophysiology of the disease. Of note, only 2/15 ChAdOx1S recipients seroreverted, compared with 3/5 BNT162b2 recipients.

These data suggest the presence of a trigger does not reduce risk of relapse in MOGAD.

g) No MOG IgG1 seroconversion among healthy donors exposed to ChAdOx1S

There were no instances of MOG IgG1 seroconversion in the 387 pairs of pre- and post-ChAdOx1S samples taken from healthy donors.

This may be due to underpowering. Although CD19+ cells reacting to the extracellular domain of MOG protein are found in healthy controls (293), the background rates of symptomatic and asymptomatic MOG antibody seroconversion are unknown. Rates are likely to be exceedingly low. One study found none of 45 healthy controls and 1 of 183 people with other neurological disease tested positive using secondary antibodies to IgG (294).

Assuming the Oxford and Liverpool NMODAS were referred all cases of post-first-dose ChAdOx1S MOGAD cases in England and that all recipients with antibodies were symptomatic, the incidence of ChAdOx1S-associated disease is 17 in 20,592,816. Thus, to detect 1 additional case of MOGAD over 1,200,000 pairs of samples would have

to be tested, which is beyond the capacity of the Oxford Neuroimmunology Laboratory.

The immunofluorescence scores of 2 patients increased from 0 at baseline to ≥2 at day 28 after ChAdOx1S when the anti-human Fc secondary antibody was used. There are four possible explanations.

1) The vaccine triggered a non-specific polyclonal B cell response, which led to an increase in titre of antibodies that bound MOG protein in 2 patients. Polyclonal activation of naïve B cells following SARS-CoV-2 infection is implied by the presence of IgM against a broad range of autoantigens in the sera of patients (295). As anti-Fc secondary antibodies bind MOG IgG2-3 and even IgA (296), antibodies in these two participants are likely to be of these subtypes.

2) A component of the vaccine stimulated MOG-specific memory B cells, either directly via molecular mimicry or indirectly via occult antigen exposure or epitope spreading. However, the immunoglobulins released were not of the pathological IgG1 subclass.

3) The vaccine triggered a MOG-specific B cell response and IgG1 increased but did not reach threshold for positivity in the anti-IgG1-based assay, which has a negative predictive value of 80% for clinical disease (35).

4) Vaccination with ChAdOx1S stimulated antibodies to the HEK-293 cells used in the assay in these patients.

As explained in the introduction (section 6.vii), ChAdOx1S adenoviral vectors are retrieved by lysis of HEK-293 cells and undergo purification to remove contaminants (217,297). Despite this, ChAdOx1S contains a raft of HEK-293 contaminants (298). It is possible the two ChAdOx1S recipients developed antibodies to HEK-293 cell antigens, which bound the anti-Fc secondary.

10.2) Questions raised by the current study

a) Although there was an increase in onset MOGAD cases during the vaccine roll-out, seasonality studies did not indicate an increase in relapse rates. Only 3 of 17 MOGAD relapses in 2021 (17.6%) occurred within 8 weeks of SARS-CoV-2 vaccination, compared with 52.8% of onset attacks.

A cross sectional study of 63 MOGAD patients reported no relapses and 3 onset cases associated with SARS-CoV-2 vaccination, two of which followed ChAdOx1S (279). An Italian study including 30 MOGAD patients reported no relapses within 8 weeks of SARS-CoV-2 vaccination. However, all patients received mRNA-based vaccines (299).

The absence of increased relapse risk is unlikely to be attributable to immunosuppression because most MOGAD patients in the Oxford NMODAS cohort are not immunosuppressed.

Vaccination may trigger disease onset by several mechanisms, including switching potentially MOG-reactive lymphocytes from anergic to activated states or driving affinity maturation of MOG-reactive lymphocytes. Thereafter, a pool of memory B cells leaves the patient at risk of relapse due to reactivation, which may be driven by different processes.

b) Although there are reports of AICS following the other commonly-used adenoviral SARS-CoV-2 vaccine, Janssen/ Johnson & Johnson's Ad26.COV2.S, these were fewer than for ChAdOx1S. Ad26.COV2.S was used infrequently in the UK but even international reports are sparse (246,300). This may have been due to differences in the purification process, as the contamination of Ad26.COV2.S was significantly lower than ChAdOx1S (298). Another potential reason for the difference in risk of AICS associated with each vaccine is the use of different adenoviral vectors (chimp Adenovirus in ChAdOx1S and human Ad26 in Ad26.COV2.S), which may drive differences in the immune response (217).

10.3) Explaining an association between ChAdOx1S and MOGAD and seronegative AICS

a) Immunological tolerance and ignorance in MOGAD

To generate a broad immune response and maximise protection against multiple pathogens, thousands of germline-encoded B and T cell receptors are generated during ontogeny due to V(D)J recombination and different combinations of either heavy and light chains (in the case of B cells) or α, β, γ and δ chains (in the case of T cells), as well as stochastic insertion of nucleotides into coding regions (for review, see reference 301). This diversity naturally generates some receptors that are capable of binding self-antigens. “Tolerance” prevents autoimmune responses.

Central tolerance of B and T cells is enabled by expression of self-antigens in the bone marrow and thymus, respectively. High-affinity interactions between lymphocytes and self-antigen can trigger clonal deletion or B cell receptor editing/ T cell receptor chain rearrangements. Lower affinity binding leads to anergy, permitting weakly self-reactive lymphocytes with a high threshold for activation into the circulation (225,302,303). Clonal deletion may be incomplete (225), meaning high- and low-affinity autoreactive lymphocytes in the circulation need regulation by peripheral tolerogenic mechanisms, including anergy and downregulation of B and T cell receptors on contact with low-affinity self-antigen.

Anergy can be overcome if the antigen is presented concurrently with other inflammatory signals (225,304). Release of cytokines such as IL-12 and IFNγ from macrophages, neutrophils and dendritic cells can stimulate activation and proliferation of anergic T cells directly or by switching antigen presenting cells from a resting to an activated state and increasing efficiency of antigen presentation (305). Engagement of pattern recognition receptors (PRRs) can also overcome anergy (306). Regulatory T cells (Tregs) are also vital in maintaining tolerance (307) and exposure to signals like IL-6 can shift the lymphocyte profile away from the Treg phenotype (308). Autoreactive CD4+ T helper cells activated via these mechanisms can provide B cell help, culminating in autoantibody synthesis (225,303).

Like T cells, autoreactive B cells can be rendered anergic by binding low-affinity antigen in the absence of T cell help but can be activated by exposure to antigen in the context of co-stimulation or activation of PRRs (225).

It has been proposed that MOG is not expressed in the thymus and that this prevents clonal deletion of MOG-reactive T cells (“immunological ignorance”), although this is debated (66,302,309–311).

The presence of MOG-reactive T cells, IgM and, rarely, IgG capable of binding MOG in healthy individuals (34,95,312,313) suggests pathogenic responses depend on more than the presence of MOG-reactive lymphocytes. Additional requirements to instigate disease could include: i) the presence of antibodies to specific encephalitogenic

MOG peptides distinct from those found in healthy controls; ii) exposure to encephalitogenic MOG peptides or mimics to activate naïve B cells and induce class-switching of pre-existing high affinity B cells; iii) a signal to overcome peripheral tolerance and stimulate weakly MOG-reactive B cells to undergo somatic hypermutation to increase affinity and stimulate pathogenic IgG1 antibody production.

The need to overcome peripheral tolerance is believed to explain why myelin-specific T cells or inoculation with myelin peptides alone are not sufficient to induce EAE in susceptible animals (304,314). EAE is an experimental paradigm initially designed to model MS but often with greater pathophysiological and clinical similarity to MOGAD. C57BL/6 mice develop EAE following inoculation with MOG peptide but only in the presence of an adjuvant (e.g., complete Freund's adjuvant) and pertussis toxin (315). In another EAE paradigm, myelin-specific T cells caused CNS inflammation and clinical disease if an additional inflammatory stimulus was delivered or in the presence of pathogens, but not in the absence of an inflammatory trigger or in pathogen-free environments (304). By extension, clinical MOGAD may also require a stimulus to overcome peripheral tolerance.

b) Evidence the immune response to ChAdOx1S could trigger MOGAD

Creating an immune environment liable to promote MOGAD (and possibly seronegative AICS) requires an event capable of: i) establishing the Th1/Th17-dominant profile necessary for clinical MOGAD; ii)

switching tolerised lymphocytes to an activated state, if peripheral tolerance is present; iii) promoting activation of B cells reactive to MOG (or other CNS antigens) and iv) increasing lymphocyte access to the CNS. ChAdOx1S fulfils all these criteria.

b.i) **ChAdOx1S creates a pro-inflammatory environment favouring the Th1/Th17 profile necessary for clinical MOGAD**

CNS expression of cytokines associated with Th1 (IFNγ, IL-12 and TNFα) and Th17 (IL-17, IL-1β, IL-6) increases during EAE attacks (316–318). *Ex vivo* stimulation of peripheral lymphocytes with myelin epitopes increases production of the same cytokines (317,318). Transgenic mice lacking IL-6 are resistant to EAE induced by inoculation with MOG peptide (319). The importance of both IL-17 and IL-1β was demonstrated by experiments showing IL-17 knockout mice were resistant to MOG-induced EAE but disease could be triggered in the presence of exogenous IL-17 or IL-1β (320).

Studies of human MOGAD have yielded similar results. The serum cytokine profile of patients with MOGAD is biased towards a Th1/Th17 response, including elevated concentrations of IFNγ, IL-6, IL-17 and IL-21 (66,321–323). CSF of patients with MOGAD contains significantly higher concentrations of cytokines associated with Th1 (IFNγ, TNFα), Th17 (IL-1β, IL-6, IL-8, IL-17) and B cell responses (CXCL13, BAFF, APRIL)

compared with non-inflammatory CNS disease controls (324). During attacks, there is an increase in peripheral Th17 cells (325), probably resulting from increased serum IL-6, and IL-1β during relapses (321).

Multiple studies have demonstrated increased levels of Th1-associated cytokines following vaccination with ChAdOx1S, including IFNγ, TNFα and IL-12 (326–329). One explanation for the occurrence of MOGAD and seronegative AICS following ChAdOx1S but not BNT162b2 is the greater intensity of the Th1 response after ChAdOx1S (328), although some studies show equivalent vigour (330,331).

Alternatively, a more marked Th17 response following ChAdOx1S could account for differences in the propensity of vaccines to cause disease. ChAdOx1S causes increases in Th17-associated cytokines, IL-1β and IL-6 (326,328,329) and IL-17 and IL-22 (332) but this has not been demonstrated with BNT162b2 (328). *Ex vivo* exposure of vaccine-naïve lymphocytes to ChAdOx1S but not BNT162b2 triggers upregulation of IL-17 and IL-22 (333).

Cytokines upregulated after ChAdOx1S are capable of overcoming peripheral tolerance The post-ChAdOx1S cytokine profile includes upregulation of IL-2, IL-12 and IFNγ (326), all of which are capable of overcoming lymphocyte anergy (334,335). In addition, IL-6 suppresses Tregs (308).

b.iii) **Cytokines upregulated after ChAdOx1S include B cell activators**

Certain cytokines upregulated following ChAdOx1S, such as IFNγ and IL-6 (326,328) are potent B cell stimulators. Pathogen-associated molecular patterns (PAMPs) found in ChAdOx1S are also capable of binding to PRRs on B cells to induce activation (see later).

b.iv) Cytokines upregulated after ChAdOx1S increase leucocyte migration across the blood brain barrier (BBB).

IFNγ has been shown to enhance leucocyte infiltration of the CNS (336). TNFα (337) and IL-17 (338) are capable of disrupting tight junctions of the BBB and IL-6 upregulates expression of cell adhesion molecules by the endothelium (339).

b.v) The post-vaccine cytokine response explains the first dose effect

There is a differential cytokine response after first and subsequent doses of ChAdOx1S. Serum IFNγ concentrations of rhesus macaques increased after the prime ChAdOx1S dose but not the boost (327). In humans, increased serum levels of IL-1β, IL-6 and TNFα following first dose ChAdOx1S were not observed following the second dose, nor following vaccination with BNT162b2 (328). This may partly explain the higher incidence of MOGAD and seronegative AICS after first dose in the current study, as well as higher incidence of MOGAD (276) and other autoimmune diseases (252) after first dose in other studies.

Mechanisms by which the cytokine profile shared by ChAdOx1S and MOGAD can trigger disease and establish a positive feedback loop leading to sustained inflammation are shown in supplementary table 229.

The evidence presented confirms the immune response to ChAdOx1S is capable of initiating a pro-inflammatory feedback loop, particularly involving IL-6, IL-17, TNFα and IL-1β, which may create a sustained immune response and potentially autoreactive state. It has characteristics that predispose to CNS inflammation, (increased permeability of the BBB, increased leucocyte infiltration of the CNS and direct cytotoxic neuronal and oligodendrocyte damage). Many aspects are shared with the inflammatory milieu of MOGAD.

Although the evidence presented above has focused on MOGAD, similar factors may drive seronegative AICS.

c) Possible mechanisms by which ChAdOx1S may provoke clinical onset of MOGAD or seronegative AICS

The cytokine response described above can support induction and persistence of CNS inflammation in general and MOG-associated inflammation in particular. As with EAE, it is likely additional mechanisms are needed to initiate the cascade that leads to MOGAD, including activation of MOG-specific lymphocytes.

Below is a summary of the possible mechanisms by which ChAdOx1S may initiate MOGAD and other antibody-mediated CNS diseases. Almost all the explanations below could induce T-cell mediated disease without need for antibody production, which may be relevant to seronegative AICS.

C.i) **Molecular mimicry**. The most frequently posited mechanism of vaccine-induced autoimmunity is molecular mimicry, in which a non-self-antigen bears sequence homology or structural similarity to a self-antigen. Exposure to cognate non-self-antigen during infection or vaccination leads to activation of autoreactive T and B lymphocytes, either by overcoming peripheral tolerance by mechanisms described above (low affinity) or due to immunological ignorance/ escape from central tolerance (high affinity) (224). Proliferation of antigen-specific cytotoxic T cells and plasma cells releasing affinity-matured antibodies can lead to damage to host cells expressing the self-antigen.

Interestingly, patients with MOGAD have antibodies to different MOG epitopes (312,314,340). Different epitope reactivities between individuals could be due to exposure to disparate molecular mimics in individuals with cognate HLA and lymphocyte receptors. Existence of multiple different susceptibility loci between patients would explain why no HLA association has been identified (219,220).

There is evidence of molecular mimicry in some autoimmune disease. For example, GBS frequently follows Campylobacter jejuni infection (341). Lipo-oligosaccharides expressed on the Campylobacter jejuni cell envelope mimic gangliosides on peripheral nerve myelin or axons, bind to host B cell receptors and stimulate synthesis of antibodies cross reactive with host gangliosides (341). Similarly, cross-reactivity between the M protein expressed by Streptococcus pyogenes and lysogangliosides expressed on cardiac myocytes is believed to underlie rheumatic fever (225).

The evidence for molecular mimicry resulting from SARS-CoV-2 infection or vaccination is mixed. One study used ELISA to identify cross reactivity between antibodies to SARS-CoV-2 spike (S) and nucleocapsid (N) proteins and human antigens (342). Antibodies to both SARS-CoV-2 antigens were capable of binding a host of human peptides, including myelin basic protein (MBP). However, ELISAs do not use antigens in their native conformations and the findings have not been replicated with whole proteins.

Another study found neutralising antibodies from patients previously infected with SARS-CoV-2 bound murine tissues, including brain (343). These antibodies had undergone only limited somatic hypermutation, suggesting B cells expressing germline-encoded autoreactive antibodies escaped tolerance or

persisted due to immunological ignorance. Whether the same targets are expressed in human tissue has not been confirmed.

There is evidence of cross-reactivity between MOG protein and SARS-CoV-2 nucleocapsid (N) protein. MOG antibodies from 1 of 11 MOGAD patients with prior SARS-CoV-2 infection bound strongly to N protein *in vitro* and SARS-CoV-2 N antibodies from the same patient bound MOG. Adsorption of antibodies to SARS-CoV-2 N reduced MOG IgG binding (344). It is not known whether this patient had cross-reactive antibodies prior to infection or whether they resulted from infection.

The existence of cross-reactivity does not prove causation. Conversely, lack of cross-reactivity with proteins S and N in 4 MOGAD patients with disease onset after SARS-CoV-2 vaccination (344) does not exclude cross-reactivity in other vaccine recipients, nor does it exclude cross-reactivity between MOG antibodies and other vaccine constituents.

There are case reports of MOGAD arising after SARS-CoV-2 infection (345–348). SARS-CoV-2-triggered MOGAD was suggested by a study showing SARS-CoV-2 seropositivity was more common among patients with new-onset MOGAD than matched controls and that diagnoses of MOGAD increased in the years of the pandemic (349). A series of 9 new onset MOGAD cases arising within 5 weeks of SARS-CoV-2 infection included 2 patients with multifocal brain lesions and TM, 2 patients with encephalopathy

and multifocal brain lesions, 2 cases of isolated TM and 3 cases of isolated ON (350). Other instances of MOGAD with multifocal brain lesions have been reported following SARS-CoV-2 infection (351). The high frequency of brain involvement and low frequency of ON mirrors our post-vaccine findings.

If SARS-CoV-2 infection can trigger MOGAD onset, the S protein is the most likely molecular mimic as the only components common to SARS-CoV-2 infection and the ChAdOx1S vaccine are SARS-CoV-2 DNA and, post translation, the S protein. The S protein is ubiquitous to SARS-CoV-2 variants and mRNA and adenoviral vaccines have utilised this to stimulate neutralising antibodies effective against multiple different strains (217,352,353). Therefore, antibodies cross reactive to MOG and the S protein would not explain the lack of association between MOGAD and BNT162b2, nor why MOGAD was reported so infrequently following the Janssen/ Johnson & Johnson Ad26.COV2.S vaccine.

An alternative ChAdOx1S component may mimic MOG or, in the case of seronegative AICS, a different CNS antigen. Substantial contamination of ChAdOx1S with adenoviral and HEK-293 components has been demonstrated and up to 70% of the vaccine protein content was derived from HEK-293 cells, compared with a maximum of 7% in Ad26COV2.S (271,298). Of the >1,000 human proteins isolated, most were structural but several neuronal and glial proteins were also identified (Prof. Lea Krutzke, personal

communication). This is consistent with the presence of neuronal mRNA and protein found in HEK-293 cells (354). Immune responses to contaminants can be inferred from a study showing memory T cells from 100% of unexposed donors were stimulated by commercial ChAdOx1S, whereas only memory T cells from only 60% responded to purified ChAdOx1S adenoviral particles (333).

No MOG protein has been found in the ChAdOx1S batches tested, but there was substantial variation in the protein profile (298). Even in the absence of MOG, a molecular mimic could exist among the contaminants. Of note, HEK-293 cells express neurofilament chains (354). MOG-specific T cells have been shown to cross-react with neurofilament medium chain and to induce EAE after passive transfer (355). Neurofilament light chain was identified in ChAdOx1S, but no medium chain was found (Prof. Lea Krutzke, personal communication). This does not exclude its presence in other batches.

C.ii) **Bystander activation**. Bystander activation involves non-specific stimulation of innate immune cells as well as activation of off-target T and B cells. PAMPs, such as viral DNA, engage PRRs on macrophages and dendritic cells to stimulate cytokine release, costimulatory molecule expression and antigen presentation. Anergic T cells bound to autoantigens with low affinity can be switched to an activated state in the presence of pro-inflammatory signals from the innate immune system, particularly

in the presence of PAMPs (224,309). This was demonstrated in EAE, when mice with MBP-specific T cell receptors developed disease in the absence of inoculation with MBP peptides if an additional pro-inflammatory stimulus was present (304). The authors propose the additional stimulus triggered an immune cascade capable of overcoming peripheral tolerance and non-specifically activating potentially autoreactive T cells.

In the case of ChAdOx1S, viral DNA, adenoviral capsid proteins and unknown contaminants could lead to bystander activation by binding PRRs on innate immune cells and lymphocytes. The broad pro-inflammatory cytokine profile described following ChAdOx1S (326–328) may be sufficient to induce innate and adaptive cell activation. Bystander activation by these means would explain non-antigen-specific increases in T cell reactivity following SARS-CoV-2 vaccination (333,356).

C.iii) **Epitope spreading**. This describes the expansion of an immune response to epitopes beyond that initially targeted (222). According to the hypothesis proposed by Vanderlugt and Miller (357), the dominant viral or vaccine epitope is presented to antigen-restricted T cells, which are activated and migrate to the sites of antigen accumulation. Here, T cells, antibodies and innate immune cells interact to initiate an inflammatory cascade leading to tissue damage. Local inflammatory signals strong enough to overcome potential tolerance stimulate autoreactive T cells with

receptors capable of binding epitopes released by damaged host cells. This establishes a cycle of tissue damage and propagates autoreactivity. As a result, a triggering epitope would not necessarily have to mimic the epitope targeted in autoimmune disease.

Epitope spreading is a feature of EAE (309). Induction of EAE by inoculation with proteolipid peptide epitope ($PLP_{139-151}$) results in activation of T cells specific for $PLP_{178-191}$ and an epitope of a distinct myelin protein (myelin basic protein, MBP_{84-104}). These secondary autoreactive T cells are capable of inducing EAE by passive transfer (357). A primate model of EAE induced by inoculation with MP4, (a fusion protein made up of MBP and PLP), resulted in antibodies to MOG, despite the absence of MOG from the inciting antigen (358).

Epitope spreading has been implicated in human autoimmune disease. For example, patients with autoimmune hepatitis expand their antibody specificities during the course of their disease (359). This may explain the polyclonal MOG antibody response in some patients (340).

ChAdOx1S is contaminated by many human proteins, including those expressed in the CNS (298). It is conceivable that CNS-reactive T cells could be activated by binding of cognate self-antigen or mimic in the vaccine or by bystander activation in the context of a vigorous inflammatory response. These T cells could

migrate to the CNS, re-encounter antigen and establish a localised inflammatory cascade, exposing dendritic cells and lymphocytes to MOG and other CNS-restricted antigens, triggering a secondary adaptive immune response causing MOGAD or seronegative AICS, respectively.

C.iv) **Cryptic antigen exposure.** The mechanism of cryptic antigen exposure is similar to epitope spreading, but the requirement for activation of autoreactive T and B cells at disease initiation is not absolute. Tissue destruction by infection, innate immune responses or adaptive immune responses expose cryptic self-antigens to which the immune system is ignorant (222).

As discussed above, the cytokine profile elicited by ChAdOx1S is capable of increasing leucocyte recruitment to the CNS, which can occur in the absence of CNS inflammation if the systemic cytokine profile is permissive (360). In addition, ChAdOx1S contains EDTA, which increases vascular permeability (271) and may increase BBB permeability (361). Exposure of antigens sequestered behind the BBB to dendritic cells and non-tolerised lymphocytes could lead to adaptive responses targeting MOG or other CNS proteins. Supporting this theory, cervical lymph nodes of people with MS contain MOG peptides (362) and MOG peptides and IgG have been detected in the sera of patients with amyotrophic lateral sclerosis (363). Together, this suggests CNS inflammation can lead to

cryptic antigen exposure, uptake by dendritic cells and successful presentation to B cells.

C.V) **Polyclonal B cell activation.** This is a type of bystander activation in which naive polyclonal extrafollicular B cells may be activated by engagement of toll-like receptors (TLRs) or by cross linking B cell receptors, even in the absence of cognate antigen binding (364–367). In this way, even if there are no self-reactive T cell receptors in the adaptive repertoire, B cells can be licenced to proliferate, differentiate into short-lived plasma cells and produce autoantibodies (364,368–370). Although it was believed T cell-independent B cell responses were not capable of generating class-switched antibodies necessary for MOG IgG1, simultaneous engagement of TLRs and the B cell receptor has been found to induce limited class switching (370–373). Low-affinity IgG to MOG produced by these B cells, as well as IgM from non-class-switched B cells, may be capable of opsonising the target. Opsonisation triggers dendritic cell antigen uptake and presentation to naïve B cells in lymph nodes. This could drive affinity maturation. Polyclonal responses to other CNS antigens could lead to seronegative AICS.

Polyclonal B cell activation has been posited to underlie other vaccine-induced autoimmune diseases (222,224,357).

Adenoviral vector capsid and DNA in ChAdOx1S are known to bind to TLRs on B cells (374,375). The serum and CSF of SARS-CoV-2

infected patients contains antibodies to a range of autoantigens, including those in the CNS (295,376,377). Together, this suggests SARS-CoV-2 infection is capable of stimulating polyclonal B cell responses to CNS antigens.

C.vi) **B cell co-capture.** It is possible for B cells to internalise self- and non-self-antigen via the B cell receptor, presenting exogenous antigen to CD4+ T cells for co-stimulation that licenses autoreactive B cells (378).

This mechanism has been demonstrated for MOG antibody synthesis *in vitro* (379). When MOG-specific B cells were cultured with tissues co-expressing MOG and haemagglutinin-ovalbumin, co-capture of MOG and haemagglutinin was visualised, MOG-specific B cells were capable of activating ovalbumin-specific T cells and co-stimulation resulted in MOG antibody synthesis. When MOG-specific co-cultured B cells were transferred to transgenic mice with ovalbumin-specific T cells, MOG antibodies could be detected in their sera. However, the experiment used co-expressed membrane-bound proteins. There is no evidence that that SARS-CoV-2 virus (380) or ChAdOx1S vaccine infiltrates the CNS and therefore oligodendrocyte expression of vaccine-derived protein and MOG is unlikely following vaccination. Co-capture is possible if a vaccine component “mimics” an autologous myelin protein. For example, dendritic cells activated in the CNS may present autologous myelin antigen and MOG simultaneously to

MOG-reactive B cells in cervical lymph nodes. These B cells could then derive costimulatory signals from T cells primed by the myelin mimic, stimulating differentiation of MOG-IgG-producing plasma cells. The same mechanism is applicable to other CNS antigens for seronegative AICS.

C.vii) **Creation of neoantigens.** Neoantigens are antigens to which an individual's immune cells have not been exposed and can be created when an autoantigen undergoes structural changes. Immunological ignorance of the altered antigen means an adaptive immune response may develop if cognate receptors are present in the lymphocyte repertoire (223). Interactions between self-antigens and vaccine contents to generate neoantigens capable of activating B cells has been proposed as the mechanism underlying VITT (240,271).

If the adaptive immune system is tolerised to native MOG, vaccine-induced structural alterations to MOG presented in lymph nodes during CNS inflammation could bypass tolerance. Interestingly, VITT antibodies binding PF4/hexon complexes were also able to bind PF4 alone in some cases (241,271), suggesting an initial response to altered self-antigen can expand to the native antigen. Formation of neoantigens could underlie MOGAD or seronegative AICS.

C.viii) **Memory response to adenoviral infection**. Adenovirus can enter the CNS and cause meningoencephalitis (381). Because we do not routinely perform lumbar punctures on healthy individuals, rates of asymptomatic or mildly symptomatic CNS infection are unknown.

Direct injection of replication-deficient adenovirus into rat brains resulted in minimal inflammatory change and no demyelination at 60 days post-injection. Animals who received peripheral inoculation with the same adenovirus 60 days after brain injection demonstrated marked inflammation with macrophage, dendritic cell and T cell infiltration and demyelination (382).

It is theoretically possible that patients presenting with post-vaccine AICS had latent CNS adenovirus infection and that peripheral challenge with a cross-reactive adenoviral vector triggered an inflammatory response that in turn led to cryptic antigen exposure, epitope spreading and/or B cell co-capture to trigger MOGAD or seronegative AICS.

Adenoviral-specific human T cells can be activated by exposure to simian adenoviruses, like that used in ChAdOx1S (383). Memory T cells from vaccine-naïve, pre-pandemic healthy controls were stimulated by ChAdOx1S but not BNT162b2 or S1 peptides (333). The antigenic stimulant may have been an adenoviral component. Multiomic studies also indicate memory responses to adenoviral peptides after ChAdOx1S (384). However, it is unclear whether

replication-competent adenoviruses can cause persistent latent CNS infection necessary for subsequent peripherally-driven inflammation.

d) Proposed model for vaccine-induced MOGAD and seronegative AICS

The model is summarised in figure 56 (see appendix 19 for legend). ChAdOx1S is more likely than other vaccines to cause MOGAD because the resulting cytokine profile is conducive, because it is capable of increasing BBB permeability, because it contains PRRs capable of eliciting bystander responses and because the range of contaminants, including CNS antigens, may increase risk of molecular mimicry and of initial CNS damage directed at antigens other than those causing autoimmune disease. The model does not assume antigen specificity as the initial response is driven largely by bystander activation and polyclonal lymphocyte responses, which can be induced by multiple inflammatory stimuli. Molecular mimicry, if it plays a role, need not be caused by a single antigen and the possibility of epitope spread, cryptic antigen exposure and B cell co-capture mean initial antigen-specific responses could converge on downstream MOG antibody synthesis. The non-specific trigger may explain the variety of different infections reported to precede MOGAD attacks (66,67), why different MOGAD

patients have antibodies that recognise different epitopes (314,340) and why no HLA risk loci have been identified (219,220).

It is important to remember that a trigger is not necessarily a cause, and the mechanisms suggested are contingent on the patient already expressing T and B cell receptors capable of binding self-antigen. Vaccination may expose a pre-existing propensity for disease. Whether the patients reported here would have demonstrated clinical manifestations in the absence of vaccination is uncertain.

Figure 56. Proposed model of ChAdOx1S-induced AICS

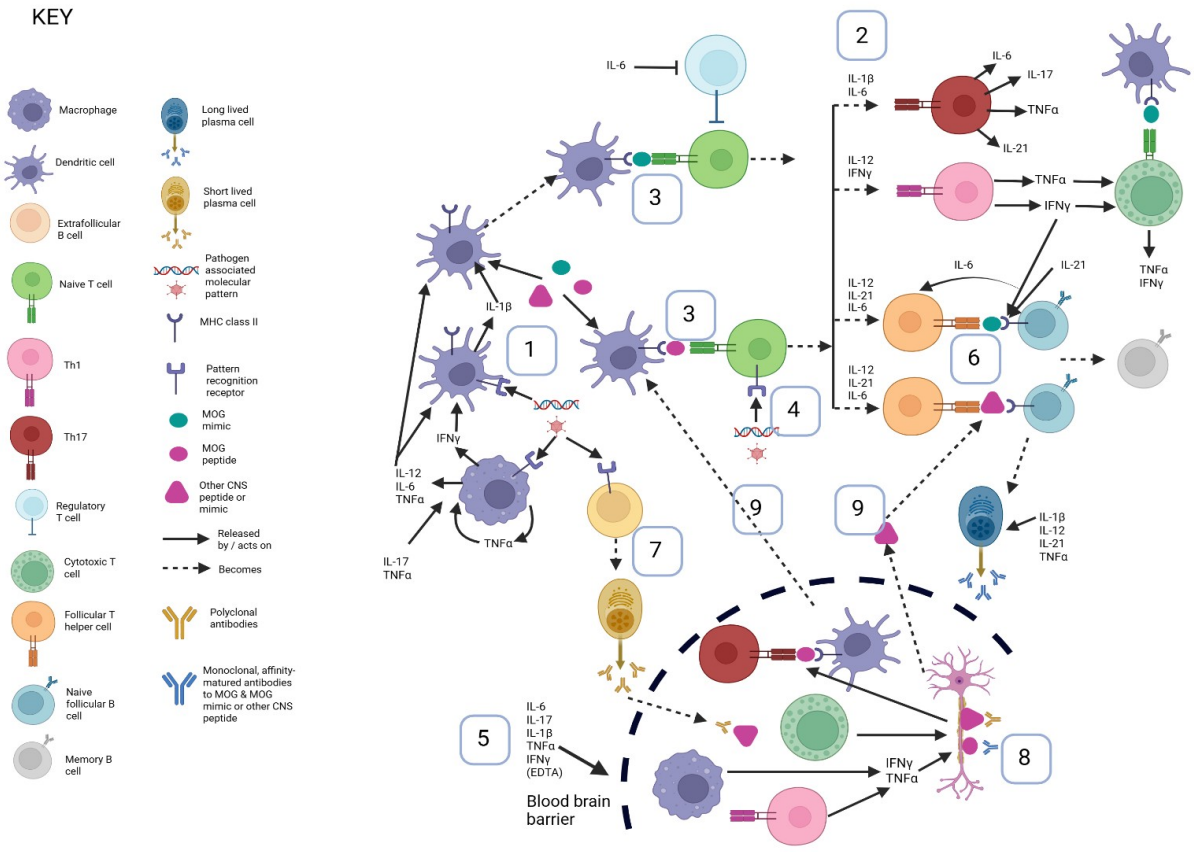

e) Can the model explain atypical phenotypes in post-ChAdOx1S MOGAD patients?

It is possible that MOGAD phenotype is determined by the precipitant:

i) Phenotypic and histological features of EAE induced by passive transfer vary according to the cytokines used to differentiate naïve T cells *in vitro*, which determines T cell subtypes (385). Pertussis toxin is capable of altering disease phenotype after initiation, suggesting the inflammatory milieu following induction modulates attacks. Different precipitants in human disease would be expected to result in different inflammatory profiles and may therefore result in different phenotypes.

ii) Severity of CNS inflammation in Lewis rats can be altered by modulating the ratio of CNS-specific T cells and MOG antibodies (386). In human disease, the ratio of T- and B-cell responses depends on the pathogen.

iii) EAE phenotype is partially determined by the specificity of the T cell receptor for different MOG peptide sequences (302). Target epitopes in human MOGAD are likely to vary according to both host genetics and presence of an original trigger (340,387).

The high frequency of ADEM in children with MOGAD has been attributed to differences in maturity of myelin and immune responses (53). Children are also at greater risk of exposure to novel antigens in the form of both infection and vaccination. Novel antigenic triggers

presented in an inflammatory context may drive an immune response that favours brain lesions and LETM over ON. Intriguingly, Bauer and colleagues reported the Th17 lymphocyte skew observed in patients with MOGAD was more prominent in children than adults (323). They suggest a preceding infectious prodrome may drive the immune response towards a Th17-dominant profile in these patients, resulting in an ADEM phenotype. If this is the case, the Th17-biased response observed after ChAdOx1S (332,333) may explain the high incidence of cerebral and brainstem lesions observed in post-ChAdOx1S MOGAD patients reported here and elsewhere (253,276,277,281). A similar effect may explain why infections more commonly precede ADEM than other MOGAD phenotypes (66).

10.4) Assessment, advantages and limitations of the study

a) Association and causation

Many studies purporting to show associations between SARS-CoV-2 vaccination and neurological sequelae were underpowered, failed to take into account disease incidence and vaccination patterns in the population and were published before adequate case ascertainment could be completed.

The current study overcame these limitations by applying validated statistical methods, such as self-controlled case series, accounting for national vaccination patterns in the analysis and collecting data for more than 3 years after the vaccine roll-out to optimise case ascertainment.

Despite the rigorous methodology used in this study, causality cannot be proven definitively without a proven biological mechanism. Acknowledging this difficulty, the WHO has produced the following criteria to assess causality of AEFIs (388).

i) **Temporal relationship: The AEFI must follow vaccination**.

We define post-vaccination events as those that occur within a given interval of vaccination. The WHO does not specify a maximum interval between vaccination and disease onset. Most assessments consider an event an AEFI if it occurs within 6 weeks of vaccination (222,247,253). All post-vaccine seronegative AICS

and all but 2 MOGAD cases in the current study occurred within 6 weeks of vaccination.

However, the 6-week interval is arbitrary in most cases and the true delay between vaccination and onset may be much longer (222). Autoantibodies associated with AQP4+ NMOSD (389) and type 1 diabetes mellitus (390) can be present years before clinical disease. This means clinical manifestations of vaccine-induced autoantibodies may emerge years after the inciting event. Conversely antibodies may have been present for years before the event believed to have triggered the disease.

The current work is unique in that it includes a case of seroconversion around the time of vaccination, demonstrating the temporal relationship.

ii) **Strength of association: The association between exposure and outcome should be statistically significant**. The current study demonstrates patients with new onset MOGAD were significantly more likely to have received ChAdOx1S than the remainder of the English population and that incidence rate of onset attacks was significantly higher during the post-exposure risk window.

iii) **Dose−response relationship: Risk of the outcome increases as intensity of exposure increases**. As noted by the WHO, evidence of a dose-response relationship may not be

possible for vaccines because the degree of exposure is usually fixed.

iv) **Consistency of evidence: Similar observations have been made in different settings**. Case reports and case series of AICS and MOGAD following ChAdOx1S have already been cited within this thesis. No epidemiological study has focused on post-SARS-CoV-2-vaccination MOGAD and the background rarity of the disease would necessitate vast numbers to confirm an association. Nevertheless, available evidence from India, Italy, Germany, Australia and the UK demonstrates a consistent association between ChAdOx1S and new-onset AICS and MOGAD.

v) **Specificity: The vaccine is the only demonstrable cause of the outcome**. MOGAD and seronegative AICS can occur sporadically or follow other infections or vaccinations. The requirement for specificity is not met in the current study. However, there are many examples of vaccines acting as *a* trigger but not *the only* trigger of a disease. For example, GBS can be idiopathic or follow infection and is therefore not specific to the 1976 H1N1 influenza vaccine but most studies agree the vaccine significantly increased the risk of disease. Thrombotic thrombocytopaenia can result from heparin therapy or surgery in the absence of heparin in predisposed individuals and is therefore not specific to ChAdOx1S, yet there is strong evidence that

ChAdOx1S can precipitate VITT. Although our study lacks specificity, it is not always a mandatory requirement for causality.

vi) **Biological plausibility: The outcome should be consistent with the mechanism of the vaccine**. The immunological effects of ChAdOx1S and the similarities with responses in people with MOGAD and animal models are explored in section 10.3.b, with potential mechanisms listed in section 10.3.c (see also appendix 19).

According to definitions proposed by Butler *et al*. (228), the available evidence points to a “possible” association between ChAdOx1S and AICS and MOGAD.

b) Limitations of the study

i) It is possible preferential referral of post-vaccine cases may have increased their representation among cases seen by the NMODAS, particularly in outreach clinics. I attempted to mitigate this by limiting certain calculations (proportion of post-vaccine new-onset cases, index dose analysis etc) to patients seen by the Oxford NMODAS at the John Radcliffe Hospital. Even within this cohort, clinicians may have been more likely to refer post-vaccine cases to the John Radcliffe Hospital. This is particularly the case for seronegative disease, as there are no referral criteria.

Clinicians may be more likely to refer severely affected seronegative cases than those with mild manifestations, increasing the proportion of patients with disabling TM or cerebral and brainstem manifestations. This may have biased the phenotype distribution.

ii) The post-vaccine MOGAD cohort included one patient who had received treatment for latent syphilis two weeks prior to onset and another who had concomitant Lyme disease with Borrelia IgG in the CSF. The clinical and paraclinical findings for both patients were felt to be more consistent with MOGAD. However, co-existing syphilitic optic neuropathy and Lyme myelopathy cannot be excluded.

The florid, fatal CNS inflammation observed in a seronegative patient who tested positive for Borrelia IgM was not consistent with neuroborreliosis, although interaction with other pathologies is possible. One seronegative patient had a positive Hepatitis E test. Although Hepatitis E virus has been associated with GBS and may explain the patient's peripheral neuropathy, meningoencephalitis is only rarely reported as a consequence of Hepatitis E infection and CSF is often negative for viral RNA (391).

iii) Antibody testing was not always performed at presentation, with delays of up to 25 months between symptom onset and first test, Given up to 25% of people with MOGAD serorevert (392), some cases classed seronegative could have been associated with

MOG antibodies that subsequently fell below the diagnostic threshold. In addition, the exact dates of acute treatments were not recorded in many cases and sampling during or after plasma exchange may have caused false negatives. However, of the 8 seronegative patients with repeat antibody testing 6 months or more after disease onset, none had become positive after treatment was discontinued.

The long intervals between presentation and testing in some cases highlights the importance of prolonged and continuous data collection to investigate vaccine-associated diseases.

iv) Few patients had serum SARS-CoV-2 N antibodies tested at presentation or subsequently so the contribution of immunological memory in MOGAD and seronegative AICS could not be inferred. It is possible “original antigenic sin” caused a shift in the immunodominant epitope and the response to the previously subdominant epitope after vaccination cross-reacted with MOG, explaining the incidence of post-vaccine but not post-infectious MOGAD and seronegative AICS. This is unlikely, as 4 of 6 patients with results did not have serological evidence of preceding exposure and because similar mechanisms would be expected to cause disease after BNT162b2.

v) Calculations of the conditional ORs of receiving ChAdOx1S compared with alternative SARS-CoV-2 vaccines in the post-vaccine cohorts were limited by small numbers, particularly after

stratifying by age and vaccine date. The modified Haldane-Anscombe correction for zero cells cannot compensate fully and the estimated ORs are inherently less accurate with wider confidence intervals. In general, the correction underestimated the OR by reducing the odds of patients receiving first dose ChAdOx1S. The ORs of non-post-first-dose group receiving ChAdO1S compared with the English population were not statistically significant and were smaller than those of the post-first-dose groups. However, some non-post-first-dose AICS and MOGAD groups were slightly smaller than equivalent post-first-dose groups, which may have reduced the power to detect significant differences between ratios of vaccines in this group compared with the English population.

A potential criticism is the possibility of calendar-time confounding when comparing ORs of post-first-dose and non-post-first-dose AICS and MOGAD vaccine exposures. However, significant ORs persisted for the post-first-dose groups after stratifying by date.

vi) One of the core assumptions of SCCS is that an event should not affect subsequent exposure (257,258). I have assumed that onset of AICS and MOGAD did not affect risk of exposure to SARS-CoV-2 vaccination but there is no way to prove this is the case, which may appear to reduce event rates during the pre-exposure “baseline” period and inflate IRRs. In addition, patients with a history of demyelinating disease may have been advised to avoid

ChAdOx1S when the association with TM was brought to public attention, further reducing exposure among patients after disease onset. In addition, limiting analyses to non-recurrent events can introduce bias, leading to clustering of cases early in the observation period, which may impact risk of exposure to ChAdOx1S versus alternative (393).

vii) We tested 387 paired pre- and post- ChAdOx1S samples from volunteers who received the vaccine as part of a clinical trial. This was likely to be underpowered to detect MOG antibody seroconversion.

viii) As SARS-CoV-2 vaccines are novel and utilise new technologies (217,218), we have relatively little knowledge of their pharmacodynamics and immunogenicity. The risk period is not the same for every vaccine (222,254). For reasons of pragmatism, the risk period was assumed to start on the day of vaccination and persist for 8 weeks. This maximised sensitivity (case detection) but may have overestimated the number of true post-vaccine cases.

This is unlikely to have caused significant misattribution, as only 1 patient presented within 5 days of vaccination and only 3 presented beyond 6 weeks of vaccination. Two of these patients had AQP4+ NMOSD and there is little evidence, in the current study and in the literature, that vaccination triggered AQP4+ NMOSD.

10.5) Conclusions

There are many case reports and case series of AICS and MOGAD following SARS-CoV-2 vaccination, most frequently after ChAdOx1S. Without proof of a mechanism, causality cannot be proven.

The current study adds to the evidence supporting a causal relationship by examining the association between vaccination and new-onset AICS and MOGAD in a well-curated, large patient cohort with a long case-ascertainment period. Rare events, such as onset of AICS and MOGAD, are difficult to detect, even in large epidemiological studies. Modelling with multiple methods, as performed here, may be the only way to detect an association.

Patients with post-SARS-CoV-2 vaccine-associated AICS and MOGAD are more likely to have received ChAdOx1S than BNT162b2 and that this was not proportional to the vaccine distribution in the English population. The SCCS confirmed a significantly increased risk of AICS and MOGAD onset during the post-exposure risk window and seasonality analysis showed a peak of MOGAD onset that coincided with the peak of ChAdOx1S administration in England.

Perhaps most convincingly, an incidence of MOG antibody seroconversion around the time of ChAdOx1S vaccination was proven.

The similarities between the post-ChAdOx1S inflammatory profile and that observed in MOGAD patients during attacks provides the foundations of a model by which the vaccine could induce MOGAD onset.

In conjunction with the existing literature, the data presented here offer robust evidence that MOGAD is triggered by ChAdOx1S.

Two facts are beyond doubt. The first is SARS-CoV-2 vaccination prevented death and morbidity. The second is that autoimmune sequelae are rare and occur after <0.005% of vaccinations (227). Any potential autoimmune consequences are far outweighed by the short- and long-term effects of serious infection. This thesis demonstrates how rare AEFIs can provide insight into disease mechanisms while recognising the crucial need for vaccination programmes.

Chapter 11

Final conclusions

Although my initial research aim was to confirm or refute the existence of cognitive deficits in AQP4+ NMOSD and MOGAD, the opportunity to study potential triggers of autoimmune inflammatory CNS diseases afforded by the SARS-CoV-2 pandemic and subsequent vaccination programme allowed two projects to dovetail.

In the introduction, I hypothesised that diagnosis of AQP4+ NMOSD or MOGAD would have a negative impact on cognition and that this would be determined, at least in part, by presence of supratentorial lesions and age at onset. The high incidence of intracranial lesions among children with both diseases is recognised, although the reason for this is not clear. It has been proposed that differences in myelin composition, blood-brain-barrier structure and immune responses between children and adults underlie this phenotypic difference (53). However, children are also at greater risk of exposure to novel antigens. Histological and phenotypic variation in experimental autoimmune encephalitis depends on environmental exposures and subsequent lymphocyte responses (385,394). It is therefore possible that risk of cerebral involvement depends on the presence and nature of novel antigen exposure in predisposed individuals.

If this were true, it is possible patients with disease onset following recognised antigen exposure would be at higher risk of cerebral lesions and therefore, according to my earlier hypothesis, increased risk of cognitive impairment.

The research presented here confirms previously reported impairments in attention and processing speed, with additional evidence of deficits in visuospatial memory and executive function, in patients with AQP4+ NMOSD. However, there was no evidence of impairments in patients with MOGAD. Performance is largely independent of supratentorial lesion status but is associated with paediatric onset.

I have used several methods to demonstrate exposure to ChAdOx1S is associated with new acute inflammatory CNS syndromes, particularly MOGAD, and proposed a model by which disease could be initiated.

The incidence of intracranial inflammatory lesions observed in post-ChAdOx1S AICS was greater than expected, supporting the theory that disease triggered by infection or vaccination confers greater risk of parenchymal brain involvement. However, the absence of cognitive impairment in MOGAD and absence of an association between supratentorial lesion status and cognitive performance mean I was unable to link vaccine exposure with cognitive outcomes in MOGAD.

More work needs to be done with larger numbers to confirm the absence of an effect of cerebral inflammation on cognition in both AQP4+ NMOSD and MOGAD, including the use of advanced MRI paradigms to study the impact of microstructural changes on

performance in these patients compared with an appropriately selected control group.

Like the studies of VITT, research is needed to identify an antigenic trigger for MOGAD within the ChAdOx1S vaccine and to study vaccine-induced pathways that permit clinical expression of MOGAD. Contamination of ChAdOx1S by CNS proteins is a tantalising target for research. Among post-vaccine seronegative patients, testing serum for antibodies to proteins expressed in central and peripheral nervous system compartments may reveal a novel target of post-vaccine autoimmunity.

Finally, an association between preceding antigen exposure and MOGAD phenotype remains an intriguing possibility and studies looking explicitly at this relationship should be undertaken.

References

1. Jarius S, Wildemann B. Aquaporin-4 antibodies (NMO-IgG) as a serological marker of neuromyelitis optica: a critical review of the literature. Brain Pathol. 2013 Nov;23(6):661–83. doi:10.1111/bpa.12084 PubMed PMID: 24118483; PubMed Central PMCID: PMC8028894.

2. Abercrombie J. Pathological and practical researches on diseases of the brain and spinal cord [Internet]. First American, Second English. Philadelphia: Carey & Lea; 1831 [cited 2024 Jan 11]. (Medicine in the Americas, 1610-1920). Located at: NIH National Library of Medicine Digital Collection. Available from: https://collections.nlm.nih.gov/bookviewer?PID=nlm:nlmuid-66111230R-bk

3. Clifford Allbutt T. ON THE OPHTHALMOSCOPIC SIGNS OF SPINAL DISEASE. The Lancet. 1870 Jan;95(2420):76–8. doi:10.1016/S0140-6736(02)68218-2

4. Jarius S, Wildemann B. The history of neuromyelitis optica. Part 2: ‘Spinal amaurosis’, or how it all began. J Neuroinflammation. 2019 Dec;16(1):280. doi:10.1186/s12974-019-1594-1

5. Devic E. Myélite aiguë dorso-lombaire avec névrite optique. - Autopsie. In: Congrès français de médecine. Première session Lyon, 1894. Procès-verbaux, mémoires et discussions. Paris: Asselin & Houzeau; Lyon: Louis Savy; 1895. p. 434–9.

6. Gault F (1873 19) A du texte. Neuromyélite optique aiguë : thèse présentée à la Faculté de médecine... / par Fernand Gault,... [Internet]. 1894 [cited 2024 Jan 12]. Located at: gallica.bnf.fr. Available from: https://gallica.bnf.fr/ark:/12148/bpt6k9766395j

7. Stansbury F. NEUROMYELITIS OPTICA (DEVIC’S DISEASE): Presentation of Five Cases, with Pathologic Study, and Review of Literature | JAMA Ophthalmology | JAMA Network. Arch Ophthalmol. 1949;42(4):465–501. doi:10.1001/archopht.1949.00900050473014

8. Stansbury F. NEUROMYELITIS OPTICA (DEVIC’S DISEASE): Presentation of Five Cases, with Pathological Study, and Review of the Literature. Arch Ophthalmol. 1949;42(3):292–335. doi:10.1001/archopht.1949.00900050298007

9. Dreschfeld J. Acute Disseminated Myelitis. The British Medical Journal. 1894;1(1744):1174–7.

10. Cree BAC, Goodin DS, Hauser SL. Neuromyelitis optica. Semin Neurol. 2002 Jun;22(2):105–22. doi:10.1055/s-2002-36534 PubMed PMID: 12524556.

11. Kim W, Kim SH, Huh SY, Kim HJ. Brain Abnormalities in Neuromyelitis Optica Spectrum Disorder. Mult Scler Int. 2012;2012:735486. doi:10.1155/2012/735486 PubMed PMID: 23259063; PubMed Central PMCID: PMC3518965.

12. Jarius S, Ruprecht K, Wildemann B, Kuempfel T, Ringelstein M, Geis C, et al. Contrasting disease patterns in seropositive and seronegative neuromyelitis optica: A multicentre study of 175 patients. J Neuroinflammation. 2012 Jan 19;9:14. doi:10.1186/1742-2094-9-14 PubMed PMID: 22260418; PubMed Central PMCID: PMC3283476.

13. Huh SY, Min JH, Kim W, Kim SH, Kim HJ, Kim BJ, et al. The usefulness of brain MRI at onset in the differentiation of multiple sclerosis and seropositive neuromyelitis optica spectrum disorders. Mult Scler. 2014 May;20(6):695–704. doi:10.1177/1352458513506953

14. Lennon VA, Wingerchuk DM, Kryzer TJ, Pittock SJ, Lucchinetti CF, Fujihara K, et al. A serum autoantibody marker of neuromyelitis optica: distinction from multiple sclerosis. The Lancet. 2004 Dec 11;364(9451):2106–12. doi:10.1016/S0140-6736(04)17551-X

15. Lennon VA, Kryzer TJ, Pittock SJ, Verkman AS, Hinson SR. IgG marker of optic-spinal multiple sclerosis binds to the aquaporin-4 water channel. J Exp Med. 2005 Aug 15;202(4):473–7. doi:10.1084/jem.20050304 PubMed PMID: 16087714; PubMed Central PMCID: PMC2212860.

16. Waters P, Reindl M, Saiz A, Schanda K, Tuller F, Kral V, et al. Multicentre comparison of a diagnostic assay: aquaporin-4 antibodies in neuromyelitis optica. J Neurol Neurosurg Psychiatry. 2016 Sep;87(9):1005–15. doi:10.1136/jnnp-2015-312601

17. Wingerchuk DM, Lennon VA, Pittock SJ, Lucchinetti CF, Weinshenker BG. Revised diagnostic criteria for neuromyelitis optica. Neurology. 2006 May 23;66(10):1485–9. doi:10.1212/01.wnl.0000216139.44259.74 PubMed PMID: 16717206.

18. Jarius S, Wildemann B. The history of neuromyelitis optica. Journal of Neuroinflammation. 2013 Jan 15;10(1):797. doi:10.1186/1742-2094-10-8

19. Fujihara K. Neuromyelitis optica spectrum disorders: still evolving and broadening. Current Opinion in Neurology. 2019 Jun;32(3):385–94. doi:10.1097/WCO.0000000000000694

20. Clarke L, Arnett S, Bukhari W, Khalilidehkordi E, Jimenez Sanchez S, O'Gorman C, et al. MRI Patterns Distinguish AQP4 Antibody Positive Neuromyelitis Optica Spectrum Disorder From Multiple Sclerosis. Front Neurol. 2021;12:1554. doi:10.3389/fneur.2021.722237

21. Wingerchuk DM, Banwell B, Bennett JL, Cabre P, Carroll W, Chitnis T, et al. International consensus diagnostic criteria for neuromyelitis optica spectrum disorders. Neurology. 2015 Jul 14;85(2):177–89. doi:10.1212/WNL.0000000000001729 PubMed PMID: 26092914; PubMed Central PMCID: PMC4515040.

22. Hor JY, Asgari N, Nakashima I, Broadley SA, Leite MI, Kissani N, et al. Epidemiology of Neuromyelitis Optica Spectrum Disorder and Its Prevalence and Incidence Worldwide. Front Neurol. 2020 Jun 26;11. doi:10.3389/fneur.2020.00501 PubMed PMID: 32670177; PubMed Central PMCID: PMC7332882.

23. Pandit L, Asgari N, Apiwattanakul M, Palace J, Paul F, Leite M, et al. Demographic and clinical features of neuromyelitis optica: A review. Mult Scler. 2015 Jun;21(7):845–53. doi:10.1177/1352458515572406 PubMed PMID: 25921037; PubMed Central PMCID: PMC4463026.

24. O'Connell K, Hamilton-Shield A, Woodhall M, Messina S, Mariano R, Waters P, et al. Prevalence and incidence of neuromyelitis optica spectrum disorder, aquaporin-4 antibody-positive NMOSD and MOG antibody-positive disease in Oxfordshire, UK. J Neurol Neurosurg Psychiatry. 2020;91(10):1126–8. doi:10.1136/jnnp-2020-323158

25. Wingerchuk DM, Pittock SJ, Lucchinetti CF, Lennon VA, Weinshenker BG. A secondary progressive clinical course is uncommon in neuromyelitis optica. Neurology. 2007 Feb 20;68(8):603–5. doi:10.1212/01.wnl.0000254502.87233.9a

26. Kitley J, Leite MI, Nakashima I, Waters P, McNeillis B, Brown R, et al. Prognostic factors and disease course in aquaporin-4 antibody-positive patients with neuromyelitis optica spectrum disorder from the United Kingdom and Japan. Brain. 2012 Jun;135(Pt 6):1834–49. doi:10.1093/brain/aws109 PubMed PMID: 22577216.

27. McKeon A, Lennon VA, Lotze T, Tenenbaum S, Ness JM, Rensel M, et al. CNS aquaporin-4 autoimmunity in children. Neurology. 2008 Jul 8;71(2):93–100. doi:10.1212/01.wnl.0000314832.24682.c6 PubMed PMID: 18509092.

28. Akaishi T, Takahashi T, Misu T, Abe M, Ishii T, Fujimori J, et al. Progressive patterns of neurological disability in multiple sclerosis and neuromyelitis optica spectrum disorders. Sci Rep. 2020 Aug 17;10(1):13890. doi:10.1038/s41598-020-70919-w PubMed PMID: 32807848; PubMed Central PMCID: PMC7431838.

29. Kitley J, Waters P, Woodhall M, Leite MI, Murchison A, George J, et al. Neuromyelitis Optica Spectrum Disorders With Aquaporin-4 and Myelin-Oligodendrocyte Glycoprotein Antibodies: A Comparative Study. JAMA Neurology. 2014 Mar 1;71(3):276–83. doi:10.1001/jamaneurol.2013.5857

30. Sato DK, Callegaro D, Lana-Peixoto MA, Waters PJ, de Haidar Jorge FM, Takahashi T, et al. Distinction between MOG antibody-positive and AQP4 antibody-positive NMO spectrum disorders. Neurology. 2014 Feb 11;82(6):474–81. doi:10.1212/WNL.0000000000000101 PubMed PMID: 24415568; PubMed Central PMCID: PMC3937859.

31. Mader S, Gredler V, Schanda K, Rostasy K, Dujmovic I, Pfaller K, et al. Complement activating antibodies to myelin oligodendrocyte glycoprotein in neuromyelitis optica and related disorders. J Neuroinflammation. 2011 Dec 28;8:184. doi:10.1186/1742-2094-8-184 PubMed PMID: 22204662; PubMed Central PMCID: PMC3278385.

32. Ambrosius W, Michalak S, Kozubski W, Kalinowska A. Myelin Oligodendrocyte Glycoprotein Antibody-Associated Disease: Current Insights into the Disease Pathophysiology, Diagnosis and Management. Int J Mol Sci. 2020 Dec 24;22(1):100. doi:10.3390/ijms22010100 PubMed PMID: 33374173; PubMed Central PMCID: PMC7795410.

33. Reindl M, Waters P. Myelin oligodendrocyte glycoprotein antibodies in neurological disease. Nat Rev Neurol. 2019 Feb;15(2):89–102. doi:10.1038/s41582-018-0112-x PubMed PMID: 30559466.

34. Waters P, Woodhall M, O'Connor KC, Reindl M, Lang B, Sato DK, et al. MOG cell-based assay detects non-MS patients with inflammatory neurologic disease. Neurol Neuroimmunol Neuroinflamm. 2015 Mar 19;2(3):e89. doi:10.1212/NXI.0000000000000089 PubMed PMID: 25821844; PubMed Central PMCID: PMC4370386.

35. Waters PJ, Komorowski L, Woodhall M, Lederer S, Majed M, Fryer J, et al. A multicenter comparison of MOG-IgG cell-based assays. Neurology. 2019 Mar 12;92(11):e1250–5. doi:10.1212/WNL.0000000000007096 PubMed PMID: 30728305; PubMed Central PMCID: PMC6511109.

36. Jurynczyk M, Messina S, Woodhall MR, Raza N, Everett R, Roca-Fernandez A, et al. Clinical presentation and prognosis in MOG-antibody disease: a UK study. Brain. 2017 Dec 1;140(12):3128–38. doi:10.1093/brain/awx276

37. Satukijchai C, Mariano R, Messina S, Sa M, Woodhall MR, Robertson NP, et al. Factors Associated With Relapse and Treatment of Myelin Oligodendrocyte Glycoprotein Antibody–Associated Disease in the United Kingdom. JAMA Network Open. 2022 Jan 10;5(1):e2142780. doi:10.1001/jamanetworkopen.2021.42780

38. de Mol C, Wong Y, van Pelt E, Wokke B, Siepman T, Neuteboom R, et al. The clinical spectrum and incidence of anti-MOG-associated

acquired demyelinating syndromes in children and adults. Mult Scler. 2020 Jun;26(7):806–14. doi:10.1177/1352458519845112 PubMed PMID: 31094288; PubMed Central PMCID: PMC7294530.

39. Cobo-Calvo A, Ruiz A, Rollot F, Arrambide G, Deschamps R, Maillart E, et al. Clinical Features and Risk of Relapse in Children and Adults with Myelin Oligodendrocyte Glycoprotein Antibody–Associated Disease. Annals of Neurology. 2021;89(1):30–41. doi:10.1002/ana.25909

40. Hor JY, Fujihara K. Epidemiology of myelin oligodendrocyte glycoprotein antibody-associated disease: a review of prevalence and incidence worldwide. Front Neurol. 2023;14:1260358. doi:10.3389/fneur.2023.1260358 PubMed PMID: 37789888; PubMed Central PMCID: PMC10542411.

41. Gupta A, Stead TS, Ganti L. Determining a Meaningful R-squared Value in Clinical Medicine. Academic Medicine & Surgery. 2024 Oct 27. doi:10.62186/001c.125154

42. Höftberger R, Sepulveda M, Armangue T, Blanco Y, Rostásy K, Calvo AC, et al. Antibodies to MOG and AQP4 in adults with neuromyelitis optica and suspected limited forms of the disease. Mult Scler. 2015 Jun;21(7):866–74. doi:10.1177/1352458514555785 PubMed PMID: 25344373; PubMed Central PMCID: PMC4824843.

43. Zhou L, Huang Y, Li H, Fan J, Zhangbao J, Yu H, et al. MOG-antibody associated demyelinating disease of the CNS: A clinical and pathological study in Chinese Han patients. J Neuroimmunol. 2017 Apr 15;305:19–28. doi:10.1016/j.jneuroim.2017.01.007 PubMed PMID: 28284341.

44. de Mol C, Wong Y, van Pelt E, Wokke B, Siepman T, Neuteboom R, et al. The clinical spectrum and incidence of anti-MOG-associated acquired demyelinating syndromes in children and adults. Mult Scler. 2020 Jun;26(7):806–14. doi:10.1177/1352458519845112 PubMed PMID: 31094288; PubMed Central PMCID: PMC7294530.

45. Lechner C, Baumann M, Hennes EM, Schanda K, Marquard K, Karenfort M, et al. Antibodies to MOG and AQP4 in children with neuromyelitis optica and limited forms of the disease. J Neurol Neurosurg Psychiatry. 2016 Aug;87(8):897–905. doi:10.1136/jnnp-2015-311743 PubMed PMID: 26645082.

46. Banwell B, Bennett JL, Marignier R, Kim HJ, Brilot F, Flanagan EP, et al. Diagnosis of myelin oligodendrocyte glycoprotein antibody-associated disease: International MOGAD Panel proposed criteria. The Lancet Neurology. 2023 Jan;S1474442222004318. doi:10.1016/S1474-4422(22)00431-8

47. Jurynczyk M, Geraldes R, Probert F, Woodhall MR, Waters P, Tackley G, et al. Distinct brain imaging characteristics of autoantibody-mediated CNS conditions and multiple sclerosis. Brain. 2017 Mar 1;140(3):617–27. doi:10.1093/brain/aww350

48. Pittock SJ, Lennon VA, Krecke K, Wingerchuk DM, Lucchinetti CF, Weinshenker BG. Brain abnormalities in neuromyelitis optica. Arch Neurol. 2006 Mar;63(3):390–6. doi:10.1001/archneur.63.3.390 PubMed PMID: 16533966.

49. Fadda G, Armangue T, Hacohen Y, Chitnis T, Banwell B. Paediatric multiple sclerosis and antibody-associated demyelination: clinical, imaging, and biological considerations for diagnosis and care. Lancet Neurol. 2021 Feb;20(2):136–49. doi:10.1016/S1474-4422(20)30432-4 PubMed PMID: 33484648.

50. Cobo-Calvo A, Ruiz A, Rollot F, Arrambide G, Deschamps R, Maillart E, et al. Clinical Features and Risk of Relapse in Children and Adults with Myelin Oligodendrocyte Glycoprotein Antibody-Associated Disease. Ann Neurol. 2021 Jan;89(1):30–41. doi:10.1002/ana.25909 PubMed PMID: 32959427.

51. Camera V, Messina S, Elhadd KT, Sanpera-Iglesias J, Mariano R, Hacohen Y, et al. Early predictors of disability of paediatric-onset AQP4-IgG-seropositive neuromyelitis optica spectrum disorders. J Neurol Neurosurg Psychiatry. 2021 Sep 28. doi:10.1136/jnnp-2021-327206 PubMed PMID: 34583946.

52. Collongues N, Marignier R, Zéphir H, Papeix C, Fontaine B, Blanc F, et al. Long-term follow-up of neuromyelitis optica with a pediatric onset. Neurology. 2010 Sep 21;75(12):1084–8. doi:10.1212/WNL.0b013e3181f39a66

53. Wender M. Acute disseminated encephalomyelitis (ADEM). Journal of Neuroimmunology. 2011 Feb 1;231(1):92–9. doi:10.1016/j.jneuroim.2010.09.019 PubMed PMID: 21237518.

54. Paolilo RB, Hacohen Y, Yazbeck E, Armangue T, Bruijstens A, Lechner C, et al. Treatment and outcome of aquaporin-4 antibody-positive NMOSD: A multinational pediatric study. Neurol Neuroimmunol Neuroinflamm. 2020 Sep;7(5). doi:10.1212/NXI.0000000000000837 PubMed PMID: 32732259; PubMed Central PMCID: PMC7413715.

55. Kim W, Park MS, Lee SH, Kim SH, Jung IJ, Takahashi T, et al. Characteristic brain magnetic resonance imaging abnormalities in central nervous system aquaporin-4 autoimmunity. Mult Scler. 2010 Oct;16(10):1229–36. doi:10.1177/1352458510376640 PubMed PMID: 20685766.

56. Ashtari F, Najarzadeh P, Shaygannejad V, Adibi I, Ramezani N, Davanian F, et al. Cognitive function and brain magnetic resonance imaging profiles in neuromyelitis optica spectrum disorder and multiple sclerosis. J Res Med Sci. 2024 Aug 2;29:49. doi:10.4103/jrms.jrms_703_23 PubMed PMID: 39403229; PubMed Central PMCID: PMC11472874.

57. Masuda H, Hirano S, Takahashi N, Hatsugano E, Uzawa A, Uchida T, et al. Comparison of cognitive and brain grey matter volume profiles between multiple sclerosis and neuromyelitis optica spectrum disorder. PLOS ONE. 2017 Aug 28;12(8):e0184012. doi:10.1371/journal.pone.0184012

58. Vanotti S, Cores EV, Eizaguirre B, Melamud L, Rey R, Villa A. Cognitive performance of neuromyelitis optica patients: comparison with multiple sclerosis. Arq Neuro-Psiquiatr. 2013 Jun;71:357–61.

59. Risi M, Altieri M, Bisecco A, Rippa V, Borgo RM, Maggi G, et al. Longitudinal assessment of cognitive function in patients with non-relapsing MOG-IgG associated disease. Journal of the Neurological Sciences. 2025 Mar 15;470:123413. doi:10.1016/j.jns.2025.123413

60. Hacohen Y, Wong YY, Lechner C, Jurynczyk M, Wright S, Konuskan B, et al. Disease Course and Treatment Responses in Children With Relapsing Myelin Oligodendrocyte Glycoprotein Antibody–Associated Disease. JAMA Neurology. 2018 Apr 1;75(4):478–87. doi:10.1001/jamaneurol.2017.4601

61. Passoke S, Stern C, Häußler V, Kümpfel T, Havla J, Engels D, et al. Cognition in patients with myelin oligodendrocyte glycoprotein antibody-associated disease: a prospective, longitudinal, multicentre study of 113 patients (CogniMOG-Study). J Neurol Neurosurg Psychiatry. 2025 Mar 13;96(3):296–305. doi:10.1136/jnnp-2024-333994 PubMed PMID: 39084862; PubMed Central PMCID: PMC12015013.

62. Correale ECC Jorge. Association between infections, the microbiome, vaccination, and neuromyelitis optica spectrum disorder - Edgar Carnero Contentti, Jorge Correale, 2023. Multiple Sclerosis Journal [Internet]. 2022 Jul 28 [cited 2026 Feb 23]. Available from: https://journals.sagepub.com/doi/full/10.1177/13524585221113272?download=true

63. Yoshimura S, Isobe N, Matsushita T, Yonekawa T, Masaki K, Sato S, et al. Distinct genetic and infectious profiles in Japanese neuromyelitis optica patients according to anti-aquaporin 4 antibody status. J Neurol Neurosurg Psychiatry. 2013 Jan 1;84(1):29–34. doi:10.1136/jnnp-2012-302925 PubMed PMID: 23038741.

64. Koga M, Takahashi T, Kawai M, Fujihara K, Kanda T. A serological analysis of viral and bacterial infections associated with neuromyelitis optica. J Neurol Sci. 2011 Jan 15;300(1–2):19–22. doi:10.1016/j.jns.2010.10.013 PubMed PMID: 21056429.

65. Kitley J, Leite MI, Küker W, Quaghebeur G, George J, Waters P, et al. Longitudinally Extensive Transverse Myelitis With and Without Aquaporin 4 Antibodies. JAMA Neurology. 2013 Nov 1;70(11):1375–81. doi:10.1001/jamaneurol.2013.3890

66. Corbali O, Chitnis T. Pathophysiology of myelin oligodendrocyte glycoprotein antibody disease. Front Neurol. 2023 Feb 28;14:1137998. doi:10.3389/fneur.2023.1137998 PubMed PMID: 36925938; PubMed Central PMCID: PMC10011114.

67. Jarius S, Ruprecht K, Kleiter I, Borisow N, Asgari N, Pitarokoili K, et al. MOG-IgG in NMO and related disorders: a multicenter study of 50 patients. Part 2: Epidemiology, clinical presentation, radiological and laboratory features, treatment responses, and long-term outcome. Journal of Neuroinflammation. 2016 Oct 28;13(1):280. doi:10.1186/s12974-016-0718-0

68. Ramanathan S, Mohammad S, Tantsis E, Nguyen TK, Merheb V, Fung VSC, et al. Clinical course, therapeutic responses and outcomes in relapsing MOG antibody-associated demyelination. J Neurol Neurosurg Psychiatry. 2018 Feb;89(2):127–37. doi:10.1136/jnnp-2017-316880 PubMed PMID: 29142145; PubMed Central PMCID: PMC5800335.

69. Florenzo B, Brenton JN. Socioeconomic, Clinical, and Laboratory Parameters Differentiating Pediatric Patients With MOG Antibody-Associated Disease and Multiple Sclerosis. J Child Neurol. 2023 Mar;38(3–4):178–85. doi:10.1177/08830738231170290 PubMed PMID: 37122175; PubMed Central PMCID: PMC10213154.

70. Torisu H, Okada K. Vaccination-associated acute disseminated encephalomyelitis. Vaccine. 2019 Feb;37(8):1126–9. doi:10.1016/j.vaccine.2019.01.021

71. López-Chiriboga AS, Majed M, Fryer J, Dubey D, McKeon A, Flanagan EP, et al. Association of MOG-IgG Serostatus With Relapse After Acute Disseminated Encephalomyelitis and Proposed Diagnostic Criteria for MOG-IgG-Associated Disorders. JAMA Neurol. 2018 Nov 1;75(11):1355–63. doi:10.1001/jamaneurol.2018.1814 PubMed PMID: 30014148; PubMed Central PMCID: PMC6248120.

72. Hennes EM, Baumann M, Schanda K, Anlar B, Bajer-Kornek B, Blaschek A, et al. Prognostic relevance of MOG antibodies in children with an acquired demyelinating syndrome. Neurology. 2017

Aug 29;89(9):900–8. doi:10.1212/WNL.0000000000004312 PubMed PMID: 28768844.

73. Di Pauli F, Mader S, Rostasy K, Schanda K, Bajer-Kornek B, Ehling R, et al. Temporal dynamics of anti-MOG antibodies in CNS demyelinating diseases. Clinical Immunology. 2011 Mar 1;138(3):247–54. doi:10.1016/j.clim.2010.11.013

74. Azumagawa K, Nakashima I, Kaneko K, Torisu H, Sakai Y, Kira R, et al. A nation-wide survey of paediatric MOG antibody-associated diseases. Brain Dev. 2021;43:705–13.

75. Banks SA, Morris PP, Chen JJ, Pittock SJ, Sechi E, Kunchok A, et al. Brainstem and cerebellar involvement in MOG-IgG-associated disorder versus aquaporin-4-IgG and MS. J Neurol Neurosurg Psychiatry. 2021 Apr 1;92(4):384–90. doi:10.1136/jnnp-2020-325121 PubMed PMID: 33372052.

76. Waters P, Fadda G, Woodhall M, O'Mahony J, Brown RA, Castro DA, et al. Serial Anti–Myelin Oligodendrocyte Glycoprotein Antibody Analyses and Outcomes in Children With Demyelinating Syndromes. JAMA Neurol. 2020 Jan;77(1). doi:10.1001/jamaneurol.2019.2940 PubMed PMID: 31545352; PubMed Central PMCID: PMC6763982.

77. Sun X, Qiu W, Wang J, Wang S, Wang Y, Zhong X, et al. Myelin oligodendrocyte glycoprotein-associated disorders are associated with HLA subtypes in a Chinese paediatric-onset cohort. J Neurol Neurosurg Psychiatry. 2020 Jul;91(7):733–9. doi:10.1136/jnnp-2019-322115 PubMed PMID: 32430437; PubMed Central PMCID: PMC7361006.

78. Harris PA, Taylor R, Minor BL, Elliott V, Fernandez M, O'Neal L, et al. The REDCap consortium: Building an international community of software platform partners. Journal of Biomedical Informatics. 2019 Jul 1;95:103208. doi:10.1016/j.jbi.2019.103208

79. Compston A, Coles A. Multiple sclerosis. Lancet. 2008 Oct 25;372(9648):1502–17. doi:10.1016/S0140-6736(08)61620-7 PubMed PMID: 18970977.

80. Chiaravalloti N, DeLuca J. Cognitive impairment in multiple sclerosis. Lancet Neurol. 2008;7:1139–51.

81. Ruano L, Portaccio E, Goretti B, Niccolai C, Severo M, Patti F, et al. Age and disability drive cognitive impairment in multiple sclerosis across disease subtypes. Mult Scler. 2017 Aug;23(9):1258–67. doi:10.1177/1352458516674367 PubMed PMID: 27738090.

82. Sumowski JF, Benedict R, Enzinger C, Filippi M, Geurts JJ, Hamalainen P, et al. Cognition in multiple sclerosis. Neurology. 2018

Feb 6;90(6):278–88. doi:10.1212/WNL.0000000000004977 PubMed PMID: 29343470; PubMed Central PMCID: PMC5818015.

83. Lorefice L, Carta E, Frau J, Contu F, Casaglia E, Coghe G, et al. The impact of deep grey matter volume on cognition in multiple sclerosis. Mult Scler Relat Disord. 2020 Oct;45:102351. doi:10.1016/j.msard.2020.102351 PubMed PMID: 32731200.

84. Kim SH, Kwak K, Hyun JW, Jeong IH, Jo HJ, Joung A, et al. Widespread cortical thinning in patients with neuromyelitis optica spectrum disorder. European Journal of Neurology. 2016;23(7):1165–73. doi:https://doi.org/10.1111/ene.13011

85. Calabrese M, Rinaldi F, Mattisi I, Grossi P, Favaretto A, Atzori M, et al. Widespread cortical thinning characterizes patients with MS with mild cognitive impairment. Neurology. 2010 Jan 26;74(4):321–8. doi:10.1212/WNL.0b013e3181cbcd03

86. Benedict RH, Hulst HE, Bergsland N, Schoonheim MM, Dwyer MG, Weinstock-Guttman B, et al. Clinical significance of atrophy and white matter mean diffusivity within the thalamus of multiple sclerosis patients. Mult Scler. 2013 Oct;19(11):1478–84. doi:10.1177/1352458513478675 PubMed PMID: 23459570.

87. Eijlers AJC, van Geest Q, Dekker I, Steenwijk MD, Meijer KA, Hulst HE, et al. Predicting cognitive decline in multiple sclerosis: a 5-year follow-up study. Brain. 2018 Sep 1;141(9):2605–18. doi:10.1093/brain/awy202

88. Saji E, Arakawa M, Yanagawa K, Toyoshima Y, Yokoseki A, Okamoto K, et al. Cognitive impairment and cortical degeneration in neuromyelitis optica. Annals of Neurology. 2013;73(1):65–76. doi:10.1002/ana.23721

89. Rimkus C de M, Avolio IMB, Miotto EC, Pereira SA, Mendes MF, Callegaro D, et al. The protective effects of high-education levels on cognition in different stages of multiple sclerosis. Mult Scler Relat Disord. 2018 May;22:41–8. doi:10.1016/j.msard.2018.03.001 PubMed PMID: 29554549.

90. Faragó P, Tóth E, Szabó N N, Kocsis K, Kincses B, Bozsik B, et al. Connection between microstructural alterations detected by diffusion MRI and cognitive dysfunction in MS: A model-free analysis approach. Multiple Sclerosis and Related Disorders. 2022 Jan 1;57:103442. doi:10.1016/j.msard.2021.103442

91. De Meo E, Portaccio E, Giorgio A, Ruano L, Goretti B, Niccolai C, et al. Identifying the Distinct Cognitive Phenotypes in Multiple Sclerosis. JAMA Neurology. 2021 Apr 1;78(4):414–25. doi:10.1001/jamaneurol.2020.4920

92. Ciotti JR, Eby NS, Wu GF, Naismith RT, Chahin S, Cross AH. Clinical and laboratory features distinguishing MOG antibody disease from multiple sclerosis and AQP4 antibody-positive neuromyelitis optica. Multiple Sclerosis and Related Disorders. 2020 Oct 1;45. doi:10.1016/j.msard.2020.102399 PubMed PMID: 32702642.

93. Du Q, Shi Z, Chen H, Zhang Y, Wang J, Qiu Y, et al. Comparison of clinical characteristics and prognoses in patients with different AQP4-Ab and MOG-Ab serostatus with neuromyelitis optica spectrum disorders. J Neuroimmunol. 2021 Apr 15;353:e577494. doi:10.1016/j.jneuroim.2021.577494 PubMed PMID: 33515897.

94. Gupta S, Rehani V, Dhull P, Somasekharan M, Sreen A. A Comparative Analysis of Clinical and Imaging Features of Aquaporin 4 (AQP4) Antibody Positive, Myelin Oligodendrocyte Glycoprotein (MOG) Antibody Positive and Double Seronegative Subtypes of Neuro Myelitis Optica Spectrum Disorder (NMOSD). Ann Indian Acad Neurol. 2022;25(2):239–45. doi:10.4103/aian.aian_406_21 PubMed PMID: 35693656; PubMed Central PMCID: PMC9175425.

95. Hofer LS, Ramberger M, Gredler V, Pescoller AS, Rostásy K, Sospedra M, et al. Comparative Analysis of T-Cell Responses to Aquaporin-4 and Myelin Oligodendrocyte Glycoprotein in Inflammatory Demyelinating Central Nervous System Diseases. Frontiers in Immunology [Internet]. 2020 [cited 2023 Aug 25];11. Available from: https://www.frontiersin.org/articles/10.3389/fimmu.2020.01188

96. Calabrese M, Rinaldi F, Mattisi I, Grossi P, Favaretto A, Atzori M, et al. Widespread cortical thinning characterizes patients with MS with mild cognitive impairment. Neurology. 2010 Jan 26;74(4):321–8. doi:10.1212/WNL.0b013e3181cbcd03 PubMed PMID: 20101038.

97. Sinnecker T, Dörr J, Pfueller CF, Harms L, Ruprecht K, Jarius S, et al. Distinct lesion morphology at 7-T MRI differentiates neuromyelitis optica from multiple sclerosis. Neurology. 2012 Aug 14;79(7):708–14. doi:10.1212/WNL.0b013e3182648bc8 PubMed PMID: 22855861.

98. Messina S, Mariano R, Roca-Fernandez A, Cavey A, Jurynczyk M, Leite MI, et al. Contrasting the brain imaging features of MOG-antibody disease, with AQP4-antibody NMOSD and multiple sclerosis. Mult Scler. 2022 Feb;28(2):217–27. doi:10.1177/13524585211018987 PubMed PMID: 34048323; PubMed Central PMCID: PMC8795219.

99. Jurynczyk M, Geraldes R, Probert F, Woodhall MR, Waters P, Tackley G, et al. Distinct brain imaging characteristics of autoantibody-mediated CNS conditions and multiple sclerosis. Brain. 2017 Mar;140(3):617–27. doi:10.1093/brain/aww350

100. Zheng F, Li Y, Zhuo Z, Duan Y, Cao G, Tian D, et al. Structural and functional hippocampal alterations in Multiple sclerosis and neuromyelitis optica spectrum disorder. Mult Scler. 2022 Apr 1;28(5):707–17. doi:10.1177/13524585211032800

101. Cortese R, Battaglini M, Prados F, Gentile G, Luchetti L, Bianchi A, et al. Grey Matter Atrophy and its Relationship with White Matter Lesions in Patients with Myelin Oligodendrocyte Glycoprotein Antibody-associated Disease, Aquaporin-4 Antibody-Positive Neuromyelitis Optica Spectrum Disorder, and Multiple Sclerosis. Ann Neurol. 2024 Aug;96(2):276–88. doi:10.1002/ana.26951 PubMed PMID: 38780377.

102. Camera V, Messina S, Tamanti A, Bontempi P, Petralia LS, Griffanti L, et al. Investigating the Presence of Neurodegeneration Independent of Relapses in MOGAD Compared to Relapsing-Remitting Multiple Sclerosis. Neurology Open Access. 2025 Jun;1(2):e000013. doi:10.1212/WN9.0000000000000013

103. Camera V, Holm-Mercer L, Ali AAH, Messina S, Horvat T, Kuker W, et al. Frequency of New Silent MRI Lesions in Myelin Oligodendrocyte Glycoprotein Antibody Disease and Aquaporin-4 Antibody Neuromyelitis Optica Spectrum Disorder. JAMA Network Open. 2021 Dec 8;4(12):e2137833. doi:10.1001/jamanetworkopen.2021.37833

104. Calabrese M, Oh MS, Favaretto A, Rinaldi F, Poretto V, Alessio S, et al. No MRI evidence of cortical lesions in neuromyelitis optica. Neurology. 2012 Oct 16;79(16):1671–6. doi:10.1212/WNL.0b013e31826e9a96

105. Popescu BFG, Guo Y, Jentoft ME, Parisi JE, Lennon VA, Pittock SJ, et al. Diagnostic utility of aquaporin-4 in the analysis of active demyelinating lesions. Neurology. 2015 Jan 13;84(2):148–58. doi:10.1212/WNL.0000000000001126 PubMed PMID: 25503621; PubMed Central PMCID: PMC4336081.

106. Kim SH, Kwak K, Hyun JW, Jeong IH, Jo HJ, Joung A, et al. Widespread cortical thinning in patients with neuromyelitis optica spectrum disorder. Eur J Neurol. 2016 Jul;23(7):1165–73. doi:10.1111/ene.13011 PubMed PMID: 27108769.

107. Kim SH, Kwak K, Jeong IH, Hyun JW, Jo HJ, Joung A, et al. Cognitive impairment differs between neuromyelitis optica spectrum disorder and multiple sclerosis. Mult Scler. 2016 Dec;22(14):1850–8. doi:10.1177/1352458516636246 PubMed PMID: 26920380.

108. Hyun JW, Park G, Kwak K, Jo HJ, Joung A, Kim JH, et al. Deep gray matter atrophy in neuromyelitis optica spectrum disorder and

multiple sclerosis. European Journal of Neurology. 2017 Feb;24(2):437–45. doi:10.1111/ene.13224

109. Messina S, Mariano R, Roca-Fernandez A, Cavey A, Jurynczyk M, Leite MI, et al. Contrasting the brain imaging features of MOG-antibody disease, with AQP4-antibody NMOSD and multiple sclerosis. Mult Scler. 2022 Feb;28(2):217–27. doi:10.1177/13524585211018987 PubMed PMID: 34048323; PubMed Central PMCID: PMC8795219.

110. Finke C, Heine J, Pache F, Lacheta A, Borisow N, Kuchling J, et al. Normal volumes and microstructural integrity of deep gray matter structures in AQP4+ NMOSD. Neurol Neuroimmunol Neuroinflamm. 2016 Apr 20;3(3):e229. doi:10.1212/NXI.0000000000000229 PubMed PMID: 27144219; PubMed Central PMCID: PMC4841641.

111. Liu Y, Fu Y, Schoonheim MM, Zhang N, Fan M, Su L, et al. Structural MRI substrates of cognitive impairment in neuromyelitis optica. Neurology. 2015 Oct 27;85(17):1491–9. doi:10.1212/WNL.0000000000002067 PubMed PMID: 26423432.

112. Zhuo Z, Duan Y, Tian DC, Wang X, Gao C, Ding J, et al. Brain structural and functional alterations in MOG antibody disease. MSJ. 2021;27(9):1350–63.

113. Kim SH, Park EY, Park B, Hyun JW, Park NY, Joung A, et al. Multimodal magnetic resonance imaging in relation to cognitive impairment in neuromyelitis optica spectrum disorder. Sci Rep. 2017 Aug 23;7(1):1. doi:10.1038/s41598-017-08889-9

114. Chen X, Roberts N, Zheng Q, Peng Y, Han Y, Luo Q, et al. Comparison of diffusion tensor imaging (DTI) tissue characterization parameters in white matter tracts of patients with multiple sclerosis (MS) and neuromyelitis optica spectrum disorder (NMOSD). Eur Radiol. 2024 Aug 1;34(8):5263–75. doi:10.1007/s00330-023-10550-1

115. Chou IJ, Tanasescu R, Mougin OE, Gowland PA, Tench CR, Whitehouse WP, et al. Reduced Myelin Signal in Normal-appearing White Matter in Neuromyelitis Optica Measured by 7T Magnetic Resonance Imaging. Sci Rep. 2019 Oct 7;9:14378. doi:10.1038/s41598-019-50928-0 PubMed PMID: 31591424; PubMed Central PMCID: PMC6779889.

116. Akaishi T, Takahashi T, Misu T, Abe M, Ishii T, Fujimori J, et al. Progressive patterns of neurological disability in multiple sclerosis and neuromyelitis optica spectrum disorders. Sci Rep. 2020 Aug 17;10(1):13890. doi:10.1038/s41598-020-70919-w PubMed PMID: 32807848; PubMed Central PMCID: PMC7431838.

117. Rice GPA. The natural history of secondary progressive multiple sclerosis: observations from the London study group. Mult Scler. 2002 Feb;8(1):81–2. doi:10.1177/135245850200800116 PubMed PMID: 11936492.

118. Czarnecka D, Oset M, Karlińska I, Stasiołek M. Cognitive impairment in NMOSD—More questions than answers. Brain and Behavior. 2020;10(11):e01842. doi:10.1002/brb3.1842

119. Meng H, Xu J, Pan C, Cheng J, Hu Y, Hong Y, et al. Cognitive dysfunction in adult patients with neuromyelitis optica: a systematic review and meta-analysis. J Neurol. 2017 Aug;264(8):1549–58. doi:10.1007/s00415-016-8345-3 PubMed PMID: 27909800.

120. Kawahara Y, Ikeda M, Deguchi K, Hishikawa N, Kono S, Omote Y, et al. Cognitive and Affective Assessments of Multiple Sclerosis (MS) and Neuromyelitis Optica (NMO) Patients Utilizing Computerized Touch Panel-type Screening Tests. Intern Med. 2014;53(20):2281–90. doi:10.2169/internalmedicine.53.2571

121. Hollinger K, Franke C, Arenivas A, Woods SR, Mealy MA, Levy M, et al. Cognition, mood, and purpose in life in neuromyelitis optica spectrum disorder. Journal of the neurological sciences. 2016 Mar 15;362:85–90. doi:10.1016/j.jns.2016.01.010 PubMed PMID: 26944124.

122. Whittam D, Wilson M, Hamid S, Keir G, Bhojak M, Jacob A. What's new in neuromyelitis optica? A short review for the clinical neurologist. J Neurol. 2017 Nov 1;264(11):2330–44. doi:10.1007/s00415-017-8445-8

123. Taylor HG, Alden J. Age-related differences in outcomes following childhood brain insults: An introduction and overview. Journal of the International Neuropsychological Society. 1997 Nov;3(6):555–67. doi:10.1017/S1355617797005559

124. Santoro JD, Jafarpour S, Boyd NK, Nguyen L, Khoshnood MM. The Impact of Neuroimmunologic Disease and Developing Nervous System. Pediatric Neurology. 2023 Nov 1;148:189–97. doi:10.1016/j.pediatrneurol.2023.06.006

125. Tan A, Hague C, Greenberg BM, Harder L. Neuropsychological outcomes of pediatric demyelinating diseases: a review. Child Neuropsychol. 2018 Jul;24(5):575–97. doi:10.1080/09297049.2017.1339785 PubMed PMID: 28637379.

126. Cacciaguerra L, Curatoli C, Vizzino C, Valsasina P, Filippi M, Rocca MA. ECTRIMS 2022 – Oral Presentations: Functional correlates of intelligence quotient and cognitive abilities vary according to maturation in pediatric MS (abstract O164). Mult Scler. 2022 Oct 1;28(3_suppl):3–129. doi:10.1177/13524585221123685

127. Harder L, Arenivas A, Tan A, Hughes S, Plumb P, Greenberg B. Pediatrics-2Neuropsychological and Academic Functioning in Pediatric Neuromyelitis Optica. Arch Clin Neuropsychol. 2015 Sep 1;30(6):481. doi:10.1093/arclin/acv046.18

128. Zhang N, Li Y, Shao J, Luo L, Shi F, Liu Y. Cognitive impairment in Chinese neuromyelitis optica. MSJ. 2015;21(14):1839–46.

129. Kong L, Lang Y, Wang X, Wang J, Chen H, Shi Z, et al. Identifying different cognitive phenotypes and their relationship with disability in neuromyelitis optica spectrum disorder. Front Neurol. 2022 Sep 16;13:958441. doi:10.3389/fneur.2022.958441 PubMed PMID: 36188400; PubMed Central PMCID: PMC9524354.

130. Salama S, Marouf H, Reda MI, Mansour AR, ELKholy O, Levy M. Cognitive function in Egyptian Neuromyelitis Optica Spectrum Disorder. Clin Neurol Neurosurg. 2020 Feb;189:105621. doi:10.1016/j.clineuro.2019.105621 PubMed PMID: 31790906; PubMed Central PMCID: PMC7002275.

131. Moore P, Methley A, Pollard C, Mutch K, Hamid S, Elsone L, et al. Cognitive and psychiatric comorbidities in neuromyelitis optica. J Neurol Sci. 2016 Jan 15;360:4–9. doi:10.1016/j.jns.2015.11.031 PubMed PMID: 26723962.

132. Cho EB, Han CE, Seo SW, Chin J, Shin JH, Cho HJ, et al. White Matter Network Disruption and Cognitive Dysfunction in Neuromyelitis Optica Spectrum Disorder. Front Neurol. 2018 Dec 17;9. doi:10.3389/fneur.2018.01104 PubMed PMID: 30619061; PubMed Central PMCID: PMC6304415.

133. Vlahovic L, McDonald J, Hinman J, Tomczak A, Lock C, Palmer CA, et al. Prevalence, Demographic, and Clinical Factors Associated With Cognitive Dysfunction in Patients With Neuromyelitis Optica Spectrum Disorder. Neurology. 2024 Jan 9;102(1):e207965. doi:10.1212/WNL.0000000000207965

134. Savoldi F, Rocca MA, Valsasina P, Riccitelli GC, Mesaros S, Drulovic J, et al. Functional brain connectivity abnormalities and cognitive deficits in neuromyelitis optica spectrum disorder. Multiple Sclerosis. 2020;26(7):pp795-805. doi:10.1177/1352458519845109

135. YABALAK A, ALTUNRENDE B, DEMİR GA. Cognitive Impairment in Neuromyelitis Optica. Noro Psikiyatr Ars. 2020 Apr 24;58(3):200–5. doi:10.29399/npa.24928 PubMed PMID: 34526842; PubMed Central PMCID: PMC8419735.

136. Fujimori J, Nakashima I, Baba T, Meguro Y, Ogawa R, Fujihara K. Cognitive impairment in neuromyelitis optica spectrum disorders: A comparison of the Wechsler Adult Intelligence Scale-III and the Wechsler Memory Scale Revised with the Rao Brief Repeatable

Neuropsychological Battery. eNeurologicalSci. 2017 Sep 21;9:3–7. doi:10.1016/j.ensci.2017.09.001 PubMed PMID: 29260040; PubMed Central PMCID: PMC5731537.

137. Liu Y, Jiang X, Butzkueven H, Duan Y, Huang J, Ren Z, et al. Multimodal characterization of gray matter alterations in neuromyelitis optica. Mult Scler. 2018 Sep;24(10):1308–16. doi:10.1177/1352458517721053

138. Griffiths-King D, Billaud C, Makusha L, Looi LL, Wassmer E, Wright S, et al. Impact of autoantibodies against myelin oligodendrocyte glycoprotein in paediatric acquired demyelinating disease: Intellectual functioning and academic performance. European Journal of Paediatric Neurology. 2024 Nov 1;53:8–17. doi:10.1016/j.ejpn.2024.09.001 PubMed PMID: 39243465.

139. Deiva K, Cobo-Calvo A, Maurey H, De Chalus A, Yazbeck E, Husson B, et al. Risk factors for academic difficulties in children with myelin oligodendrocyte glycoprotein antibody-associated acute demyelinating syndromes. Developmental Medicine & Child Neurology. 2020;62(9):1075–81. doi:10.1111/dmcn.14594

140. Brill L, Ganelin-Cohen E, Dabby R, Rabinowicz S, Zohar-Dayan E, Rein N, et al. Age-Related Clinical Presentation of MOG-IgG Seropositivity in Israel. Frontiers in Neurology. 2021;11:1739. doi:10.3389/fneur.2020.612304

141. Jacobs RK, Anderson VA, Neale JL, Shield LK, Kornberg AJ. Neuropsychological outcome after acute disseminated encephalomyelitis: Impact of age at illness onset. Pediatric Neurology. 2004 Sep 1;31(3):191–7. doi:10.1016/j.pediatrneurol.2004.03.008

142. Suppiej A, Cainelli E, Casara G, Cappellari A, Nosadini M, Sartori S. Long-term neurocognitive outcome and quality of life in pediatric acute disseminated encephalomyelitis. Pediatr Neurol. 2014 Apr;50(4):363–7. doi:10.1016/j.pediatrneurol.2013.12.006 PubMed PMID: 24630282.

143. Mittelman A, Pique J, Desportes V, Deiva K, Poulat AL, Marignier R. Cognitive and academic outcomes in children with myelin oligodendrocyte glycoprotein antibody-associated disease. Developmental Medicine & Child Neurology. n/a(n/a). doi:10.1111/dmcn.16093

144. Armangue T, Olivé-Cirera G, Martínez-Hernandez E, Sepulveda M, Ruiz-Garcia R, Muñoz-Batista M, et al. Associations of paediatric demyelinating and encephalitic syndromes with myelin oligodendrocyte glycoprotein antibodies: a multicentre

observational study. Lancet Neurol. 2020 Mar;19(3):234–46. doi:10.1016/S1474-4422(19)30488-0 PubMed PMID: 32057303.

145. Kogel AK, Ladopoulos T, Schwake C, Kleiter I, Teegen B, Siems N, et al. Cognitive Impairment, Associated Clinical Factors, and MR Volumetric Measures in Myelin Oligodendrocyte Glycoprotein-IgG-Associated Disease. Neurol Neuroimmunol Neuroinflamm. 2024 Dec;11(6):e200325. doi:10.1212/NXI.0000000000200325 PubMed PMID: 39393044.

146. Yazbeck E, Maurey H, Leroy C, Horellou P, Napuri S, Lali M, et al. Progressive Leukodystrophy-Like Demyelinating Syndromes with MOG-Antibodies in Children: A Rare Under-Recognized Phenotype. Neuropediatrics. 2021 Aug;52(4):337–40. doi:10.1055/s-0041-1726289 PubMed PMID: 33792000.

147. Wang J, Qiu Z, Li D, Yang X, Ding Y, Gao L, et al. Clinical and Imaging Features of Patients With Encephalitic Symptoms and Myelin Oligodendrocyte Glycoprotein Antibodies. Frontiers in Immunology [Internet]. 2021 [cited 2022 Jul 21];12. Available from: https://www.frontiersin.org/articles/10.3389/fimmu.2021.722404

148. Jacobs RK, Anderson VA, Neale JL, Shield LK, Kornberg AJ. Neuropsychological outcome after acute disseminated encephalomyelitis: impact of age at illness onset. Pediatr Neurol. 2004 Sep;31(3):191–7. doi:10.1016/j.pediatrneurol.2004.03.008 PubMed PMID: 15351018.

149. Toga AW, Thompson PM, Sowell ER. Mapping brain maturation. Trends in Neurosciences. 2006 Mar 1;29(3):148–59. doi:10.1016/j.tins.2006.01.007 PubMed PMID: 16472876.

150. Pujol J, Vendrell P, Junqué C, Martí-Vilalta JL, Capdevila A. When does human brain development end? Evidence of corpus callosum growth up to adulthood. Annals of Neurology. 1993;34(1):71–5. doi:10.1002/ana.410340113

151. Wingerchuk DM, Banwell B, Bennett JL, Cabre P, Carroll W, Chitnis T, et al. International consensus diagnostic criteria for neuromyelitis optica spectrum disorders. Neurology. 2015 Jul 14;85(2):177–89. doi:10.1212/WNL.0000000000001729 PubMed PMID: 26092914; PubMed Central PMCID: PMC4515040.

152. Keesey JC. Does myasthenia gravis affect the brain? Journal of the Neurological Sciences. 1999 Nov 30;170(2):77–89. doi:10.1016/S0022-510X(99)00205-1

153. Kenny RA, Coen RF, Frewen J, Donoghue OA, Cronin H, Savva GM. Normative Values of Cognitive and Physical Function in Older Adults: Findings from The Irish Longitudinal Study on Ageing. Journal of the

American Geriatrics Society. 2013;61(s2):S279–90. doi:10.1111/jgs.12195

154. Faul F, Erdfelder E, Lang AG, Buchner A. G*Power 3: a flexible statistical power analysis program for the social, behavioral, and biomedical sciences. Behav Res Methods. 2007 May;39(2):175–91. doi:10.3758/bf03193146 PubMed PMID: 17695343.

155. Guo X, Zhu J, Zhang N, Zhang L, Qi Y, Cai H, et al. Altered neurovascular coupling in neuromyelitis optica. Hum Brain Mapp. 2018 Oct 13;40(3):976–86. doi:10.1002/hbm.24426 PubMed PMID: 30315685; PubMed Central PMCID: PMC6865682.

156. Amato MP, Portaccio E, Goretti B, Zipoli V, Ricchiuti L, De Caro MF, et al. The Rao's Brief Repeatable Battery and Stroop test: normative values with age, education and gender corrections in an Italian population. Mult Scler. 2006 Nov 1;12(6):787–93. doi:10.1177/1352458506070933

157. Nasreddine ZS, Phillips NA, Bédirian V, Charbonneau S, Whitehead V, Collin I, et al. The Montreal Cognitive Assessment, MoCA: a brief screening tool for mild cognitive impairment. J Am Geriatr Soc. 2005 Apr;53(4):695–9. doi:10.1111/j.1532-5415.2005.53221.x PubMed PMID: 15817019.

158. Freitas S, Batista S, Afonso AC, Simões MR, de Sousa L, Cunha L, et al. The Montreal Cognitive Assessment (MoCA) as a screening test for cognitive dysfunction in multiple sclerosis. Applied Neuropsychology: Adult. 2018 Jan 2;25(1):57–70. doi:10.1080/23279095.2016.1243108 PubMed PMID: 27791389.

159. Han Y, Liu Y, Zeng C, Luo Q, Xiong H, Zhang X, et al. Functional Connectivity Alterations in Neuromyelitis Optica Spectrum Disorder. Clin Neuroradiol. 2020 Sep 1;30(3):559–68. doi:10.1007/s00062-019-00802-3

160. Wittich W, Phillips N, Nasreddine ZS, Chertkow H. Sensitivity and Specificity of the Montreal Cognitive Assessment Modified for Individuals who are Visually Impaired. Journal of Visual Impairment & Blindness. 2010 Jun;104(6):360–8. doi:10.1177/0145482X1010400606

161. Dunn PK, Smyth GK. Chapter 2: Linear Regression Models. In: Dunn PK, Smyth GK, editors. Generalized Linear Models With Examples in R [Internet]. New York, NY: Springer; 2018 [cited 2024 Aug 4]. p. 31–91. Available from: https://doi.org/10.1007/978-1-4419-0118-7_2 doi:10.1007/978-1-4419-0118-7_2

162. van Buuren S. Flexible Imputation of Missing Data [Internet]. Second Edition. CRC Press; 2018 [cited 2024 Nov 7]. (Chapman &

Hall/ CRC Interdisciplinary Statistics Series). Available from: https://stefvanbuuren.name/fimd/

163. R Core Team. R: A language and environment for statistical computing. [Internet]. Vienna, Austria.: R Foundation for Statistical Computing,; 2021. Available from: https://www.R-project.org/

164. Ayzenberg I, Richter D, Henke E, Asseyer S, Paul F, Trebst C, et al. Pain, Depression, and Quality of Life in Neuromyelitis Optica Spectrum Disorder. Neurol Neuroimmunol Neuroinflamm. 2021 Apr 20;8(3):e985. doi:10.1212/NXI.0000000000000985 PubMed PMID: 34108267; PubMed Central PMCID: PMC8058953.

165. Chanson JB, Zéphir H, Collongues N, Outteryck O, Blanc F, Fleury M, et al. Evaluation of health-related quality of life, fatigue and depression in neuromyelitis optica: HRQOL, fatigue and depression in NMO. European Journal of Neurology. 2011 Jun;18(6):836–41. doi:10.1111/j.1468-1331.2010.03252.x

166. Cacciaguerra L, Valsasina P, Meani A, Riccitelli GC, Radaelli M, Rocca MA, et al. Volume of hippocampal subfields and cognitive deficits in neuromyelitis optica spectrum disorders. European Journal of Neurology. 2021;28(12):4167–77. doi:10.1111/ene.15073

167. Lopes C, Sousa C, Fraga A, Guimarães J, Vicente S, Sá MJ. Cognitive impairment in Neuromyelitis Optica Spectrum Disorder: A retrospective study using the Brief International cognitive Assessment for Multiple Sclerosis (BICAMS). Appl Neuropsychol Adult. 2025;32(3):761–7. doi:10.1080/23279095.2023.2210242 PubMed PMID: 37195824.

168. Yang Y, Yu Q, Wu P, Dai H, Wu X, Han S, et al. Reduced GABA levels in the medial prefrontal cortex are associated with cognitive impairment in patients with NMOSD. Multiple Sclerosis and Related Disorders. 2022 Feb 1;58:103496. doi:10.1016/j.msard.2022.103496

169. Blanc F, Noblet V, Jung B, Rousseau F, Renard F, Bourre B, et al. White Matter Atrophy and Cognitive Dysfunctions in Neuromyelitis Optica. PLoS One. 2012 Apr 3;7(4). doi:10.1371/journal.pone.0033878 PubMed PMID: 22509264; PubMed Central PMCID: PMC3317931.

170. Diamond BJ, Johnson SK, Kaufman M, Graves L. Relationships between information processing, depression, fatigue and cognition in multiple sclerosis. Arch Clin Neuropsychol. 2008 Mar;23(2):189–99. doi:10.1016/j.acn.2007.10.002 PubMed PMID: 18053682.

171. Arnett PA. Longitudinal consistency of the relationship between depression symptoms and cognitive functioning in multiple

sclerosis. CNS Spectr. 2005 May;10(5):372–82. doi:10.1017/s1092852900022744 PubMed PMID: 15858455.

172. Arnett PA, Barwick FH, Beeney JE. Depression in multiple sclerosis: Review and theoretical proposal. Journal of the International Neuropsychological Society. 2008 Sep;14(5):691–724. doi:10.1017/S1355617708081174

173. Guillemin C, Lommers E, Delrue G, Gester E, Maquet P, Collette F. The Complex Interplay Between Trait Fatigue and Cognition in Multiple Sclerosis | Psychologica Belgica [Internet]. 2022 Jan 10. doi:10.5334/pb.1125

174. Mattioli F, Bellomi F, Stampatori C, Parrinello G, Capra R. Depression, disability and cognitive impairment in multiple sclerosis: a cross sectional Italian study. Neurol Sci. 2011 Oct 1;32(5):825–32. doi:10.1007/s10072-011-0624-2

175. Heesen C, Schulz KH, Fiehler J, Von der Mark U, Otte C, Jung R, et al. Correlates of cognitive dysfunction in multiple sclerosis. Brain, Behavior, and Immunity. 2010 Oct;24(7):1148–55. doi:10.1016/j.bbi.2010.05.006

176. Dagenais E, Rouleau I, Demers M, Jobin C, Roger E, Chamelian L, et al. Value of the MoCA test as a screening instrument in multiple sclerosis. Can J Neurol Sci. 2013 May;40(3):410–5. doi:10.1017/s0317167100014384 PubMed PMID: 23603179.

177. Meng H, Xu J, Pan C, Cheng J, Hu Y, Hong Y, et al. Cognitive dysfunction in adult patients with neuromyelitis optica: a systematic review and meta-analysis. Journal of Neurology. 2017 Aug 1;264. doi:10.1007/s00415-016-8345-3

178. Kazzi C, Alpitsis R, O'Brien TJ, Malpas CB, Monif M. Cognitive and psychopathological features of neuromyelitis optica spectrum disorder and myelin oligodendrocyte glycoprotein antibody-associated disease: A narrative review. Multiple Sclerosis and Related Disorders. 2024 May 1;85:105596. doi:10.1016/j.msard.2024.105596

179. Chavarro VS, Bellmann-Strobl J, Zimmermann HG, Scheel M, Chien C, Oertel FC, et al. Visual system damage and network maladaptation are associated with cognitive performance in neuromyelitis optica spectrum disorders. Mult Scler Relat Disord. 2020 Oct;45:102406. doi:10.1016/j.msard.2020.102406 PubMed PMID: 32707533.

180. Maniscalco GT, Ziello AR, Mantovani E, Dinoto A, Di Giulio Cesare D, Moreggia O, et al. Cognitive Profile in Adult Patients With Myelin Oligodendrocyte Glycoprotein Antibody-Associated Disease: A

Comparative Study With Multiple Sclerosis. Euro J of Neurology. 2025 Mar;32(3):e70115. doi:10.1111/ene.70115

181. Meca-Lallana V, Gascón-Giménez F, Ginestal-López RC, Higueras Y, Téllez-Lara N, Carreres-Polo J, et al. Cognitive impairment in multiple sclerosis: diagnosis and monitoring. Neurol Sci. 2021;42(12):5183–93. doi:10.1007/s10072-021-05165-7 PubMed PMID: 33796947; PubMed Central PMCID: PMC8642331.

182. Scarpina F, Tagini S. The Stroop Color and Word Test. Front Psychol. 2017 Apr 12;8:557. doi:10.3389/fpsyg.2017.00557 PubMed PMID: 28446889; PubMed Central PMCID: PMC5388755.

183. Damasceno A, Amaral JMSDS, Barreira AA, Becker J, Callegaro D, Campanholo KR, et al. Normative values of the Brief Repeatable Battery of Neuropsychological Tests in a Brazilian population sample: discrete and regression–based norms. Arq Neuro-Psiquiatr. 2018 Mar;76(3):163–9. doi:10.1590/0004-282x20180006

184. Rao SM, Leo GJ, Bernardin L, Unverzagt F. Cognitive dysfunction in multiple sclerosis.: I. Frequency, patterns, and prediction. Neurology. 1991 May 1;41(5):685–91. doi:10.1212/WNL.41.5.685 PubMed PMID: 2027484.

185. He D, Wu Q, Chen X, Zhao D, Gong Q, Zhou H. Cognitive impairment and whole brain diffusion in patients with neuromyelitis optica after acute relapse. Brain Cogn. 2011 Oct;77(1):80–8. doi:10.1016/j.bandc.2011.05.007 PubMed PMID: 21723024.

186. Blanc F, Zéphir H, Lebrun C, Labauge P, Castelnovo G, Fleury M, et al. Cognitive functions in neuromyelitis optica. Arch Neurol. 2008 Jan;65(1):84–8. doi:10.1001/archneurol.2007.16 PubMed PMID: 18195143.

187. Constantinescu C, Chou IJ, Tanasescu R, Tench C, Lim SY, Podda G. Cognitive Function and Fatigue in Patients with Neuromyelitis Optica: comparison with MS subtypes (P5.256). Neurology [Internet]. 2015 Apr 6 [cited 2022 Mar 16];84(14 Supplement). Available from: https://n.neurology.org/content/84/14_Supplement/P5.256

188. Foolad F, Khodagholi F, Nabavi SM, Javan M. Changes in mitochondrial function in patients with neuromyelitis optica; correlations with motor and cognitive disabilities. PLOS ONE. 2020 Mar 26;15(3):e0230691. doi:10.1371/journal.pone.0230691

189. Cacciaguerra L, Valsasina P, Meani A, Riccitelli GC, Radaelli M, Rocca MA, et al. Volume of hippocampal subfields and cognitive deficits in neuromyelitis optica spectrum disorders. European Journal of Neurology. 2021;28(12):4167–77. doi:10.1111/ene.15073

190. Höftberger R, Guo Y, Flanagan EP, Lopez-Chiriboga AS, Endmayr V, Hochmeister S, et al. The pathology of central nervous system inflammatory demyelinating disease accompanying myelin oligodendrocyte glycoprotein autoantibody. Acta Neuropathol. 2020 May 1;139(5):875–92. doi:10.1007/s00401-020-02132-y

191. Roemer SF, Parisi JE, Lennon VA, Benarroch EE, Lassmann H, Bruck W, et al. Pattern-specific loss of aquaporin-4 immunoreactivity distinguishes neuromyelitis optica from multiple sclerosis. Brain. 2007 May 1;130(5):1194–205. doi:10.1093/brain/awl371

192. Takai Y, Misu T, Kaneko K, Chihara N, Narikawa K, Tsuchida S, et al. Myelin oligodendrocyte glycoprotein antibody-associated disease: an immunopathological study. Brain. 2020 May 1;143(5):1431–46. doi:10.1093/brain/awaa102

193. Zhao M, Li X, Li F, Hu X, Wang J, Liu Y, et al. Identification of neurotransmitter imbalances in the cingulate cortex of NMOSD patients using magnetic resonance spectroscopy. Cerebral Cortex. 2024 Jul 1;34(7):bhae304. doi:10.1093/cercor/bhae304

194. Cha H, Choi JH, Jeon H, Kim JH, Kim M, Kim SJ, et al. Aquaporin-4 Deficiency is Associated with Cognitive Impairment and Alterations in astrocyte-neuron Lactate Shuttle. Mol Neurobiol. 2023 Nov 1;60(11):6212–26. doi:10.1007/s12035-023-03475-9

195. Duan Y, Zhuo Z, Li H, Tian DC, Li Y, Yang L, et al. Brain structural alterations in MOG antibody diseases: a comparative study with AQP4 seropositive NMOSD and MS. J Neurol Neurosurg Psychiatry. 2021 Jul;92(7):709–16. doi:10.1136/jnnp-2020-324826 PubMed PMID: 33687975; PubMed Central PMCID: PMC8223649.

196. Schmidt FA, Chien C, Kuchling J, Bellmann-Strobl J, Ruprecht K, Siebert N, et al. Differences in Advanced Magnetic Resonance Imaging in MOG-IgG and AQP4-IgG Seropositive Neuromyelitis Optica Spectrum Disorders: A Comparative Study. Front Neurol. 2020 Sep 30;11. doi:10.3389/fneur.2020.499910

197. Lotan I, Billiet T, Ribbens A, Van Hecke W, Huang B, Kister I, et al. Volumetric brain changes in MOGAD: A cross-sectional and longitudinal comparative analysis. Multiple Sclerosis and Related Disorders. 2023 Jan 1;69:104436. doi:10.1016/j.msard.2022.104436

198. Zhuo Z, Duan Y, Tian D, Wang X, Gao C, Ding J, et al. Brain structural and functional alterations in MOG antibody disease. Mult Scler. 2021 Aug 1;27(9):1350–63. doi:10.1177/1352458520964415

199. Zhao DD, Zhou HY, Wu QZ, Liu J, Chen XY, He D, et al. Diffusion tensor imaging characterization of occult brain damage in relapsing neuromyelitis optica using 3.0T magnetic resonance imaging

techniques. NeuroImage. 2012 Feb 15;59(4):3173–7. doi:10.1016/j.neuroimage.2011.11.022

200. Liu Y, Liang P, Duan Y, Jia X, Wang F, Yu C, et al. Abnormal baseline brain activity in patients with neuromyelitis optica: A resting-state fMRI study. European Journal of Radiology. 2011 Nov 1;80(2):407–11. doi:10.1016/j.ejrad.2010.05.002

201. Fan Y, Liu M, Wu X, Wang F, Ding J, Chen J, et al. Aquaporin-4 promotes memory consolidation in Morris water maze. Brain Struct Funct. 2013 Jan;218(1):39–50. doi:10.1007/s00429-011-0373-2 PubMed PMID: 22193336.

202. Hubbard JA, Szu JI, Binder DK. The role of aquaporin-4 in synaptic plasticity, memory and disease. Brain Res Bull. 2018 Jan;136:118–29. doi:10.1016/j.brainresbull.2017.02.011 PubMed PMID: 28274814.

203. Oliveira AI, Monteiro IR, Alferes AR, Santos I, Machado R, Correia I, et al. Cognitive outcomes in late-onset versus adult-onset Multiple Sclerosis. Multiple Sclerosis and Related Disorders. 2024 Oct 1;90:105845. doi:10.1016/j.msard.2024.105845

204. Eyre M, Absoud M, Abdel-Mannan O, Crichton S, Hacohen Y, Rossor T, et al. Academic outcomes before and after clinical onset of acquired demyelinating syndromes in children: a matched cohort data linkage study. Ann Clin Transl Neurol. 2024 Oct 2. doi:10.1002/acn3.52198 PubMed PMID: 39359055.

205. Carroll S, Chalder T, Hemingway C, Heyman I, Bear H, Sweeney L, et al. Adolescent and parent factors related to fatigue in paediatric multiple sclerosis and chronic fatigue syndrome: A comparative study. European Journal of Paediatric Neurology. 2019 Jan 1;23(1):70–80. doi:10.1016/j.ejpn.2018.10.006 PubMed PMID: 30455131.

206. Douglas JW. Early hospital admissions and later disturbances of behaviour and learning. Developmental Medicine & Child Neurology. 1975;17(4):456–80. doi:10.1111/j.1469-8749.1975.tb03497.x

207. Harder LL, Holland AA, Frohman E, Graves D, Greenberg BM. Cognitive functioning in pediatric transverse myelitis. Mult Scler. 2013 Jun 1;19(7):947–52. doi:10.1177/1352458512466606

208. He D, Chen X, Zhao D, Zhou H. Cognitive Function, Depression, Fatigue, and Activities of Daily Living in Patients With Neuromyelitis Optica After Acute Relapse. null. 2011 Nov 11;121(12):677–83. doi:10.3109/00207454.2011.608456

209. Tarhan B, Rempe T, Rahman S, Rodriguez E, Sladky J, Tuna IS, et al. A Comparison of Pediatric- and Adult-Onset Aquaporin-4

Immunoglobulin G-Positive Neuromyelitis Optica Spectrum Disorder: A Review of Clinical and Radiographic Characteristics. J Child Neurol. 2022 Aug;37(8–9):727–37. doi:10.1177/08830738221103085 PubMed PMID: 35673711.

210. Zhou X, Yang Y, Zhu F, Chen X, Zhu Y, Gui T, et al. Neurometabolic and Brain Functional Alterations Associated with Cognitive Impairment in Patients with Myasthenia Gravis: A Combined 1H-MRS and fMRI Study. Neuroscience. 2024 Apr 19;544:12–27. doi:10.1016/j.neuroscience.2024.02.021 PubMed PMID: 38423165.

211. Iwasaki Y, Kinoshita M, Ikeda K, Takamiya K, Shiojima T. Cognitive dysfunction in myasthenia gravis. Int J Neurosci. 1990 Sep;54(1–2):29–33. doi:10.3109/00207459008986619 PubMed PMID: 2265963.

212. Klaus B, Müller P, van Wickeren N, Dordevic M, Schmicker M, Zdunczyk Y, et al. Structural and functional brain alterations in patients with myasthenia gravis. Brain Communications. 2022 Feb 1;4(1):fcac018. doi:10.1093/braincomms/fcac018

213. Bartel PR, Lotz BP. Neuropsychological test performance and affect in myasthenia gravis. Acta Neurologica Scandinavica. 1995 Apr;91(4):266–70. doi:10.1111/j.1600-0404.1995.tb07002.x

214. Lewis SW, Ron MA, Newsom-Davis J. Absence of central functional cholinergic deficits in myasthenia gravis. J Neurol Neurosurg Psychiatry. 1989 Feb;52(2):258–61. doi:10.1136/jnnp.52.2.258 PubMed PMID: 2703842; PubMed Central PMCID: PMC1032516.

215. Glennerster A, Palace J, Warburton D, Oxbury S, Newsom-Davis J. Memory in myasthenia gravis. Neurology. 1996 Apr;46(4):1138–42. doi:10.1212/WNL.46.4.1138

216. Kyriakidis NC, López-Cortés A, González EV, Grimaldos AB, Prado EO. SARS-CoV-2 vaccines strategies: a comprehensive review of phase 3 candidates. npj Vaccines. 2021 Feb 22;6(1):1–17. doi:10.1038/s41541-021-00292-w

217. Heinz FX, Stiasny K. Distinguishing features of current COVID-19 vaccines: knowns and unknowns of antigen presentation and modes of action. npj Vaccines. 2021 Aug 16;6(1):1. doi:10.1038/s41541-021-00369-6

218. Federico M. The conundrum of current anti-SARS-CoV-2 vaccines. Cytokine Growth Factor Rev. 2021 Aug;60:46–51. doi:10.1016/j.cytogfr.2021.03.001 PubMed PMID: 33714693; PubMed Central PMCID: PMC7936752.

219. Grant-Peters M, Passos GRD, Yeung HY, Jacob A, Huda S, Leite MI, et al. No strong HLA association with MOG antibody disease in the

UK population. Ann Clin Transl Neurol. 2021 Jul;8(7):1502–7. doi:10.1002/acn3.51378 PubMed PMID: 33991459; PubMed Central PMCID: PMC8283171.

220. Bruijstens AL, Wong YYM, Van Pelt DE, Van Der Linden PJE, Haasnoot GW, Hintzen RQ, et al. HLA association in MOG-IgG– and AQP4-IgG–related disorders of the CNS in the Dutch population. Neurol Neuroimmunol Neuroinflamm. 2020 May;7(3):e702. doi:10.1212/NXI.0000000000000702

221. Ramanathan S, Reddel SW, Henderson A, Parratt JDE, Barnett M, Gatt PN, et al. Antibodies to myelin oligodendrocyte glycoprotein in bilateral and recurrent optic neuritis. Neurol Neuroimmunol Neuroinflamm. 2014 Oct 29;1(4):e40. doi:10.1212/NXI.0000000000000040 PubMed PMID: 25364774; PubMed Central PMCID: PMC4215392.

222. Agmon-Levin N, Paz Z, Israeli E, Shoenfeld Y. Vaccines and autoimmunity. Nat Rev Rheumatol. 2009 Nov;5(11):11. doi:10.1038/nrrheum.2009.196

223. Mustelin T, Andrade F. Autoimmunity: the neoantigen hypothesis. Front Immunol. 2024 Jun 27;15. doi:10.3389/fimmu.2024.1432985

224. Wraith DC, Goldman M, Lambert PH. Vaccination and autoimmune disease: what is the evidence? The Lancet. 2003 Nov 15;362(9396):1659–66. doi:10.1016/S0140-6736(03)14802-7

225. Wang L, Wang FS, Gershwin ME. Human autoimmune diseases: a comprehensive update. Journal of Internal Medicine. 2015;278(4):369–95. doi:10.1111/joim.12395

226. Olivieri B, Betterle C, Zanoni G. Vaccinations and Autoimmune Diseases. Vaccines (Basel). 2021 Jul 22;9(8):815. doi:10.3390/vaccines9080815 PubMed PMID: 34451940; PubMed Central PMCID: PMC8402446.

227. Schattner A. Consequence or coincidence? The occurrence, pathogenesis and significance of autoimmune manifestations after viral vaccines. Vaccine. 2005 Jun 10;23(30):3876–86. doi:10.1016/j.vaccine.2005.03.005 PubMed PMID: 15917108.

228. Butler M, Tamborska A, Wood GK, Ellul M, Thomas RH, Galea I, et al. Considerations for causality assessment of neurological and neuropsychiatric complications of SARS-CoV-2 vaccines: from cerebral venous sinus thrombosis to functional neurological disorder. J Neurol Neurosurg Psychiatry. 2021 Nov 1;92(11):1144–51. doi:10.1136/jnnp-2021-326924 PubMed PMID: 34362855.

229. Sejvar JJ, Pfeifer D, Schonberger LB. Guillain-Barré Syndrome Following Influenza Vaccination: Causal or Coincidental? Curr Infect Dis Rep. 2011 Aug 1;13(4):387–98. doi:10.1007/s11908-011-0194-8

230. Whitaker HJ, Farrington CP, Spiessens B, Musonda P. Tutorial in biostatistics: the self-controlled case series method. Stat Med. 2006 May 30;25(10):1768–97. doi:10.1002/sim.2302 PubMed PMID: 16220518.

231. Black C, Kaye JA, Jick H. MMR vaccine and idiopathic thrombocytopaenic purpura. Br J Clin Pharmacol. 2003 Jan;55(1):107–11. doi:10.1046/j.1365-2125.2003.01790.x PubMed PMID: 12534647; PubMed Central PMCID: PMC1884189.

232. Tenembaum S, Chitnis T, Ness J, Hahn JS, International Pediatric MS Study Group. Acute disseminated encephalomyelitis. Neurology. 2007 Apr 17;68(16 Suppl 2):S23-36. doi:10.1212/01.wnl.0000259404.51352.7f PubMed PMID: 17438235.

233. Krupp LB, Tardieu M, Amato MP, Banwell B, Chitnis T, Dale RC, et al. International Pediatric Multiple Sclerosis Study Group criteria for pediatric multiple sclerosis and immune-mediated central nervous system demyelinating disorders: revisions to the 2007 definitions. Mult Scler. 2013 Sep;19(10):1261–7. doi:10.1177/1352458513484547 PubMed PMID: 23572237.

234. Karussis D, Petrou P. The spectrum of post-vaccination inflammatory CNS demyelinating syndromes. Autoimmun Rev. 2014 Mar;13(3):215–24. doi:10.1016/j.autrev.2013.10.003 PubMed PMID: 24514081.

235. Ketelslegers I, Visser I, Neuteboom R, Boon M, Catsman-Berrevoets C, Hintzen R. Disease course and outcome of acute disseminated encephalomyelitis is more severe in adults than in children. Mult Scler. 2011 Apr 1;17(4):441–8. doi:10.1177/1352458510390068

236. Huynh W, Cordato D, Kehdi E, Masters L, Dedousis C. Post-vaccination encephalomyelitis: Literature review and illustrative case | Elsevier Enhanced Reader. J Clin Neurol. 2008;15:1315–22. doi:10.1016/j.jocn.2008.05.002

237. Kumar N, Graven K, Joseph NI, Johnson J, Fulton S, Hostoffer R, et al. Case Report: Postvaccination Anti-Myelin Oligodendrocyte Glycoprotein Neuromyelitis Optica Spectrum Disorder: A Case Report and Literature Review of Postvaccination Demyelination. Int J MS Care. 2020 Apr;22(2):85–90. doi:10.7224/1537-2073.2018-104 PubMed PMID: 32410903; PubMed Central PMCID: PMC7204366.

238. Cobo-Calvo A, Ruiz A, Maillart E, Audoin B, Zephir H, Bourre B, et al. Clinical spectrum and prognostic value of CNS MOG

autoimmunity in adults: The MOGADOR study. Neurology. 2018 May 22;90(21):e1858–69. doi:10.1212/WNL.0000000000005560

239. GOV.UK [Internet]. [cited 2021 Dec 30]. COVID-19: estimated administrative vaccine uptake for people aged 18 and over. Available from: https://www.gov.uk/government/publications/covid-19-vaccine-estimated-coverage-for-people-aged-18-and-over

240. McLean-Tooke A, Lucas M, French M. Autoimmunity elicited by the chemokine response to adenovirus vector vaccines may underlie vaccine-induced immune thrombotic thrombocytopaenia: a hypothesis. Clin Transl Immunology. 2021 Oct 14;10(10):e1349. doi:10.1002/cti2.1349 PubMed PMID: 34691454; PubMed Central PMCID: PMC8517088.

241. Cines DB, Greinacher A. Spotlight on vaccine-induced thrombosis and thrombocytopenia (VITT). Blood. 2023 Jan 20;blood.2022017696. doi:10.1182/blood.2022017696

242. Greinacher A, Thiele T, Warkentin TE, Weisser K, Kyrle PA, Eichinger S. Thrombotic Thrombocytopenia after ChAdOx1 nCov-19 Vaccination. New England Journal of Medicine. 2021 Jun 3;384(22):2092–101. doi:10.1056/NEJMoa2104840 PubMed PMID: 33835769.

243. Schulz JB, Berlit P, Diener HC, Gerloff C, Greinacher A, Klein C, et al. COVID-19 Vaccine-Associated Cerebral Venous Thrombosis in Germany. Annals Of Neurology. 2021;90(4):pp627-639. doi:10.1002/ana.26172

244. Kim KH, Kim SH, Park NY, Hyun JW, Kim HJ. Onset of various CNS inflammatory demyelination diseases following COVID-19 vaccinations. Mult Scler Relat Disord. 2022 Dec;68:104141. doi:10.1016/j.msard.2022.104141 PubMed PMID: 36037757; PubMed Central PMCID: PMC9392895.

245. Kaulen LD, Doubrovinskaia S, Mooshage C, Jordan B, Purrucker J, Haubner C, et al. Neurological autoimmune diseases following vaccinations against SARS-CoV-2: a case series. Eur J Neurol. 2022 Feb;29(2):555–63. doi:10.1111/ene.15147 PubMed PMID: 34668274; PubMed Central PMCID: PMC8652629.

246. Jara LJ, Vera-Lastra O, Mahroum N, Pineda C, Shoenfeld Y. Autoimmune post-COVID vaccine syndromes: does the spectrum of autoimmune/inflammatory syndrome expand? Clin Rheumatol. 2022;41(5):1603–9. doi:10.1007/s10067-022-06149-4 PubMed PMID: 35378658; PubMed Central PMCID: PMC8979721.

247. Patone M, Handunnetthi L, Saatci D, Pan J, Katikireddi SV, Razvi S, et al. Neurological complications after first dose of COVID-19

vaccines and SARS-CoV-2 infection. Nature medicine. 2021;27(12):2144–53. doi:10.1038/s41591-021-01556-7

248. Walker JL, Schultze A, Tazare J, Tamborska A, Singh B, Donegan K, et al. Safety of COVID-19 vaccination and acute neurological events: A self-controlled case series in England using the OpenSAFELY platform. Vaccine. 2022 Jul 30;40(32):4479–87. doi:10.1016/j.vaccine.2022.06.010 PubMed PMID: 35715350; PubMed Central PMCID: PMC9170533.

249. Medicines & Healthcare Products Regulatory Agency. Coronavirus Vaccines Summary of Yellow Card reporting. 2022.

250. GOV.UK [Internet]. [cited 2021 Nov 24]. Information for UK recipients on COVID-19 Vaccine AstraZeneca (Regulation 174). Available from: https://www.gov.uk/government/publications/regulatory-approval-of-covid-19-vaccine-astrazeneca/information-for-uk-recipients-on-covid-19-vaccine-astrazeneca

251. GOV.UK [Internet]. [cited 2021 Nov 30]. Information for UK recipients on Pfizer/BioNTech COVID-19 vaccine (Regulation 174). Available from: https://www.gov.uk/government/publications/regulatory-approval-of-pfizer-biontech-vaccine-for-covid-19/information-for-uk-recipients-on-pfizerbiontech-covid-19-vaccine

252. Faksova K, Walsh D, Jiang Y, Griffin J, Phillips A, Gentile A, et al. COVID-19 vaccines and adverse events of special interest: A multinational Global Vaccine Data Network (GVDN) cohort study of 99 million vaccinated individuals. Vaccine. 2024 Apr 2;42(9):2200–11. doi:10.1016/j.vaccine.2024.01.100

253. Netravathi M, Dhamija K, Gupta M, Tamborska A, Nalini A, Holla VV, et al. COVID-19 vaccine associated demyelination & its association with MOG antibody. Multiple Sclerosis and Related Disorders. 2022 Apr 1;60. doi:10.1016/j.msard.2022.103739 PubMed PMID: 35306244.

254. Rowhani-Rahbar A, Klein NP, Dekker CL, Edwards KM, Marchant CD, Vellozzi C, et al. Biologically plausible and evidence-based risk intervals in immunization safety research. Vaccine. 2012 Dec 17;31(1):271–7. doi:10.1016/j.vaccine.2012.07.024

255. GOV.UK [Internet]. [cited 2023 Feb 12]. Use of the AstraZeneca COVID-19 (AZD1222) vaccine: updated JCVI statement, 7 May 2021. Available from: https://www.gov.uk/government/publications/use-of-the-astrazeneca-covid-19-vaccine-jcvi-statement-7-may-2021/use-of-the-astrazeneca-covid-19-azd1222-vaccine-updated-jcvi-statement-7-may-2021

256. Public Health England. GOV.UK [Internet]. 2021 [cited 2022 Jan 3]. JCVI advises on COVID-19 vaccine for people aged under 40. Available from: https://www.gov.uk/government/news/jcvi-advises-on-covid-19-vaccine-for-people-aged-under-40

257. Farrington P, Whitaker H, Weldeselassie YG. Self-Controlled Case Series Studies (a modelling guide with R). CRC Press; 2018. (Chapman & Hall/ CRC Biostatistics Series).

258. Petersen I, Douglas I, Whitaker H. Self controlled case series methods: an alternative to standard epidemiological study designs. BMJ. 2016 Sep 12;354:i4515. doi:10.1136/bmj.i4515 PubMed PMID: 27618829.

259. Farrington CP. Relative Incidence Estimation from Case Series for Vaccine Safety Evaluation. Biometrics. 1995;51(1):228–35. doi:10.2307/2533328

260. Nohynek H, Jokinen J, Partinen M, Vaarala O, Kirjavainen T, Sundman J, et al. AS03 adjuvanted AH1N1 vaccine associated with an abrupt increase in the incidence of childhood narcolepsy in Finland. PLoS One. 2012;7(3):e33536. doi:10.1371/journal.pone.0033536 PubMed PMID: 22470453; PubMed Central PMCID: PMC3314666.

261. Li X, Raventós B, Roel E, Pistillo A, Martinez-Hernandez E, Delmestri A, et al. Association between covid-19 vaccination, SARS-CoV-2 infection, and risk of immune mediated neurological events: population based cohort and self-controlled case series analysis. The BMJ. 2022 Mar 16;376:e068373. doi:10.1136/bmj-2021-068373 PubMed PMID: 35296468.

262. Weldeselassie YG, Whitaker H, Farrington P. SCCS: The Self-Controlled Case Series Method [Internet]. 2024 [cited 2025 Mar 22]. Available from: https://cran.r-project.org/web/packages/SCCS/index.html

263. Partinen M, Saarenpää-Heikkilä O, Ilveskoski I, Hublin C, Linna M, Olsén P, et al. Increased Incidence and Clinical Picture of Childhood Narcolepsy following the 2009 H1N1 Pandemic Vaccination Campaign in Finland. PLOS ONE. 2012 Mar 28;7(3):e33723. doi:10.1371/journal.pone.0033723

264. Abramson JH. WINPEPI updated: computer programs for epidemiologists, and their teaching potential. Epidemiol Perspect Innov. 2011 Feb 2;8:1. doi:10.1186/1742-5573-8-1 PubMed PMID: 21288353; PubMed Central PMCID: PMC3041648.

265. Angyal A, Longet S, Moore SC, Payne RP, Harding A, Tipton T, et al. T-cell and antibody responses to first BNT162b2 vaccine dose in previously infected and SARS-CoV-2-naive UK health-care workers: a

multicentre prospective cohort study. The Lancet Microbe. 2022 Jan 1;3(1):e21–31. doi:10.1016/S2666-5247(21)00275-5

266. Borelli WV, da Silveira ALM, Finkelsztejn A, Hansel G, Sato DK, Saute JAM. Simultaneous bilateral optic neuritis and longitudinally extensive transverse myelitis following vaccination against COVID-19: A case report. Neuroimmunology Reports. 2021 Dec;1:100041. doi:10.1016/j.nerep.2021.100041 PubMed PMID: null; PubMed Central PMCID: PMC8592852.

267. Nagaratnam SA, Ferdi AC, Leaney J, Lee RLK, Hwang YT, Heard R. Acute disseminated encephalomyelitis with bilateral optic neuritis following ChAdOx1 COVID-19 vaccination. BMC Neurol. 2022 Feb 12;22(1):54. doi:10.1186/s12883-022-02575-8

268. Permezel F, Borojevic B, Lau S, de Boer HH. Acute disseminated encephalomyelitis (ADEM) following recent Oxford/AstraZeneca COVID-19 vaccination. Forensic Sci Med Pathol. 2022;18(1):74–9. doi:10.1007/s12024-021-00440-7 PubMed PMID: 34735684; PubMed Central PMCID: PMC8567127.

269. Kania K, Ambrosius W, Tokarz Kupczyk E, Kozubski W. Acute disseminated encephalomyelitis in a patient vaccinated against SARS-CoV-2. Ann Clin Transl Neurol. 2021 Oct;8(10):2000–3. doi:10.1002/acn3.51447 PubMed PMID: 34480527; PubMed Central PMCID: PMC8528462.

270. Cao L, Ren L. Acute disseminated encephalomyelitis after severe acute respiratory syndrome coronavirus 2 vaccination: a case report. Acta Neurol Belg. 2022;122(3):793–5. doi:10.1007/s13760-021-01608-2 PubMed PMID: 33527327; PubMed Central PMCID: PMC7849959.

271. Greinacher A, Selleng K, Ralankar R, WescheJ J, Handtke S, M W, et al. Insights in ChAdOx1 nCoV-19 vaccine-induced immune thrombotic thrombocytopenia. Blood. 2021 Feb 12;138(22). doi:10.1182/blood.2021013231 PubMed PMID: 34587242.

272. Román GC, Gracia F, Torres A, Palacios A, Gracia K, Harris D. Acute Transverse Myelitis (ATM):Clinical Review of 43 Patients With COVID-19-Associated ATM and 3 Post-Vaccination ATM Serious Adverse Events With the ChAdOx1 nCoV-19 Vaccine (AZD1222). Frontiers in Immunology [Internet]. 2021 [cited 2022 May 26];12. Available from: https://www.frontiersin.org/article/10.3389/fimmu.2021.653786

273. Francis AG, Elhadd K, Camera V, Ferreira dos Santos M, Rocchi C, Adib-Samii P, et al. Acute Inflammatory Diseases of the Central Nervous System After SARS-CoV-2 Vaccination. Neurol Neuroimmunol Neuroinflamm. 2022 Nov 21;10(1):e200063.

doi:10.1212/NXI.0000000000200063 PubMed PMID: 36411077; PubMed Central PMCID: PMC9679888.

274. Francis A, Palace J, Fugger L. MOG antibody-associated disease after vaccination with ChAdOx1 nCoV-19. The Lancet Neurology. 2022 Mar;21(3):217–8. doi:10.1016/S1474-4422(22)00043-6

275. Ostovan VR, Sahraian MA, Karazhian N, Rostamihosseinkhani M, Salimi M, Marbooti H. Clinical characteristics, radiological features and prognostic factors of transverse myelitis following COVID-19 vaccination: A systematic review. Multiple Sclerosis and Related Disorders. 2022 Oct 1;66:104032. doi:10.1016/j.msard.2022.104032

276. Jarius S, Bieber N, Haas J, Wildemann B. MOG encephalomyelitis after vaccination against severe acute respiratory syndrome coronavirus type 2 (SARS-CoV-2): case report and comprehensive review of the literature. J Neurol. 2022 Oct 1;269(10):5198–212. doi:10.1007/s00415-022-11194-9

277. Dams L, Kraemer M, Becker J. MOG-antibody-associated longitudinal extensive myelitis after ChAdOx1 nCoV-19 vaccination. Mult Scler. 2022 Jun 1;28(7):1159–62. doi:10.1177/13524585211057512

278. Sehgal V, Bansal P, Arora S, Kapila S, Bedi GS. Myelin Oligodendrocyte Glycoprotein Antibody Disease After COVID-19 Vaccination - Causal or Incidental? Cureus. 2022 Jul 19;14(7). doi:10.7759/cureus.27024

279. Hümmert MW, Bütow F, Tkachenko D, Ayzenberg I, Pakeerathan T, Hellwig K, et al. Effects of the COVID-19 Pandemic on Patients With NMO Spectrum Disorders and MOG-Antibody-Associated Diseases: COPANMO(G)-Study. Neurol Neuroimmunol Neuroinflamm. 2023 Mar;10(2):e200082. doi:10.1212/NXI.0000000000200082 PubMed PMID: 36693760; PubMed Central PMCID: PMC10108387.

280. Gernert JA, Zimmermann H, Oswald E, Christmann T, Kümpfel T, Havla J. Clinical onset of CNS demyelinating disease after COVID-19 vaccination: denovo disease? Multiple Sclerosis and Related Disorders. 2022 Nov 1;67:104175. doi:10.1016/j.msard.2022.104175

281. Mumoli L, Vescio V, Pirritano D, Russo E, Bosco D. ADEM anti-MOG antibody-positive after SARS-CoV2 vaccination. Neurol Sci. 2021 Nov 19. doi:10.1007/s10072-021-05761-7

282. Matsumoto Y, Ohyama A, Kubota T, Ikeda K, Kaneko K, Takai Y, et al. MOG Antibody-Associated Disorders Following SARS-CoV-2 Vaccination: A Case Report and Literature Review. Front Neurol. 2022 Mar 1;13:845755. doi:10.3389/fneur.2022.845755 PubMed PMID: 35299613; PubMed Central PMCID: PMC8922017.

283. Notghi AA, Atley J, Silva M. Lessons of the month 1: Longitudinal extensive transverse myelitis following AstraZeneca COVID-19 vaccination. Clin Med (Lond). 2021 Sep;21(5):e535–8. doi:10.7861/clinmed.2021-0470 PubMed PMID: 34507942; PubMed Central PMCID: PMC8439525.

284. Pagenkopf C, Südmeyer M. A case of longitudinally extensive transverse myelitis following vaccination against Covid-19. J Neuroimmunol. 2021 Sep 15;358:577606. doi:10.1016/j.jneuroim.2021.577606 PubMed PMID: 34182207; PubMed Central PMCID: PMC8223023.

285. Maramattom BV, Krishnan P, Paul R, Padmanabhan S, Cherukudal Vishnu Nampoothiri S, Syed AA, et al. Guillain-Barré Syndrome following ChAdOx1-S/nCoV-19 Vaccine. Ann Neurol. 2021 Aug;90(2):312–4. doi:10.1002/ana.26143 PubMed PMID: 34114256.

286. Cortese A, Franciotta D, Alfonsi E, Visigalli N, Zardini E, Diamanti L, et al. Combined central and peripheral demyelination: Clinical features, diagnostic findings, and treatment. Journal of the Neurological Sciences. 2016 Apr 15;363:182–7. doi:10.1016/j.jns.2016.02.022

287. AlKolfat F, Elfatatry A, Mekky J, Aly AS. Combined peripheral and central nervous system demyelination post-COVID-19 vaccination: A case report. Neuroimmunology Reports. 2022 Jan 1;2:100057. doi:10.1016/j.nerep.2022.100057

288. Coelho P, Paula A, Martins IV, de Campos CF, Ferreira J, Antunes AP, et al. Combined central and peripheral demyelination after COVID-19 vaccination. J Neurol. 2022 Sep 1;269(9):4618–22. doi:10.1007/s00415-022-11188-7

289. Matteo E, Romoli M, Calabrò C, Piccolo L, Lazzarotto T, Suserea M, et al. Combined Central and Peripheral Demyelination with Anti-Neurofascin155 IgG Following COVID-19 Vaccination. Canadian Journal of Neurological Sciences. 2023 Jan;50(1):141–3. doi:10.1017/cjn.2021.256

290. Kauffman L, El Seblani N, Grogan J, Zachariah JJ, Kochar P, Bacharach R. A Combined Central and Peripheral Demyelination (CPPD) Syndrome After COVID-19 Vaccination (P4-4.008). Neurology. 2024 Apr 14;102(7_supplement_1):6976. doi:10.1212/WNL.0000000000208211

291. Badrawi N, Kumar N, Albastaki U. Post COVID-19 vaccination neuromyelitis optica spectrum disorder: Case report & MRI findings. Radiol Case Rep. 2021 Oct 13;16(12):3864–7. doi:10.1016/j.radcr.2021.09.033 PubMed PMID: 34659602; PubMed Central PMCID: PMC8512112.

292. Lopez-Chiriboga S, Sechi E, Buciuc M, Chen JJ, Pittock SJ, Lucchinetti CF, et al. Long-term Outcomes in Patients With Myelin Oligodendrocyte Glycoprotein Immunoglobulin G–Associated Disorder. JAMA Neurol. 2020 Dec;77(12):1575–7. doi:10.1001/jamaneurol.2020.3115 PubMed PMID: 32865549; PubMed Central PMCID: PMC7489431.

293. Degauque N, Ngono AE, Akl A, Lepetit M, Crochette R, Giral M, et al. Characterization of Antigen-Specific B Cells Using Nominal Antigen-Coated Flow-Beads. PLOS ONE. 2013 Dec 30;8(12):e84273. doi:10.1371/journal.pone.0084273

294. Jarius S, Ruprecht K, Kleiter I, Borisow N, Asgari N, Pitarokoili K, et al. MOG-IgG in NMO and related disorders: a multicenter study of 50 patients. Part 1: Frequency, syndrome specificity, influence of disease activity, long-term course, association with AQP4-IgG, and origin. Journal of Neuroinflammation. 2016 Oct 27;13(1):279. doi:10.1186/s12974-016-0717-1

295. Wong AKH, Woodhouse I, Schneider F, Kulpa DA, Silvestri G, Maier CL. Broad auto-reactive IgM responses are common in critically ill patients, including those with COVID-19. Cell Rep Med. 2021 May 28;2(6):100321. doi:10.1016/j.xcrm.2021.100321 PubMed PMID: 34075365; PubMed Central PMCID: PMC8160082.

296. Gastaldi M, Scaranzin S, Jarius S, Wildeman B, Zardini E, Mallucci G, et al. Cell-based assays for the detection of MOG antibodies: a comparative study. J Neurol. 2020 Dec 1;267(12):3555–64. doi:10.1007/s00415-020-10024-0

297. Singh S, Kumar R, Agrawal B, Singh S, Kumar R, Agrawal B. Adenoviral Vector-Based Vaccines and Gene Therapies: Current Status and Future Prospects. In: Adenoviruses [Internet]. IntechOpen; 2018 [cited 2025 Jul 31]. Available from: https://www.intechopen.com/chapters/62883 doi:10.5772/intechopen.79697

298. Krutzke L, Rösler R, Allmendinger E, Engler T, Wiese S, Kochanek S. Process- and product-related impurities in the ChAdOx1 nCov-19 vaccine. Sawyer SL, Harper DM, Klimkait T, Wagner R, editors. eLife. 2022 Jul 4;11:e78513. doi:10.7554/eLife.78513

299. Dinoto A, Sechi E, Ferrari S, Gajofatto A, Orlandi R, Solla P, et al. Risk of disease relapse following COVID-19 vaccination in patients with AQP4-IgG-positive NMOSD and MOGAD. Mult Scler Relat Disord. 2022 Feb;58:103424. doi:10.1016/j.msard.2021.103424 PubMed PMID: 35216793; PubMed Central PMCID: PMC8607690.

300. Ismail II, Salama S. A systematic review of cases of CNS demyelination following COVID-19 vaccination. J Neuroimmunol.

2022 Jan 15;362:577765. doi:10.1016/j.jneuroim.2021.577765 PubMed PMID: 34839149; PubMed Central PMCID: PMC8577051.

301. Jackson KJL, Kidd MJ, Wang Y, Collins AM. The shape of the lymphocyte receptor repertoire: lessons from the B cell receptor. Front Immunol. 2013 Sep 2;4:263. doi:10.3389/fimmu.2013.00263 PubMed PMID: 24032032; PubMed Central PMCID: PMC3759170.

302. Seamons A, Perchellet A, Goverman J. Immune tolerance to myelin proteins. Immunol Res. 2003 Dec 1;28(3):201–21. doi:10.1385/IR:28:3:201

303. Meffre E, O'Connor KC. Impaired B-cell tolerance checkpoints promote the development of autoimmune diseases and pathogenic autoantibodies. Immunol Rev. 2019 Nov;292(1):90–101. doi:10.1111/imr.12821 PubMed PMID: 31721234; PubMed Central PMCID: PMC9145185.

304. Goverman J, Woods A, Larson L, Weiner LP, Hood L, Zaller DM. Transgenic mice that express a myelin basic protein-specific T cell receptor develop spontaneous autoimmunity. Cell. 1993 Feb 26;72(4):551–60. doi:10.1016/0092-8674(93)90074-Z

305. Trinchieri G. Interleukin-12 and the regulation of innate resistance and adaptive immunity. Nat Rev Immunol. 2003 Feb;3(2):133–46. doi:10.1038/nri1001

306. Oh JZ, Kurche JS, Burchill MA, Kedl RM. TLR7 enables cross-presentation by multiple dendritic cell subsets through a type I IFN-dependent pathway. Blood. 2011 Sep 15;118(11):3028–38. doi:10.1182/blood-2011-04-348839 PubMed PMID: 21813451; PubMed Central PMCID: PMC3175780.

307. Vignali DAA, Collison LW, Workman CJ. How regulatory T cells work. Nat Rev Immunol. 2008 Jul;8(7):523–32. doi:10.1038/nri2343 PubMed PMID: 18566595; PubMed Central PMCID: PMC2665249.

308. Hirano T. IL-6 in inflammation, autoimmunity and cancer. Int Immunol. 2020 Dec 18;33(3):127–48. doi:10.1093/intimm/dxaa078 PubMed PMID: 33337480; PubMed Central PMCID: PMC7799025.

309. Sospedra M, Martin R. IMMUNOLOGY OF MULTIPLE SCLEROSIS*. Annual Review of Immunology. 2005 Apr 23;23(Volume 23, 2005):683–747. doi:10.1146/annurev.immunol.23.021704.115707

310. Uhlen M, Oksvold P, Fagerberg L, Lundberg E, Jonasson K, Forsberg M, et al. Towards a knowledge-based Human Protein Atlas. Nat Biotechnol. 2010 Dec;28(12):1248–50. doi:10.1038/nbt1210-1248 PubMed PMID: 21139605.

311. www.proteinatlas.org [Internet]. [cited 2025 Aug 6]. Tissue expression of MOG - Summary - The Human Protein Atlas. Available from: https://www.proteinatlas.org/ENSG00000204655-MOG/tissue

312. Schanda K, Peschl P, Lerch M, Seebacher B, Mindorf S, Ritter N, et al. Differential Binding of Autoantibodies to MOG Isoforms in Inflammatory Demyelinating Diseases. Neurology - Neuroimmunology Neuroinflammation. 2021 Sep 1;8(5). doi:10.1212/NXI.0000000000001027 PubMed PMID: 34131067.

313. Reindl M, Schanda K, Woodhall M, Tea F, Ramanathan S, Sagen J, et al. International multicenter examination of MOG antibody assays. Neurol Neuroimmunol Neuroinflamm. 2020 Feb 5;7(2):e674. doi:10.1212/NXI.0000000000000674 PubMed PMID: 32024795; PubMed Central PMCID: PMC7051197.

314. Spadaro M, Winklmeier S, Beltrán E, Macrini C, Höftberger R, Schuh E, et al. Pathogenicity of human antibodies against myelin oligodendrocyte glycoprotein. Ann Neurol. 2018 Aug;84(2):315–28. doi:10.1002/ana.25291 PubMed PMID: 30014603.

315. Lazarević M, Stanisavljević S, Nikolovski N, Dimitrijević M, Miljković Đ. Complete Freund's adjuvant as a confounding factor in multiple sclerosis research. Front Immunol. 2024 Feb 15;15:1353865. doi:10.3389/fimmu.2024.1353865 PubMed PMID: 38426111; PubMed Central PMCID: PMC10902151.

316. Murphy ÁC, Lalor SJ, Lynch MA, Mills KHG. Infiltration of Th1 and Th17 cells and activation of microglia in the CNS during the course of experimental autoimmune encephalomyelitis. Brain, Behavior, and Immunity. 2010 May 1;24(4):641–51. doi:10.1016/j.bbi.2010.01.014

317. Diab A, Zhu J, Xiao BG, Mustafa M, Link H. High IL-6 and Low IL-10 in the Central Nervous System Are Associated with Protracted Relapsing EAE in DA Rats. Journal of neuropathology and experimental neurology. 1997;56(6):641–50. doi:10.1097/00005072-199706000-00002

318. Issazadeh S, Lorentzen JC, Mustafa MI, Höjeberg B, Miissener Å, Olsson T. Cytokines in relapsing experimental autoimmune encephalomyelitis in DA rats: persistent mRNA expression of proinflammatory cytokines and absent expression of interleukin-10 and transforming growth factor-β. Journal of neuroimmunology. 1996;69(1):103–15. doi:10.1016/0165-5728(96)00076-8

319. Eugster HP, Frei K, Kopf M, Lassmann H, Fontana A. IL-6-deficient mice resist myelin oligodendrocyte glycoprotein-induced autoimmune encephalomyelitis. European Journal of Immunology.

1998;28(7):2178–87. doi:10.1002/(SICI)1521-4141(199807)28:07<2178::AID-IMMU2178>3.0.CO;2-D

320. McGinley AM, Sutton CE, Edwards SC, Leane CM, DeCourcey J, Teijeiro A, et al. Interleukin-17A Serves a Priming Role in Autoimmunity by Recruiting IL-1β-Producing Myeloid Cells that Promote Pathogenic T Cells. Immunity. 2020 Feb 18;52(2):342-356.e6. doi:10.1016/j.immuni.2020.01.002 PubMed PMID: 32023490.

321. Kwon YN, Kim B, Ahn S, Seo J, Kim SB, Yoon SS, et al. Serum level of IL-1β in patients with inflammatory demyelinating disease: Marked upregulation in the early acute phase of MOG antibody associated disease (MOGAD). Journal of Neuroimmunology. 2020 Nov 15;348:577361. doi:10.1016/j.jneuroim.2020.577361

322. Villacieros-Álvarez J, Espejo C, Arrambide G, Dinoto A, Mulero P, Rubio-Flores L, et al. Profile and Usefulness of Serum Cytokines to Predict Prognosis in Myelin Oligodendrocyte Glycoprotein Antibody−Associated Disease. Neurol Neuroimmunol Neuroinflamm. 2025 Mar;12(2):e200362. doi:10.1212/NXI.0000000000200362

323. Bauer A, Rudzki D, Berek K, Dinoto A, Lechner C, Wendel EM, et al. Increased peripheral inflammatory responses in myelin oligodendrocyte glycoprotein associated disease and aquaporin-4 antibody positive neuromyelitis optica spectrum disorder. Front Immunol. 2022 Nov 14;13. doi:10.3389/fimmu.2022.1037812

324. Lee S, Kong J, Lyu S, Nam SO, Lim TJ, Song JY, et al. Relationship between cerebrospinal fluid cytokines/chemokines and clinical impact of myelin oligodendrocyte glycoprotein antibody-associated disorders in children. Brain and Development. 2025 Aug 1;47(4):104389. doi:10.1016/j.braindev.2025.104389

325. Liu J, Mori M, Sugimoto K, Uzawa A, Masuda H, Uchida T, et al. Peripheral blood helper T cell profiles and their clinical relevance in MOG-IgG-associated and AQP4-IgG-associated disorders and MS. BMJ Publishing; 2020.

326. Ewer KJ, Barrett JR, Belij-Rammerstorfer S, Sharpe H, Makinson R, Morter R, et al. T cell and antibody responses induced by a single dose of ChAdOx1 nCoV-19 (AZD1222) vaccine in a phase 1/2 clinical trial. Nat Med. 2021 Feb;27(2):2. doi:10.1038/s41591-020-01194-5

327. van Doremalen N, Lambe T, Spencer A, Belij-Rammerstorfer S, Purushotham JN, Port JR, et al. ChAdOx1 nCoV-19 vaccine prevents SARS-CoV-2 pneumonia in rhesus macaques. Nature. 2020 Oct;586(7830):578–82. doi:10.1038/s41586-020-2608-y PubMed PMID: 32731258; PubMed Central PMCID: PMC8436420.

328. Heo JY, Seo YB, Kim EJ, Lee J, Kim YR, Yoon JG, et al. COVID-19 vaccine type-dependent differences in immunogenicity and inflammatory response: BNT162b2 and ChAdOx1 nCoV-19. Front Immunol. 2022 Sep 2;13. doi:10.3389/fimmu.2022.975363

329. Willems LH, Nagy M, Ten Cate H, Spronk HMH, Jacobs LMC, Kranendonk J, et al. ChAdOx1 vaccination, blood coagulation, and inflammation: No effect on coagulation but increased interleukin-6. Research and Practice in Thrombosis and Haemostasis. 2021 Dec 1;5(8):e12630. doi:10.1002/rth2.12630

330. Fernández-Ciriza L, González Á, del Pozo JL, Fernández-Montero A, Carmona-Torre F, Carlos S, et al. Humoral and cellular immune response over 9 months of mRNA-1273, BNT162b2 and ChAdOx1 vaccination in a University Hospital in Spain. Sci Rep. 2022 Oct 7;12:15606. doi:10.1038/s41598-022-19537-2 PubMed PMID: 36207324; PubMed Central PMCID: PMC9546941.

331. Kim JY, Bae S, Park S, Kwon JS, Lim SY, Park JY, et al. Comparison of Antibody and T Cell Responses Induced by Single Doses of ChAdOx1 nCoV-19 and BNT162b2 Vaccines. Immune Netw. 2021 Aug;21(4):e29. doi:10.4110/in.2021.21.e29 PubMed PMID: 34522442; PubMed Central PMCID: PMC8410992.

332. Familiar-Macedo D, Vieira Damasco P, Fiestas Solórzano VE, Carnevale Rodrigues J, Sampaio de Lemos ER, Barreto dos Santos F, et al. Inflammatory and cytotoxic mediators in COVID-19 patients and in ChAdOx1 nCoV-19 (AZD1222) vaccine recipients. Cytokine. 2023 Nov 1;171:156350. doi:10.1016/j.cyto.2023.156350

333. Gardner J, Abrams ST, Toh CH, Parker AL, Lovatt C, Nicolson PLR, et al. Identification of cross reactive T cell responses in adenovirus based COVID 19 vaccines. npj Vaccines. 2024 Jun 5;9(1):1–12. doi:10.1038/s41541-024-00895-z

334. Dure M, Macian F. IL-2 signaling prevents T cell anergy by inhibiting the expression of anergy inducing genes. Mol Immunol. 2009 Feb;46(5):999–1006. doi:10.1016/j.molimm.2008.09.029 PubMed PMID: 18990450; PubMed Central PMCID: PMC2667138.

335. Broderick L, Brooks SP, Takita H, Baer AN, Bernstein JM, Bankert RB. IL-12 reverses anergy to T cell receptor triggering in human lung tumor-associated memory T cells. Clin Immunol. 2006;118(2–3):159–69. doi:10.1016/j.clim.2005.09.008 PubMed PMID: 16271513.

336. Popko B, Corbin JG, Baerwald KD, Dupree J, Garcia AM. The effects of interferon-γ on the central nervous system. Mol Neurobiol. 1997;14(1):19–35. doi:10.1007/BF02740619 PubMed PMID: 9170099; PubMed Central PMCID: PMC7091409.

337. Versele R, Sevin E, Gosselet F, Fenart L, Candela P. TNF-α and IL-1β Modulate Blood-Brain Barrier Permeability and Decrease Amyloid-β Peptide Efflux in a Human Blood-Brain Barrier Model. Int J Mol Sci. 2022 Sep 6;23(18):10235. doi:10.3390/ijms231810235 PubMed PMID: 36142143; PubMed Central PMCID: PMC9499506.

338. Kebir H, Kreymborg K, Ifergan I, Dodelet-Devillers A, Cayrol R, Bernard M, et al. Human TH17 lymphocytes promote blood-brain barrier disruption and central nervous system inflammation. Nat Med. 2007 Oct;13(10):1173–5. doi:10.1038/nm1651

339. Erta M, Quintana A, Hidalgo J. Interleukin-6, a Major Cytokine in the Central Nervous System. Int J Biol Sci. 2012;8(9):1254–66. doi:10.7150/ijbs.4679

340. Mayer MC, Breithaupt C, Reindl M, Schanda K, Rostásy K, Berger T, et al. Distinction and Temporal Stability of Conformational Epitopes on Myelin Oligodendrocyte Glycoprotein Recognized by Patients with Different Inflammatory Central Nervous System Diseases. The Journal of Immunology. 2013 Oct 1;191(7):3594–604. doi:10.4049/jimmunol.1301296

341. Finsterer J. Triggers of Guillain–Barré Syndrome: Campylobacter jejuni Predominates. Int J Mol Sci. 2022 Nov 17;23(22):14222. doi:10.3390/ijms232214222 PubMed PMID: 36430700; PubMed Central PMCID: PMC9696744.

342. Vojdani A, Kharrazian D. Potential antigenic cross-reactivity between SARS-CoV-2 and human tissue with a possible link to an increase in autoimmune diseases. Clin Immunol. 2020 Aug;217:108480. doi:10.1016/j.clim.2020.108480 PubMed PMID: 32461193; PubMed Central PMCID: PMC7246018.

343. Kreye J, Reincke SM, Kornau HC, Sánchez-Sendin E, Corman VM, Liu H, et al. A Therapeutic Non-self-reactive SARS-CoV-2 Antibody Protects from Lung Pathology in a COVID-19 Hamster Model. Cell. 2020 Nov 12;183(4):1058-1069.e19. doi:10.1016/j.cell.2020.09.049 PubMed PMID: 33058755; PubMed Central PMCID: PMC7510528.

344. Schanda K, Mariotto S, Rudzki D, Bauer A, Dinoto A, Rossi P, et al. Is there an immunological cross-reactivity of antibodies to the myelin oligodendrocyte glycoprotein and coronaviruses? Brain Communications. 2024 Apr 1;6(2):fcae106. doi:10.1093/braincomms/fcae106

345. Ide T, Kawanami T, Eriguchi M, Hara H. SARS-CoV-2-related Myelin Oligodendrocyte Glycoprotein Antibody-associated Disease: A Case Report and Literature Review. Intern Med. 2022 Apr 15;61(8):1253–8. doi:10.2169/internalmedicine.8709-21 PubMed PMID: 35135920; PubMed Central PMCID: PMC9107978.

346. Ismail II, Salama S. Association of CNS demyelination and COVID-19 infection: an updated systematic review. J Neurol. 2021 Aug 12;1–36. doi:10.1007/s00415-021-10752-x

347. Kogure C, Kikushima W, Fukuda Y, Hasebe Y, Takahashi T, Shibuya T, et al. Myelin oligodendrocyte glycoprotein antibody-associated optic neuritis in a COVID-19 patient. Medicine (Baltimore). 2021 May 14;100(19):e25865. doi:10.1097/MD.0000000000025865 PubMed PMID: 34106635; PubMed Central PMCID: PMC8133173.

348. Zhou S, Jones-Lopez EC, Soneji DJ, Azevedo CJ, Patel VR. Myelin Oligodendrocyte Glycoprotein Antibody-Associated Optic Neuritis and Myelitis in COVID-19. J Neuroophthalmol. 2020 Sep;40(3):398–402. doi:10.1097/WNO.0000000000001049 PubMed PMID: 32604245; PubMed Central PMCID: PMC7382408.

349. Mariotto S, Carta S, Dinoto A, Lippi G, Salvagno GL, Masin L, et al. Is there a correlation between MOG-associated disorder and SARS-CoV-2 infection? European Journal of Neurology. 2022;29(6):1855–8. doi:10.1111/ene.15304

350. Lambe J, McGinley MP, Moss BP, Mao-Draayer Y, Kassa R, Ciotti JR, et al. Myelin oligodendrocyte glycoprotein-IgG associated disorders (MOGAD) following SARS-CoV-2 infection: A case series. J Neuroimmunol. 2022 Sep 15;370:577933. doi:10.1016/j.jneuroim.2022.577933 PubMed PMID: 35878436; PubMed Central PMCID: PMC9279254.

351. Peters J, Saleh A, Vogels CBF, Grubaugh ND, Farhadian S, Longbrake EE. MOG-associated encephalitis following SARS-COV-2 infection. Mult Scler Relat Disord. 2021 May 1;50:102857. doi:10.1016/j.msard.2021.102857

352. Arashkia A, Jalilvand S, Mohajel N, Afchangi A, Azadmanesh K, Salehi-Vaziri M, et al. Severe acute respiratory syndrome-coronavirus-2 spike (S) protein based vaccine candidates: State of the art and future prospects. Rev Med Virol. 2020 Oct 15;e2183. doi:10.1002/rmv.2183 PubMed PMID: 33594794; PubMed Central PMCID: PMC7646037.

353. Chung YH, Beiss V, Fiering SN, Steinmetz NF. COVID-19 Vaccine Frontrunners and Their Nanotechnology Design. ACS Nano. 2020 Oct 9;acsnano.0c07197. doi:10.1021/acsnano.0c07197 PubMed PMID: 33034449; PubMed Central PMCID: PMC7553041.

354. Shaw G, Morse S, Ararat M, Graham FL. Preferential transformation of human neuronal cells by human adenoviruses and the origin of HEK 293 cells. The FASEB Journal. 2002;16(8):869–71. doi:10.1096/fj.01-0995fje

355. Krishnamoorthy G, Saxena A, Mars LT, Domingues HS, Mentele R, Ben-Nun A, et al. Myelin-specific T cells also recognize neuronal autoantigen in a transgenic mouse model of multiple sclerosis. Nat Med. 2009 Jun;15(6):626–32. doi:10.1038/nm.1975 PubMed PMID: 19483694.

356. Langgartner D, Winkler R, Brunner-Weisser J, Rohleder N, Jarczok MN, Gündel H, et al. COVID-19 vaccination exacerbates ex vivo IL-6 release from isolated PBMCs. Sci Rep. 2023 Jun 12;13(1):9496. doi:10.1038/s41598-023-35731-2 PubMed PMID: 37308487; PubMed Central PMCID: PMC10261110.

357. Vanderlugt CL, Miller SD. Epitope spreading in immune-mediated diseases: implications for immunotherapy. Nat Rev Immunol. 2002 Feb;2(2):85–95. doi:10.1038/nri724

358. McFarland HI, Lobito AA, Johnson MM, Nyswaner JT, Frank JA, Palardy GR, et al. Determinant Spreading Associated with Demyelination in a Nonhuman Primate Model of Multiple Sclerosis. J Immunol. 1999 Feb 1;162(4):2384–90. doi:10.4049/jimmunol.162.4.2384

359. Hintermann E, Holdener M, Bayer M, Loges S, Pfeilschifter JM, Granier C, et al. Epitope spreading of the anti-CYP2D6 antibody response in patients with autoimmune hepatitis and in the CYP2D6 mouse model. Journal of Autoimmunity. 2011 Nov 1;37(3):242–53. doi:10.1016/j.jaut.2011.06.005

360. Mapunda JA, Tibar H, Regragui W, Engelhardt B. How Does the Immune System Enter the Brain? Front Immunol. 2022 Feb 22;13. doi:10.3389/fimmu.2022.805657

361. Ohbuchi M, Shibuta M, Tetsuka K, Sasaki-Iwaoka H, Oishi M, Shimizu F, et al. Modeling of Blood–Brain Barrier (BBB) Dysfunction and Immune Cell Migration Using Human BBB-on-a-Chip for Drug Discovery Research. Int J Mol Sci. 2024 Jun 12;25(12):6496. doi:10.3390/ijms25126496 PubMed PMID: 38928202; PubMed Central PMCID: PMC11204321.

362. van Zwam M, Huizinga R, Melief MJ, Wierenga-Wolf AF, van Meurs M, Voerman JS, et al. Brain antigens in functionally distinct antigen-presenting cell populations in cervical lymph nodes in MS and EAE. J Mol Med. 2009 Mar 1;87(3):273–86. doi:10.1007/s00109-008-0421-4

363. Trivedi RR, Archambault AS, Pavlak C, Gastaldi M, Cantoni C, Ghezzi L, et al. Prevalence of anti-myelin oligodendrocyte glycoprotein antibodies across neuroinflammatory and neurodegenerative diseases. Journal of the Neurological Sciences. 2024 Jun 15;461. doi:10.1016/j.jns.2024.123041 PubMed PMID: 38744216.

364. Montes CL, Acosta-Rodríguez EV, Merino MC, Bermejo DA, Gruppi A. Polyclonal B cell activation in infections: infectious agents' devilry or defense mechanism of the host? J Leukoc Biol. 2007 Nov 1;82(5):1027–32. doi:10.1189/jlb.0407214

365. Sindhava VJ, Bondada S. Multiple Regulatory Mechanisms Control B-1 B Cell Activation. Front Immunol. 2012 Dec 17;3:372. doi:10.3389/fimmu.2012.00372 PubMed PMID: 23251136; PubMed Central PMCID: PMC3523257.

366. Doherty DG, Melo AM, Moreno-Olivera A, Solomos AC. Activation and Regulation of B Cell Responses by Invariant Natural Killer T Cells. Front Immunol. 2018 Jun 18;9. doi:10.3389/fimmu.2018.01360

367. Voss LF, Howarth AJ, Wittenborn TR, Hummelgaard S, Juul-Madsen K, Kastberg KS, et al. The extrafollicular response is sufficient to drive initiation of autoimmunity and early disease hallmarks of lupus. Front Immunol. 2022 Dec 14;13. doi:10.3389/fimmu.2022.1021370

368. Luo W, Yin Q. B Cell Response to Vaccination. Immunological Investigations. 2021 Oct 3;50(7):780–801. doi:10.1080/08820139.2021.1903033 PubMed PMID: 33779464.

369. Rawlings DJ, Schwartz MA, Jackson SW, Meyer-Bahlburg A. Integration of B cell responses through Toll-like receptors and antigen receptors. Nat Rev Immunol. 2012 Mar 16;12(4):282–94. doi:10.1038/nri3190 PubMed PMID: 22421786; PubMed Central PMCID: PMC3437941.

370. Sha Z, Compans RW. Induction of CD4+ T-Cell-Independent Immunoglobulin Responses by Inactivated Influenza Virus. Journal of Virology. 2000 Jun;74(11):4999. doi:10.1128/jvi.74.11.4999-5005.2000 PubMed PMID: 10799573.

371. Lapuente D, Winkler TH, Tenbusch M. B-cell and antibody responses to SARS-CoV-2: infection, vaccination, and hybrid immunity. Cell Mol Immunol. 2024 Feb;21(2):144–58. doi:10.1038/s41423-023-01095-w

372. Pone EJ, Zhang J, Mai T, White CA, Li G, Sakakura JK, et al. BCR-signalling synergizes with TLR-signalling for induction of AID and immunoglobulin class-switching through the non-canonical NF-κB pathway. Nat Commun. 2012 Apr 3;3(1):767. doi:10.1038/ncomms1769

373. Hjálmsdóttir Á, Hasler F, Waeckerle-Men Y, Duda A, López-Deber MP, Pihlgren M, et al. T cell independent antibody responses with class switch and memory using peptides anchored on liposomes.

npj Vaccines. 2024 Jun 22;9(1):115. doi:10.1038/s41541-024-00902-3

374. Shirley JL, Jong YP de, Terhorst C, Herzog RW. Immune Responses to Viral Gene Therapy Vectors. Molecular Therapy. 2020 Mar 4;28(3):709–22. doi:10.1016/j.ymthe.2020.01.001 PubMed PMID: 31968213.

375. Sakurai F, Tachibana M, Mizuguchi H. Adenovirus vector-based vaccine for infectious diseases. Drug Metabolism and Pharmacokinetics. 2022 Feb;42:100432. doi:10.1016/j.dmpk.2021.100432 PubMed PMID: 34974335.

376. Wang EY, Mao T, Klein J, Dai Y, Huck JD, Jaycox JR, et al. Diverse functional autoantibodies in patients with COVID-19. Nature. 2021 Jul;595(7866):7866. doi:10.1038/s41586-021-03631-y

377. Franke C, Ferse C, Kreye J, Reincke SM, Sanchez-Sendin E, Rocco A, et al. High frequency of cerebrospinal fluid autoantibodies in COVID-19 patients with neurological symptoms. Brain, Behavior, and Immunity. 2021 Mar 1;93:415–9. doi:10.1016/j.bbi.2020.12.022

378. Prüss H. Autoantibodies in neurological disease. Nat Rev Immunol. 2021 Dec;21(12):798–813. doi:10.1038/s41577-021-00543-w

379. Sanderson NSR, Zimmermann M, Eilinger L, Gubser C, Schaeren-Wiemers N, Lindberg RLP, et al. Cocapture of cognate and bystander antigens can activate autoreactive B cells. PNAS. 2017 Jan 24;114(4):734–9. doi:10.1073/pnas.1614472114 PubMed PMID: 28057865.

380. Neumann B, Schmidbauer ML, Dimitriadis K, Otto S, Knier B, Niesen WD, et al. Cerebrospinal fluid findings in COVID-19 patients with neurological symptoms. J Neurol Sci. 2020 Nov 15;418:117090. doi:10.1016/j.jns.2020.117090 PubMed PMID: 32805440; PubMed Central PMCID: PMC7417278.

381. Vidal LR, de Almeida SM, Cavalli BM, Dieckmann TG, Raboni SM, Salvador GLO, et al. Human adenovirus meningoencephalitis: a 3-years' overview. J Neurovirol. 2019 Aug;25(4):589–96. doi:10.1007/s13365-019-00758-7 PubMed PMID: 31102186.

382. Byrnes AP, MacLaren RE, Charlton HM. Immunological Instability of Persistent Adenovirus Vectors in the Brain: Peripheral Exposure to Vector Leads to Renewed Inflammation, Reduced Gene Expression, and Demyelination. J Neurosci. 1996 May 1;16(9):3045–55. doi:10.1523/JNEUROSCI.16-09-03045.1996

383. Hutnick NA, Carnathan D, Demers K, Makedonas G, Ertl HCJ, Betts MR. Adenovirus-specific human T cells are pervasive, polyfunctional,

and cross-reactive. Vaccine. 2010 Feb 23;DNA Vaccines 200928(8):1932–41. doi:10.1016/j.vaccine.2009.10.091

384. Ryan FJ, Norton TS, McCafferty C, Blake SJ, Stevens NE, James J, et al. A systems immunology study comparing innate and adaptive immune responses in adults to COVID-19 mRNA and adenovirus vectored vaccines. Cell Rep Med. 2023 Feb 17;4(3):100971. doi:10.1016/j.xcrm.2023.100971 PubMed PMID: 36871558; PubMed Central PMCID: PMC9935276.

385. Jäger A, Dardalhon V, Sobel RA, Bettelli E, Kuchroo VK. Th1, Th17 and Th9 effector cells induce experimental autoimmune encephalomyelitis with different pathological phenotypes. J Immunol. 2009 Dec 1;183(11):7169–77. doi:10.4049/jimmunol.0901906 PubMed PMID: 19890056; PubMed Central PMCID: PMC2921715.

386. Lassmann H, Brunner C, Bradl M, Linington C. Experimental allergic encephalomyelitis: the balance between encephalitogenic T lymphocytes and demyelinating antibodies determines size and structure of demyelinated lesions. Acta Neuropathol. 1988 Nov 1;75(6):566–76. doi:10.1007/BF00686201

387. Peschl P, Bradl M, Höftberger R, Berger T, Reindl M. Myelin Oligodendrocyte Glycoprotein: Deciphering a Target in Inflammatory Demyelinating Diseases. Frontiers in Immunology [Internet]. 2017 [cited 2023 Apr 11];8. Available from: https://www.frontiersin.org/articles/10.3389/fimmu.2017.00529

388. World Health Organization. 9789241516990-eng.pdf [Internet]. 2019 [cited 2025 Feb 8]. Causality assessment of an adverse event following immunization (AEFI) User manual for the revised WHO classification. Available from: https://iris.who.int/bitstream/handle/10665/340802/9789241516990-eng.pdf?sequence=1

389. Leite MI, Coutinho E, Lana-Peixoto M, Apostolos S, Waters P, Sato D, et al. Myasthenia gravis and neuromyelitis optica spectrum disorder. Neurology. 2012 May 15;78(20):1601–7. doi:10.1212/WNL.0b013e31825644ff PubMed PMID: 22551731; PubMed Central PMCID: PMC3348852.

390. HOPPU S, RONKAINEN MS, KULMALA P, ÅKERBLOM HK, KNIP M. GAD65 antibody isotypes and epitope recognition during the prediabetic process in siblings of children with type I diabetes. Clin Exp Immunol. 2004 Apr;136(1):120–8. doi:10.1111/j.1365-2249.2004.02416.x PubMed PMID: 15030523; PubMed Central PMCID: PMC1809002.

391. Lhomme S, Abravanel F, Cintas P, Izopet J. Hepatitis E Virus Infection: Neurological Manifestations and Pathophysiology. Pathogens. 2021 Dec 3;10(12):1582. doi:10.3390/pathogens10121582 PubMed PMID: 34959537; PubMed Central PMCID: PMC8705630.

392. Kwon YN, Kim B, Kim JS, Park KS, Seo DY, Kim H, et al. Time to Treat First Acute Attack of Myelin Oligodendrocyte Glycoprotein Antibody-Associated Disease. JAMA Neurol. 2024 Oct 1;81(10):1073–84. doi:10.1001/jamaneurol.2024.2811

393. Whitaker H, Ghebremichael-Weldesselassie Y, Musonda P, Hocine MN. SELF-CONTROLLED CASE SERIES STUDIES [Internet]. [cited 2025 Mar 24]. Self controlled case series studies. Available from: http://sccs-studies.info/r.html

394. Pierson ER, Goverman JM. GM-CSF is not essential for experimental autoimmune encephalomyelitis but promotes brain-targeted disease. JCI Insight. 2(7). doi:10.1172/jci.insight.92362 PubMed PMID: 28405624; PubMed Central PMCID: PMC5374070.

395. Aylard PR, Gooding JH, McKenna PJ, Snaith RP. A validation study of three anxiety and depression self-assessment scales. Journal of Psychosomatic Research. 1987 Jan 1;31(2):261–8. doi:10.1016/0022-3999(87)90083-3

396. Honarmand K, Feinstein A. Validation of the Hospital Anxiety and Depression Scale for use with multiple sclerosis patients. Mult Scler. 2009 Dec;15(12):1518–24. doi:10.1177/1352458509347150 PubMed PMID: 19965520.

397. Yeo T, dos Passos GR, Muhammed L, Everett R, Reeve S, Messina S, et al. Factors associated with fatigue in CNS inflammatory diseases with AQP4 and MOG antibodies. Annals of Clinical and Translational Neurology. 2020;7(3):375–83. doi:10.1002/acn3.51008

398. Fischer JS, LaRocca NG, Miller DM, Ritvo PG, Andrews H, Paty D. Recent developments in the assessment of quality of life in multiple sclerosis (MS). Mult Scler. 1999 Aug;5(4):251–9. doi:10.1177/135245859900500410 PubMed PMID: 10467384.

399. Kos D, Kerckhofs E, Carrea I, Verza R, Ramos M, Jansa J. Evaluation of the Modified Fatigue Impact Scale in four different European countries. Mult Scler. 2005 Feb 1;11(1):76–80. doi:10.1191/1352458505ms1117oa

400. Téllez N, Río J, Tintoré M, Nos C, Galán I, Montalban X. Does the Modified Fatigue Impact Scale offer a more comprehensive assessment of fatigue in MS? Mult Scler. 2005 Apr 1;11(2):198–202. doi:10.1191/1352458505ms1148oa

401. Calabrese M, Rinaldi F, Grossi P, Mattisi I, Bernardi V, Favaretto A, et al. Basal ganglia and frontal/parietal cortical atrophy is associated with fatigue in relapsing—remitting multiple sclerosis. Mult Scler. 2010 Oct 1;16(10):1220–8. doi:10.1177/1352458510376405

402. Masuda H, Mori M, Uzawa A, Uchida T, Ohtani R, Kobayashi S, et al. Validation of the Modified Fatigue Impact Scale and the relationships among fatigue, pain and serum interleukin-6 levels in patients with neuromyelitis optica spectrum disorder. J Neurol Sci. 2018 Feb 15;385:64–8. doi:10.1016/j.jns.2017.11.041 PubMed PMID: 29406915.

403. Cleeland CS. The Brief Pain Inventory. User Guide. 2009.

404. Keller S, Bann C, Dodd S, Schein J, Mendoza TR, Cleeland CS. Validity of the Brief Pain Inventory for Use in Documenting the Outcomes of Patients With Noncancer Pain. Clin J Pain. 2004;20(5):309–18.

405. Osborne TL, Raichle KA, Jensen MP, Ehde DM, Kraft G. The Reliability and Validity of Pain Interference Measures in Persons with Multiple Sclerosis. Journal of Pain and Symptom Management. 2006 Sep 1;32(3):217–29. doi:10.1016/j.jpainsymman.2006.03.008

406. Dunn PK, Smyth GK. Generalized Linear Models With Examples in R [Internet]. New York, NY: Springer; 2018 [cited 2024 Aug 4]. (Springer Texts in Statistics). Available from: http://link.springer.com/10.1007/978-1-4419-0118-7 doi:10.1007/978-1-4419-0118-7

407. Rao SM, Leo GJ, Bernardin L, Unverzagt F. Cognitive dysfunction in multiple sclerosis.: I. Frequency, patterns, and prediction. Neurology. 1991 May 1;41(5):685–91. doi:10.1212/WNL.41.5.685 PubMed PMID: 2027484.

408. Buschke H. Selective reminding for analysis of memory and learning. Journal of Verbal Learning and Verbal Behavior. 1973 Oct 1;12(5):543–50. doi:10.1016/S0022-5371(73)80034-9

409. Rao S. Instructions for the Paced Auditory Serial Addition Test [Internet]. Available from: http://pasat.us/PDF/PASAT_Manual.pdf

410. Anscombe FJ. On Estimating Binomial Response Relations. Biometrika. 1956;43(3/4):461–4. doi:10.2307/2332926

411. Edwards JH. The recognition and estimation of cyclic trends. Annals of Human Genetics. 1961;25(1):83–7. doi:10.1111/j.1469-1809.1961.tb01501.x

412. ROGER JH. A significance test for cyclic trends in incidence data. Biometrika. 1977 Apr 1;64(1):152–5. doi:10.1093/biomet/64.1.152

413. Rau R. Chapter 3. Measuring seasonality. In: Seasonality in Human Mortality: A Demographic Approach. 1st edn. Springer Berlin, Heidelberg. p. 39–81. (Demographic Research Monographs).

414. Sedger LM, McDermott MF. TNF and TNF-receptors: From mediators of cell death and inflammation to therapeutic giants – past, present and future. Cytokine & Growth Factor Reviews. 2014 Aug 1;25(4):453–72. doi:10.1016/j.cytogfr.2014.07.016

415. Galozzi P, Bindoli S, Doria A, Sfriso P. The revisited role of interleukin-1 alpha and beta in autoimmune and inflammatory disorders and in comorbidities. Autoimmunity Reviews. 2021 Apr 1;20(4):102785. doi:10.1016/j.autrev.2021.102785

416. Kaneko N, Kurata M, Yamamoto T, Morikawa S, Masumoto J. The role of interleukin-1 in general pathology. Inflammation and Regeneration. 2019 Jun 6;39(1):12. doi:10.1186/s41232-019-0101-5

417. Elsner RA, Shlomchik MJ. Germinal Center and Extrafollicular B Cell Responses in vaccination, immunity and autoimmunity. Immunity. 2020 Dec 15;53(6):1136–50. doi:10.1016/j.immuni.2020.11.006 PubMed PMID: 33326765; PubMed Central PMCID: PMC7748291.

418. Lydyard P, Whelan A, Fanger M. B-cell activation. In: Immunology. Third. CRC Press; 2003. (BIOS Instant Notes).

419. Höftberger R, Guo Y, Flanagan EP, Lopez-Chiriboga AS, Endmayr V, Hochmeister S, et al. The pathology of central nervous system inflammatory demyelinating disease accompanying myelin oligodendrocyte glycoprotein autoantibody. Acta Neuropathol. 2020 May;139(5):875–92. doi:10.1007/s00401-020-02132-y PubMed PMID: 32048003; PubMed Central PMCID: PMC7181560.

420. Spadaro M, Gerdes LA, Mayer MC, Ertl-Wagner B, Laurent S, Krumbholz M, et al. Histopathology and clinical course of MOG-antibody-associated encephalomyelitis. Ann Clin Transl Neurol. 2015 Mar;2(3):295–301. doi:10.1002/acn3.164 PubMed PMID: 25815356; PubMed Central PMCID: PMC4369279.

421. Kinzel S, Lehmann-Horn K, Torke S, Häusler D, Winkler A, Stadelmann C, et al. Myelin-reactive antibodies initiate T cell-mediated CNS autoimmune disease by opsonization of endogenous antigen. Acta Neuropathol. 2016 Jul;132(1):43–58. doi:10.1007/s00401-016-1559-8

Appendix 1

Excerpts from the protocol for the Neuromyelitis Optica Spectrum Disorders and Multiple Sclerosis Research Tissue Bank

Date and Version No: **V6.0 07.06.2020**	Tissue for the study of Neuromyelitis Optica Spectrum Disorders (NMOSD), Multiple Sclerosis (MS) and related disorders: clinical, genetic and immunological studies. Ethics ref:16/SC/0224.

Study Title: Tissue for the study of Neuromyelitis Optica Spectrum Disorders (NMOSD), Multiple Sclerosis (MS) and related conditions: clinical, genetic and immunological studies

Short title: Neuromyelitis Optica Spectrum Disorders and Multiple Sclerosis Research Tissue Bank

Ethics Ref: 16/SC/0224

Date and Version No: V6.0 07.06.2020

Chief Investigator:	Dr Jacqueline Palace Consultant Neurologist Department of Clinical Neurology Level 3 West Wing John Radcliffe Hospital Oxford OX3 9DU
Investigators:	Dr Maria Isabel Leite (principal investigator), Dr Gabriel DeLuca and members of the NMO and MS teams, Department of Clinical Neurology, John Radcliffe Hospital
License Holder (Institute)	Weatherall Institute of Molecular Medicine, Oxford University
Designated Individual	Dr Kathryn Robson
Designated Person	Professor Lars Fugger
Licence Number	12433
Funder:	NMO and MS charitable and research funds
Signatures:	No conflicts of interest.

Version 6.0 of the Protocol has been prepared for Substantial Amendment 3 07.06.2020

2. SYNOPSIS

Research Tissue Bank Title	**Tissue for the study of Neuromyelitis Optica Spectrum Disorders (NMOSD), Multiple Sclerosis (MS) and related disorders: clinical, genetic and immunological studies**
Ethics Ref:	**10/H0606/56**
Collection methods	To collect donations of blood and urine samples, that would not be part of the normal patient care
Material Collected	DNA/serum/plasma/CSF/urine/tissue-blocks/sections, clinical data, imaging and additional demographic and clinical information (including questionnaires)
Number of Samples	Approximately 500 samples per year (approx. 200 NMO; 200 MS/other disease groups; 100 Healthy Volunteers).
Planned Approval Period	Samples will be stored in a research tissue bank that will be available to supply material for medical research for ongoing and future research projects
Primary Objective	To provide tissue samples and data to serve as a research resource to study NMOSD, MS and related disorders (e.g. acute disseminated encephalomyelitis, ADEM, neurosarcoidosis), and compare with controls.
Secondary Objectives	A. To supply samples from NMOSD, MS and related disorders, for instance to 1) identify genetic factors that may influence the presentation and course of disease and response to treatment; 2) understand the molecular mechanisms of disease in these neurological disorders; 3) understand the role of autoantibodies in triggering the disease and relapses with distinct manifestations; 4) study the response to therapies for these disorders; 5) improve diagnostic methods and identify new target antigens in some neurological disorders thought to be autoimmune and belong to the NMOSD, MS and related disorders (such as ADEM), which serum samples are found negative for the currently available antibody. B. To supply clinical material, for instance to 1) characterise the patients affected; 2) identify the range of neurological syndromes (clinical manifestations, neurological deficits and imaging); 3) identify associated non-neurological manifestations or diseases; 4) improve diagnosis and define diagnostic criteria; 5) study patient responses to treatments and disease outcomes. These data will be collected from the patients' notes

	and from speaking to the patients and families in clinical setting (regular visits in the outpatient clinic or elective admissions in the inpatient ward, as needed for the patient clinical care). C: To supply additional demographic and clinical information for instance to 1) understand the influence of certain factors in the disease manifestations (e.g. ethnicity, age at onset and gender); 2) study the incidence and role of other associated conditions (eg. autoimmune diseases) in patients or in family; 3) identify possible factors that may trigger the disease. D. To collate and analyse all clinical Information from B and C, which is crucial to accumulate clinical knowledge about NMOSD, MS and related disorders such as ADEM. E. To correlate the results from A with those from B and C, to achieve overall understanding of the NMOSD, MS and related disorders

Appendix 2

Group size calculation for the MoCA

Group means and SDs of patients with NMOSD and controls from Guo *et al*., 2018 (155). No paper provides mean MoCA score and SD of patients with MOGAD, so values were assumed to be equivalent to those of patients with NMOSD.

A linear regression of a continuous variable against a factor with 3 levels is equivalent to an ANOVA with 3 levels. Therefore, the group size for an ANOVA with 3 levels, $\alpha = 0.05$ and power = 0.80 was calculated.

Mean MoCA score in controls = 25.21 (84.03%)

Mean MoCA score in patients with NMOSD = 22.55 (75.17%)

SD controls = SD_1 = 2.76 (9.20%)

SD NMOSD (%) = SD_2 = 4.61 (15.37%)

Number of patients with NMOSD = n_1 = 43

Number of controls = n_2 = 42

Pooled mean (assuming MOGAD scores equivalent to NMOSD scores) =

$$\frac{84.03+75.17+75.17}{3}$$

Pooled mean = 78.12%

Pooled SD = $$\sqrt{\frac{(n_1-1).SD_1^2+(n_2-1).SD_2^2}{n_1+n_2-2}}$$

Pooled SD = 12.63

$$f=\sqrt{\frac{\sum p_i(\mu_i-\mu)^2}{\sigma^2}}$$

$$\sum p_i(\mu_i-\mu)^2=\frac{1}{3}(84.03-78.12)^2+\frac{1}{3}(75.17-78.12)^2+¿\frac{1}{3}(75.17-78.12)^2¿$$

$$\sum p_i(\mu_i-\mu)^2= 11.64 + 8.70 + 8.70 = 1.77$$

$$f=\sqrt{\frac{29.05}{159.52}} = 0.427$$

G*Power calculation of group sizes to detect group difference with α = 0.05 and power = 0.80 is 19 per group.

Appendix 3

Montreal Cognitive Assessment (MoCA) scoring sheet (157)

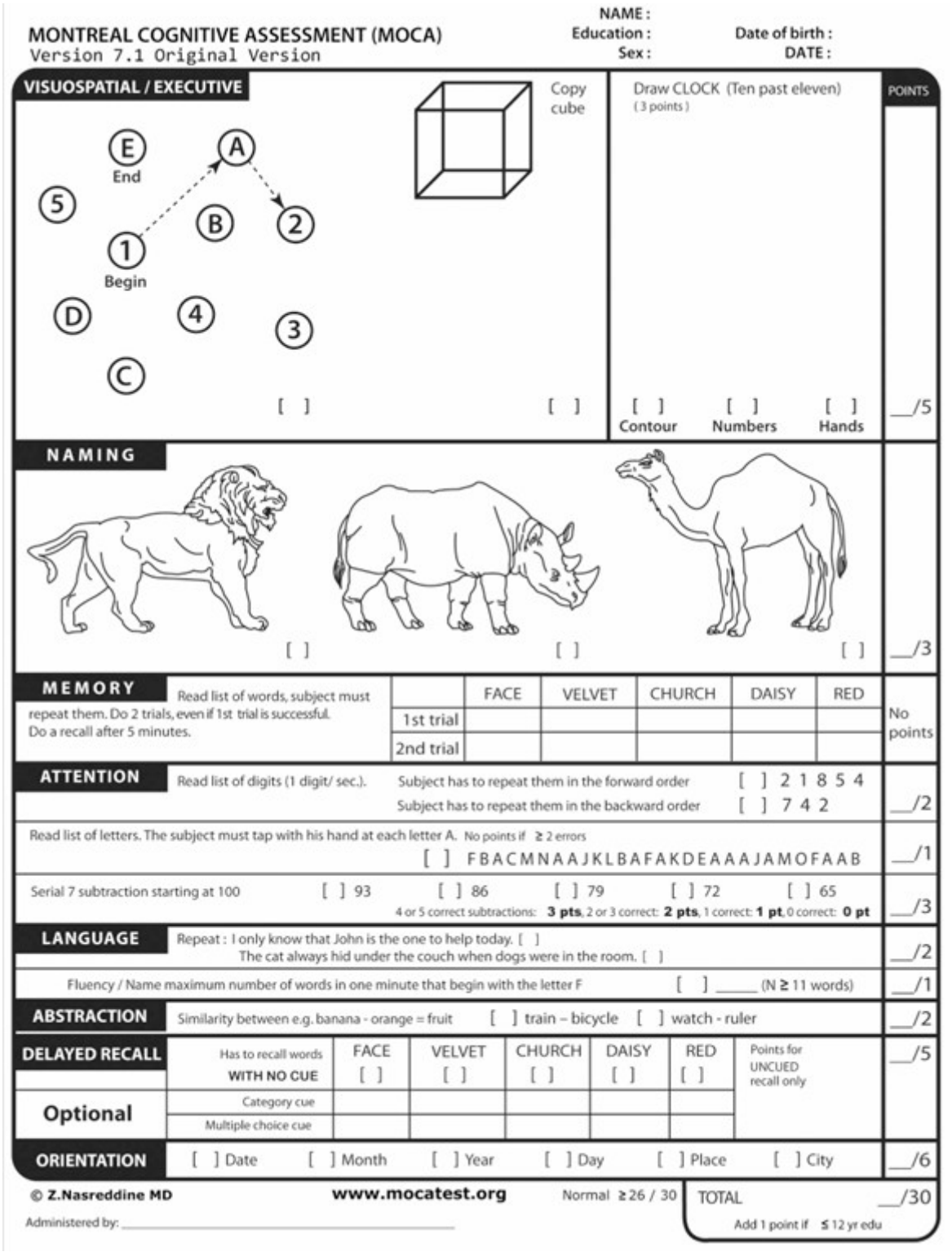

MONTREAL COGNITIVE ASSESSMENT (MOCA)
Version 7.1 Original Version

NAME :
Education : Date of birth :
Sex : DATE :

VISUOSPATIAL / EXECUTIVE — Copy cube — Draw CLOCK (Ten past eleven) (3 points) — POINTS

E End, A, 5, B, 2, 1 Begin, D, 4, 3, C

[ ] [ ]

[ ] Contour [ ] Numbers [ ] Hands __/5

NAMING [ ] [ ] [ ] __/3

MEMORY Read list of words, subject must repeat them. Do 2 trials, even if 1st trial is successful. Do a recall after 5 minutes.

	FACE	VELVET	CHURCH	DAISY	RED
1st trial					
2nd trial					

No points

ATTENTION Read list of digits (1 digit/ sec.).
Subject has to repeat them in the forward order [ ] 2 1 8 5 4
Subject has to repeat them in the backward order [ ] 7 4 2 __/2

Read list of letters. The subject must tap with his hand at each letter A. No points if ≥ 2 errors
[ ] F B A C M N A A J K L B A F A K D E A A A J A M O F A A B __/1

Serial 7 subtraction starting at 100 [ ] 93 [ ] 86 [ ] 79 [ ] 72 [ ] 65
4 or 5 correct subtractions: **3 pts**, 2 or 3 correct: **2 pts**, 1 correct: **1 pt**, 0 correct: **0 pt** __/3

LANGUAGE Repeat : I only know that John is the one to help today. [ ]
The cat always hid under the couch when dogs were in the room. [ ] __/2

Fluency / Name maximum number of words in one minute that begin with the letter F [ ] _____ (N ≥ 11 words) __/1

ABSTRACTION Similarity between e.g. banana - orange = fruit [ ] train – bicycle [ ] watch - ruler __/2

DELAYED RECALL

	Has to recall words WITH NO CUE	FACE	VELVET	CHURCH	DAISY	RED	Points for UNCUED recall only
		[ ]	[ ]	[ ]	[ ]	[ ]	
Optional	Category cue						
	Multiple choice cue						

__/5

ORIENTATION [ ] Date [ ] Month [ ] Year [ ] Day [ ] Place [ ] City __/6

© Z.Nasreddine MD www.mocatest.org Normal ≥ 26 / 30

TOTAL __/30
Add 1 point if ≤ 12 yr edu

Administered by: _____

Montreal Cognitive Assessment (Blind) (160)

MONTREAL COGNITIVE ASSESSMENT (MoCA®)

Version 8.1 BLIND English

NAME:
EDUCATION :
Sex :
Date of birth :
DATE :

MEMORY		FACE	VELVET	CHURCH	DAISY	RED	POINTS
Read list of words, subject must repeat them. Do 2 trials, even if 1st trial is successful. Do a recall after 5 minutes.	1st TRIAL						NO POINTS
	2nd TRIAL						

ATTENTION		
Read list of digits (1 digit / sec.).	Subject has to repeat in the forward order. [ ] 2 1 8 5 4 Subject has to repeat in the backward order. [ ] 7 4 2	___ /2
Read list of letters. The subject must tap at each letter A. No points if ≥ 2 errors [ ] F B A C M N A A J K L B A F A K D E A A A J A M O F A A B		____ /1
Seria 7 subtraction starting at 100 4 or 5 correct subtractions: 3 pts,	[ ] 93 [ ] 86 [ ] 79 [ ] 72 [ ] 65 2 or 3 correct: 2 pts, 1 correct: 1 pt, 0 correct: 0 pt	____ /3
LANGUAGE	I only know that John is the one to help today. [ ]	____ /2
Repeat:	The cat always hid under the couch when dogs were in the room [ ]	
Fluency: Name maximum number of words in one minute that begin with the letter F.	[ ] _____ (N ≥ 11words)	____ /1
ABSTRACTION Similarity between e.g. orange - banana = fruit	[ ] train - bicycle [ ] watch - ruler	____ /2

DELAYED RECALL		Has to recall words WITH NO CUE	FACE	VELVET	CHURCH	DAISY	RED	
Memory	(MIS) X3		[ ]	[ ]	[ ]	[ ]	[ ]	____ /5
Index	X2	Category cue						NO POINTS
Score	X1	Multiple choice cue						

ORIENTATION	[ ] Date [ ] Month [ ] Year [ ] Day [ ] Place [ ] City	____ /6

© Z. Nasreddine MD www.mocatest.org

TOTAL ____ /22

Administered by : _____ Add 1 point if ≤ 12 yr edu

MIS: /15 (Normal ≥ 19/22)

Appendix 4

Description and validation of psychosocial questionnaires

The Hospital Anxiety and Depression Scale (HADS) asks patients to rate frequency or severity of 7 items reflecting anxiety (HADS-A) and 7 items reflecting depression (HADS-D) on a scale of 0 to 3.

The HADS has good external validity in patients with and without depression and anxiety with sensitivity and specificity >95% (395). It loads on psychosocial rather than somatic symptoms of depression, avoiding score inflation by physical manifestations of CNS disease (395). It has been validated in MS (396) and has been used to assess depression and anxiety in MS, NMOSD and MOGAD (131,180,397).

The Modified Fatigue Impact Scale (MFIS) is part of the MS Quality of Life Index (398) and consists of 21 self-rated items assessing cognitive (10 items), physical (9 items) and social (2 items) domains of fatigue over the preceding 4 weeks. Patients rate each item on a 5-point Likert scale, with 0 indicating no interference and 4 indicating maximum interference. Global and domain scores can be obtained.

The MFIS demonstrates good construct validity (399) and internal consistency (397). It has been validated and used to assess fatigue in MS (174,175,400,401) and in NMOSD (180,397,402).

The Brief Pain Inventory (BPI) (403) requires patients to rate 4 items related to pain severity (worst, least, average and current) and 7 items related to interference of pain with mood, enjoyment of life, relationships with others, sleep, general activities, walking and working. Items are scored with 10-point Likert scales (0 = no pain, 10 = “worst pain imaginable” for severity items and “completely interferes” for interference items) according to the patient’s experience over the preceding 24 hours.

The BPI demonstrates high internal consistency, validity and test-retest reliability in different diseases (403,404), including MS (405). It has

been to measure pain in NMOSD (164). Total scores were calculated for each participant.

HOSPITAL ANXIETY AND DEPRESSION SCALE (HADS)

Read each item below and underline the reply which comes closest to how you have been feeling in the past week. Don't take too long over your replies; your immediate reaction to each item will probably be more accurate than a long, thought-out response.

1. I feel tense or wound up

3 Most of the time
2 A lot of the time
1 From time to time
0 Not at all

2. I still enjoy the things I used to enjoy

0 Definitely as much
1 Not quite so much
2 Only a little
3 Hardly at all

3. I get a frightened feeling as if something awful is about to happen

3 Very definitely and quite badly
2 Yes, but not too badly
1 A little, but it doesn't worry me
0 Not at all

4. I can laugh and see the funny side of things

0 As much as I always could
1 Not quite so much now
2 Definitely not so much now
3 Not at all

5. Worrying thoughts go through my mind

3 A great deal of the time
2 A lot of the time
1 Not too often
0 Very little

6. I feel cheerful

3 Never
2 Not often
1 Sometimes
0 Most of the time

7. I can sit at ease and feel relaxed

0 Definitely
1 Usually
2 Not often
3 Not at all

8. I feel as if I am slowed down

3 Nearly all the time
2 Very Often
1 Sometimes
0 Not at all

9. I get a sort of frightened feeling like 'butterflies' in the stomach

0 Not at all
1 Occasionally
2 Quite often
3 Very often

10. I have lost interest in my appearance

3 Definitely
2 I don't take as much care as I should
1 I may not take quite as much care
0 I take just as much care as ever

11. I feel restless as if I have to be on the move

3 Very much indeed
2 Quite a lot
1 Not very much
0 Not at all

12. I look forward with enjoyment to things

0 As much as I ever did

1 Rather less than I used to
2 Definitely less than I used to
3 Hardly at all

13. I get sudden feelings of panic

3 Very often indeed
2 Quite often
1 Not very often
0 Not at all

14. I can enjoy a good book or radio or television programme

0 Often
1 Sometimes
2 Not often
3 Very seldom

Visual Analogue Scale for Fatigue

How much fatigue are you having now?

0	1	2	3	4	5	6	7	8	9	10
No Fatigue										Worst possible fatigue

MODIFIED FATIGUE IMPACT SCALE (MFIS)

Following is a list of statements that describe how fatigue may affect a person. Fatigue is a feeling of physical tiredness and lack of energy that many people experience from time to time. In medical conditions like NMO, feelings of fatigue can occur more often and have a greater impact than usual. Please read each statement carefully and then circle the one number that best indicates how often fatigue has affected you in this way during the past 4 weeks. Please answer every question. If you are not sure which answer to select, please choose the one answer that comes closest to describing you.

Because of my fatigue during the past 4 weeks…

	Never	Rarely	Sometimes	Often	Almost Always
1. I have been less alert.	0	1	2	3	4
2. I have had difficulty paying attention for long periods of time.	0	1	2	3	4
3. I have been unable to think clearly.	0	1	2	3	4
4. I have been clumsy and uncoordinated.	0	1	2	3	4
5. I have been forgetful.	0	1	2	3	4
6. I have had to pace myself in my physical activities.	0	1	2	3	4
7. I have been less motivated to do anything that requires physical effort.	0	1	2	3	4
8. I have been less motivated to participate in social activities.	0	1	2	3	4
9. I have been limited in my ability to do things away from home.	0	1	2	3	4

Because of my fatigue during the past 4 weeks....

	Never	Rarely	Sometimes	Often	Almost always
10. I have had trouble maintaining physical effort for long periods.	0	1	2	3	4
11. I have had difficulty making decisions.	0	1	2	3	4
12. I have been less motivated to do anything that requires thinking.	0	1	2	3	4

13. My muscles have felt weak.	0	1	2	3	4
14. I have been physically uncomfortable.	0	1	2	3	4
15. I have had trouble finishing tasks that require thinking.	0	1	2	3	4
16. I have had difficulty organizing my thoughts when doing things at home or at work.	0	1	2	3	4
17. I have been less able to complete tasks that require physical effort.	0	1	2	3	4
18. my thinking has been slowed down.	0	1	2	3	4
19. I have had trouble concentrating.	0	1	2	3	4
20. I have limited my physical activities.	0	1	2	3	4
21. I have needed to rest more often or for longer periods.	0	1	2	3	4

BRIEF PAIN INVENTORY (BPI)

1. **Throughout our lives, most of us have had pain from time to time (such as minor headaches, sprains and toothaches). Have you have pain other than these everyday kinds of pain today?**

   Yes No (please circle you response)

2. **On the diagram shade in the areas where you feel pain. And put a cross on the area that hurts the most.**

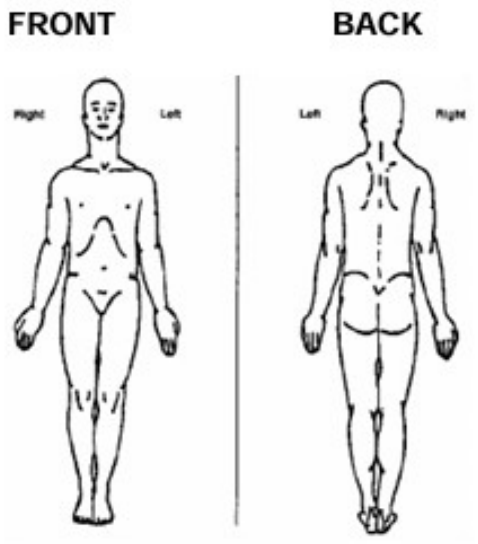

3. **Please rate your pain by circling the one number that best describes your pain at its <u>worst</u> in the <u>last 24 hours</u>.**

0	1	2	3	4	5	6	7	8	9	10
No Pain										Pain as bad as you can imagine

4. **Please rate your pain by circling the one number that best describes your pain at its <u>least</u> in the <u>last 24 hours</u>.**

0	1	2	3	4	5	6	7	8	9	10
No Pain										Pain as bad as you can imagine

5. **Please rate your pain by circling the one number that best describes your pain on <u>average</u>.**

0 1 2 3 4 5 6 7 8 9 10

No Pain — Pain as bad as you can imagine

6. **Please rate your pain by circling the one number that tells how much pain you have right now.**

0 1 2 3 4 5 6 7 8 9 10

No Pain — Pain as bad as you can imagine

7. **What treatments or medications are you receiving for your pain?**

_____

8. **In the last 24 hours, how much relief have pain treatments or medications provided? Please circle the one number that shows how much relief you have received?**

0% 10% 20% 30% 40% 50% 60% 70% 80% 90% 100%

No Relief — Complete Relief

9. **Circle the one number that describes how, during the past 24 hours, pain has interfered with your:**

A. General Activity

0 1 2 3 4 5 6 7 8 9 10

Does not Interfere — completely Interferes

B. Mood

0 1 2 3 4 5 6 7 8 9 10

Does not Interfere — completely Interferes

C. Walking Ability

0 1 2 3 4 5 6 7 8 9 10

Does not Interfere — Completely Interferes

D. Normal Work (includes both work outside the home and housework)

0 1 2 3 4 5 6 7 8 9 10

Does not Interfere — Completely Interferes

E. Relations with other people

0 1 2 3 4 5 6 7 8 9 10

Does not Interfere — Completely Interferes

F. Sleep

0 1 2 3 4 5 6 7 8 9 10

Does not Interfere — Completely Interferes

G. Enjoyment of life

0 1 2 3 4 5 6 7 8 9 10

Does not Interfere — Completely Interferes

Appendix 5

Explanation and analysis of linear regression and data distribution

Application of linear regression models is only appropriate if the relationships between the independent and dependent variables are linear, there is homoscedasticity of the residuals, the residuals approximate a normal distribution and there are no or few significant outliers (161).

Simple linear regression depends on least mean squares to fit the regression line and, more importantly, define the residuals, calculate the standard deviation (SD) and estimate the standard error (SE) and 95% confidence intervals of the regression line. In a simple linear regression, for a matrix of p independent variables ($x_1 \ldots x_p$) and an observed dependent variable y_i with n values ($y_1 \ldots y_n$) the regression coefficients for p independent variables ($\beta_1, \ldots \beta_q$) are calculated by fitting the line that minimises the loss function.

The residuals, or errors ($r_1 \ldots r_n$) are given by:

$r_i = y_i - \mu$

where μ is the fitted value, i.e., the predicted value of y for a given value of independent variable x, or for a combination of variables, x_p.

$\mu_i = ¿\beta_0 + \beta_1 x_{i1} + \beta_2 x_{i2} \ldots \beta_q x_{ip}$,

where β_0 is the intercept (the value of μ_i when $x_p = 0$).

The loss function is the sum square of the errors (SSE), i.e., the sum square of the residuals:

$SSE = \Sigma (y_i - \mu)^2$

If we assume there is only one independent predictor, x_1, then

$\mu_i = ¿\beta_0 + \beta_1 x_{i1}$

$SSE = \Sigma (y_i - \beta_0 - \beta_1 x_{i1})^2$

The aim of least mean squares methods is to minimise the SSE. This is achieved by solving the partial derivative of the SSE with respect to β_1. When solved for 0, the value of β_1 is the value at which the standard deviation (SD) is at its nadir:

$$\frac{\delta \sum (y_i - \beta_0 - \beta_1 x_{i1})^2}{\delta \beta_1} = 0$$

$$2\sum x_i (y_i - \beta_0 - \beta_1 x_{i1}) = 0$$

Therefore,

$$\sum x_i (y_i - \beta_0 - \beta_1 x_{i1}) = 0 \qquad (1)$$

Simultaneously, the partial derivative of the SSE with respect to β_0 can be solved for 0:

$$\frac{\delta \sum (y_i - \beta_0 - \beta_1 x_{i1})^2}{\delta \beta_0} = 0$$

$$\frac{\delta \sum (y_i - \beta_0 - \beta_1 x_{i1})^2}{\delta \beta_0} = ¿ -2\sum (y_i - \beta_0 - \beta_1 x_{i1}) = 0$$

$$= \sum (y_i - \sum \beta_0 - \beta_1 \sum x_{i1}) = 0$$

$$\sum \beta_0 = n\beta_0$$

Rearranging to solve for β_0:

$$n\beta_0 = \sum y_i - \beta_1 \sum x_{i1}$$

$$\beta_0 = \frac{1}{n}\sum y_i - \frac{1}{n}\beta_1 \sum x_{i1}$$

$$\overline{y} = \frac{1}{n}\sum y_i; \qquad \overline{x} = \frac{1}{n}\beta_1 \sum x_{i1}$$

$$\beta_0 = \overline{y} - \beta_1 \overline{x} \qquad (2)$$

Substituting (2) into (1):

$$\sum x_i (y_i - \overline{y} + \beta_1 \overline{x} - \beta_1 x_{i1}) = 0$$

$$\beta_1 = \frac{\sum (x_i - \overline{x}) y_i}{\sum (x_i - \overline{x})^2} \quad (161)$$

This provides the value of β_1 at which the SSE is at its minimum, i.e., the residual sum of squares (RSS). For an overview, see reference 406.

A least mean squares method to minimise the residuals cannot be applied when the residuals are non-parametric because the numeric mean is not a good measure of central tendency. For example, data that are positively skewed will have few high values, which will cause the mean to exceed the median. This has two effects.

The first effect is on the estimate of the beta regression coefficient (β_1, i.e., the line that minimises the SSE to give the RSS). If y_i is far from the mean, $(y_i - \beta_0 - \beta_1 x_{i1})$ is large. The effect of y_i on β_1 is proportional to the square of the residual (SSE = $\Sigma (y_i - \beta_0 - \beta_1 x_{i1})^2$). To minimise the SSE, the beta regression coefficient is distorted towards the values from the extremes of the distribution. This may lead to errors in the estimation of the regression coefficient, although effects are usually small.

The second effect is that the estimates of the standard errors and standard deviation of the model, which depend on the residuals, are inaccurate.

The standard error of the model is estimated from the variance in the sample data:

Variance = $SD^2 = \sigma^2$

$$\sigma^2 = \frac{\sum (y_i - \mu)^2}{n}$$

$$SD\ (\sigma) = \sqrt{\frac{\sum (y_i - \mu)^2}{n}}$$

The value of σ describes the spread of the data around the mean under the assumption that the data are from a normal distribution. If the data are skewed, the RSS is increased and σ and σ^2 are inflated.

The variance is minimal when the RSS is optimised, i.e., when μ is the value that minimises the SSE. To account for this optimisation, the estimated variance of the model is:

S^2 (mean square error, MSE) ¿ $\frac{\sum (y_i-\mu)^2}{n-p}$

S (residual standard error, RSE) = $\sqrt{\frac{\sum (y_i-\mu)^2}{n-p}}$

The RSE of the model is therefore an indicator of the fit of the model to the data, with a larger RSE reflecting greater residuals and poorer fit. A non-normal distribution would exaggerate the RSE.

The standard error of the regression coefficients is also calculated using the mean squared error (MSE):

$SE(\beta_j) = \sqrt{\frac{S^2}{\sum (x_i-\overline{x})^2}} = \frac{S}{\sqrt{\sum (x_i-\overline{x})^2}}$

where x_i is the ith value of the independent variable and $\overline{x}$ is the mean of the independent variable.

A non-normal distribution will alter the MSE and thus the standard error of the regression coefficient.

If the residuals are taken from a standard normal distribution, the RSS will follow a Chi squared (χ^2) distribution. Therefore, the SE is derived from a square root of a χ^2 distribution. Dividing normally distributed data by the square root of a χ^2 distribution gives rise to a t distribution, which is essential when calculating the t- statistic:

$t = \frac{\beta_j - 0}{SE(\beta ¿ ¿ j) ¿}$

The t statistic is used to calculate the probability that the estimated value of β_j is not 0, i.e., to reject the Null hypothesis. If residuals do not follow a normal distribution, the t statistic derived is not taken from a t distribution and the p value is invalid.

Confidence intervals are also calculated from the critical t statistic (the t statistic corresponding to a probability of 0.975 for the relevant degrees of freedom) and the standard error. Evidently, if these are derived under false assumptions, the confidence intervals will also be incorrect.

The F statistic that is used to assess the statistical significance of the model also depends on the RSS following a χ^2 distribution. Therefore, the statistical significance of the model can only be determined if the residuals follow a normal distribution.

Incorrect assumptions regarding the distribution of the data will therefore affect not only the estimate of the model fit (RSE) but also measures of precision (e.g., standard error of the β coefficients) and indicators of significance (confidence intervals and p values), potentially leading to incorrect inferences.

Similarly, outliers affect both the beta regression coefficient by exerting disproportionate influence in least mean squares calculations, distorting the line that minimises the RSS towards themselves, and lead to inaccurate estimates of standard errors, confidence intervals and t statistics.

Homoscedasticity is important because each squared error term in a linear regression $(y_i-\mu)^2$ is assumed to estimate the underlying variance (σ^2). If error terms are unequal for different values of μ, a single estimate of variance is not appropriate and does not represent the observed variance throughout the data. The accuracy of a predicted outcome (e.g., %MoCA score) for a given value of a predictor is assumed to be constant by the model, even if the data show heteroscedasticity of the residuals. Measures of accuracy, such as

standard errors, are therefore overestimated or underestimated depending on the value of the predictor.

Meeting assumptions of linear regression

Untransformed data did not meet assumptions of linear regression:

a) MoCA scores did not follow a normal distribution (fig a5.i). More importantly, the standardised residuals generated by linear regression did not approximate normal distributions (for examples, see figs a5.ii – v, tables a5.i - iv).

b) Outliers were identified in univariable linear regression of MoCA scores against several independent variables (for examples, see tables a5.i – iv).

c) Plots of the standardised residuals against fitted values revealed heteroscedasticity for several continuous independent variables. Levene's test indicated unequal variance for sex at birth and first language (for examples, see tables a5.i - iv).

Figure a5.i. Distribution of %MoCA scores of all participants

a. Histogram of %MoCA scores for all groups

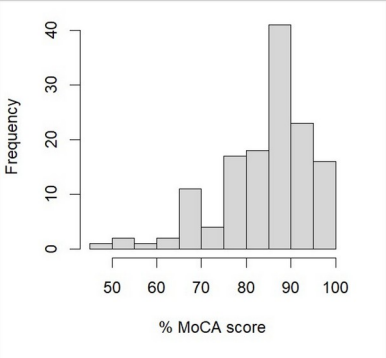

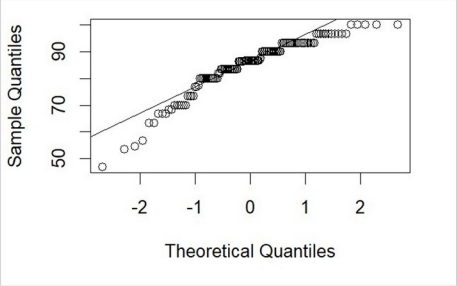

Figure a5.ii. Linear regression of %MoCA score against diagnosis

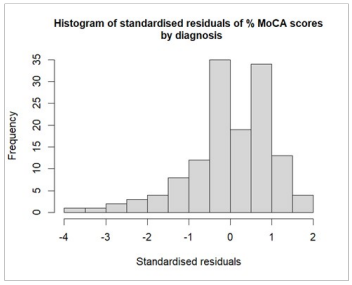

a. Histogram of standardised residuals for MoCA scores vs diagnosis

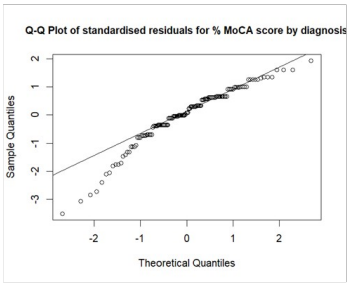

b. QQ plot of standardised residuals for MoCA scores vs diagnosis

Table a5.i. Univariable linear regression of MoCA scores by diagnosis

Parameter	Result
R^2	0.074
RSE (DoF)	9.855 (133)
β AQP4+ NMOSD (p)	-6.082 (0.007)
β MOGAD (p)	-0.349 (0.870)
F statistic (DoF)	5.350 (2, 133)
Shapiro Wilk residuals (p)	0.94 ($p < 0.001$)
N outliers	2
Cook's distances	0
Levene's test (F value) (p)	1.739 ($p = 0.180$)

Figure a5.iii. Linear regression of %MoCA score against disease duration

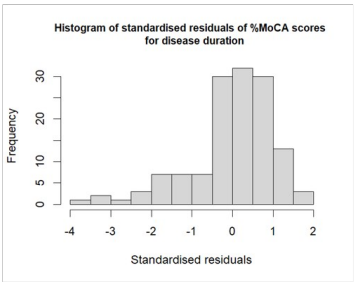

a. Histogram of standardised residuals for MoCA scores vs disease duration

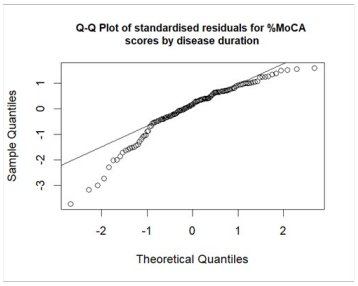

b. QQ plot of standardised residuals for MoCA scores vs disease duration

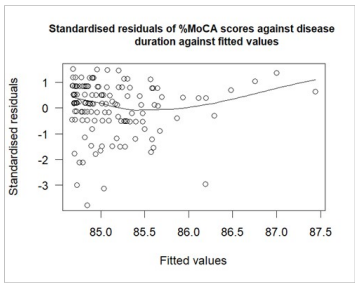

c. Scatter plot of standardised residuals against predicted MoCA scores

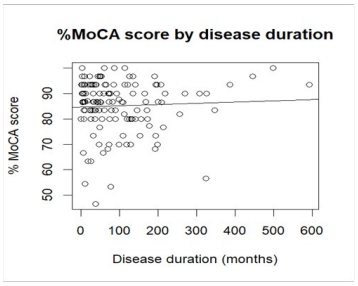

d. Scatterplot of MoCA score against disease duration

Supplementary table a5.ii. Univariable linear regression of MoCA scores by disease duration

Parameter	Result
R^2	0.002
RSE (DoF)	10.18 (131)
β (p)	0.005 (0.587)
F statistic (DoF)	0.297 (1, 131)
Shapiro Wilk residuals (p)	0.91 (<0.001)
N outliers	4
Cook's distances	0
Heteroscedasticity	Yes

Figure a5.iv. Linear regression of %MoCA score against BPI score

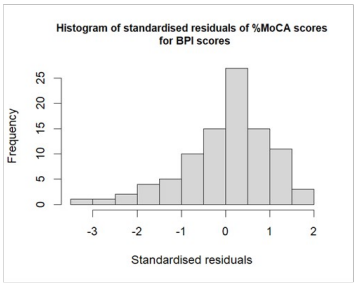

a. Histogram of standardised residuals for MoCA scores vs BPI score

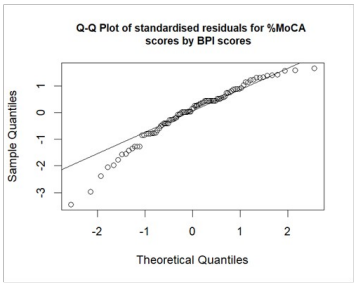

b. QQ plot of standardised residuals for MoCA scores vs BPI score

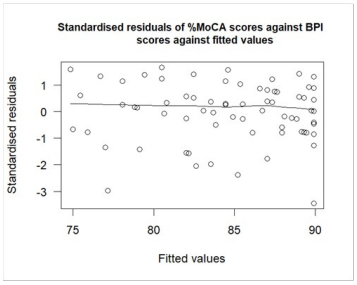

c. Scatter plot of standardised residuals against predicted MoCA scores

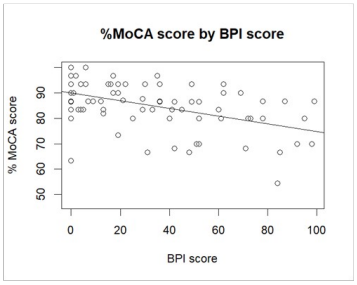

d. Scatterplot of MoCA score against BPI score

Supplementary table a5.iii. Univariable linear regression of MoCA scores by BPI score

Parameter	Result
R^2	0.253
RSE (DoF)	7.82 (92)
β (p)	-0.152 (<0.001)
F statistic (DoF)	31.22 (1, 92)
Shapiro Wilk residuals (p)	0.95 (<0.001)
N outliers	2
Cook's distances	0
Heteroscedasticity	No

Figure a5.v. Linear regression of %MoCA score against sex at birth

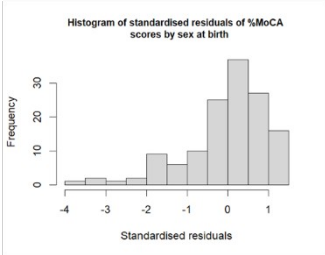

a. Histogram of standardised residuals for MoCA scores by sex at birth

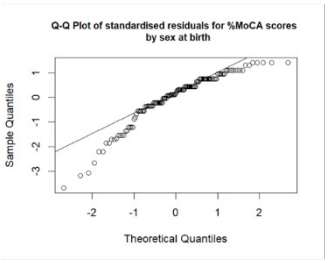

b. QQ plot of standardised residuals for MoCA scores by sex at birth

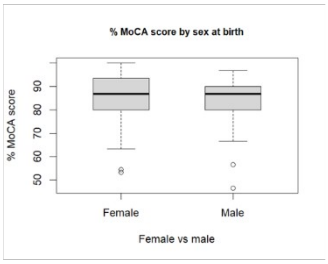

c. Boxplot of MoCA score by sex at birth

Table a5.iv. Univariable linear regression of MoCA scores by sex at birth

Parameter	Result
R^2	0.008
RSE (DoF)	10.16 (134)
B (male) (p)	-1.989 (0.300)
F statistic (DoF)	1.081 (1, 134)
Shapiro Wilk residuals (p)	0.91 (<0.001)
N outliers	3
Cook's distances	0
Levene's test (F value) (p)	7.858 (0.006)

Appendix 6

Transforming %MoCA scores

Various transforms were applied to %MoCA scores to overcome non-normality and heteroscedasticity of the residuals and the presence of outliers.

The examples shown below model linear relationships between a function of %MoCA score and age at onset (table a6.i).

Table a6.i: Analysis of linear regressions of untransformed and transformed %MoCA scores against age at onset

Model	Non-linearity	Normality of residuals (Shapiro Wilk p value)	Heteroscedasticity	R^2	B(p)	N outliers
% MoCA	No	No (<0.001)	Yes	0.014	-0.092 (0.175)	4
% MoCA score^2 (Box-Cox transform)	No	No (<0.001)	Yes	0.014	-14.87 (0.169)	1
% MoCA score^3	No	No (0.03)	Yes	0.015	-1846 (0.162)	0
Log (100 – % MoCA score) + 0.1	No	No (<0.001)	No	0.014	0.010 (0.013)	5
√(101 - % MoCA score)	No	Yes (0.261)	No	0.016	0.012 (0.147)	0

The method that compelled the residuals to normal distributions while preserving linearity, avoiding heteroscedasticity and eliminating outliers was the square root reflect transform (fig a6.i; table a6.ii).

Figure a6.i. Regression of √(101 - % MoCA score) against age at onset

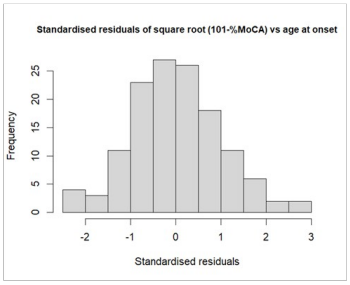

a. Histogram of standardised residuals for √(101 - % MoCA score) by age at onset

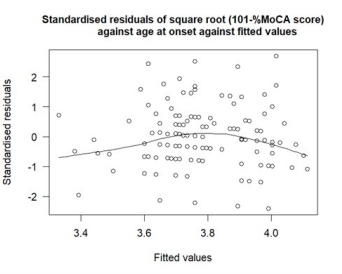

b. Scatter plot of standardised residuals against predicted √(101 - % MoCA score)

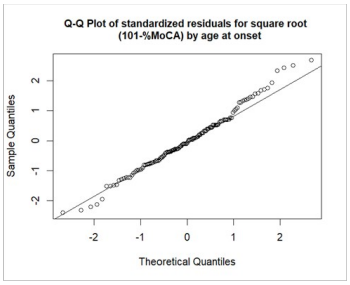

c. QQ plot of standardised residuals for √(101 - % MoCA score) vs age at onset

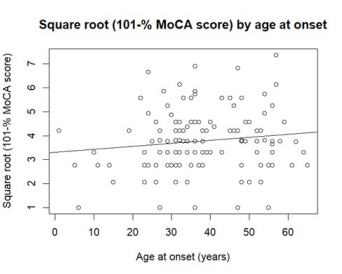

d. Scatter plot of √(101 - % MoCA score) by age at onset (years)

Table a6.ii. Results of univariable linear regression for √(101 - % MoCA score) by age at onset

Parameter	Result
R^2	0.016
RSE (DoF)	1.255 (131)
B (p)	0.012 (0.147)
F statistic (DoF)	2.124 (1, 131)
P (F Statistic)	0.147
Shapiro Wilk residuals (p)	0.99 (0.422)
N outliers	0
Cook's distances	0
Heteroscedasticity	No
β_0 (p)	3.319 (<0.001)
AIC (eDOF)	62.35 (2)

A square root reflect transform is a method of normalising negatively skewed data.

The square root reflect transform is the square root of the maximum score minus the observed score:

$$Transformed\ MoCA\ score = \sqrt{101 - \%MoCA\ score}$$

For a categorical variable, let μ represent the predicted value of the dependent variable (% MoCA score) in response space and μ_t represent the predicted transformed value. Let β_0 represent the model intercept. In a linear regression with 1 categorical variable with 2 levels (A and B), the value of the intercept (β_0¿ is the predicted mean value of the reference variable, A, in transformed space (μ_{tA}¿. β_1 represents the beta regression coefficient associated with the group of interest, B, in transformed space, i.e., the change in μ_t associated with group B compared with group A.

$$\mu_t = \sqrt{max\ score + 1 - \mu}$$

$$\mu_t^2 = max\ score + 1 - ¿\,\mu\,¿ \qquad \text{(Equation 1)}$$

The predicted value of μ_t for group B relative to group A (μ_{tB}¿ is:

$$\mu_{tB} = \beta_0 + \beta_1 + e$$

Ignore for now the error term, which does not represent the effects of the independent variable.

$$\mu_{tB}^2 = (\beta_0 + \beta_1)^2$$

Substitute Equation 1:

$$max\ score + 1 - \mu_B = (\beta_0 + \beta_1)^2$$

$$\mu_B = max\ score + 1 - (\beta_0 + \beta_1)^2$$

Recall $\beta_0 = \mu_{tA} = \sqrt{max\ score + 1 - \mu_A}$

$$\mu_B = max\ score + 1 - (\sqrt{max\ score + 1 - \mu_A} + \beta_1)^2$$

$$\mu_B = max\ score + 1 - (max\ score + 1 - \mu_A + 2\beta_1(\sqrt{max\ score + 1 - y_A}) + \beta_1 ¿¿ 2)¿$$

$$\mu_B = \mu_A - 2\beta_1(\sqrt{max\ score + 1 - \mu_A}) - \beta_1^{\,2}$$

$$\mu_B = \mu_A - 2\beta_1(\beta_0) - \beta_1^{\,2} \qquad \text{(Equation 2)}$$

I.e.,

$$Mean\ predicted\ \%MoCA\ score\ group\ B = Mean\ predicted\ \%MoCA\ score\ group\ A - 2\beta_1(\beta_0) - \beta_1^2$$

Therefore, $2\beta_1(\beta_0)+\beta_1^2$ is the predicted difference between the groups.

E.g.,

$$\%\,MoCA_{AQP4+NMOSD} = \%\,MoCA_{MG} - 2(0.700).(3.548) - (0.700)^2$$

$$\%\,MoCA_{AQP4+NMOSD} = \%\,MoCA_{MG} - 4.48$$

For continuous variables, let μ represent the dependent variable (% MoCA score) and μ_t represent the predicted value of the transformed dependent variable. Let x_1 represent the independent variable, let β_0 represent the intercept and let β_1 represent the beta regression coefficient associated with the independent variable, x_1, in transformed space.

$$\mu_t = \sqrt{max\ score + 1 - \mu}$$

$$\mu_t^2 = max\ score + 1 - \mu \qquad \text{(Equation 1)}$$

$$\mu_t = \beta_0 + \beta_1 x_1 + e$$

Ignore for now the error term, which does not represent the effect of the independent variable.

$$\mu_t^2 = (\beta_0 + \beta_1 x_1)^2$$

Substitute Equation 1:

$$max\ score + 1 - \mu = (\beta_0 + \beta_1 x_1)^2$$

$$\mu = max\ score + 1 - (\beta_0 + \beta_1 x_1)^2$$

$$\mu = max\ score + 1 - \beta_0^2 - 2(\beta_0 \beta_1 x_1) - (\beta_1 x_1)^2$$

To express the change in MoCA score caused by a 1 unit change in the independent variable, x_1:

$$\mu_x = max\ score + 1 - (\beta_0 + \beta_1 x_1)^2$$

$$\mu_{x+1} = max\ score + 1 - ¿¿$$

$$\mu_{x+1} = max\ score + 1 - (\beta_0 + \beta_1 x_1 + \beta_1)^2$$

$$\Delta\mu = \mu_{x+1} - \mu_x$$

$$\Delta\mu = [max\ score + 1 - (\beta_0 + \beta_1 x_1 + \beta_1) ¿¿¿ 2] - [max\ score + 1 - (\beta_0 + \beta_1 x_1)^2]$$

$$\Delta\mu = (\beta_0 + \beta_1 x_1)^2 - (\beta_0 + \beta_1 x_1 + \beta_1)^2$$

Algebraically, $A^2 - B^2 = (A + B)(A - B)$

$A = \beta_0 + \beta_1 x_1$

$B = \beta_0 + \beta_1 x_1 + \beta_1$

$$\Delta\mu = (\beta ¿¿ 0 + \beta_1 x_1 + \beta_0 + \beta_1 x_1 + \beta_1)(\beta_0 + \beta_1 x_1 - \beta_0 - \beta_1 x_1 - \beta_1) ¿$$

$$\Delta\mu = (2\beta ¿¿ 0 + 2\beta_1 x_1 + \beta_1)(-\beta_1) ¿$$

$$\Delta\mu = (-2\beta ¿¿ 0\beta_1 - 2\beta_1^2 x_1 - \beta_1^2) ¿ \qquad \text{(Equation 3)}$$

I.e.,

$$Change \in \%MoCA\ score = (-2\beta ¿¿ 0\beta_1 - 2\beta_1^2 x_1 - \beta_1^2) ¿$$

Appendix 7

Method: Multiple Imputation with Chained Equations for the MoCA

Data were assumed to be missing at random (MAR).

Variables missing most values in the original incomplete data set were identified. A data set containing only complete data (trial complete data set) was created from the original, incomplete data set and 15% of the values of variables with most data missing from the original data set (HADS-A, HADS-D, total MFIS, MFIS cognitive and BPI scores) were deleted at random (trial data set).

Fully conditional specification (FCS) was used to impute missing values separately. Five imputations were run for each variable with up to 20 iterations. Methods trialled were predictive mean matching (PMM), stochastic regression and Bayesian regression .

Values from each imputation were compared with the observed (deleted) values from the trial complete data set and percentage bias was calculated. Values of around 5% are considered acceptable (162).

Multivariable regression models were applied to each of the 5 imputed data sets and the results were pooled using Rubin’s rules. The output of the model using the trial imputed data set was compared with the output of the model applied to the trial complete data set.

The multivariable relative increase in variance (RIV) was calculated for each imputation method[21]. Convergence was assessed with convergence plots and feasibility of the distribution was checked with strip plots.

The most appropriate method of imputation was selected based on a combination of adequate convergence, imputed values within the range of observed values, low percentage bias, low variance inflation and

[21] Values of 0 indicate imputation caused no increase in variance above that caused by sampling, RIV ≤ 0.2 is considered modest, values 0.2 – 0.3 are considered moderately large and values > 0.3 are considered high (162).

similarity of the model estimates using the complete data set and the trial data set. This method was then used to impute missing values in the original, incomplete data set.

This method was repeated for the AQP4+ NMOSD and MOGAD cohort only. Ten percent of the most commonly missing variables were deleted from the trial data set with complete data. The number of imputations was increased to 20.

Appendix 8

Results: MICE feasibility study and method selection for MoCA analysis (whole cohort)

One-hundred and ninety-five data points were missing for 136 participants (fig a8.i).

Figure a8.i. Patterns of missingness

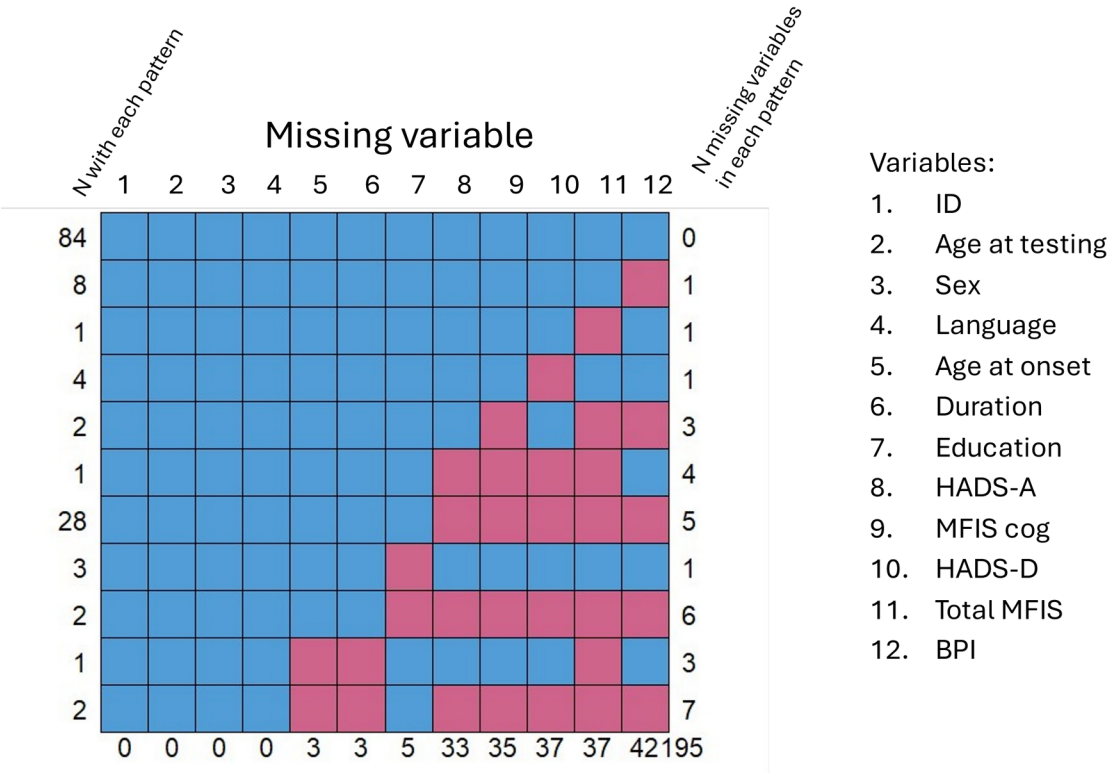

Complete data from 84 patients were incorporated into a trial data set for the feasibility study. Predictor variables for imputation were diagnosis, age at onset, onset age group, age at testing, disease duration, sex, first language, education and scores for HADS-A, HADS-D, total MFIS, cognitive MFIS, BPI and transformed MoCA score. Variables imputed were HADS-A, HADS-D, total MFIS, MFIS cognitive and BPI scores.

Predictive mean matching (PMM), stochastic regression and Bayesian regression all showed adequate convergence without trends. Imputed values were drawn from outside observed values when stochastic or

Bayesian methods were used. Percentage bias of most imputed values was lowest using PMM (table a8.i).

The RIV for all models was low (table a8.ii).

Table a8.i. Percentage bias in estimates of imputed variables with different imputation methods from trial data

Imputed covariate	% bias with PMM	% bias with Bayesian imputation	% bias with stochastic imputation
HADS-A	-18.15	-26.33	-23.69
HADS-D	3.55	15.62	6.96
Total MFIS	0.75	5.68	1.21
Cognitive MFIS	8.82	15.16	19.81
BPI	-26.68	-15.59	0.60

Table a8.ii. Regression model parameters with different imputation methods in MICE (trial data)

	Complete data subset	Imputed data with PMM	Imputed data with Bayesian method	Imputed data with stochastic method
R^2	0.392	0.383	0.386	0.385
β_{AQP4} (SE) (p)	0.826 (0.185)* (0.005)	0.815 (0.289) (0.006)	0.828 (0.287) (0.005)	0.817 (0.288) (0.006)
β_{MOGAD} (SE) (p)	0.389 (0.279) (0.167)	0.237 (0.281) (0.221)	0.355 (0.281) (0.210)	0.337 (0.281) (0.233)
F statistic (DOF) (p)	8.257 (6, 77)	7.821 (6, 74.93)	7.859 (6, 74.83)	7.934 (6, 74.99)
P (F statistic)	<0.001	<0.001	<0.001	<0.001
RIV	N/A	0.015	0.021	0.011

PMM was selected to impute missing study values (fig a8.ii & a8.iii). Estimates of regression coefficients, F statistics and R^2 generated from the trial data set after imputation with PMM were similar to those obtained using the complete trial data set, confirming models using imputed data were accurate (table a8.ii).

Figure a8.ii. Convergence of MICE models using PMM method (feasibility trial data)

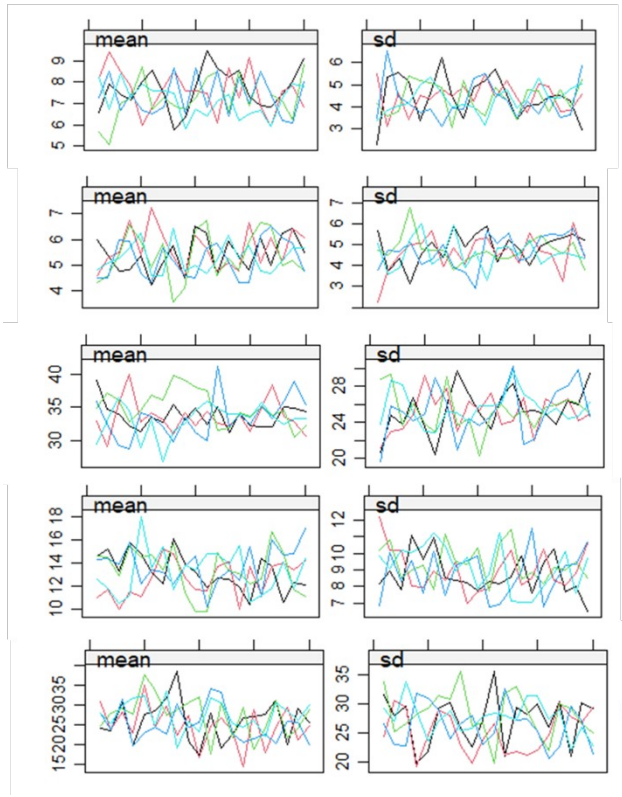

a. Convergence of imputed values of HADS-A score

b. Convergence of imputed values of HADS-D score

c. Convergence of imputed values of total MFIS score

d. Convergence of imputed values of MFIS-cognitive subscore

e. Convergence of imputed values of BPI score

Figure a8.iii. Strip plots of imputed values using PMM (feasibility trial data)

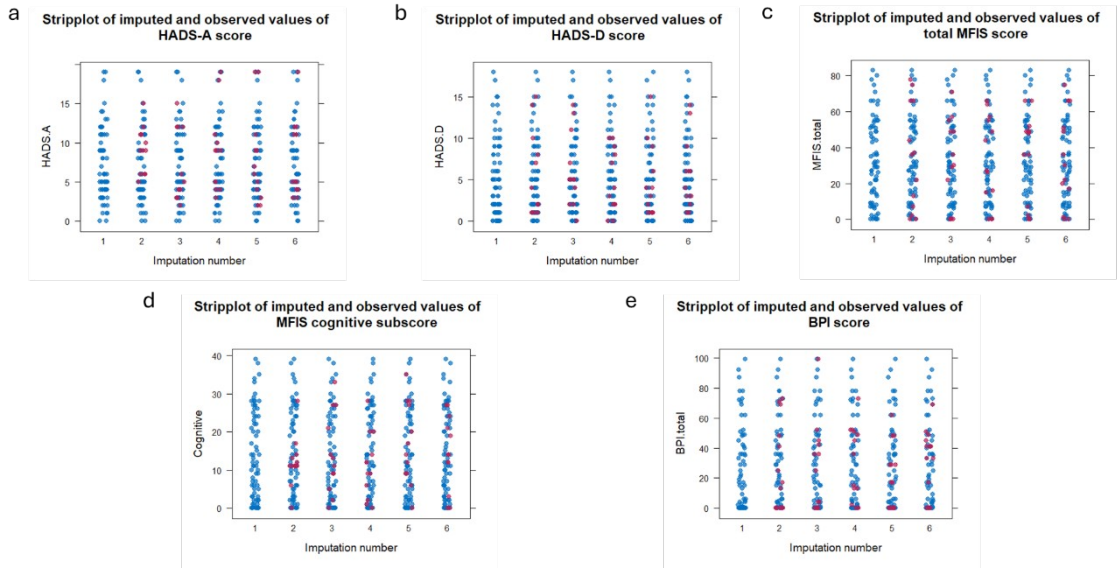

Blue dots indicate observed values, red dots indicate imputed values

The maximum number of iterations was increased to 50 when missing values were imputed for the original, incomplete data set to improve convergence. Imputations demonstrated adequate convergence and were from realistic distributions (fig a8.iv & a8.v).

Figure a8.iv. Convergence of MICE models using PMM method applied to original, incomplete data set

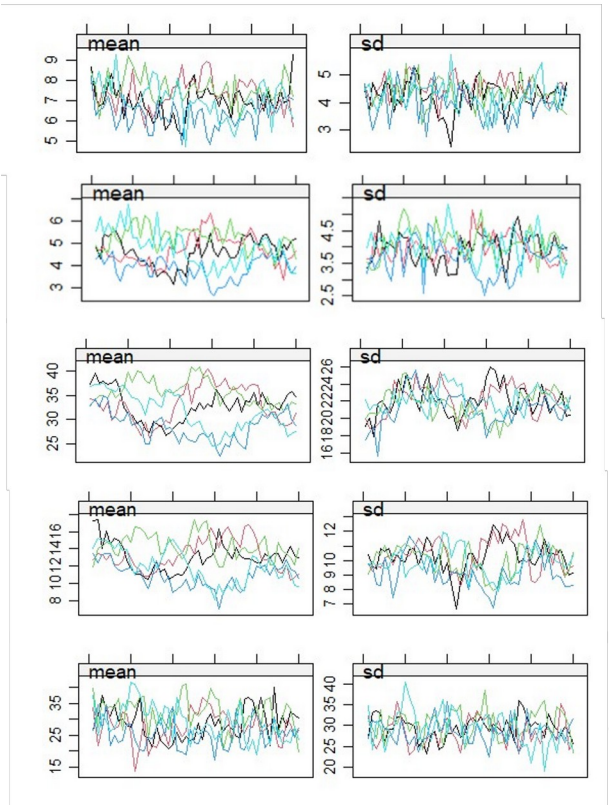

a. Convergence of imputed values of HADS-A score

b. Convergence of imputed values of HADS-D score

c. Convergence of imputed values of total MFIS score

d. Convergence of imputed values of MFIS-cognitive subscore

e. Convergence of imputed values of BPI score

Figure a8.v. Strip plots of imputed values using PMM applied to original, incomplete data set

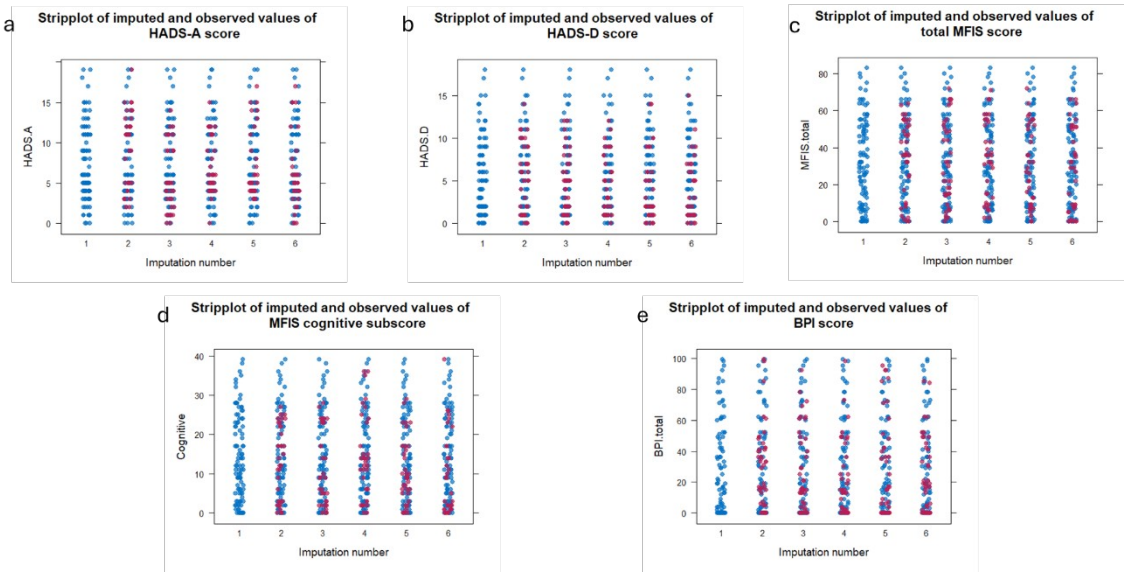

Blue dots indicate observed values, red dots indicate imputed values

Multiple imputation with chained equations: Results of feasibility study (AQP4+ NMOSD and MOGAD only)

When the same process was applied to the trial complete data set of patients with AQP4+ NMOSD and MOGAD, PMM only imputed variables from a narrow range of data and convergence of MFIS cognitive scores was poor (fig a8.vi & a8.vii). Stochastic and Bayesian methods imputed impossible values (fig a8.viii – a8.xi. Therefore, multiple imputation was not applied to the data set limited to AQP4+ NMOSD and MOGAD.

Figure a8.vi. Convergence of MICE models using PMM method for AQP4+ NMOSD and MOGAD only (feasibility trial data)

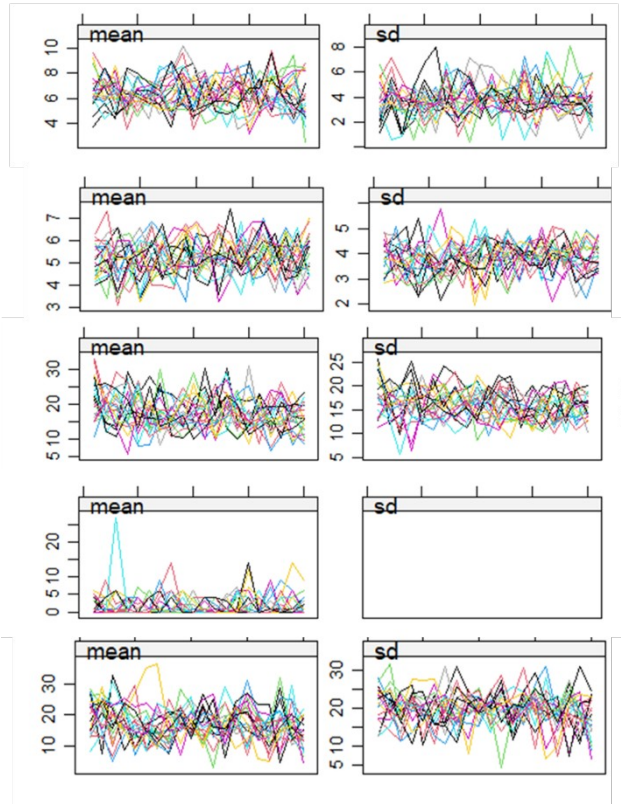

a. Convergence of imputed values of HADS-A score

b. Convergence of imputed values of HADS-D score

c. Convergence of imputed values of total MFIS score

d. Convergence of imputed values of MFIS-cognitive subscore

e. Convergence of imputed values of BPI score

Figure a8.vii. Strip plots of imputed values using PMM for AQP4+ NMOSD and MOGAD only (feasibility trial data)

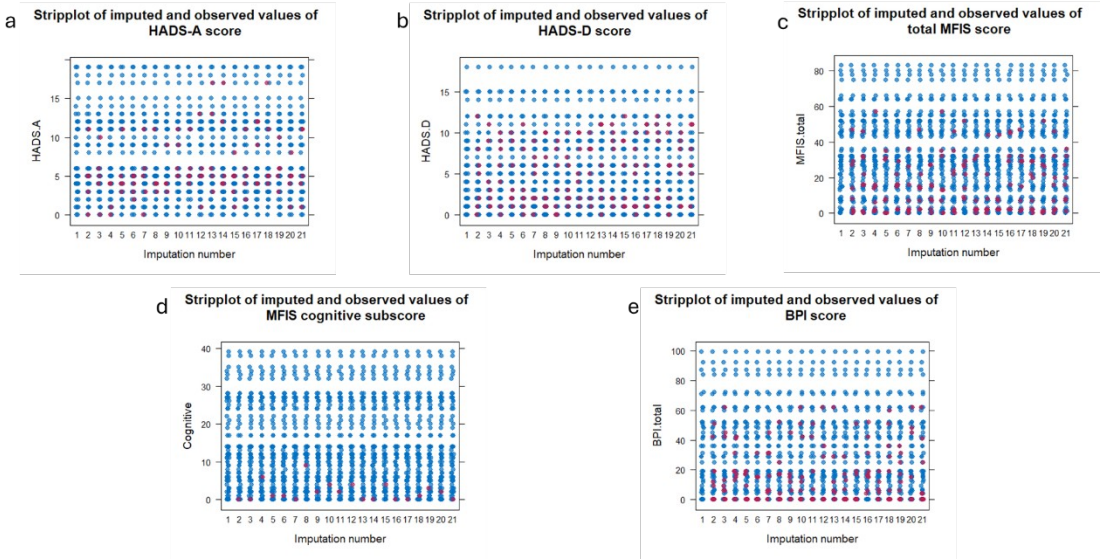

Blue dots indicate observed values, red dots indicate imputed values

Figure a8.viii Convergence of MICE models using stochastic method for AQP4+ NMOSD and MOGAD only (feasibility trial data)

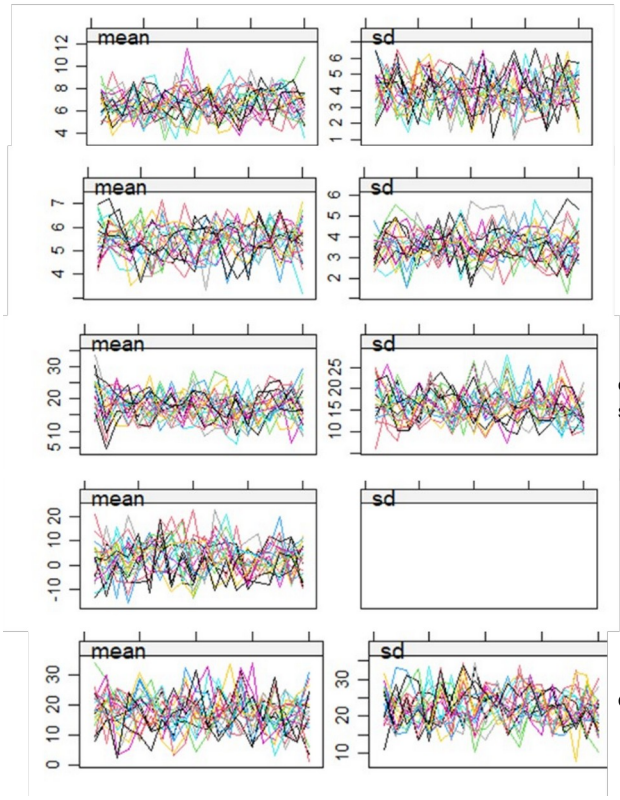

a. Convergence of imputed values of HADS-A score

b. Convergence of imputed values of HADS-D score

c. Convergence of imputed values of total MFIS score

d. Convergence of imputed values of MFIS-cognitive subscore

e. Convergence of imputed values of BPI score

Figure a8.ix. Strip plots of imputed values using stochastic imputation for AQP4+ NMOSD and MOGAD only (feasibility trial data)

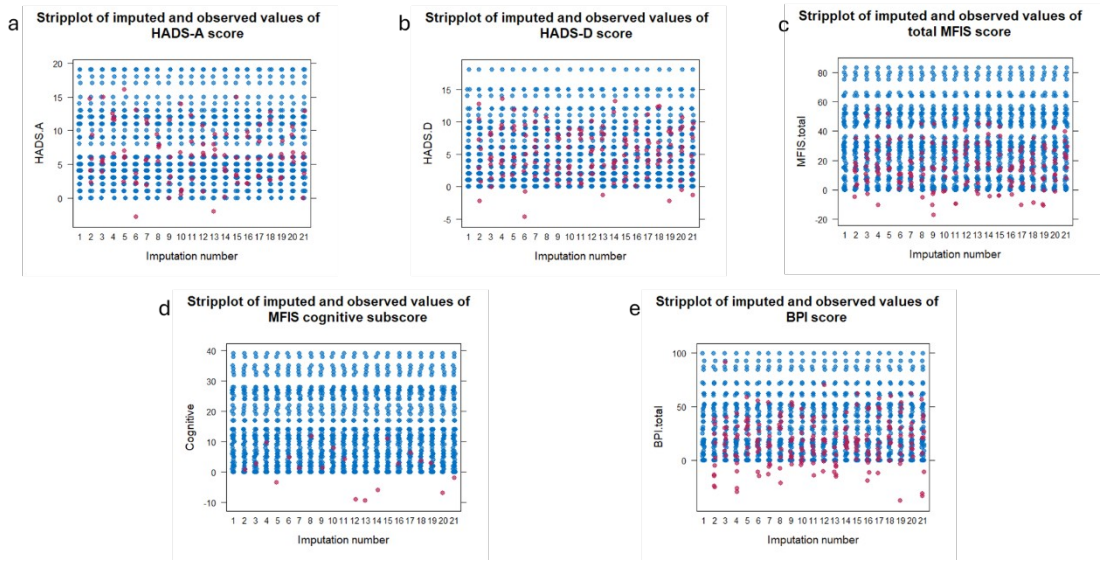

Blue dots indicate observed values, red dots indicate imputed values

Figure a8.x. Convergence of MICE models using Bayesian method for AQP4+ NMOSD and MOGAD only (feasibility trial data)

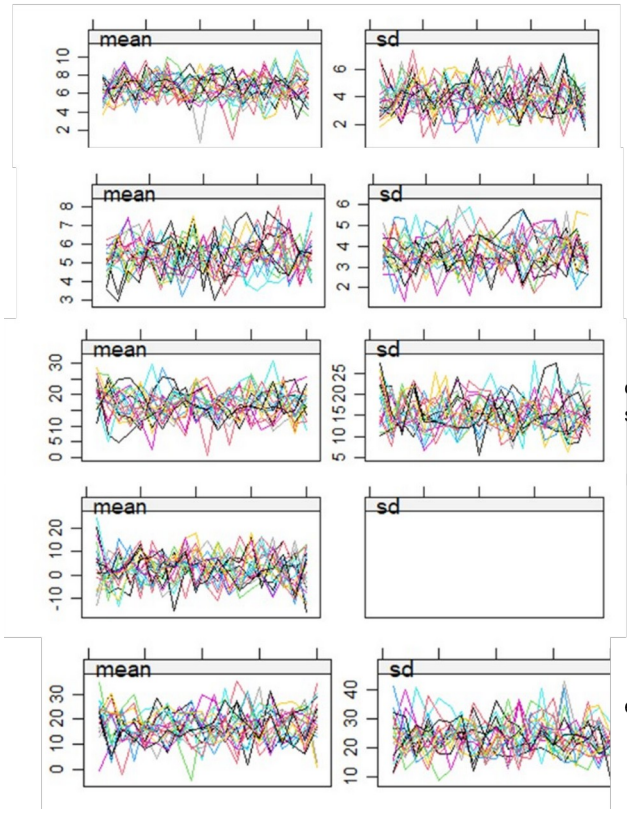

a. Convergence of imputed values of HADS-A score

b. Convergence of imputed values of HADS-D score

c. Convergence of imputed values of total MFIS score

d. Convergence of imputed values of MFIS-cognitive subscore

e. Convergence of imputed values of BPI score

Figure a8.xi. Strip plots of imputed values using Bayesian imputation for AQP4+ NMOSD and MOGAD only (feasibility trial data)

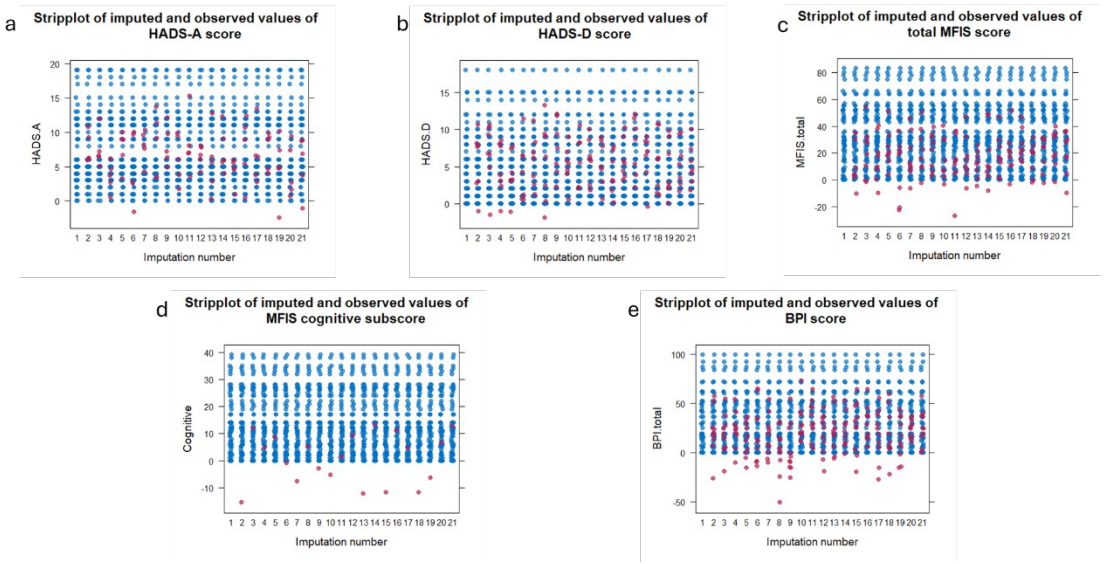

Blue dots indicate observed values, red dots indicate imputed values

Appendix 9

Rao Brief Repeatable Battery of Neurocognitive Tests and Stroop Colour Word Test

The version of the Selective Reminding Test (SRT) used in the Rao BRB-N includes 6 repetitions (156,183,407). Items were read by the examiner at a rate of 1 every 2 seconds. Scoring was as described by Buschke (408). Long-term storage (LTS) was indicated if an item was recalled on two successive trials. Consistent long-term retrieval (CLTR) was indicated if an item was recalled on successive trials, including the final trial. Delayed recall (DR) was assessed after a delay of approximately 10 minutes, when participants had completed the Spatial Recall Test-immediate recall (SPART-IR), Symbol Digit Modalities Test (SDMT) and Paced Auditory Serial Additions Test (PASAT).

The SPART-10/36 stimulus consists of a printed 6 x 6 grid with black circles in 10 of the spaces (below). Participants were shown the stimulus for 10s and asked to replicate the pattern on a blank grid. Once the participant had finished, the stimulus was represented for a further 10s and the participant replicated the pattern again. The stimulus was presented 3 times and the SPART-IR score was the sum of the correct boxes over 3 trials. Delayed recall was assessed directly after the SRT-DR by presenting another blank grid without an interval stimulus.

The SDMT comprises different symbols corresponding with numbers 1-9 in a key the participant can see throughout the test. Beneath the key are 120 symbols presented in a random order across 8 rows with blank boxes below each symbol (below). Participants were asked to write the numbers corresponding to the initial 10 symbols in the associated blank boxes to confirm understanding. Participants then had 90s to write as many numbers corresponding to the symbols above as they could. Correctly matched numbers were scored without penalty for incorrect responses.

The PASAT-3s auditory stimulus was presented using an approved recording (409). Single digit numbers were read at a rate of one every

3s and the participant had to add each consecutive number to the number preceding it, *not* to give a cumulative total. A trial of 10 items was presented before the test items. Only the 3s version was presented, as in several other studies (100,107,115,132,187,208), because patients find the 2s version too stressful.

The WLGT required participants to produce as many words as they could beginning with the letter F in 60s. This was repeated for the letters O and J. Repetitions and intrusions were excluded. Proper nouns, numbers and conjugations or derivations were not permitted.

For the Stroop Colour-Word test, participants were presented with a list of 100 colour words (“green”, “red” and “blue”) printed in black ink in 5 vertical columns (below). Patients were asked to read aloud as many words as they were able over 45s (words task). Participants were then asked to state the colour (red, green or blue) of 5 columns of coloured X symbols over 45s (colour task). Finally, participants were presented with a list of the same words printed in an incongruous colour. Participants were given 45s to state the ink colour of as many words as possible (colour-word incongruous task).

The Stroop interference score (IS) was calculated using the most popular method described by Scarpina and Tagini (182):

$$IS = CW - Predicted\,CW$$

$$Predicted\,CW = \frac{(W\,x\,C)}{(W + C)},$$

where CW is the number of colours correctly named on the incongruous colour-word task in 45s, W is the number of words correctly named on the congruent word task and C is the number of colours correctly named on the congruent colour task.

Rao BRB-N Examiner Marksheet

Trial Words	1	2	3	4	5	6
Direction						
memory						
Owner						
Mountain						
Victim						
City						
Victory						
Dream						
Hotel						
Wife						
Virtue						
slave						

Selective Reminding Test

	1	2	3	4	5	6	Tot
LTS							
CLTR							
Intrusions							
Repetitions							

10/36 Spatial Recall Test

1st trial	2nd trial	3rd trial	Master copy
			x
			x
			x
			x
			x
			x

correct ☐ correct ☐ correct ☐ Total correct ☐

wrong ☐ wrong ☐ wrong ☐ Total wrong ☐

SYMBOL DIGIT MODALITIES TEST

										2	1	6	1	2

4	6	1	2	5	6	3	4	1	2	6	9	4	3	8

4	5	7	8	1	3	7	4	8	5	2	9	3	4	7

2	4	5	1	6	4	1	5	6	7	9	8	3	6	4

9	5	8	3	6	7	4	5	2	3	7	9	2	8	1

6	9	7	2	3	6	4	9	1	7	2	5	6	8	4

2	8	7	9	3	7	8	5	1	9	2	1	4	3	6

5	2	1	6	4	2	1	6	9	7	3	5	4	8	9

Paced Auditory Serial Addition Test (PASAT)

Addestramento	9+1	3	5	2	6	4	9	7	1	4
	10___	4___	8___	7___	8___	10___	13___	16___	8___	5___

(3")

1+4	8	1	5	1	3	7	2	6	9
5___	12___	9___	6___	6___	4___	10___	9___	8___	15___
4	7	3	5	3	6	8	2	5	1
13___	11___	10___	8___	8___	9___	14___	10___	7___	6___
5	4	6	3	8	1	7	4	9	3
6___	9___	10___	9___	11___	9___	8___	11___	13___	12___
7	2	6	9	5	2	4	8	3	1
10___	9___	8___	15___	14___	7___	6___	12___	11___	4___
8	5	7	1	8	2	4	9	7	9
9___	13___	12___	8___	9___	10___	6___	13___	16___	16___
3	1	5	7	4	8	1	3	8	2
12___	4___	6___	12___	11___	12___	9___	4___	11___	10___

Addestramento	3+8	2	7	9	1	8	5	2	6	4
	11___	10___	9___	16___	10___	9___	13___	7___	8___	10___

(2")

4+3	7	2	5	1	8	6	9	1	7
7___	10___	9___	7___	6___	9___	14___	15___	10___	8___
9	4	6	3	5	8	1	6	2	7
16___	13___	10___	9___	8___	13___	9___	7___	8___	9___
5	9	4	5	2	6	4	8	3	5
12___	14___	13___	9___	7___	8___	10___	12___	11___	8___
9	7	4	2	8	5	2	1	6	4
14___	16___	11___	6___	10___	13___	7___	3___	7___	10___
7	3	5	9	6	4	5	3	9	4
11___	10___	8___	14___	15___	10___	9___	8___	12___	13___
1	8	3	1	6	8	5	4	2	6
5___	9___	11___	4___	7___	14___	13___	9___	6___	8___

Total correct 3”	**Total correct 2”**

Selective Reminding Test - Delayed Recall

Now try to remeber the words I asked you at the beginning of the test	**TOT**	

Direction		**Mountain**		**Victory**		**Wife**	
Memory		**Victim**		**Dream**		**Virtue**	
Owner		**City**		**Hotel**		**Slave**	

Correct	
wrong	

Word List Generation

F words

O words					
J words					
Tot correct		**Tot perseverations**		**Tot Intrusions**	

STROOP TEST (correct answers)

Blue	**Red**	**Blue**	**Green**	**red**
Red	**Blue**	**Green**	**Red**	**blue**
Green	**Green**	**Red**	**Blue**	**Green**
Blue	**Red**	**Blue**	**Green**	**Red**
Green	**Green**	**Red**	**Red**	**Blue**
Red	**Blue**	**Green**	**Blue**	**Green**
Green	**Green**	**Red**	**Green**	**Red**
Red	**Red**	**Blue**	**Red**	**Blue**
Blue	**Blue**	**Green**	**Blue**	**Green**
Red	**Red**	**Red**	**Green**	**Blue**
Blue	**Blue**	**Green**	**Blue**	**Green**
Green	**Green**	**Blue**	**Red**	**Red**
Red	**Blue**	**Red**	**Blue**	**Blue**
Green	**Green**	**Green**	**Red**	**Green**
Blue	**Red**	**Blue**	**Green**	**Red**
Green	**Green**	**Green**	**Blue**	**Blue**
Blue	**Red**	**Red**	**Green**	**Red**
Red	**Blue**	**Blue**	**Red**	**Green**
Green	**Red**	**Green**	**Blue**	**blue**
blue	**Green**	**Blue**	**Red**	**red**

Total number correct:
Candidate SPART 10/36 stimulus

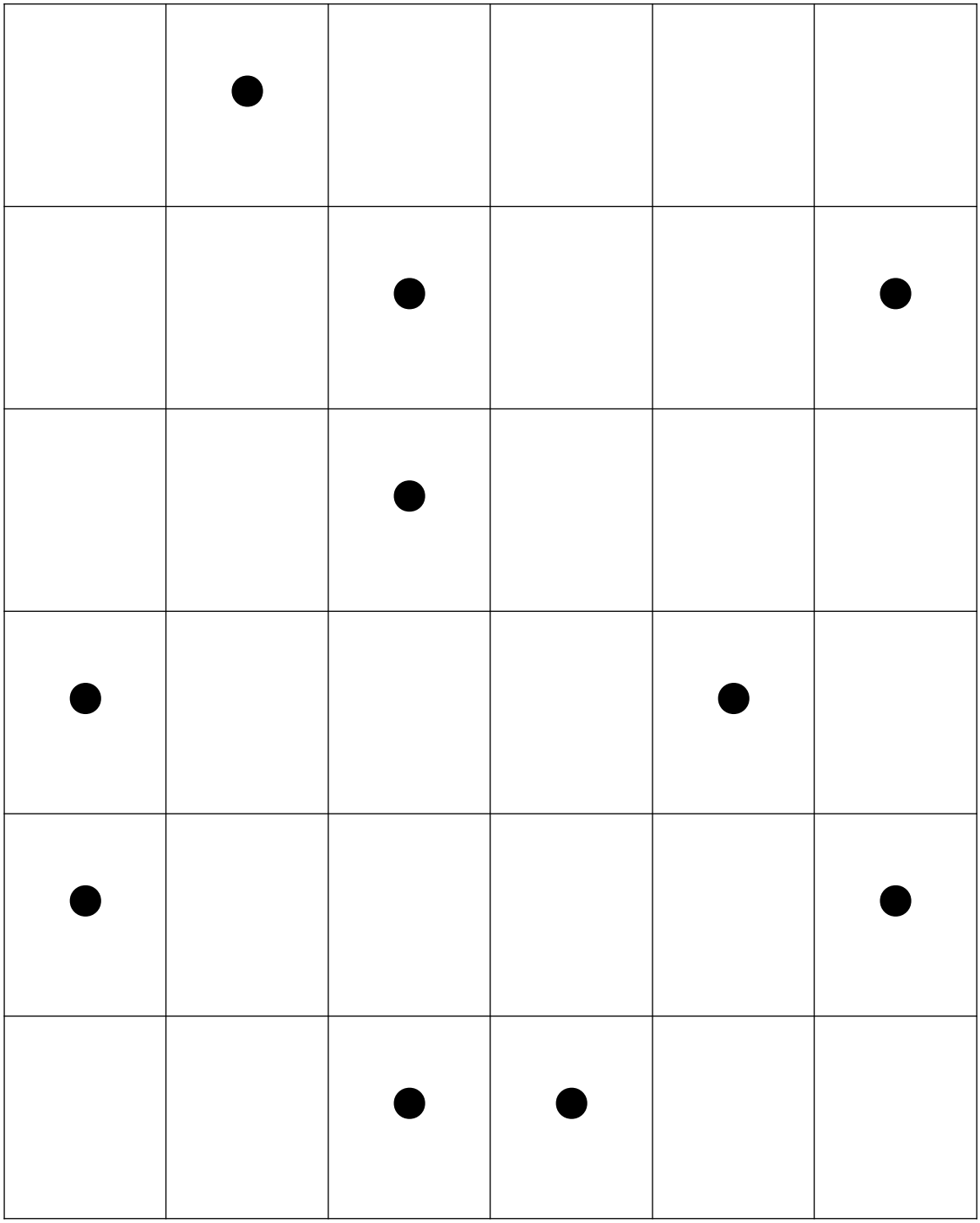

Example candidate SPART 10/36 worksheet

Candidate SDMT worksheet

KEY

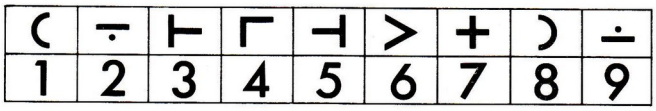

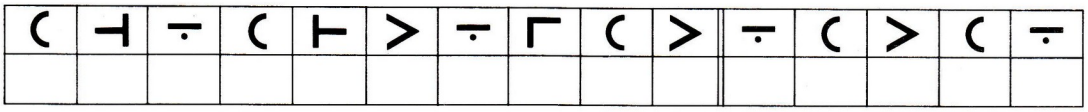

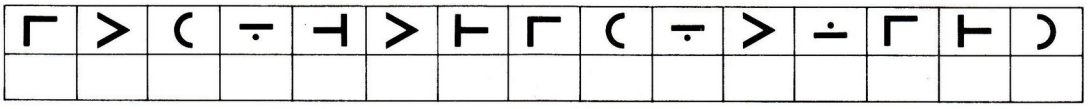

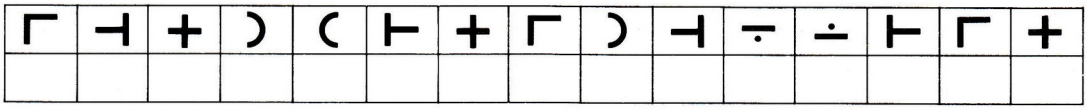

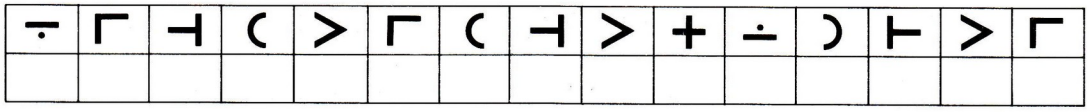

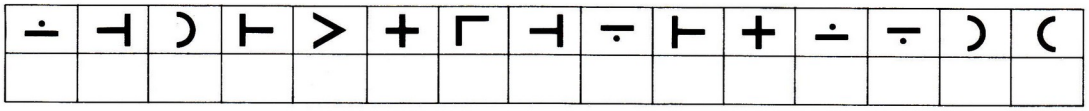

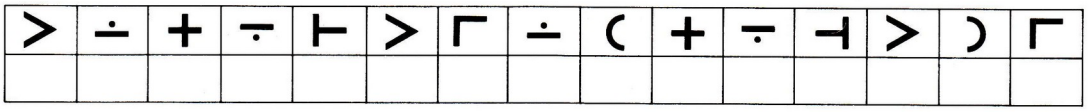

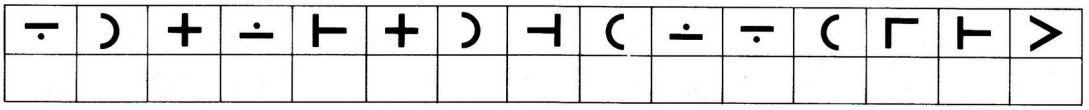

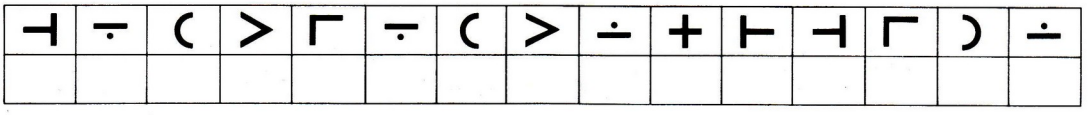

Candidate Stroop colour-word stimulus

RED	BLUE	GREEN	RED	BLUE
GREEN	GREEN	RED	BLUE	GREEN
BLUE	RED	BLUE	GREEN	RED
GREEN	BLUE	RED	RED	BLUE
RED	RED	GREEN	BLUE	GREEN
BLUE	GREEN	BLUE	GREEN	RED
RED	BLUE	GREEN	BLUE	GREEN
BLUE	GREEN	RED	GREEN	RED
GREEN	RED	BLUE	RED	BLUE
BLUE	GREEN	GREEN	BLUE	GREEN
GREEN	RED	BLUE	RED	RED
RED	BLUE	RED	GREEN	BLUE
GREEN	RED	BLUE	RED	GREEN
BLUE	BLUE	RED	GREEN	RED
RED	GREEN	GREEN	BLUE	BLUE
BLUE	BLUE	RED	GREEN	RED
RED	GREEN	BLUE	RED	GREEN
GREEN	RED	GREEN	BLUE	BLUE
RED	BLUE	RED	GREEN	RED
GREEN	RED	GREEN	BLUE	GREEN

XXXX	XXXX	XXXX	XXXX	XXXX
XXXX	XXXX	XXXX	XXXX	XXXX
XXXX	XXXX	XXXX	XXXX	XXXX
XXXX	XXXX	XXXX	XXXX	XXXX
XXXX	XXXX	XXXX	XXXX	XXXX
XXXX	XXXX	XXXX	XXXX	XXXX
XXXX	XXXX	XXXX	XXXX	XXXX
XXXX	XXXX	XXXX	XXXX	XXXX
XXXX	XXXX	XXXX	XXXX	XXXX
XXXX	XXXX	XXXX	XXXX	XXXX
XXXX	XXXX	XXXX	XXXX	XXXX
XXXX	XXXX	XXXX	XXXX	XXXX
XXXX	XXXX	XXXX	XXXX	XXXX
XXXX	XXXX	XXXX	XXXX	XXXX
XXXX	XXXX	XXXX	XXXX	XXXX
XXXX	XXXX	XXXX	XXXX	XXXX
XXXX	XXXX	XXXX	XXXX	XXXX
XXXX	XXXX	XXXX	XXXX	XXXX
XXXX	XXXX	XXXX	XXXX	XXXX
XXXX	XXXX	XXXX	XXXX	XXXX

RED	BLUE	GREEN	RED	BLUE
GREEN	GREEN	RED	BLUE	GREEN
BLUE	RED	BLUE	GREEN	RED
GREEN	BLUE	RED	RED	BLUE
RED	RED	GREEN	BLUE	GREEN
BLUE	GREEN	BLUE	GREEN	RED
RED	BLUE	GREEN	BLUE	GREEN
BLUE	GREEN	RED	GREEN	RED
GREEN	RED	BLUE	RED	BLUE
BLUE	GREEN	GREEN	BLUE	GREEN
GREEN	RED	BLUE	RED	RED
RED	BLUE	RED	GREEN	BLUE
GREEN	RED	BLUE	RED	GREEN
BLUE	BLUE	RED	GREEN	RED
RED	GREEN	GREEN	BLUE	BLUE
BLUE	BLUE	RED	GREEN	RED
RED	GREEN	BLUE	RED	GREEN
GREEN	RED	GREEN	BLUE	BLUE
RED	BLUE	RED	GREEN	RED
GREEN	RED	GREEN	BLUE	GREEN

Appendix 10

Data transform and univariable regression of Rao BRB-N and Stroop test scores for all diagnostic groups

Relationships between predictors and individual test scores were linear with no heteroscedasticity of the residuals. Residuals of SRT-LTS, SRT-DR, SPART-DR and PASAT scores violated assumption of normal distributions (for examples, see fig a10.i – a10.ix).

The transform that coerced them closest to an approximation of a normal distribution was the square root reflect transform (for example, see fig a10.x).

Figure a10.i. Linear regression of SRT-LTS score against age at onset

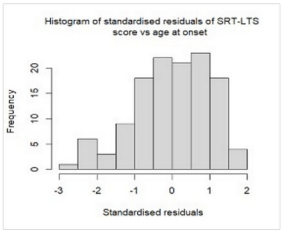

a. Histogram of standardised residuals for SRT-LTS scores vs age at onset

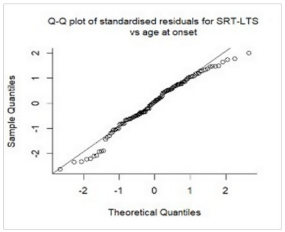

b. QQ plot of standardised residuals for SRT-LTS scores vs age at onset

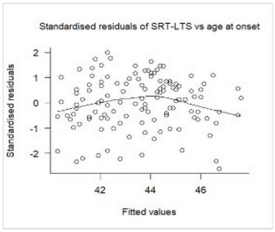

c. Scatter plot of standardised residuals against predictedSRT-LTS scores

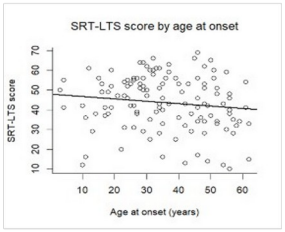

d. Scatterplot of SRT-LTS score vs age at onset

Figure a10.ii. Linear regression of SRT-CLTR score against age at onset

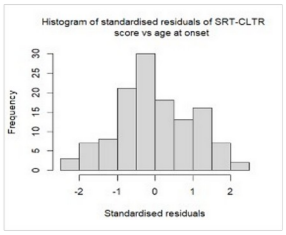

a. Histogram of standardised residuals for SRT-CLTR scores vs age at onset

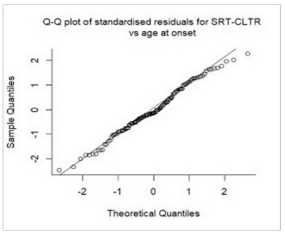

b. QQ plot of standardised residuals for SRT-CLTR scores vs age at onset

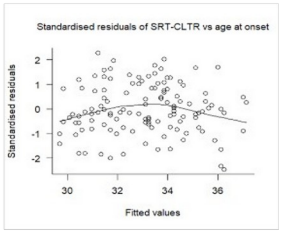

c. Scatter plot of standardised residuals against predictedSRT-CLTR scores

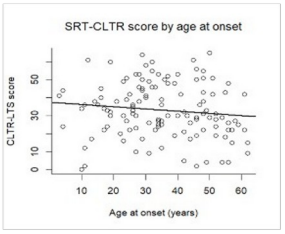

d. Scatterplot of SRT-CLTR score vs age at onset

Figure a10.iii. Linear regression of SRT-DR score against age at onset

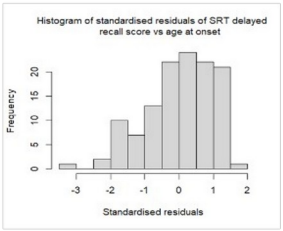

a. Histogram of standardised residuals for SRT-DR scores vs age at onset

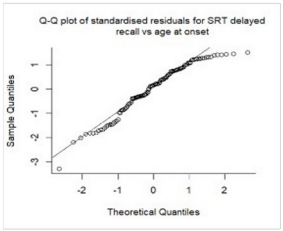

b. QQ plot of standardised residuals for SRT-DR scores vs age at onset

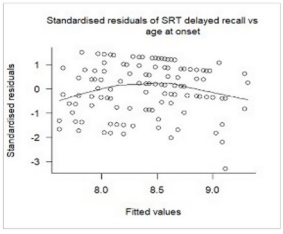

c. Scatter plot of standardised residuals against predictedSRT-DR scores

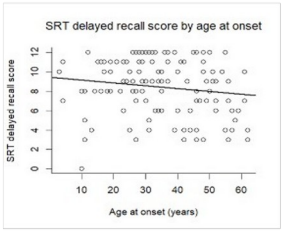

d. Scatterplot of SRT-DR score vs age at onset

Figure a10.iv. Linear regression of SPART-IR score against age at onset

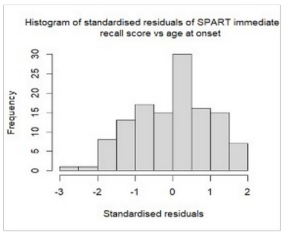

a. Histogram of standardised residuals for SPART-IR scores vs age at onset

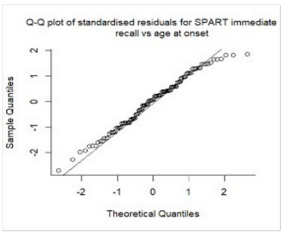

b. QQ plot of standardised residuals for SPART-IR scores vs age at onset

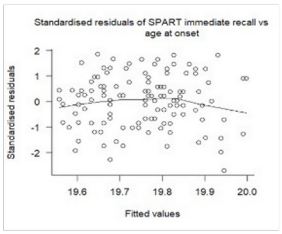

c. Scatter plot of standardised residuals against predicted SPART-IR scores

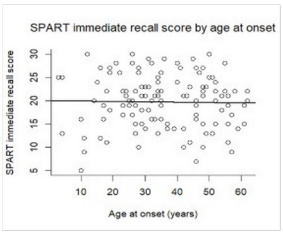

d. Scatterplot of SPART-IR score vs age at onset

Figure a10.v. Linear regression of SPART-DR score against age at onset

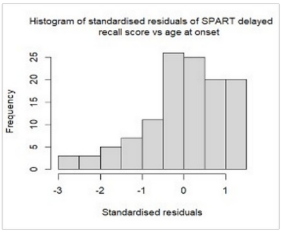

a. Histogram of standardised residuals for SPART-DR scores vs age at onset

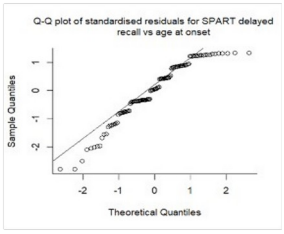

b. QQ plot of standardised residuals for SPART-DR scores vs age at onset

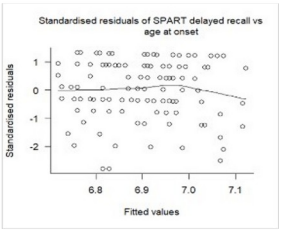

c. Scatter plot of standardised residuals against predicted SPART-DR scores

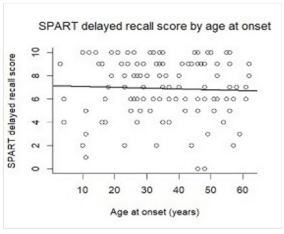

d. Scatterplot of SPART-DR score vs age at onset

Figure a10.vi. Linear regression of SDMT score against age at onset

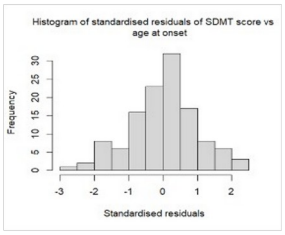

a. Histogram of standardised residuals for SDMT scores vs age at onset

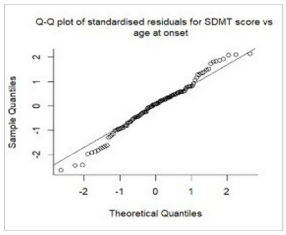

b. QQ plot of standardised residuals for SDMT scores vs age at onset

c. Scatter plot of standardised residuals against predictedSDMT scores

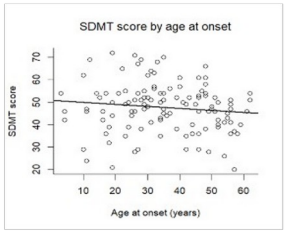

d. Scatterplot of SDMT score vs age at onset

Figure a10.vii. Linear regression of PASAT score against age at onset

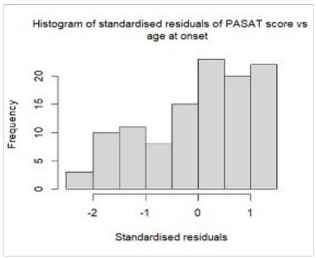

a. Histogram of standardised residuals for PASAT scores vs age at onset

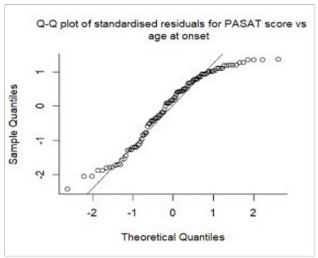

b. QQ plot of standardised residuals for PASAT scores vs age at onset

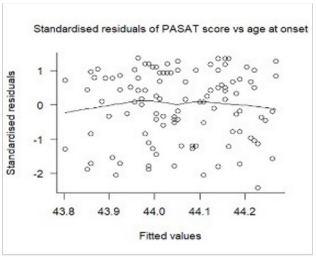

c. Scatter plot of standardised residuals against predictedPASAT scores

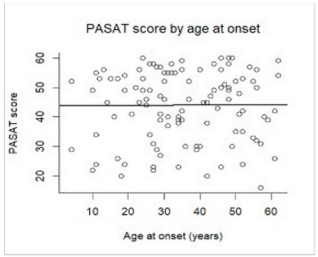

d. Scatterplot of PASAT score vs age at onset

Figure a10.viii. Linear regression of WLGT score against age at onset

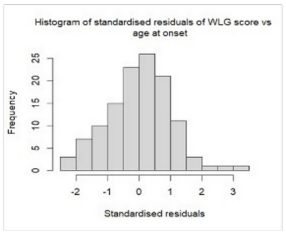

a. Histogram of standardised residuals for WLGT scores vs age at onset

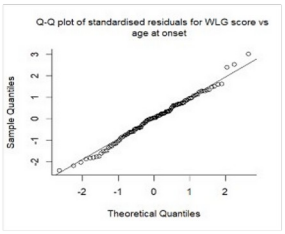

b. QQ plot of standardised residuals for WLGT scores vs age at onset

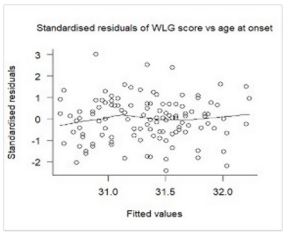

c. Scatter plot of standardised residuals against predictedWLGT scores

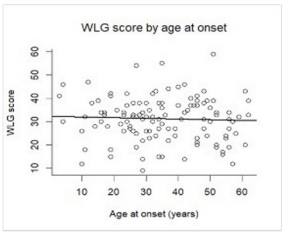

d. Scatterplot of WLGT score vs age at onset

Figure a10.ix. Linear regression of Stroop interference score against age at onset

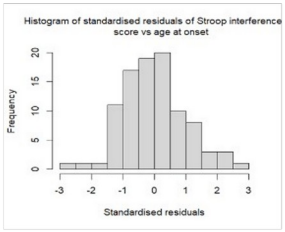

a. Histogram of standardised residuals for Stroop interference scores vs age at onset

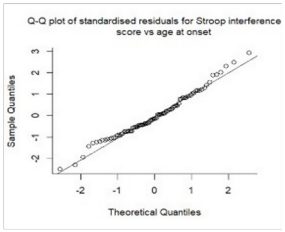

b. QQ plot of standardised residuals for Stroop interference scores vs age at onset

c. Scatter plot of standardised residuals against predicted Stroop interference score

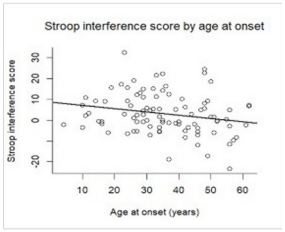

d. Scatterplot of Stroop interference score vs age at onset

Figure a10.x. Standardised residuals of SPART-DR scores regressed against age at onset before and after transformation

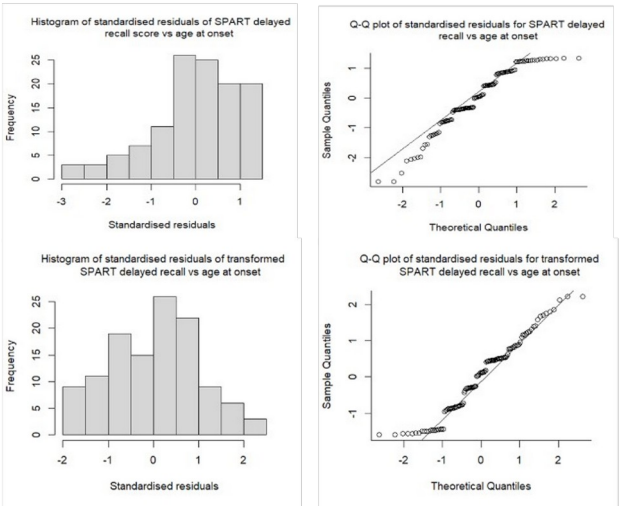

Before square root reflect transform

After square root reflect transform

Regression of WLGT score against age at onset revealed 2 outliers and regression against disease duration, BPI and HADS-A revealed 1 outlier. Regression of Stroop interference score against diagnosis, disease duration, sex at birth, education, HADS-D score, total MFIS score and BPI score revealed 1 outlier in each regression. Inclusion of outliers data did not affect any univariable regression. One patient's PASAT score was excluded from analysis as they were unable to progress beyond the first addition, despite completing the training phase successfully.

Appendix 11

MICE feasibility study and method selection for Rao BRB-N and Stroop test analyses (whole cohort)

When all 3 diagnostic groups were included, 205 data points were missing for 63 patients (fig a11.i). The independent variables most frequently missing values were HADS-A, HADS-D, total MFIS score, MFIS cognitive score and BPI score.

Figure a11.i. Patterns of missingness

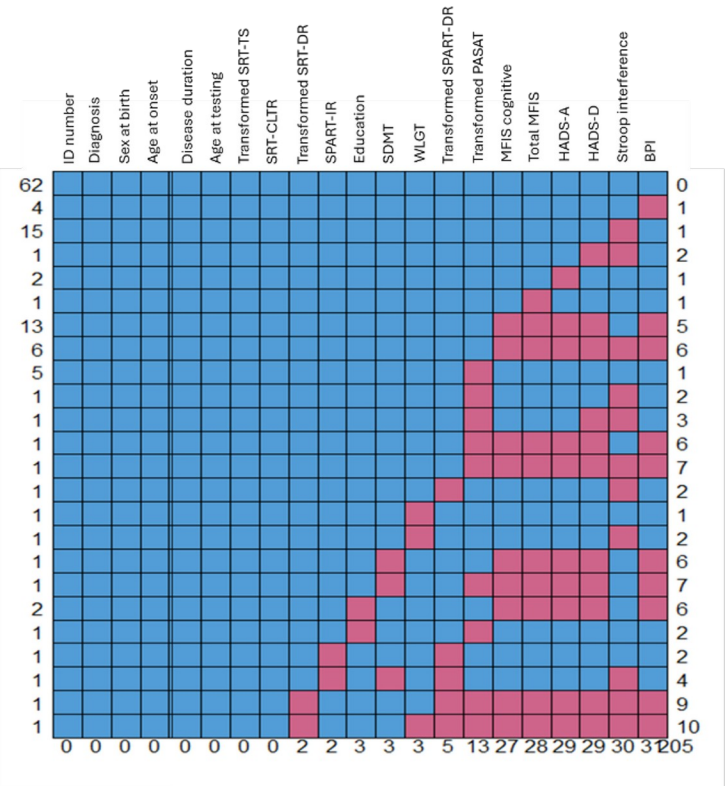

Predictor variables for imputation were diagnosis, age at onset, onset age group, age at testing, disease duration, sex, first language, education and scores for HADS-A, HADS-D, total MFIS, cognitive MFIS, BPI and Rao BRN-N and Stroop interference scores. Variables imputed were HADS-A, HADS-D, total MFIS, MFIS cognitive and BPI scores.

As described in appendix 7, a trial data set was created by identifying individuals with complete data and randomly deleting 15% of the values of variables to be imputed. Different methods were used to impute the missing data with 5 imputations and a maximum of 20 iterations for each.

The trial data set confirmed PMM was the best method for imputation as percentage bias was lower than with stochastic and Bayesian methods, convergence was adequate and no imputed values were selected from impossible ranges (fig a11.ii & a11.iii).

Figure a11.ii. Convergence plots for trial data using PMM

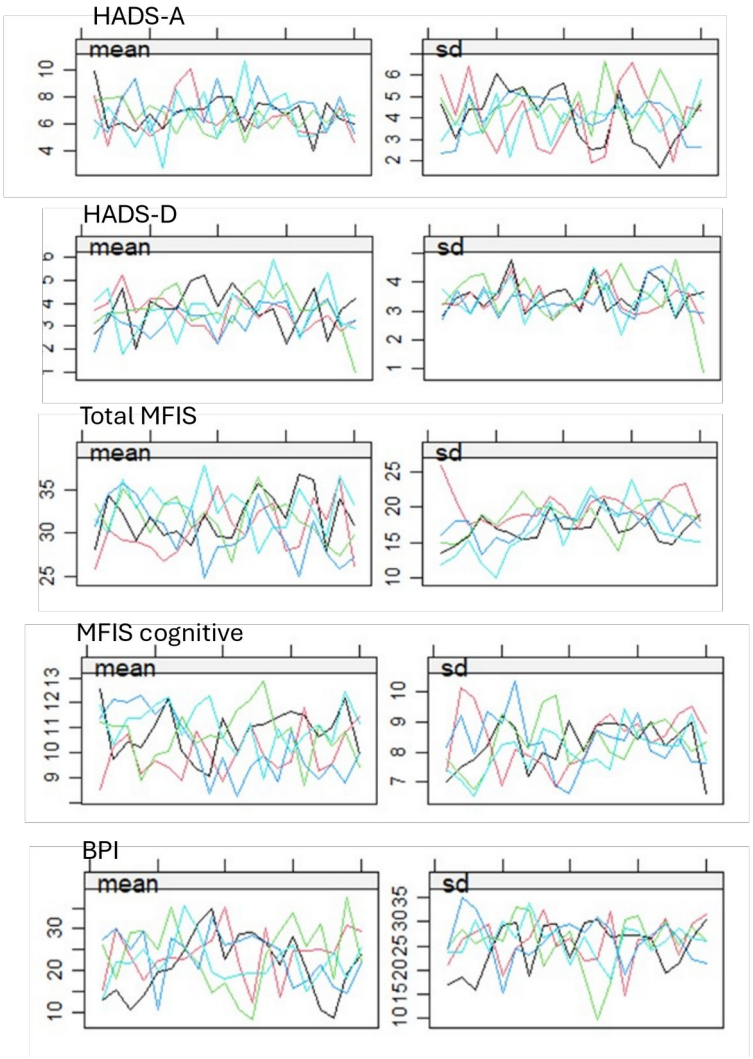

Figure a11.iii. Strip plots for trial data using PMM

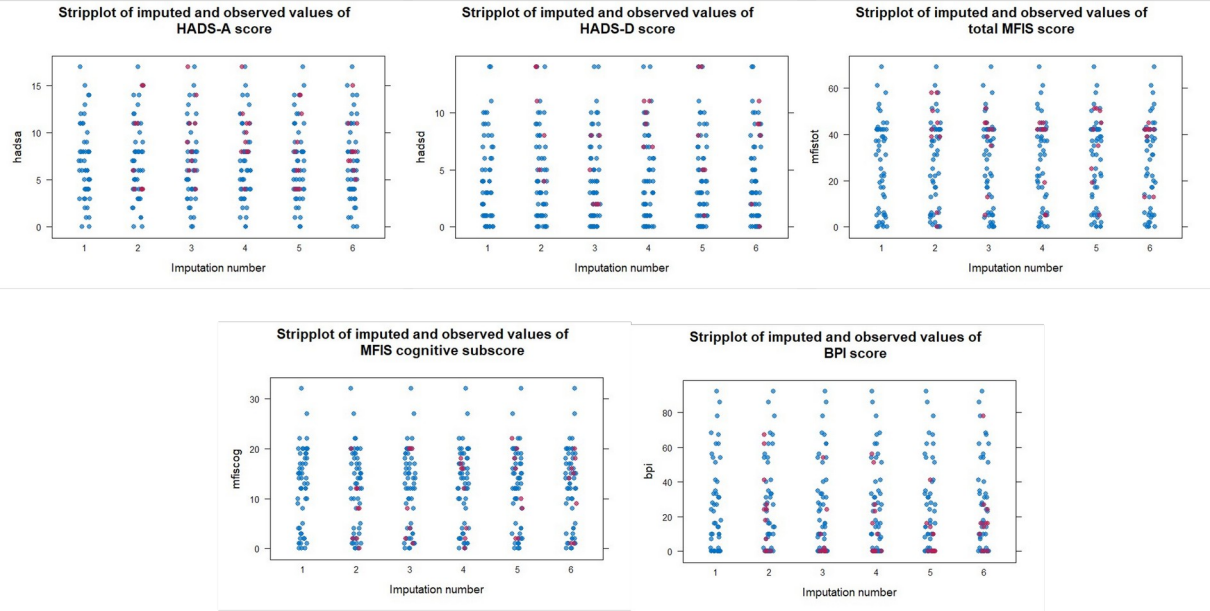

Blue dots indicate observed values, red dots indicate imputed values

Comparison of imputed values with actual values in the complete trial data set confirmed imputation was accurate. Percentage bias was >5% for all imputed variables other than total MFIS score (table a11.i).

Table a11.i: Percentage bias in imputed trial dataset (PMM)

Imputed variable	Percentage bias
HADS-A	7.91
HADS-D	-18.13
Total MFIS	0.43
MFIS cognitive	13.84
BPI	-22.52

Multivariable regression models for SPART-IR, SDMT, PASAT, WLGT and Stroop interference scores contained the variables imputed. Non-optimised models that included diagnosis as an *a priori* predictor were used, rather than optimal models, which may not include diagnosis as a factor.

Coefficients, R^2 and F statistics of models using the complete trial data set were similar to values when missing data were imputed in the incomplete trial data set, indicating imputation with PMM was a valid method, despite moderate percentage bias in HADS-D and BPI scores (tables a11.ii – a11.vi).

Table a11.ii. MICE for multivariable regression of SPART-IR scores

	Trial complete data set (n = 61)	Trial imputed data set (n = 61)	Original data set with missing values (n = 90)	Imputed full data set (n = 123)
R^2	0.027	0.028	0.029	0.058
$\beta_{(AQP4+\ NMOSD)}$ (SE)	-1.835 (2.215)	-1.746 (2.214)	-2.614 (1.695)	-1.970 (1.397)
$p_{(\beta AQP4+\ NMOSD)}$	0.411	0.444	0.127	0.161
$\beta_{(MOGAD)}$ (SE)	0.511 (1.572)	0.487 (1.587)	0.291 (1.289)	0.649 (1.137)
$p_{(MOGAD)}$	0.746	0.725	0.822	0.569
F (DOF)	0.316 (5, 56)	0.289 (5, 53.80)	1.536 (5, 84)	1.289 (5, 108.59)
p (F)	0.902	0.917	0.187	0.084
RIV	N/A	0.027	N/A	0.084

Table a11.iii. MICE for multivariable regression of SDMT scores

	Trial complete data set (n = 61)	Trial imputed data set (n = 61)	Original data set with missing values (n = 89)	Imputed full data set (n = 119)
R^2	0.374	0.391	0.284	0.326
$\beta_{(AQP4+\ NMOSD)}$ (SE)	-4.351 (3.139)	-4.353 (3.173)	-6.564 (2.721)	-4.412 (2.443)
$p_{(\beta AQP4+\ NMOSD)}$	0.171	0.159	0.018*	0.074
$\beta_{(MOGAD)}$ (SE)	2.616 (2.179)	2.641 (2.190)	2.600 (2.039)	5.075 (1.938)
$p_{(MOGAD)}$	0.235	0.411	0.206	0.010*
F (DOF)	3.954 (8, 53)	2.657 (8, 48.84)	5.363 (8, 80)	5.497 (8, 96.29)
p (F)	<0.001	0.002	<0.001	<0.001
RIV	N/A	0.138	N/A	0.187

Table a11.iv. MICE for multivariable regression of transformed PASAT scores

	Trial complete data set (n = 61)	Trial imputed data set (n = 61)	Original data set with missing values (n = 84)	Imputed full data set (n = 112)
R^2	0.213	0.210	0.159	0.243
$\beta_{(AQP4+\ NMOSD)}$ (SE)	1.169 (0.552)	1.159 (0.558)	0.972 (0.451)	1.007 (0.378)
$p_{(\beta AQP4+\ NMOSD)}$	0.039*	0.046*	0.034*	0.009*
$\beta_{(MOGAD)}$ (SE)	0.057 (0.394)	0.052 (0.404)	-0.056 (0.345)	-0.302 (0.295)
$p_{(MOGAD)}$	0.886	0.786	0.872	0.308
F (DOF)	2.482 (6, 55)	2.057 (6, 49.72)	3.623 (6, 77)	4.764 (6, 92.28)
p (F)	0.034	0.075	0.003	<0.001
RIV	N/A	0.143	N/A	0.150

Table a11.v MICE for multivariable regression of WLGT scores

	Trial complete data set (n = 61)	Trial imputed data set (n = 61)	Original data set with missing values (n = 88)	Imputed full data set (n = 119)
R^2	0.248	0.252	0.080	0.148
$\beta_{(AQP4+\ NMOSD)}$ (SE)	-5.241 (3.925)	-5.153 (3.975)	-0.808 (3.086)	-1.050 (2.315)
$p_{(\beta AQP4+\ NMOSD)}$	0.188	0.169	0.794	0.651
$\beta_{(MOGAD)}$ (SE)	1.513 (2.768)	1.293 (2.832)	1.842 (2.421)	0.330 (1.888)
$p_{(MOGAD)}$	0.587	0.791	0.449	0.862
F (DOF)	2.185 (8, 53)	1.693 (8, 46.60)	1.879 (8, 73)	2.279 (8, 107.50)
p (F)	0.043	0.125	0.076	0.027
RIV	N/A	0.220	N/A	0.030

Table a11.vi. MICE for multivariable regression of Stroop interference scores

	Trial complete data set (n = 61)	Trial imputed data set (n = 61)	Original data set with missing values (n = 76)	Imputed full data set (n = 95)
R^2	0.212	0.207	0.086	0.157
$\beta_{(AQP4+\ NMOSD)}$ (SE)	-1.937 (3.876)	-1.921 (3.884)	-1.906 (3.253)	-3.594 (2.705)
$p_{(\beta AQP4+\ NMOSD)}$	0.619	0.651	0.560	0.188
$\beta_{(MOGAD)}$ (SE)	0.547 (3.074)	0.557 (3.112)	0.983 (2.753)	1.467 (2.280)
$p_{(MOGAD)}$	0.860	0.851	0.722	0.522
F (DOF)	2.459 (6, 55)	2.311 (6, 52.85)	2.171 (6, 69)	2.560 (6, 84.84)
p (F)	0.035	0.047	0.056	0.025
RIV	N/A	0.03	N/A	0.049

Table a11.vii. Comparison of coefficients for diagnosis with and without imputation

a. SPART-IR

		β without imputation	p	β with imputation	p
	AQP4+ NMOSD	-2.614	0.127	-1.970	0.161
	MOGAD	0.291	0.822	0.649	0.569

b SDMT

		β without imputation	p	β with imputation	p
	AQP4+ NMOSD	-6.564 *	0.018	-4.412	0.074
	MOGAD	2.600	0.206	5.705*	0.010

c. PASAT

		β without imputation	p	β_1 with imputation	p
	AQP4+ NMOSD*	0.972*	0.034	1.007*	0.009
	MOGAD	-0.056	0.854	-0.302	0.310

d. WLGT

		β without imputation	p	β_1 with imputation	P
	AQP4+ NMOSD	-0.808	0.794	-1.050	0.651
	MOGAD	1.842	0.457	0.330	0.633

e. Stroop test

		β witout imputation	p	β_1 with imputation	p
	AQP4+ NMOSD	-1.906	0.560	-3.594	0.188
	MOGAD	0.983	0.722	1.467	0.522

When models were applied to the data imputed from the original, incomplete data set, convergence was moderate to poor and all values were realistic (fig a11.iv). Increasing the maximum number of iterations to 50 did not improve convergence.

Figure a11.iv. Convergence plots of data imputed from full dataset

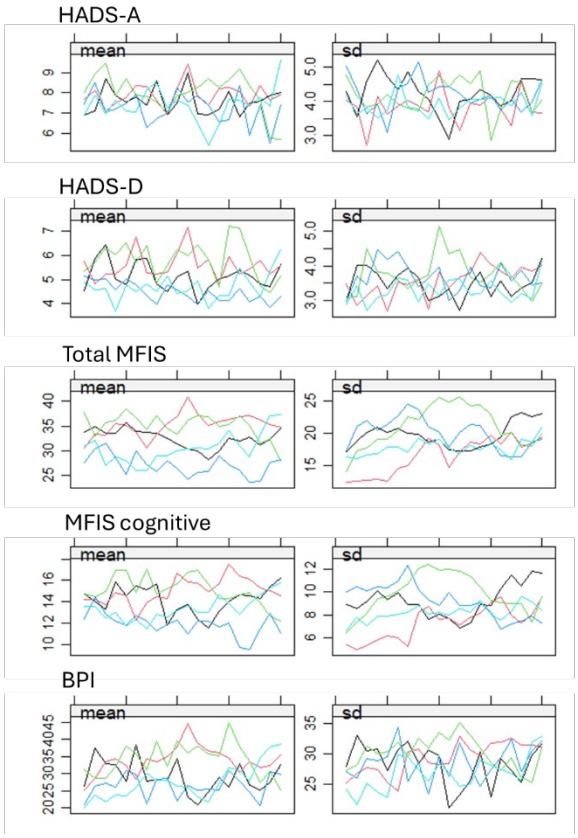

Figure a11.v. Strip plots of data with imputations from full dataset

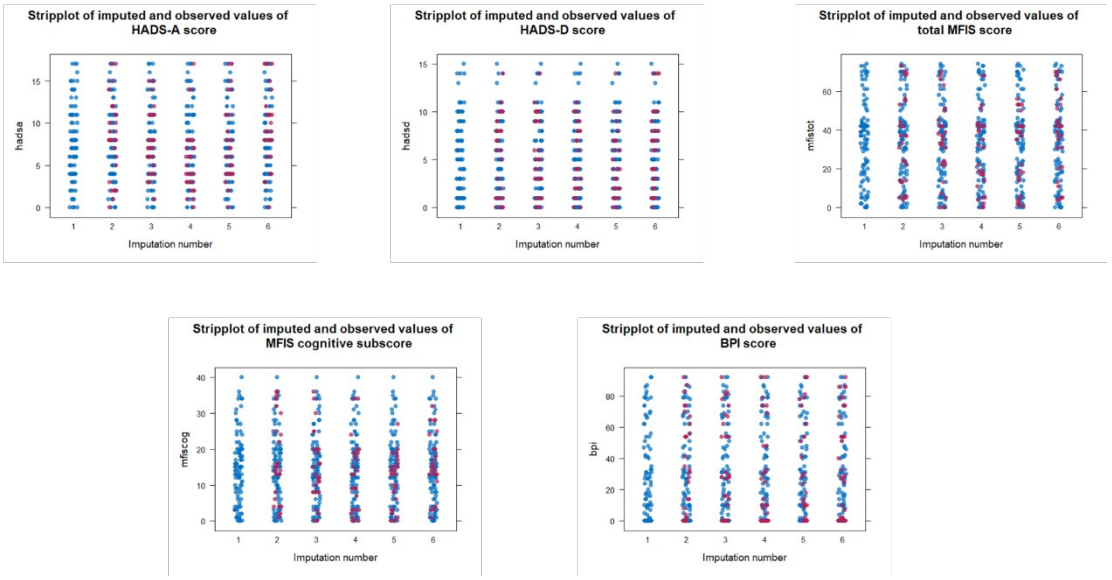

AQP4+ NMOSD and MOGAD groups only

When analysis was restricted to the AQP4+ NMOSD and MOGAD groups, 117 data points were missing from 75 patients. The independent variables most commonly lacking values were as above (fig a11.vi).

Figure a11.vi. Pattern of missingness (NMOSD and MOGAD only)

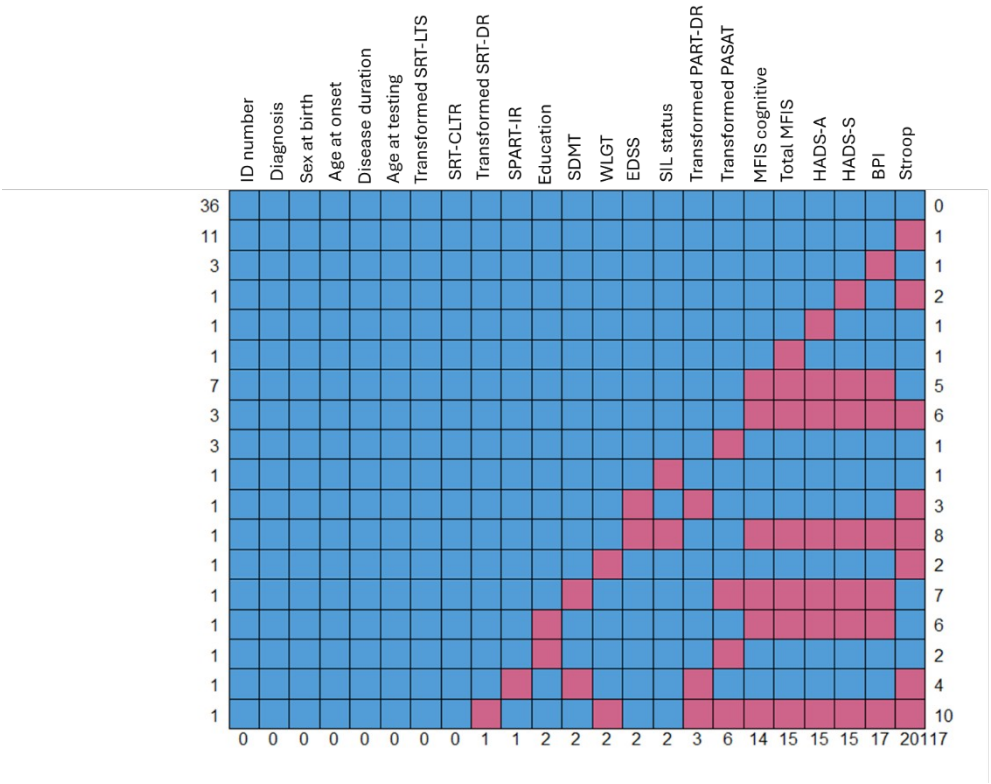

The number of imputations was increased to 20. Imputation of the trial data set (in which 10% of the values of HADS-A, HADS-D, total MFIS, MFS cognitive subscore and BPI were deleted) with PMM showed convergence was adequate and no values were from impossible ranges (fig a11.vii & a11.viii). Percentage bias was generally high (table a11.viii). Coefficients, R^2 and F statistics of the model using the complete test data set were similar to coefficients from the test data set with 10% values deleted, suggesting PMM generated valid imputations, despite percentage bias (table a11.ix – a11.xii).

Figure a11.vii. Convergence plots for trial data using PMM (NMOSD and MOGAD only)

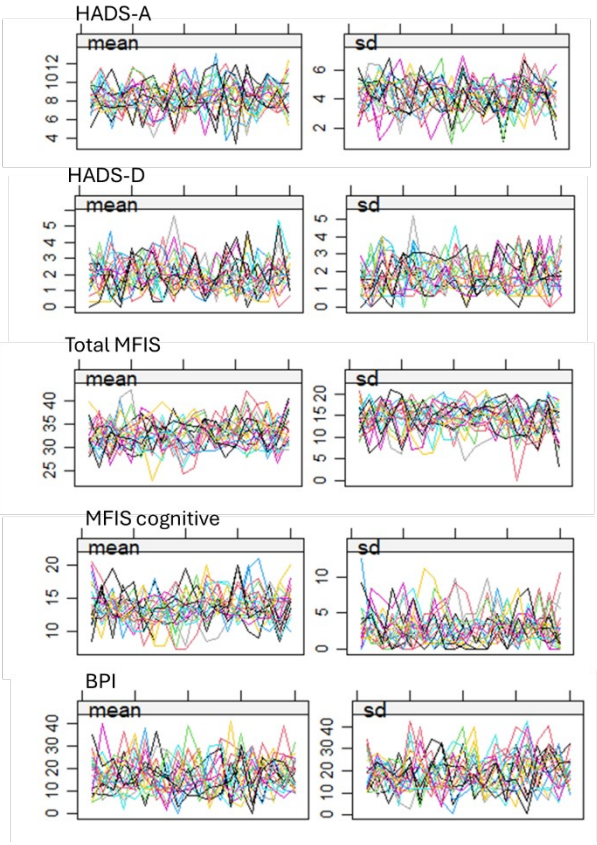

Supplementary figure a11.viii. Strip plots for trial data using PMM (AQP4+ NMOSD and MOGAD only)

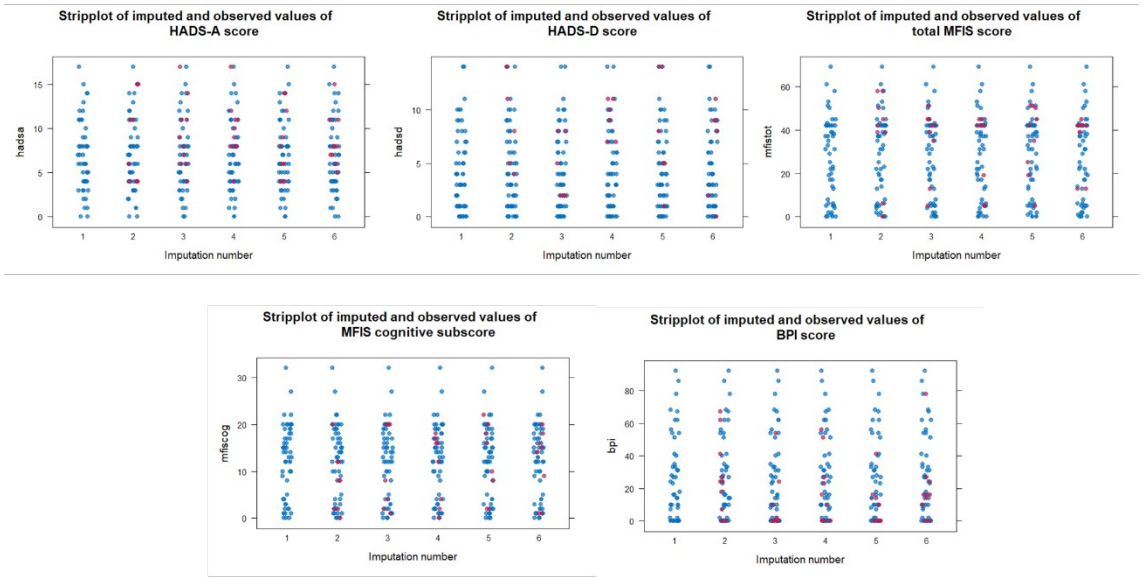

Table a11.viii.Percentage bias in imputed trial data set (NMOSD and MOGAD only)

	PPM	Stochastic	Bayesian
HADS-A	7.27	25.67	25.62
HADS-D	-44.17	-57.71	-58.12
Total MFIS	-4.52	-3.58	-5.86
MFIS cognitive	-34.44	-27.50	-31.99
BPI	-46.23	-41.12	-44.92

Table a11.ix. MICE for multivariable regression of SDMT scores (NMOSD and MOGAD only)

	Trial complete data set (n = 35)	Trial imputed data set (n = 35)	Data set with missing values (n = 52)	Imputed full data set (n = 70)
R^2	0.378	0.396	0.335	0.441
$\beta_{(AQP4+\ NMOSD)}$ (SE)	-6.047 (3.748)	-6.350 (3.750)	-8.901 (3.131)	-9.628 (2.547)
$p_{(\beta AQP4+\ NMOSD)}$	0.118	0.103	0.007	<0.001
F (DOF)	2.053 (8, 27)	2.121 (8, 25.10)	4.273 (8, 44)	5.272 (8, 58.34)
p (F)	0.078	0.072	<0.001	<0.001
RIV	N/A	0.024	N/A	0.115

Table a11.x. MICE for multivariable regression of transformed PASAT scores (NMOSD and MOGAD only)

	Trial complete data set (n = 35)	Trial imputed data set	Data set with missing values (n = 49)	Imputed full data set (n = 65)
R^2	0.365	0.366	0.223	0.383
$\beta_{(AQP4+\ NMOSD)}$ (SE)	1.298 (0.576)	1.316 (0.582)	1.179 (0.448)	1.433 (0.347)
$p_{(\beta AQP4+\ NMOSD)}$	0.033	0.033	0.012	<0.001
F (DOF)	1.941 (8, 27)	1.872 (8, 25.09)	2.760 (8, 41)	4.154 (8, 53.96)
p (F)	0.095	0.110	0.015	<0.001
RIV	N/A	0.026	N/A	0.031

Table a11.xi. MICE for multivariable regression of WLGT scores (NMOSD and MOGAD only)

	Trial complete data set (n = 35)	Trial imputed data set	Data set with missing values (n = 56)	Imputed full data set (n = 69)
R^2	0.163	0.163	0.055	0.114
$\beta_{(AQP4+\ NMOSD)}$ (SE)	-2.540 (3.204)	-2.260 (3.234)	-1.742 (2.323)	-0.678 (1.986)
$p_{(\beta AQP4+\ NMOSD)}$	0.434	0.490	0.457	0.734
F (DOF)	1.166 (5, 30)	1.157 (5, 28.16)	0.140 (5, 51)	1.546 (5, 60.96)
p (F)	0.349	0.354	0.163	0.189
RIV	N/A	0.006	N/A	0.026

Table a11.xii. MICE for multivariable regression of Stroop interference scores (NMOSD and MOGAD only)

	Trial complete data set (n = 35)	Trial imputed data set	Data set with missing values (n = 43)	Imputed full data set (n = 54)
R^2	0.228	0.273	0.055	0.220
$\beta_{(AQP4+\ NMOSD)}$ (SE)	-4.015 (3.986)	-4.159 (3.958)	-3.880 (3.429)	-4.352 (2.890)
$p_{(\beta AQP4+\ NMOSD)}$	0.322	0.302	0.265	0.139
F (DOF)	1.768 (5, 30)	1.866 (5, 28.17)	1.497 (5, 38)	2.603 (5, 46.02)
p (F)	0.150	0.134	0.214	0.037
RIV	N/A	0.003	N/A	0.021

When models were applied to the data set imputed from the original, incomplete data, convergence was adequate/poor and all values were realistic (fig a11.ix & a11.x).

Figure a11.ix. Convergence plots of data imputed from original, incomplete data set (NMOSD and MOGAD only)

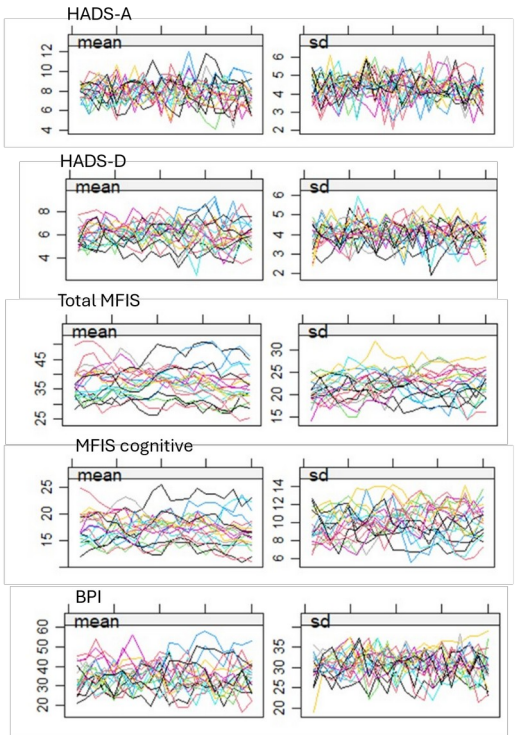

Figure a11.x. Strip plots of data imputed original, incomplete data set (NMOSD and MOGAD only)

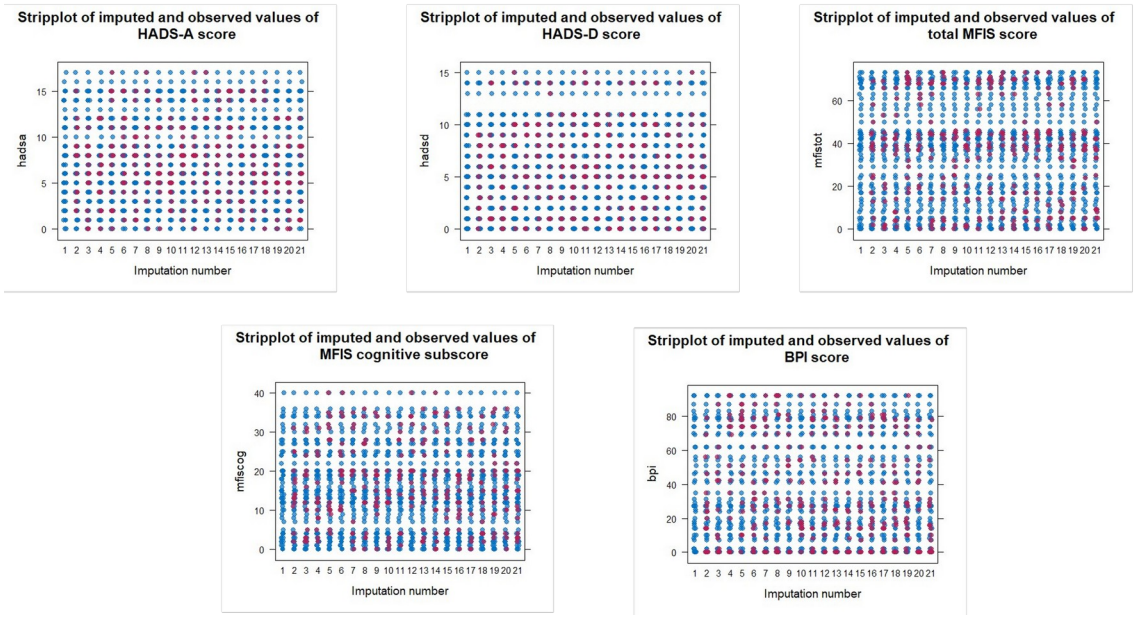

Appendix 12

Fitting restricted cubic splines to the data

Conducting linear regression on populations stratified by age group imposes constraints on the regression model by compelling separate least mean square estimates within each age group and assumes a discontinuity at the chosen threshold (30 years). Although this threshold has been justified (section 2.1.g), the true relationship may not be linear and may not change at that threshold. Therefore, cubic splines were fitted to model continuous, non-linear relationships. If optimum fit indicates test scores increase with increasing onset age up to approximately 30 years and then decline, the interaction between age at onset and onset age group demonstrated by linear regression is substantiated.

Knots were placed at the 5^{th}, 35^{th}, 65^{th} and 95^{th} percentiles. F tests were used to compare model fit with the age at onset variable compared with the Null model and to compare model fit with a single linear term compared with a model that included spline terms.

Appendix 13

1. Effects of interactions between age parameters and SIL status on Rao BRB-N and Stroop test scores: Are interactions between age and SIL status better explained by age at onset or age at testing?

The *a priori* hypothesis was that age at onset would determine cognitive outcomes. Because age at onset and age at testing were closely correlated, it is possible the significant and non-significant interactions between age at testing and SIL status demonstrated in section 5.2.c were due to confounding by the interaction between age at onset and SIL status.

To determine whether the interactions between age at onset and SIL status could possibly explain the putative interactions between age at testing and SIL status, scores were regressed against the following model:

$$Test\ score \quad age\ at\ onset + SIL\ status + age\ at\ onset * SIL\ status$$

Interactions between age at onset and SIL status resembled interactions between age at testing and SIL status for all tests, as may be predicted from the strong correlation between age at onset and age at testing (fig a13.i).

No age at onset x SIL status interaction reached statistical significance (table a13.i – viii).

Figure 13a.i. Comparison of interactions between SIL status and age at onset and between SIL status and age at testing

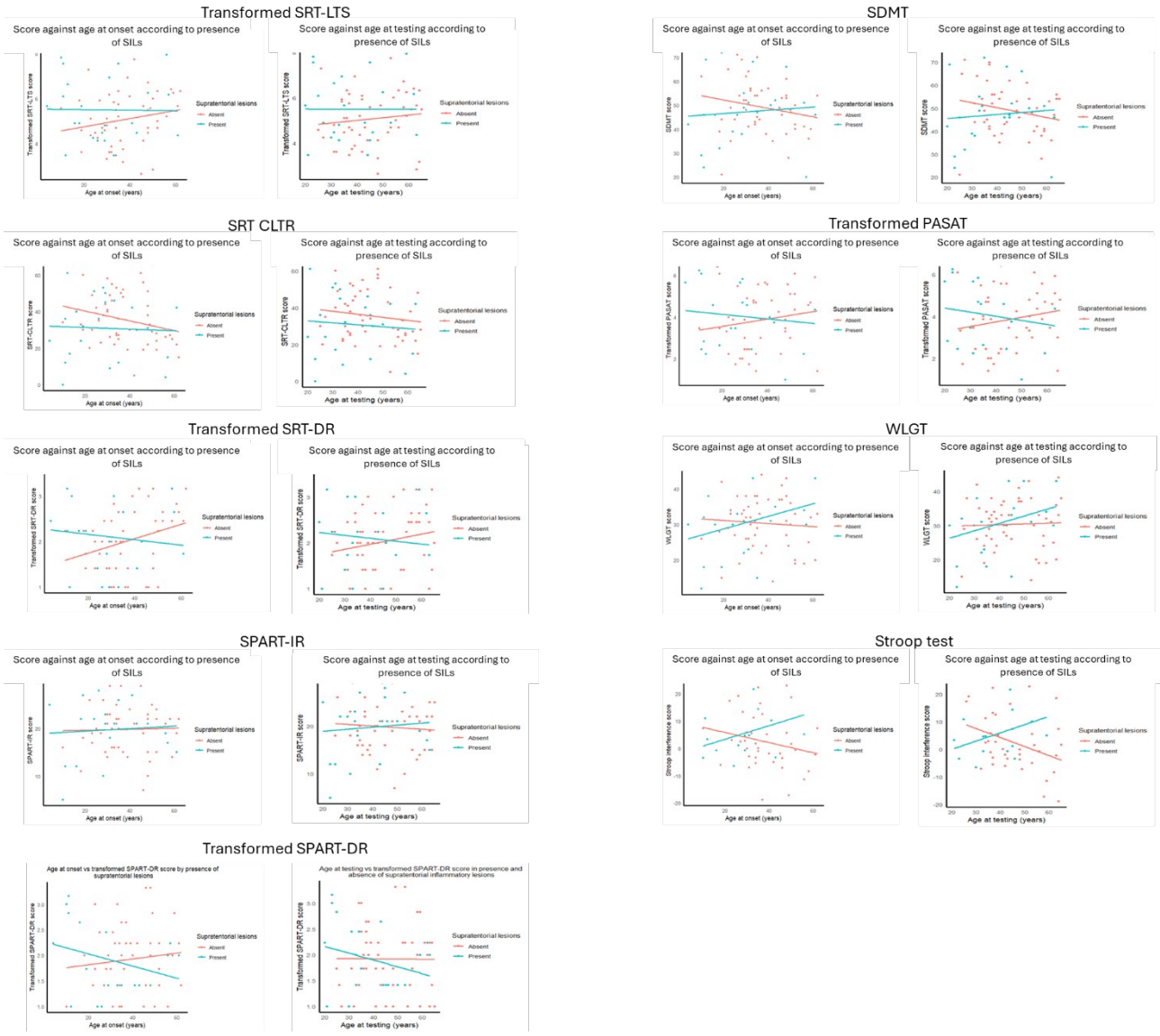

Table a13.i. Multivariable regression of transformed SRT-LTS score against presence of SILs, age at onset and SIL*age at onset interaction

a. Values of regression coefficients

Independent variable	β (SE)	T statistic	p
SILs present	0.470 (0.336)	1.398	0.167
Age at onset	0.018 (0.014)	1.260	0.212
SIL*onset age interaction	-0.019 (0.022)	-0.889	0.377

b. Assessment of model

Adj R^2	RSE (DoF)	F statistic (DoF)	P (F statistic)
0.006	1.25 (69)	1.152 (3, 69)	0.335

**p ≤0.05

Table a13.ii. Multivariable regression of SRT-CLTR score against presence of SILs, onset age and SIL*onset age interaction

a. Values of regression coefficients

Independent variable	β (SE)	T statistic	p
SILs present	-5.590 (3.990)	-1.401	0.166
Age at onset	-0.268 (0.171)	-1.564	0.122
SIL*onset age interaction	0.223 (0.259)	0.863	0.391

b. Assessment of model

Adj R^2	RSE (DoF)	F statistic (DoF)	P (F statistic)
0.014	14.88 (69)	1.336 (3, 69)	0.270

**p ≤0.05

Table a13.iii. Multivariable regression of transformed SRT-DR score against presence of SILs, onset age and SIL*onset age interaction

a. Values of regression coefficients

Independent variable	β (SE)	T statistic	p
SILs present	0.083 (0.185)	0.447	0.656
Age at onset**	0.016 (0.008)	2.020	0.047
SIL*onset age interaction	-0.022 (0.012)	-1.828	0.072

b. Assessment of model

Adj R^2	RSE (DoF)	F statistic (DoF)	P (F statistic)
0.024	0.68 (68)	1.574 (3, 68)	0.204

**p ≤0.05

Table a13.iv. Multivariable regression of SPART-IR score against presence of SILs, onset age and SIL*onset age interaction

a. Values of regression coefficients

Independent variable	β (SE)	T statistic	p
SILs present	0.052 (1.554)	0.033	0.973
Age at onset	0.010 (0.066)	0.158	0.875
SIL*onset age interaction	0.016 (0.101)	0.157	0.875

b. Assessment of model

Adj R^2	RSE (DoF)	F statistic (DoF)	P (F statistic)
-0.042	5.77 (68)	0.050 (3, 68)	0.985

**p ≤0.05

Table a13.v Multivariable regression of transformed SPART-DR score against presence of SILs, onset age and SIL*onset age interaction

a. Values of regression coefficients

Independent variable	β (SE)	T statistic	p
SILs present	0.562 (0.426)	1.318	0.192
Age at onset	0.006 (0.008)	0.741	0.462
SIL*onset age interaction	-0.018 (0.012)	-1.506	0.137

b. Assessment of model

Adj R^2	RSE (DoF)	F statistic (DoF)	P (F statistic)
-0.009	0.65 (66)	0.794 (3, 68)	0.502

**p ≤0.05

Table a13.vi. Multivariable regression of SDMT score against presence of SILs, onset age and SIL*onset age interaction

a. Values of regression coefficients

Independent variable	β (SE)	T statistic	p
SILs present	-1.963 (3.164)	-0.620	0.537
Age at onset	-0.176 (0.135)	-1.302	0.197
SIL*onset age interaction	0.244 (0.206)	1.182	0.241

b. Assessment of model

Adj R^2	RSE (DoF)	F statistic (DoF)	P (F statistic)
-0.010	11.70 (67)	0.762 (3, 67)	0.519

Table a13.vii. Multivariable regression of transformed PASAT score against presence of SILs, onset age and SIL*onset age interaction

a. Values of regression coefficients

Independent variable	β (SE)	T statistic	p
SILs present	0.151 (0.410)	0.367	0.715
Age at onset	0.018 (0.017)	1.014	0.315
SIL*onset age interaction	-0.029 (0.026)	-1.094	0.278

b. Assessment of model

Adj R^2	RSE (DoF)	F statistic (DoF)	P (F statistic)
-0.022	1.48 (63)	0.521 (3, 63)	0.670

**p ≤0.05

Table a13.viii. Multivariable regression of WLGT score against presence of SILs, onset age and SIL*onset age interaction

a. Values of regression coefficients

Independent variable	β (SE)	T statistic	p
SILs present	-6.711 (5.059)	-1.327	0.189
Age at onset	0.974 (2.187)	0.445	0.658
SIL*onset age interaction	0.219 (0.140)	1.567	0.122

b. Assessment of model

Adj R^2	RSE (DoF)	F statistic (DoF)	P (F statistic)
0.000	7.98 (67)	0.043 (3, 67)	0.395

**p ≤0.05

Table a13.ix. Multivariable regression of Stroop interference score against presence of SILs, onset age and SIL*onset age interaction

a. Values of regression coefficients

Independent variable	β (SE)	T statistic	p
SILs present	4.071 (3.141)	1.296	0.201
Age at onset	-0.185 (0.133)	-1.391	0.170
SIL*onset age interaction	0.433 (0.230)	1.883	0.066

b. Assessment of model

Adj R^2	RSE (DoF)	F statistic (DoF)	P (F statistic)
0.034	9.68 (50)	1.624 (3, 50)	0.196

Multivariable regression was performed to distinguish whether the interaction of SIL status with age at onset or with age at testing was most influential. Regressions took the form:

$$Test\ score \quad age\ at\ onset + age\ at\ testing + SIL\ status + age\ at\ onset * SIL\ status + age\ at\ testing * SIL\ status$$

There were no significant main effects of age at onset, age at testing or SIL status for any test. There were no significant interactions between age at onset and SIL status, nor between age at testing and SIL status (table a13.x – a13.xviii).

VIF values of some predictors were moderate (5 – 10) due to collinearity between age at onset and onset age group. The residual degrees of freedom were reduced by the relatively high number of predictors and the incomplete test batteries of some participants. These considerations, in addition to high variance for most tests, caused wide standard errors that may have diminished statistical significance of any main effect or interaction. The total variance explained by the models (R^2) was low. The imprecision of regression estimates and low overall predictive value of models means it was not possible to determine which age parameter drove putative interactions with SIL status.

Table a13.x. Multivariable regression of transformed SRT-LTS score against age at onset, age at testing, SIL status, age at onset*SIL status and age at testing*SIL status

a. Values of regression coefficients

Independent variable	B (SE)	T statistic	P
Age at onset	0.026 (0.024)	1.068	0.289
Age at testing	-0.010 (0.026)	-0.381	0.705
SIL status	0.471 (0.341)	1.380	0.172
Age at onset*SIL status	-0.031 (0.049)	-0.648	0.519
Age at testing*SIL status	0.017 (0.059)	0.238	0.778

**p ≤0.05

b. Assessment of model

Adj R^2	RSE (DoF)	F statistic (DoF)	P (F statistic)
-0.021	1.27 (67)	0.705 (5, 67)	0.622

c. Variance inflation factors

$VIF_{age\ at\ onset}$	$VIF_{age\ at\ testing}$	$VIF_{SIL\ status}$	$VIF_{age\ at\ onset*SIL\ status}$	$VIF_{age\ at\ testing*SIL\ status}$
5.12	4.52	1.14	9.63	9.08

Table a13.xi. Multivariable regression of SRT-CLTR score against age at onset, age at testing, SIL status, age at onset*SIL status and age at testing*SIL status

a. Values of regression coefficients

Independent variable	B (SE)	T statistic	P
Age at onset	-0.387 (0.280)	-1.385	0.171
Age at testing	0.165 (0.303)	0.544	0.588
SIL status	-5.704 (4.038)	-1.412	0.162
Age at onset*SIL status	0.604 (0.574)	1.052	0.297
Age at testing*SIL status	-0.517 (0.693)	-0.747	0.458

**p ≤0.05

b. Assessment of model

Adj R^2	RSE (DoF)	F statistic (DoF)	P (F statistic)
-0.006	15.03 (67)	0.909 (5, 67)	0.481

c. Variance inflation factors

$VIF_{age\ at\ onset}$	$VIF_{age\ at\ testing}$	$VIF_{SIL\ status}$	$VIF_{age\ at\ onset*SIL\ status}$	$VIF_{age\ at\ testing*SIL\ status}$
5.12	4.52	1.14	9.63	9.08

Table a13.xii. Multivariable regression of transformed SRT-DR score against age at onset, age at testing, SIL status, age at onset*SIL status and age at testing*SIL status

a. Values of regression coefficients

Independent variable	B (SE)	T statistic	P
Age at onset	0.021 (0.013)	1.605	0.113
Age at testing	-0.007 (0.014)	-0.473	0.638
SIL status	0.083 (0.187)	0.441	0.661
Age at onset*SIL status	-0.029 (0.027)	-1.099	0.276
Age at testing*SIL status	0.010 (0.032)	0.312	0.756

**p ≤0.05

b. Assessment of model

Adj R^2	RSE (DoF)	F statistic (DoF)	P (F statistic)
-0.002	0.69 (66)	0.967 (5, 66)	0.444

c. Variance inflation factors

$VIF_{age\ at\ onset}$	$VIF_{age\ at\ testing}$	$VIF_{SIL\ status}$	$VIF_{age\ at\ onset*SIL\ status}$	$VIF_{age\ at\ testing*SIL\ status}$
5.02	4.41	1.12	9.33	8.75

Table a13.xiii. Multivariable regression of SPART-IR score against age at onset, age at testing, SIL status, age at onset*SIL status and age at testing*SIL status

a. Values of regression coefficients

Independent variable	B (SE)	T statistic	P
Age at onset	0.091 (0.108)	0.843	0.402
Age at testing	-0.111 (0.117)	-0.949	0.346
SIL status	0.080 (1.571)	0.051	0.959
Age at onset*SIL status	-0.121 (0.228)	-0.573	0.569
Age at testing*SIL status	0.199 (0.271)	0.731	0.468

**p ≤0.05

b. Assessment of model

Adj R^2	RSE (DoF)	F statistic (DoF)	P (F statistic)
-0.057	5.81 (66)	0.235 (5, 66)	0.946

c. Variance inflation factors

$VIF_{age\ at\ onset}$	$VIF_{age\ at\ testing}$	$VIF_{SIL\ status}$	$VIF_{age\ at\ onset*SIL\ status}$	$VIF_{age\ at\ testing*SIL\ status}$
4.95	4.46	1.18	9.51	9.10

Table a13.xiv. Multivariable regression of transformed SPART-DR score against age at onset, age at testing, SIL status, age at onset*SIL status and age at testing*SIL status

a. Values of regression coefficients

Independent variable	B (SE)	T statistic	P
Age at onset	0.015 (0.012)	1.225	0.225
Age at testing	-0.013 (0.013)	-0.981	0.330
SIL status	-0.056 (0.179)	-0.312	0.756
Age at onset*SIL status	-0.028 (0.026)	-1.079	0.285
Age at testing*SIL status	0.014 (0.309)	0.460	0.647

**p ≤0.05

b. Assessment of model

Adj R^2	RSE (DoF)	F statistic (DoF)	P (F statistic)
-0.025	0.66 (64)	0.662 (5, 64)	0.654

c. Variance inflation factors

$VIF_{age\ at\ onset}$	$VIF_{age\ at\ testing}$	$VIF_{SIL\ status}$	$VIF_{age\ at\ onset*SIL\ status}$	$VIF_{age\ at\ testing*SIL\ status}$
4.83	4.29	1.10	9.19	8.72

Table a13.xv. Multivariable regression of SDMT score against age at onset, age at testing, SIL status, age at onset*SIL status and age at testing*SIL status

a. Values of regression coefficients

Independent variable	B (SE)	T statistic	P
Age at onset	-0.057 (0.221)	-0.259	0.797
Age at testing	-0.164 (0.242)	-0.679	0.500
SIL status	-1.978 (3.212)	-0.616	0.540
Age at onset*SIL status	0.068 (0.4640	0.147	0.883
Age at testing*SIL status	0.240 (0.555)	0.432	0.667

**p ≤0.05

b. Assessment of model

Adj R^2	RSE (DoF)	F statistic (DoF)	P (F statistic)
-0.034	11.84 (65)	0.544 (5, 65)	0.743

c. Variance inflation factors

$VIF_{age\ at\ onset}$	$VIF_{age\ at\ testing}$	$VIF_{SIL\ status}$	$VIF_{age\ at\ onset*SIL\ status}$	$VIF_{age\ at\ testing*SIL\ status}$
5.00	4.55	1.12	9.52	9.14

Table a13.xvi. Multivariable regression of transformed PASAT score against age at onset, age at testing, SIL status, age at onset*SIL status and age at testing*SIL status

a. Values of regression coefficients

Independent variable	B (SE)	T statistic	P
Age at onset	0.005 (0.028)	0.169	0.866
Age at testing	0.018 (0.028)	0.589	0.558
SIL status	0.139 (0.415)	0.336	0.738
Age at onset*SIL status	0.018 (0.057)	0.317	0.752
Age at testing*SIL status	-0.064 (0.070)	-0.922	0.360

**p ≤0.05

b. Assessment of model

Adj R^2	RSE (DoF)	F statistic (DoF)	P (F statistic)
-0.041	1.49 (61)	0.485 (5, 61)	0.786

c. Variance inflation factors

$VIF_{age\ at\ onset}$	$VIF_{age\ at\ testing}$	$VIF_{SIL\ status}$	$VIF_{age\ at\ onset*SIL\ status}$	$VIF_{age\ at\ testing*SIL\ status}$
5.01	4.39	1.12	9.40	8.81

Table a13.xvii. Multivariable regression of WLGT score against age at onset, age at testing, SIL status, age at onset*SIL status and age at testing*SIL status

a. Values of regression coefficients

Independent variable	B (SE)	T statistic	P
Age at onset	-0.153 (0.150)	-1.023	0.310
Age at testing	0.153 (0.163)	0.940	0.351
SIL status	0.994 (2.205)	0.451	0.654
Age at onset*SIL status	0.276 (0.317)	0.870	0.387
Age at testing*SIL status	-0.080 (0.388)	-0.207	0.387

**p ≤0.05

b. Assessment of model

Adj R^2	RSE (DoF)	F statistic (DoF)	P (F statistic)
-0.016	8.05 (65)	0.780 (5, 65)	0.568

c. Variance inflation factors

$VIF_{age\ at\ onset}$	$VIF_{age\ at\ testing}$	$VIF_{SIL\ status}$	$VIF_{age\ at\ onset*SIL\ status}$	$VIF_{age\ at\ testing*SIL\ status}$
5.00	4.35	1.11	9.84	9.15

Table a13.xviii. Multivariable regression of Stroop interference score against age at onset, age at testing, SIL status, age at onset*SIL status and age at testing*SIL status

a. Values of regression coefficients

Independent variable	B (SE)	T statistic	P
Age at onset	0.084 (0.190)	0.442	0.661
Age at testing	-0.394 (0.203)	-1.936	0.058
SIL status	4.051 (3.093)	1.310	0.197
Age at onset*SIL status	0.049 (0.409)	0.121	0.904
Age at testing*SIL status	0.554 (0.480)	1.154	0.254

**p ≤0.05

b. Assessment of model

Adj R^2	RSE (DoF)	F statistic (DoF)	P (F statistic)
0.069	9.50 (48)	1.788 (5, 48)	0.133

c. Variance inflation factors

$VIF_{age\ at\ onset}$	$VIF_{age\ at\ testing}$	$VIF_{SIL\ status}$	$VIF_{age\ at\ onset*SIL\ status}$	$VIF_{age\ at\ testing*SIL\ status}$
3.50	3.19	1.15	5.53	5.25

Appendix 14

Effects of interaction between age at onset, onset age group and SIL status on Rao BRB-N and Stroop test data

As those with onset aged <30 years were more likely to have SILs, it is possible the interactions between age at onset and onset age group was mediated by an interaction between age at onset and SIL status.

It is also possible that the interaction between age at onset and SIL status was partially attenuated by the interaction between age at onset and onset age group. For example, SRT-LTS and -CLTR scores appeared stable with increasing age at onset in patients with SILs and declined in the absence of SILs. Scores of patients with onset aged <30 years improved with increasing age at onset. An overall decline in scores among patients with SILs may have been partially masked by an interaction between age at onset and onset age group.

Additionally, onset age group may have modulated the interactions between SIL status and age at onset (3-way interactions). For example, it is possible the SRT-LTS and -CLTR scores in patients with SILs was modulated by onset age group, such that among patients with SILs and onset aged ≥30 years, scores declined with increasing age at onset but in patients with SILs and onset aged <30 years, scores were stable with age at onset. As the majority of patients with SILs experienced onset aged <30 years, the overall effect would resemble that of the interaction between age at onset and patients with SILs and onset aged <30 years.

To interrogate the separate interactions of age at onset with onset age group and with SIL status and to identify 3-way interactions, test scores were plotted against age at onset for those with and without SILs separately according to onset age group[22].

[22] If an apparent interaction between age at onset and onset age group was mediated by an interaction between age at onset and SIL status, interactions between age at onset and onset age group observed prior to stratification would diminish after stratification. The effects of age at onset in groups with SILs would be distinct from the effects of age at onset in groups without SILs, regardless of onset age group.

Statistical confirmation was sought using multivariable regressions in the form:

$$\textit{Test score} \quad \textit{onset age group} + \textit{age at onset} + \textit{SIL status} + \textit{onset age group} * \textit{age at onset} + \textit{onset age group} * \textit{SIL sta}$$

Interactions between age at onset and onset age group for SRT-DR, SPART-DR, SDMT, PASAT and Stroop interference scores resembled the interactions between age at onset and SIL status. Interactions between age at onset and onset age group for the remaining tests were dissimilar to interactions between age at onset and SIL status (fig 14a.i).

If the non-significant interactions between age at onset and SIL status observed in regression plots were positively confounded by interactions between age at onset and onset age group, the effects of age at onset in presence or absence of SILs should be similar, but the effects of age at onset should vary according to onset age group.
If there was a 3-way interaction, the differences in the gradients of the scores in patients with onset <30 years and the group with onset ≥30 years would be different in those with and without SILs.
Finally, if presence of SILs and onset age group interacted with age at onset independently, the gradients of the regression lines in presence and absence of SILs would be different and the gradients of regression lines in onset age groups would be different but the *differences* between the gradients in those <30 at onset and those ≥30 at onset will be the same in the presence and absence of lesions.

Figure a14.i. Comparison of interactions between onset age group and age at onset and between SIL status and age at onset

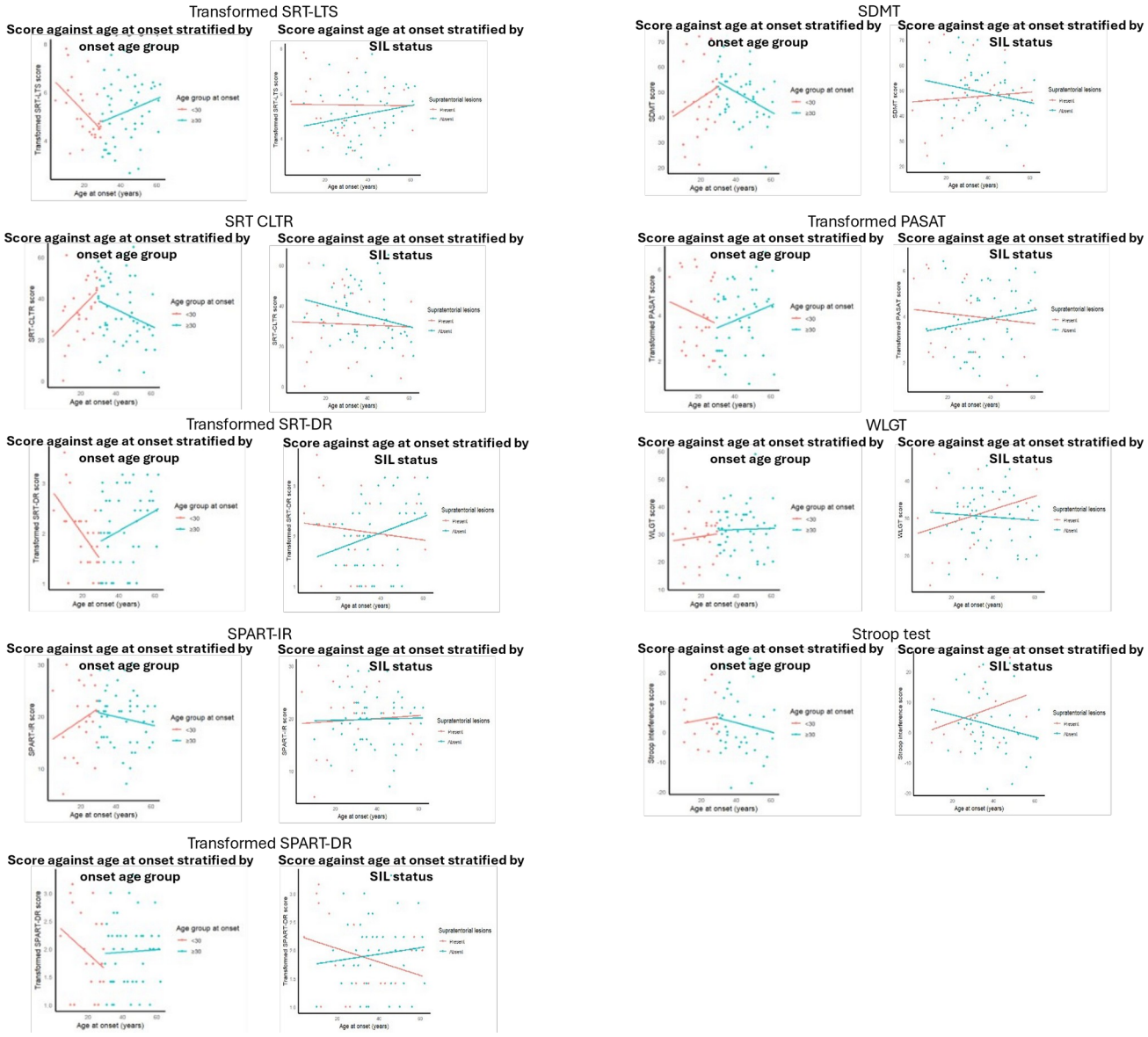

Although inspection of 3-way plots indicated mixed patterns of interplay between variables across different Rao BRB-N subtests (fig a14.ii – x), formal analysis with multivariable regressions revealed no significant main effects or interactions (table a14.i – ix). VIF values were high, subgroups were small and variance was wide, making regression coefficient estimates unreliable. Therefore, no reliable inferences could be drawn from the analyses. Small values of R^2 means any main effects or interactions would have negligible clinical impact.

Although the data were insufficient to confidently elucidate the independent and interactive effect of variables, inspection of 3-way interaction plots for transformed SRT-LTS, transformed SRT-DR, SPART-IR and SDMT scores were suggestive of interactions between age at onset and onset age group that were independent of SIL status (fig a14.ii, a14.iv, a14.v and a14.vii), with little effect of SIL status after stratifying by onset age group. If this were the case, interactions between age at onset and onset age group for SRT-DR and SDMT scores, (i.e., two of the tests for which the interaction between age at onset and onset age group resembled the interaction between age at onset and SIL status) were not mediated by interactions between age at onset and SIL status and apparent interactions between age at onset and SIL status were partially due to the interaction between age at onset and onset age group.

Interactions between age at onset and onset age group appeared to persist in either or both of the SIL status categories for all tests, including SPART-DR and PASAT, indicating independent interactions between age at onset and onset age group, with possible modulation by SIL status. The interaction between age at onset and onset age group for PASAT score approached statistical significance (table a14.vii; $\beta = 0.151$, $p = 0.088$), despite high VIF values and small subgroups.

The apparent interaction between age at onset and onset age group on Stroop test scores was diminished after stratifying for SIL status, while the interaction between age at onset and SIL status persisted for those

aged <30 years at onset[23]. Assuming a real effect, this suggests the interaction between age at onset and onset age group for the Stroop test was partially explained by an interaction between age at onset and SIL status. The interaction between age at onset and SIL status approached statistical significance for Stroop interference score (β = 21.654, p = 0.081). In conjunction with statistically significant interactions between onset age group and SIL status (supp table 130) and age at testing and SIL status (supp table 148), and borderline significant interactions between age at onset and SIL status (table a13.ix), the evidence suggests an interaction between age parameters and SIL status for Stroop interference scores.

Figure a14.iia & b. Effect of age at onset on transformed SRT-LTS score in patients with onset aged <30 and onset aged ≥30 according in presence or absence of SILs

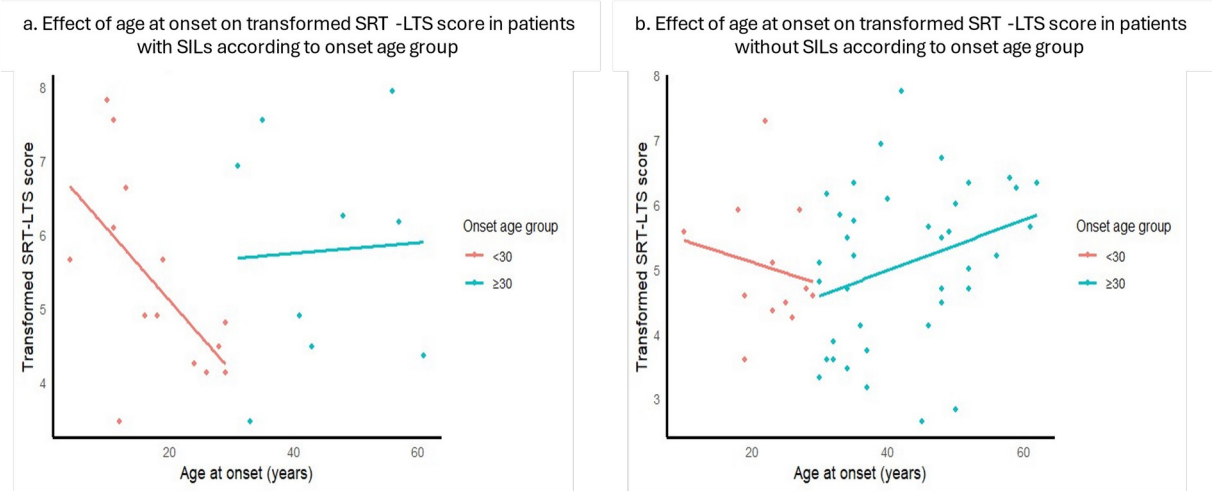

[23] Stroop interference score increased with increasing age at onset in the presence of SILs and declined in their absence (fig a14.i.i). However, after stratifying by onset age group, scores declined with increasing age at onset in the presence of lesions in both onset age groups (fig a14.x.a). The interaction between onset age group and SIL status approached statistical significance after adjusting for age at onset, but the interaction between age at onset and SIL status no longer approached statistical significance after adjusting for onset age group, i.e., Simpson's paradox.

Figure a14.iic & d. Effect of age at onset on transformed SRT-LTS score in patients with and without SILs according to onset age group

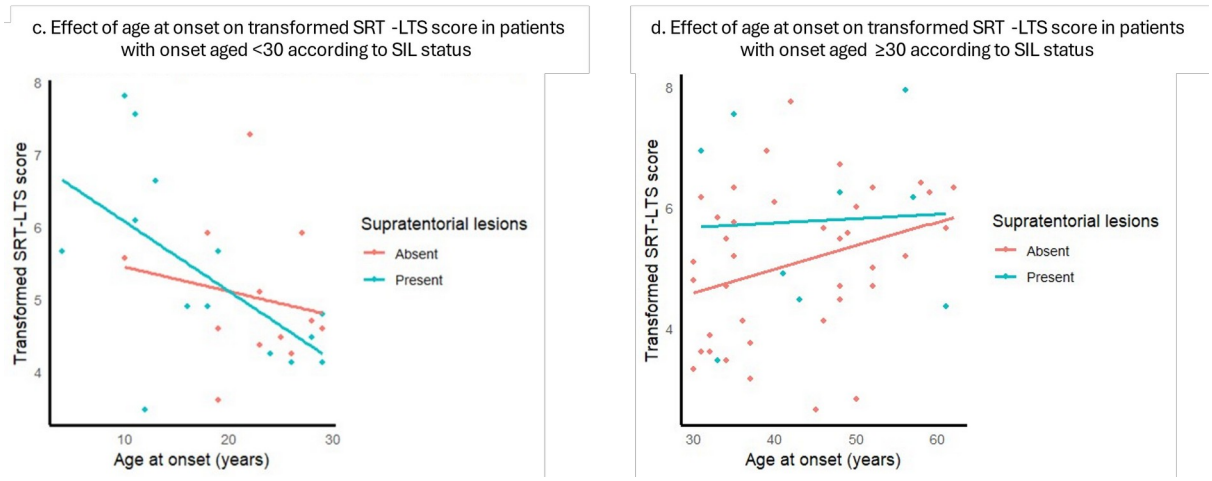

Figure a14.iiia& b. Effect of age at onset on SRT-CLTR score in patients with onset aged <30 and onset aged ≥30 according in presence or absence of SILs

Figure a14.iiic & d. Effect of age at onset on SRT-CLTR score in patients with and without SILs according to onset age group

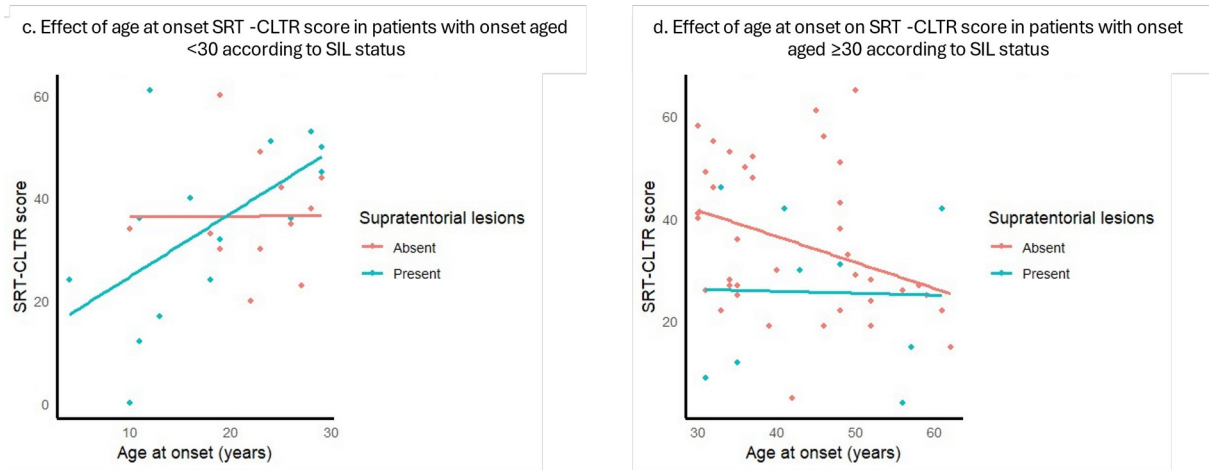

Figure a14.iva & b. Effect of age at onset on transformed SRT-DR score in patients with onset aged <30 and onset aged ≥30 according in presence or absence of SILs

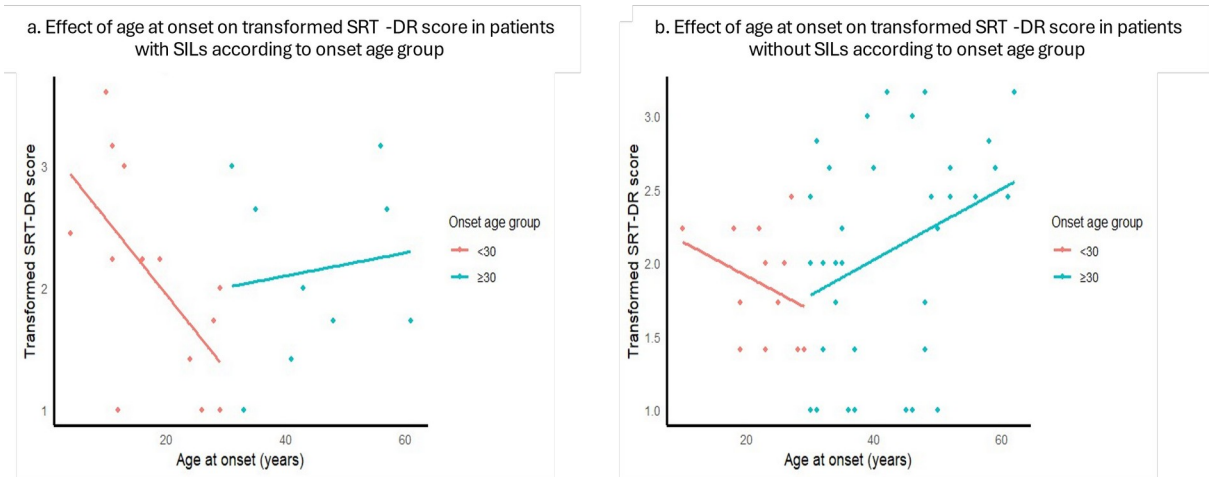

Figure a14.ivc & d. Effect of age at onset on transformed SRT-DR score in patients with and without SILs according to onset age group

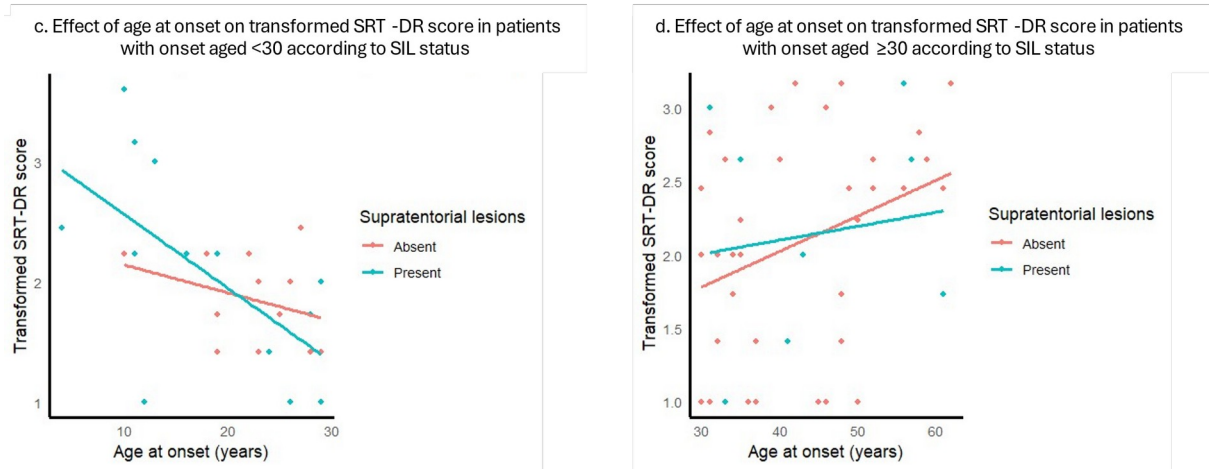

Figure a14.va & b. Effect of age at onset on SPART-IR score in patients with onset aged <30 and onset aged ≥30 according in presence or absence of SILs

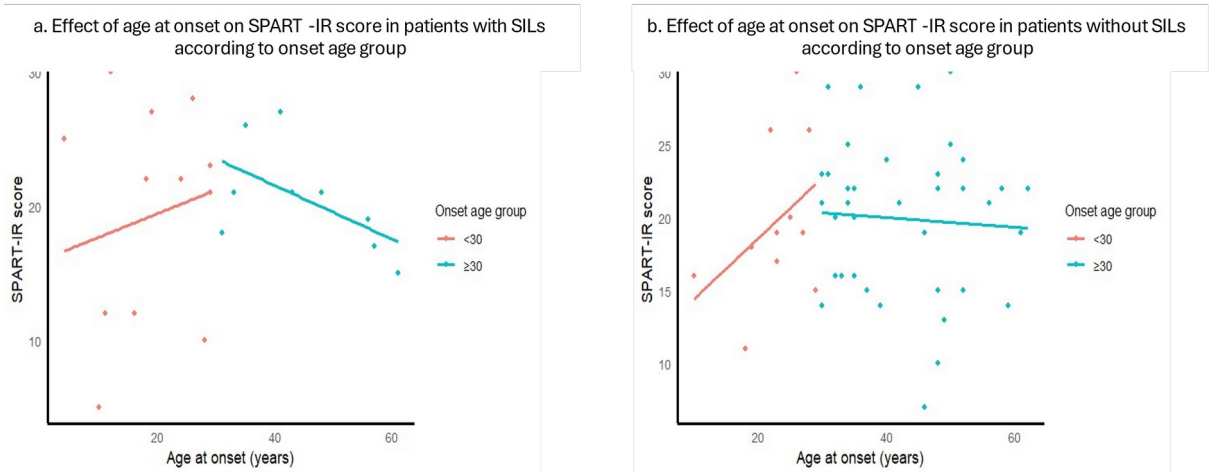

Figure a14.vc & d. Effect of age at onset on SPART-IR score in patients with and without SILs according to onset age group

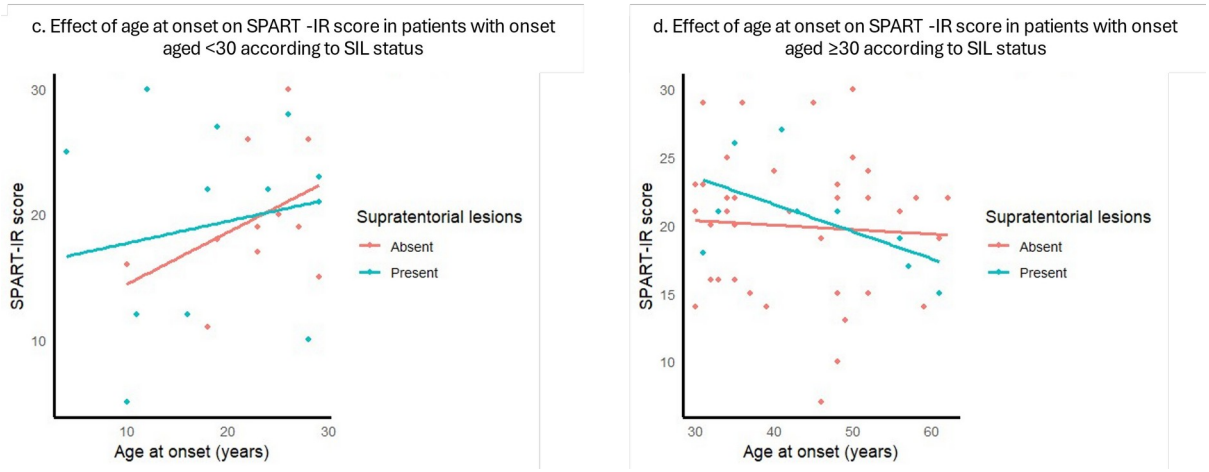

Figure a14.via & b. Effect of age at onset on transformed SPART-DR score in patients with onset aged <30 and onset aged ≥30 according in presence or absence of SILs

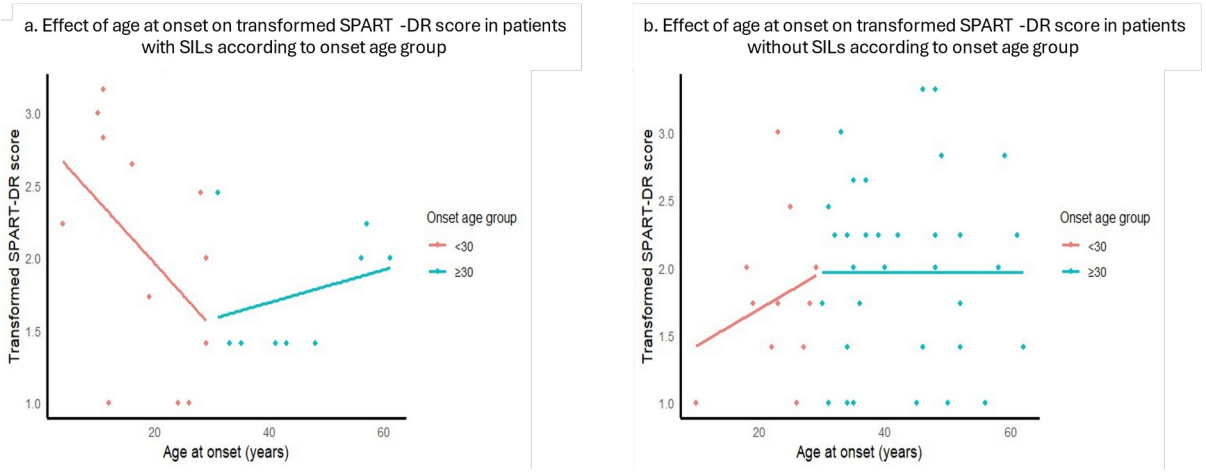

Figure a14.vic & d. Effect of age at onset on transformed SPART-DR score in patients with and without SILs according to onset age group

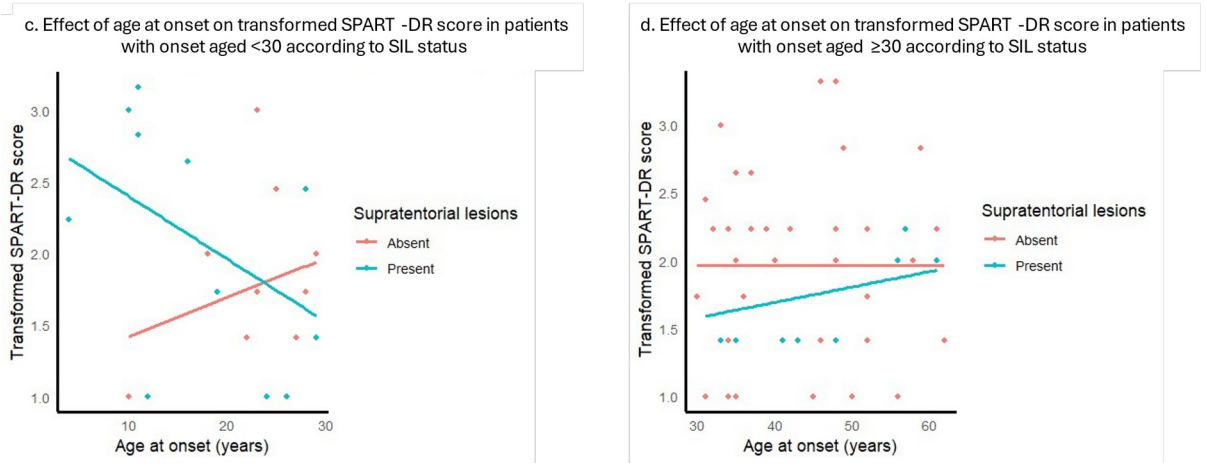

Figure a14.viia& b. Effect of age at onset on SDMT score in patients with onset aged <30 and onset aged ≥30 according in presence or absence of SILs

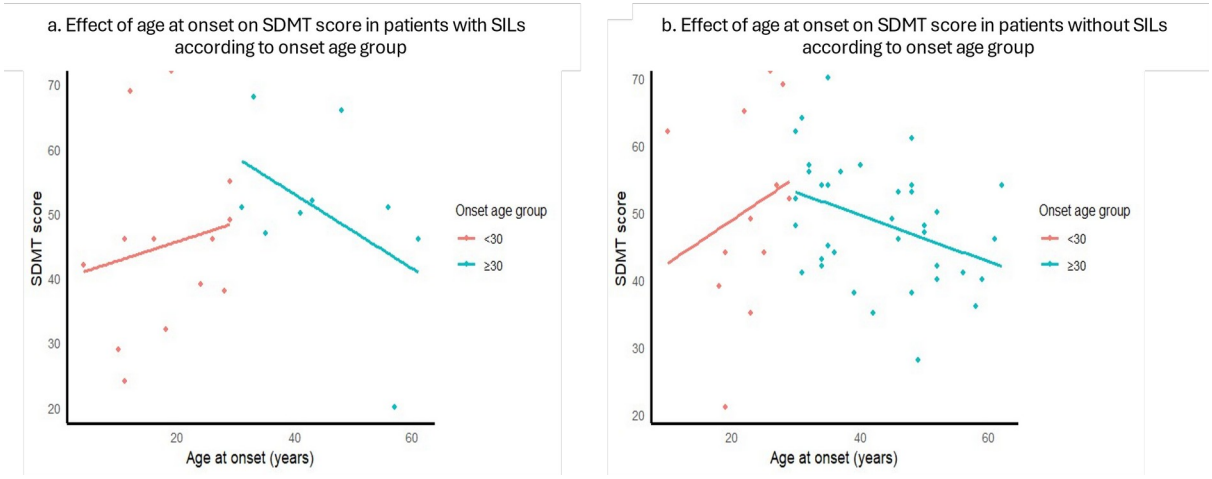

Figure a14.viic & d. Effect of age at onset on SDMT score in patients with and without SILs according to onset age group

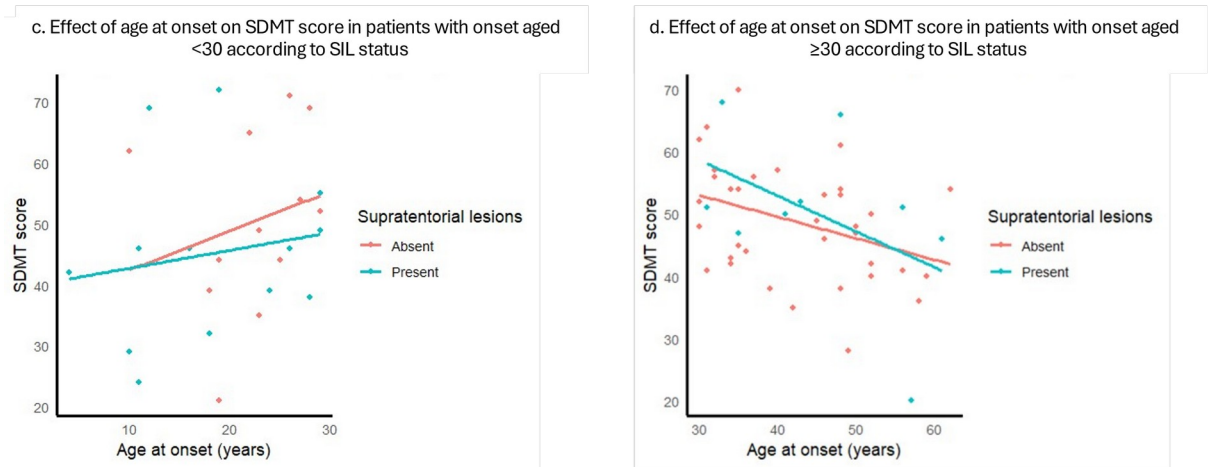

Figure a14.viiia& b. Effect of age at onset on transformed PASAT score in patients with onset aged <30 and onset aged ≥30 according in presence or absence of SILs

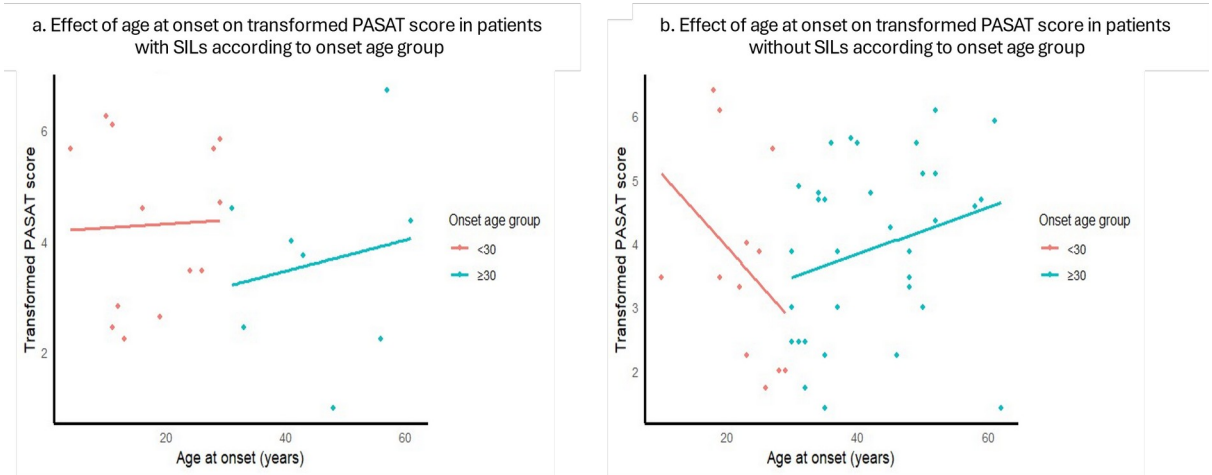

Figure a14.viiic& d. Effect of age at onset on transformed PASAT score in patients with and without SILs according to onset age group

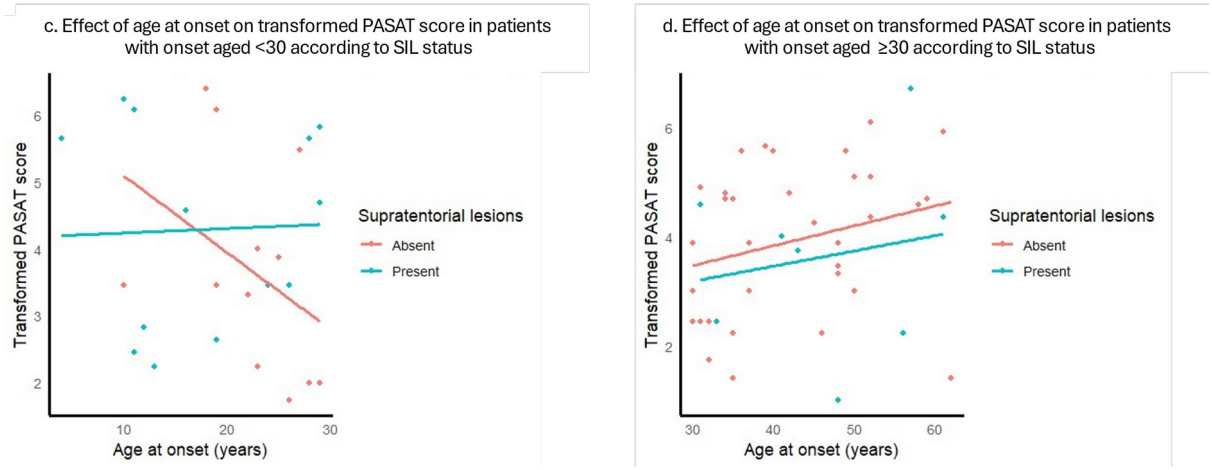

Figure a14.ixa & b. Effect of age at onset on WLGT score in patients with onset aged <30 and onset aged ≥30 according in presence or absence of SILs

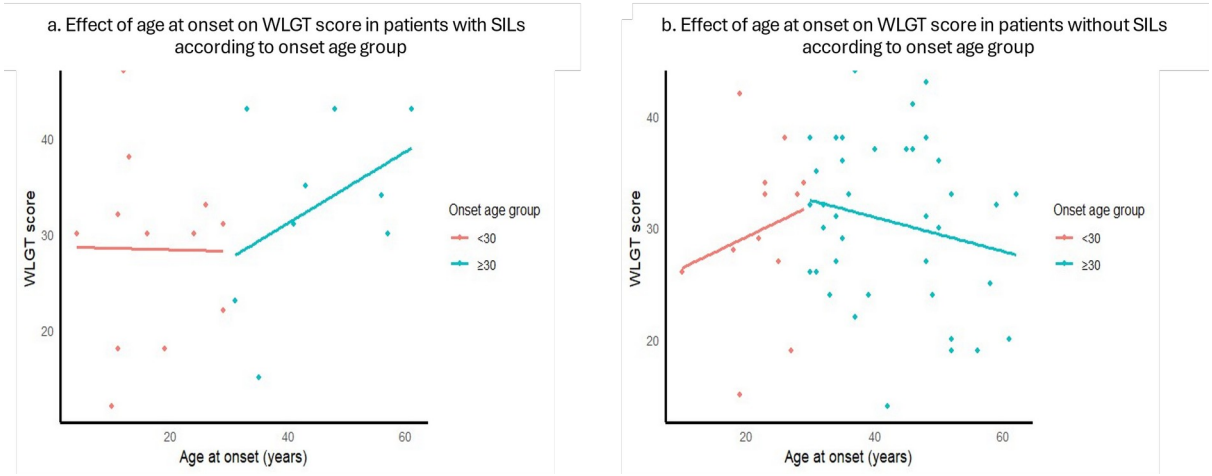

Figure a14.ixc & d. Effect of age at onset on WLGT score in patients with and without SILs according to onset age group

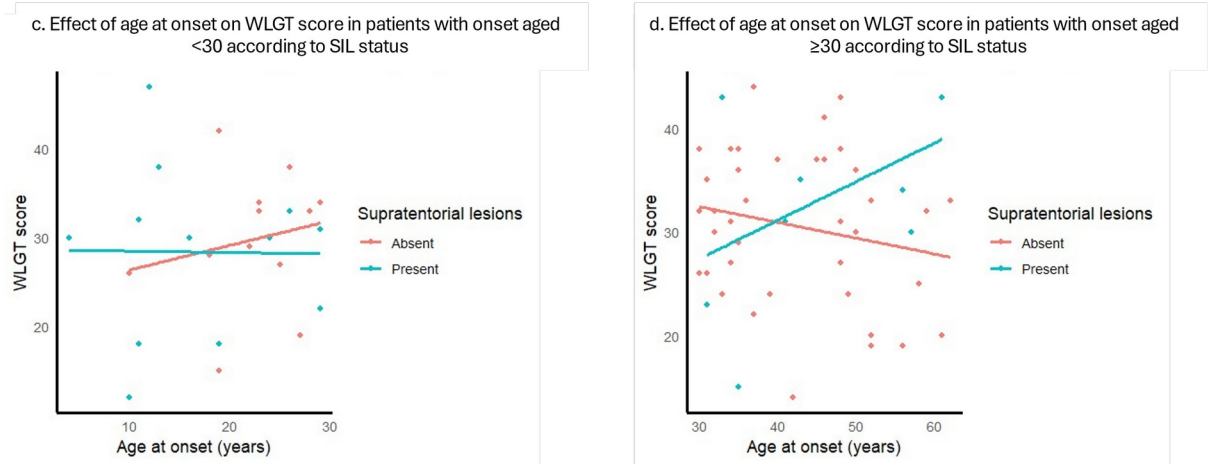

Figure a14.xa & b. Effect of age at onset on Stroop interference score in patients with onset aged <30 and onset aged ≥30 according in presence or absence of SILs

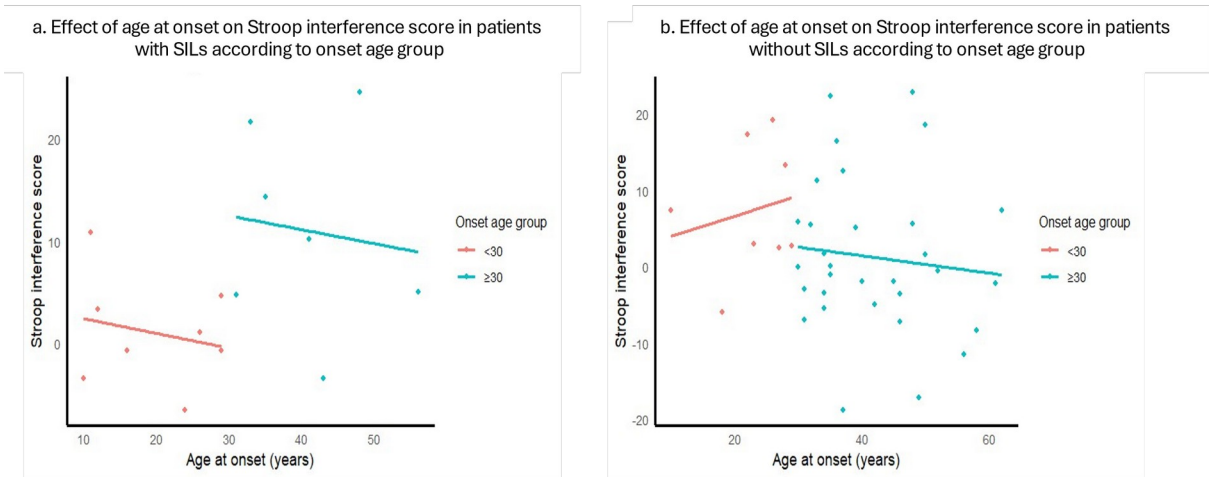

Figure a14.xc & d. Effect of age at onset on Stroop interference score in patients with and without SILs according to onset age group

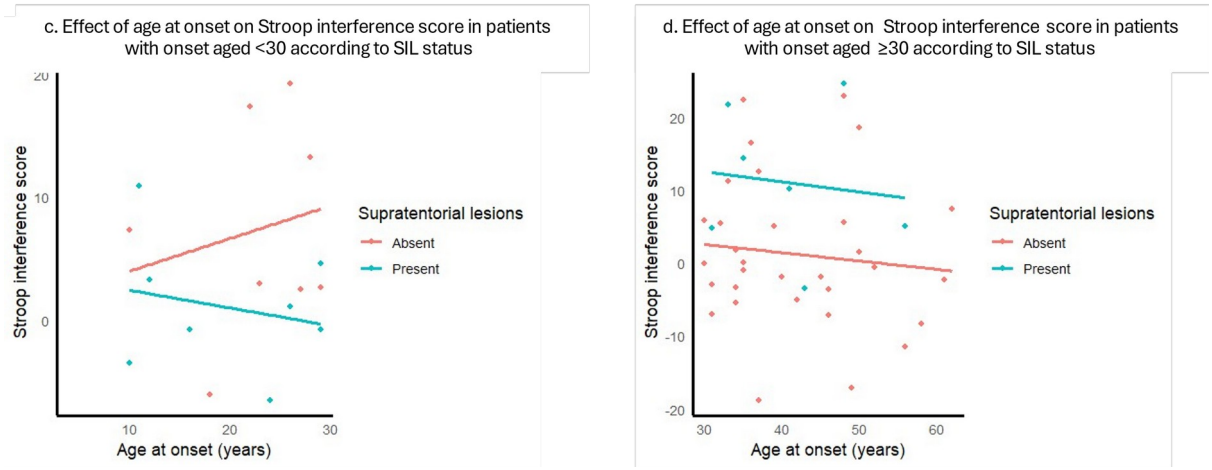

Table a14.i. Multivariable regression of transformed SRT-LTS score against age at onset * onset age group * SILs

a. Values of beta regression coefficients

Term	β (SE)	T statistic	P
Age at onset	-0.034 (0.069)	-0.490	0.626
Onset age group ≥30	0.192 (0.974)	0.197	0.844
SIL present	-0.947 (1.225)	-0.773	0.443
Age at onset*onset age group	0.073 (0.072)	1.014	0.314
Age at onset*SILs	-0.063 (0.080)	-0.781	0.437
Onset age group*SILs	1.865 (1.368)	1.364	0.177
Age at onset*onset age group*SILs	0.031 (0.091)	0.338	0.736

b. Values of parameters

Adj R^2	RSE (DoF)	F statistic (DoF)	P (F statistic)
0.067	1.21 (65)	1.738 (7, 65)	0.116

c. Variance inflation factors

$VIF_{age\ at\ onset}$	$VIF_{onset\ age\ group}$	$VIF_{SIL\ status}$	$VIF_{age\ at\ onset*onset\ age\ group}$	$VIF_{age\ at\ onset*SIL\ status}$	$VIF_{onset\ age\ group*SIL\ status}$	$VIF_{age\ at\ onset*age\ group\ *SIL\ status}$
47.28	10.76	16.04	19.54	28.68	10.01	9.91

Table a14.ii. Multivariable regression of SRT-CLTR score against age at onset * onset age group * SILs

a. Values of beta regression coefficients

Term	β (SE)	T statistic	P
Age at onset	0.011 (0.805)	0.014	0.989
Onset age group≥30	2.380 (11.415)	0.208	0.836
SIL present	19.019 (14.363)	1.324	0.190
Age at onset*onset age group	-0.519 (0.840)	-0.618	0.539
Age at onset*SILs	1.221 (0.939)	1.300	0.198
Onset age group*SILs*	-32.006 (16.036)	-1.996	0.050
Age at onset*onset age group*SILs	-0.751 (1.069)	-0.702	0.485

b. Values of parameters

Adj R^2	RSE (DoF)	F statistic (DoF)	P (F statistic)
0.097	14.24 (65)	2.108 (7, 65)	0.055

c. Variance inflation factors

$VIF_{age\ at\ onset}$	$VIF_{onset\ age\ group}$	$VIF_{SIL\ status}$	$VIF_{age\ at\ onset*onset\ age\ group}$	$VIF_{age\ at\ onset*SIL\ status}$	$VIF_{onset\ age\ group*SIL\ status}$	$VIF_{age\ at\ onset*age\ group\ *SIL\ status}$
47.28	10.76	16.04	19.53	28.68	10.01	9.91

Table a14.iii. Multivariable regression of transformed SRT-DR score against age at onset * onset age group * SILs

a. Values of beta regression coefficients

Term	β (SE)	T statistic	P
Age at onset	-0.023 (0.037)	-0.622	0.536
Onset age group≥30	0.346 (0.529)	0.654	0.516
SIL present	-0.542 (0.668)	-0.812	0.420
Age at onset*onset age group	0.047 (0.039)	1.214	0.229
Age at onset*SILs	-0.038 (0.044)	-0.879	0.383
Onset age group*SILs	0.690 (0.745)	0.926	0.358
Age at onset*onset age group*SILs	0.024 (0.050)	0.476	0.636

b. Values of parameters

Adj R^2	RSE (DoF)	F statistic (DoF)	P (F statistic)	Max VIF	VIF (age at onset x onset group)
0.092	0.660 (64)	2.026 (7, 64)	0.065	46.36	19.44

c. Variance inflation factors

$VIF_{age\ at\ onset}$	$VIF_{onset\ age\ group}$	$VIF_{SIL\ status}$	$VIF_{age\ at\ onset*onset\ age\ group}$	$VIF_{age\ at\ onset*SIL\ status}$	$VIF_{onset\ age\ group*SIL\ status}$	$VIF_{age\ at\ onset*age\ group\ *SIL\ status}$
46.36	10.49	15.64	19.44	27.68	10.04	9.90

Table a14.iv. Multivariable regression of SPART-IR score against age at onset * onset age group * SILs

a. Values of beta regression coefficients

Term	β (SE)	T statistic	P
Age at onset	0.416 (0.326)	1.274	0.207
Onset age group ≥30	-4.682 (4.627)	-1.012	0.315
SIL present	-2.751 (5.824)	-0.472	0.638
Age at onset*onset age group	-0.449 (0.340)	-1.319	0.192
Age at onset*SILs	-0.24 (0.382)	-0.628	0.532
Onset age group*SILs	5.084 (6.502)	0.782	0.437
Age at onset*onset age group*SILs	0.073 (0.435)	0.169	0.867

b. Values of parameters

Adj R^2	RSE (DoF)	F statistic (DoF)	P (F statistic)
-0.043	5.77 (64)	0.581 (7, 64)	0.769

c. Variance inflation factors

$VIF_{age\ at\ onset}$	$VIF_{onset\ age\ group}$	$VIF_{SIL\ status}$	$VIF_{age\ at\ onset*onset\ age\ group}$	$VIF_{age\ at\ onset*SIL\ status}$	$VIF_{onset\ age\ group*SIL\ status}$	$VIF_{age\ at\ onset*age\ group\ *SIL\ status}$
45.73	10.49	15.56	19.44	27.12	10.00	9.96

Table a14.v.Interaction terms from multivariable regression of transformed SPART-DR score against age at onset * onset age group * SILs

a. Values of beta regression coefficients

Term	β (SE)	T statistic	P
Age at onset	0.027 (0.038)	0.727	0.470
Onset age group ≥30	-0.142 (0.523)	-0.272	0.787
SIL present	-0.811 (0.659)	-1.231	0.223
Age at onset*onset age group	-0.027 (0.039)	-0.701	0.486
Age at onset*SILs	-0.071 (0.044)	-1.627	0.109
Onset age group*SILs	0.484 (0.735)	0.658	0.513
Age at onset*onset age group*SILs	0.083 (0.050)	1.666	0.101

b. Values of parameters

Adj R^2	RSE (DoF)	F statistic (DoF)	P (F statistic)
-0.008	0.65 (62)	0.920 (7, 62)	0.497

c. Variance inflation factors

$VIF_{age\ at\ onset}$	$VIF_{onset\ age\ group}$	$VIF_{SIL\ status}$	$VIF_{age\ at\ onset*onset\ age\ group}$	$VIF_{age\ at\ onset*SIL\ status}$	$VIF_{onset\ age\ group*SIL\ status}$	$VIF_{age\ at\ onset*age\ group\ *SIL\ status}$
45.78	9.98	15.11	20.01	26.88	10.03	10.18

Table a14.vi Interaction terms from multivariable regression of SDMT score against age at onset * onset age group * SILs

a. Values of beta regression coefficients

Term	β (SE)	T statistic	P
Age at onset	0.642 (0.650)	0.988	0.327
Onset age group≥30	-7.285 (9.236)	-0.789	0.433
SIL present	-8.473 (11.605)	-0.730	0.468
Age at onset*onset age group	-0.989 (0.679)	-1.457	0.150
Age at onset*SILs	-0.349 (0.761)	-0.458	0.649
Onset age group*SILs	12.943 (12.967)	0.998	0.322
Age at onset*onset age group*SILs	0.121 (0.867)	0.139	0.890

b. Values of parameters

Adj R^2	RSE (DoF)	F statistic (DoF)	P (F statistic)
0.024	11.50 (63)	1.250 (7, 63)	0.290

c. Variance inflation factors

$VIF_{age\ at\ onset}$	$VIF_{onset\ age\ group}$	$VIF_{SIL\ status}$	$VIF_{age\ at\ onset*onset\ age\ group}$	$VIF_{age\ at\ onset*SIL\ status}$	$VIF_{onset\ age\ group*SIL\ status}$	$VIF_{age\ at\ onset*age\ group\ *SIL\ status}$
45.72	10.45	15.47	19.30	27.11	10.00	9.97

Table a14.vii Interaction terms from multivariable regression of transformed PASAT score against age at onset * onset age group * SILs

a. Values of beta regression coefficients

Term	β (SE)	T statistic	P
Age at onset	-0.115 (0.083)	-1.381	0.172
Onset age group ≥30	1.451 (1.186)	1.223	0.226
SIL present	2.206 (1.491)	1.479	0.144
Age at onset*onset age group	0.151 (0.087)	1.735	0.088
Age at onset*SILs	0.122 (0.097)	1.253	0.215
Onset age group*SILs	-2.537 (1.704)	-1.489	0.142
Age at onset*onset age group*SILs	-0.130 (0.112)	-1.161	0.250

b. Values of parameters

Adj R^2	RSE (DoF)	F statistic (DoF)	P (F statistic)
-0.021	1.47 (59)	0.810 (7, 59)	0.583

c. Variance inflation factors

$VIF_{age\ at\ onset}$	$VIF_{onset\ age\ group}$	$VIF_{SIL\ status}$	$VIF_{age\ at\ onset*onset\ age\ group}$	$VIF_{age\ at\ onset*SIL\ status}$	$VIF_{onset\ age\ group*SIL\ status}$	$VIF_{age\ at\ onset*age\ group\ *SIL\ status}$
44.52	10.16	14.76	18.22	27.60	9.41	10.13

Table a14.viii Interaction terms from multivariable regression of WLGT score against age at onset * onset age group * SILs

a. Values of beta regression coefficients

Term	β (SE)	T statistic	P
Age at onset	0.277 (0.456)	0.608	0.545
Onset age group≥30	-1.684 (6.473)	-0.260	0.796
SIL present	-5.238 (8.548)	-0.613	0.542
Age at onset*onset age group	-0.430 (0.476)	-0.903	0.370
Age at onset*SILs	-0.293 (0.543)	-0.540	0.591
Onset age group*SILs	2.883 (9.457)	0.305	0.761
Age at onset*onset age group*SILs	0.819 (0.616)	1.330	0.188

b. Values of parameters

Adj R^2	RSE (DoF)	F statistic (DoF)	P (F statistic)
-0.022	8.07 (63)	0.783 (7, 63)	0.604

c. Variance inflation factors

$VIF_{age\ at\ onset}$	$VIF_{onset\ age\ group}$	$VIF_{SIL\ status}$	$VIF_{age\ at\ onset*onset\ age\ group}$	$VIF_{age\ at\ onset*SIL\ status}$	$VIF_{onset\ age\ group*SIL\ status}$	$VIF_{age\ at\ onset*age\ group\ *SIL\ status}$
46.20	10.22	16.58	19.35	28.65	10.79	10.19

Table a14.ix. Interaction terms from multivariable regression of Stroop interference score against age at onset * onset age group * SILs

a. Values of beta regression coefficients

Term	β (SE)	T statistic	P
Age at onset	0.266 (0.58)	0.458	0.649
Onset age group≥30	-8.673 (8.186)	-1.160	0.295
SIL present	-11.834 (11.057)	-1.070	0.295
Age at onset*onset age group	-0.379 (0.609)	-0.623	0.536
Age at onset*SILs	-0.410 (0.732)	-0.560	0.578
Onset age group*SILs	21.654 (12.128)	1.785	0.081
Age at onset*onset age group*SILs	0.387 (0.876)	0.441	0.661

b. Values of parameters

Adj R^2	RSE (DoF)	F statistic (DoF)	P (F statistic)
0.026	9.72 (46)	1.206 (7, 46)	0.319

c. Variance inflation factors

$VIF_{age\ at\ onset}$	$VIF_{onset\ age\ group}$	$VIF_{SIL\ status}$	$VIF_{age\ at\ onset*onset\ age\ group}$	$VIF_{age\ at\ onset*SIL\ status}$	$VIF_{onset\ age\ group*SIL\ status}$	$VIF_{age\ at\ onset*age\ group\ *SIL\ status}$
31.04	7.99	14.02	14.56	16.96	9.49	5.58

Appendix 15

Effects of interactions between diagnosis and paediatric onset on Rao BRB-N and Stroop test (AQP4+ NMOSD and MOGAD)

For a summary of the data, see table a15.i.

a) Paediatric onset was a predictor of SRT-LTS and SRT-DR scores in combined AQP4+ NMOSD and MOGAD groups. The effect persisted after stratifying by diagnosis, i.e., the effect was statistically significant in the AQP4+ NMOSD cohort. The interaction between paediatric onset and diagnosis reached statistical significance for SRT-DR score and approached statistical significance ($p = 0.064$) for SRT-LTS score, indicating the effect of paediatric onset was more profound among patients with AQP4+ NMOSD than MOGAD, although it does not exclude a weaker interaction between paediatric onset and MOGAD that may contribute to the effect of paediatric onset in combined diagnostic groups. A similar pattern was observed for SRT-CLTR scores, although the significant effects of AQP4+ NMOSD within the paediatric-onset group was insufficient to produce a main effect of paediatric onset when AQP4+ NMOSD and MOGAD were combined.

Diagnosis was not an independent predictor of SRT subscores, indicating detrimental effects of AQP4+ NMOSD were restricted to those with paediatric onset and the effect was insufficient to produce a significant difference between diagnostic groups.

These results indicate patients with onset of AQP4+ NMOSD in childhood are at risk of poorer verbal recall than patients with onset in adulthood or patients with MOGAD.

b) Diagnosis was a statistically significant predictor of SPART-IR and -DR scores when cohorts were combined but statistical significance was abolished after stratifying by paediatric vs adult onset disease. This may be due to lack of power to detect effects in smaller subgroups or because the difference in scores between diagnostic

groups was driven partly by the effects of paediatric onset within these groups (either a true interaction or structural overlap, caused by almost paediatric cases comprising almost 23% of AQP4+ NMOSD cases and only 10% of MOGAD cases).

In favour of a loss of statistical power is the absence of a significant interaction term. Structural overlap is more likely to explain group differences in SPART-IR score than SPART-DR score, as paediatric onset was only a significant predictor of SPART-IR score. In favour of a non-significant interaction, box plots seem to show a clearer drop in scores associated with paediatric onset in the AQP4+ NMOSD group compared with the MOGAD group but the wide variance in scores within the paediatric onset cohort with MOGAD make it difficult to interpret. A non-significant interaction may contribute to the effect of diagnosis and explain loss of effect after stratifying (fig 26d & e).

For SPART-IR score, there was a main effect of paediatric onset when diagnoses were combined and a main effect of paediatric onset in multivariable regression, indicating paediatric onset predicted lower score in the AQP4+ NMOSD group. The effect of paediatric onset in the MOGAD group was not statistically significantly different to the effect in the AQP4+ NMOSD group (no significant interaction term), suggesting an effect of paediatric onset that may be partly independent of diagnosis.

There was no effect of paediatric onset on SPART-DR score across combined diagnostic groups, nor after stratification (i.e., in the AQP4+ NMOSD group) and no significant interaction. Absence of an effect of diagnosis after stratification was mostly attributable to lack of statistical power, although the box plot was suggestive of a small contribution by a minor diagnosis x paediatric onset interaction.

Therefore, visuospatial memory is poorer among patients with AQP4+ NMOSD than patients with MOGAD. Paediatric onset is an independent predictor of immediate visuospatial recall.

c) The deleterious effect of paediatric onset on SDMT performance was not present when diagnostic groups were combined and only emerged after stratifying by diagnosis. The diagnosis x paediatric onset term for SDMT approached statistical significance ($p = 0.057$), indicating the effect of paediatric onset was more marked in the AQP4+ NMOSD group. Persistence of a main effect of diagnosis in multivariable regression with paediatric onset suggests AQP4+ NMOSD is an independent predictor of poorer visual processing speed and attention, and that paediatric onset may compound this effect.

d) There were main effects of diagnosis on PASAT and Stroop scores in the mixed paediatric and adult onset group that persisted after stratification (i.e., the effect of diagnosis was significant in adults alone). There was no statistically significant effect of paediatric onset in combined diagnostic groups, nor after stratification (i.e., in the AQP4+ NMOSD group).
Patients with AQP4+ NMOSD are at risk of poorer auditory processing speed and executive function than patients with MOGAD, with no significant effect of paediatric onset.

WLGT scores were not sensitive to paediatric onset, diagnosis or their interactions.

Diagnosis predicted poorer performance on SDMT, PASAT and Stroop tests. Paediatric onset predicted poorer performance on SRT scores. The effect of paediatric onset on SRT and SDMT scores was more marked in the AQP4+ NMOSD group.

Table a15.i. Presence of significant main effects and interactions of diagnosis and paediatric onset in univariable and multivariable regressions (AQP4+ NMOSD & MOGAD)

	Diagnosis (univariable, combined paediatric and adult onset)	Paediatric onset (univariable, combined AQP4+ NMOSD & MOGAD)	Diagnosis (multivariable)	Paediatric onset (multivariable)	Diagnosis* paediatric onset (multivariable)
SRT-LTS	No	Yes	No	Yes	Borderline
SRT-CLTR	No	No	No	Yes	Yes
SRT-DR	No	Yes	No	Yes	Yes
SPART-IR	Yes	Yes	No	Yes	No
SPART-DR	Yes	No	No	No	No
SDMT	Yes	No	Yes	Yes	Borderline
PASAT	Yes	No	Yes	No	No
WLGT	No	No	No	No	No
Stroop	Yes	No	Yes	No	No

Significant interaction terms in multivariable regressions indicate a differential effect of paediatric onset within the AQP4+ NMOSD and MOGAD cohorts but do not exclude an effect of paediatric onset in MOGAD. Conversely, in the presence of a main effect of paediatric onset, interaction terms that fail to reach statistical significance demonstrate the effect of paediatric onset is not significantly different between AQP4+ NMOSD and MOGAD but do not confirm a significant effect within the MOGAD group.

When scores were regressed against paediatric onset in the MOGAD cohort, there was no significant effect on any subtest (table a15.ii). While this may reflect a loss of statistical power with a low n (only 5 MOGAD patients had onset in childhood), plots of SRT, SPART and SDMT scores in patients with AQP4+ NMOSD showed clear differences between adult and paediatric onset (fig 27), while plots for patients with MOGAD did not (fig a15.i).

Table a15.ii. Univariable regression of test scores against paediatric onset in the MOGAD group

Test	$\beta_{(paediatric)}$	T statistic	P (β)	F (df)	R^2
Transformed SRT-LTS	-0.021 (0.593)	-0.036	0.972	0.001	0.000
SRT-CLTR	4.163 (6.646)	0.626	0.534	0.392	0.008
Transformed SRT-DR	0.021 (0.316)	0.067	0.947	0.004	0.000
SPART-IR	-1.837 (2.578)	-0.713	0.480	0.508	0.011
Transformed SPART-DR	0.122 (0.284)	0.428	0.671	0.183	0.004
SDMT	1.429 (5.056)	0.283	0.779	0.080	0.002
Transformed PASAT	0.475 (0.591)	0.804	0.426	0.646	0.015
WLGT	1.429 (3.725)	0.383	0.703	0.147	0.003
Stroop interference	-0.104 (4.933)	-0.021	0.983	0.000	0.000

Figure a15.i. Effect of paediatric onset on test scores in the MOGAD group

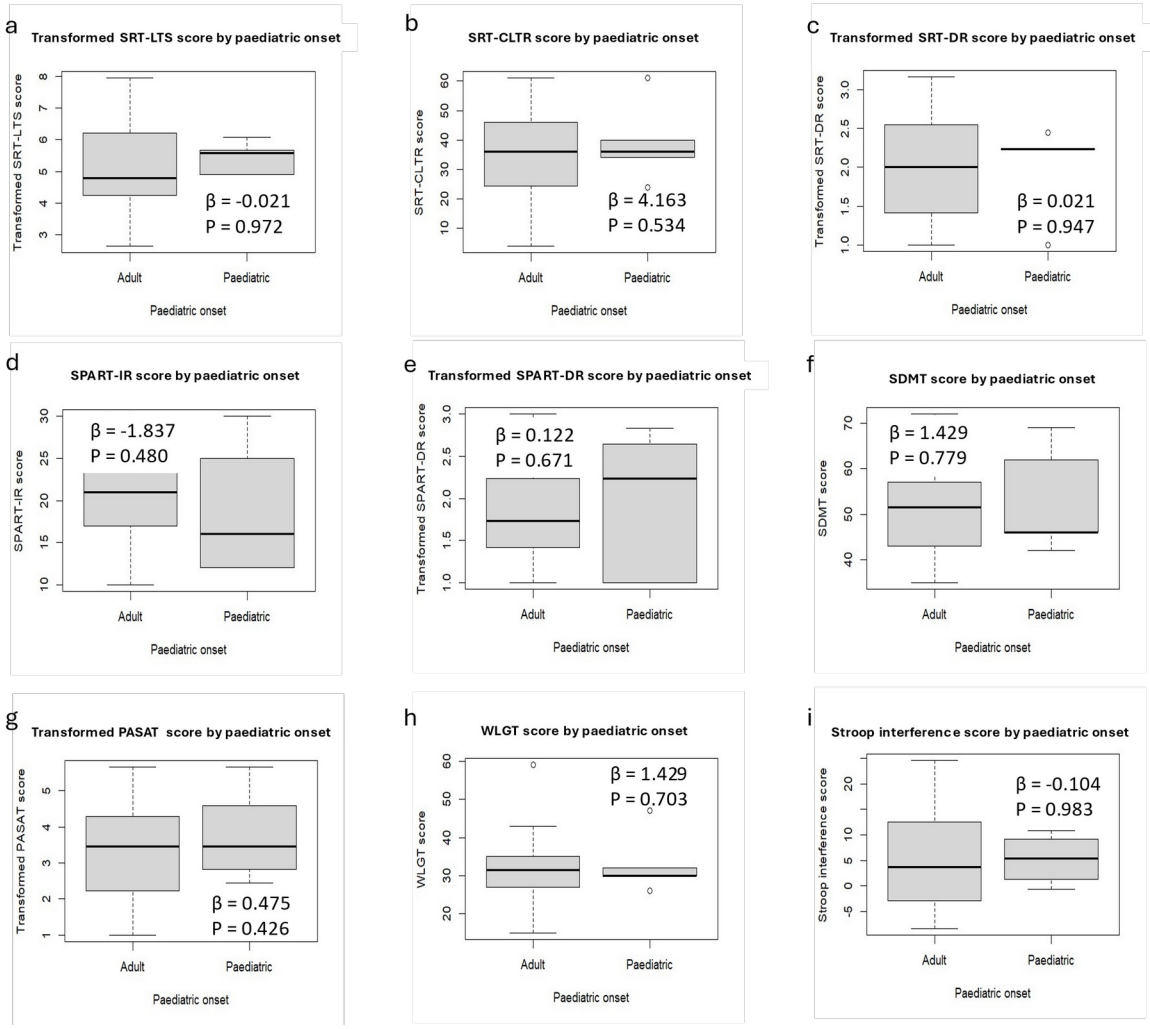

Appendix 16

Calculating conditional ORs of ChAdOx1S versus alternative vaccine

Odds of a post-first-dose AICS patient seen at the John Radcliffe Hospital having received a first vaccination with ChAdOx1S compared with an alternative SARS-CoV-2 vaccine were calculated using the formula:

$$\frac{No.\ of\ post-first-dose\ AICS\ cases\ that\ received\ first\ dose\ Ch\ AdOx1S}{No.\ of\ post-first-dose\ AICS\ cases\ that\ received\ alternative\ SARS-CoV-2\ vaccine}$$

Conditional odds of an adult in England receiving a first dose of ChAdOx1S compared with a first dose of alternative SARS-CoV-2 vaccine were calculated using the formula:

$$\frac{No.\ of\ adults \in England\ that\ received\ a\ first\ SARS-CoV-2\ vaccination\ with\ Ch\ AdOx1S}{No.\ of\ adults \in England\ that\ received\ a\ first\ SARS-CoV-2\ vaccination\ with\ an\ alternative\ vaccine}$$

Inclusion in the calculation was conditional on receiving a first dose SARS-CoV-2 vaccine in the period from 7th December 2020 to 5th December 2021[24].

Only first doses were considered because confidential MHRA data did not distinguish between homologous and heterologous dosing. Additionally, most post-vaccine AICS and almost all post-vaccine MOGAD cases occurred after the first dose of vaccine and patients often declined subsequent vaccination.

To check any significant ORs were due to increased odds of having received ChAdOx1S in the post-first-vaccine AICS group and not due to some demographic factor common to all patients with AICS increasing odds of receiving the vaccine (reverse causality), the conditional odds of

[24] The odds were conditional on receiving at least 1 dose of SARS-CoV-2 vaccine. This is because the question of interest was whether the post-vaccine AICS groups were more likely to have received ChAdOx1S as opposed to an alternative vaccine than the general population. Unvaccinated AICS patients were not included in the analysis because they are *de facto* not part of the post-vaccine cohort. Inclusion of the unvaccinated English population would falsely inflate the OR.

receiving ChadOx1S versus alternative in the Oxford post-first-dose AICS and MOGAD cohorts were compared with the conditional odds of receiving ChAdOx1S in new-onset AICS with onset outside 8 weeks of SARS-CoV-2 vaccination for the whole cohort (the non-post-first-dose cohort).

Additionally, the conditional odds of Oxford non-post-first-dose AICS cases receiving a first dose of ChAdOx1S were compared with the conditional odds in the English population. If a significant OR was observed when comparing odds of receiving ChAdOx1S in the post-first-dose AICS cases with the English population, a significant OR when comparing non-post-first-dose vaccine cases with the English population would suggest some demographic factor that predisposes patients to both AICS and vaccination with ChAdOx1S.

Odds of a non-post-first-dose AICS patient receiving a first dose of ChAdOx1S were calculated as for post-first-dose cases but limited to the non-post-first-vaccine Oxford AICS cohort.

Due to small numbers of patients, 95% confidence intervals were calculated using Fisher’s exact conditional confidence interval. Any cells with zero counts were corrected using the Haldane-Anscombe method (410). This slightly underestimates the OR by reducing the odds of receiving first dose ChAdOx1S in the post-first-dose AICS subgroups.

Appendix 17

Explanation of the self-controlled case series

The basic method was described by Farrington and colleagues (257).

An observation period is specified. Events of interest (cases) that occur during this period are identified. The time each individual spends in the observation period is divided into intervals according to exposure status (pre-exposure baseline, post-exposure “risk period”, post-risk-period baseline) and other time-variant factors that are believed to modify risk (e.g., age). It is assumed every individual *i* has a unique baseline rate (ϕ_i) determined by time-invariant factors, and each interval is associated with an incidence rate (λ) that is determined by the baseline rate and some factor associated with exposure status (e^{β}) and any other time-variant predictors (e.g., age). The incidence rate (λ) during the exposure period is the baseline rate (ϕ_i) multiplied by the exposure factor (e^{β}); e^{β} is the change in incidence rate between baseline and exposure (incidence rate ratio, IRR). Similarly, age can be categorised and the change in incidence rate associated with different age categories estimated.

For each individual, the number of events in a given interval is modelled as the event rate (λ) in the interval multiplied by the time (t) in the interval.

For all ages *j* from j = 0… j = r and all exposures *k* from k = 0… k = s, the event number experienced by individual *i* can be defined by:

Event number = $\lambda_{ijk}.t_{ijk}$

The conditional probability of n events occurring in interval jk can be modelled as:

$$P(n_{ijk}) = \left(\frac{\lambda_{ijk}.t_{ijk}}{\sum_{j}\sum_{k}\lambda_{irs}.t_{irs}}\right)^{nijk}$$

The likelihood of an individual’s event distribution (l_i) is the product of their interval probabilities:

$$l_i = \prod_{jk} \left(\frac{\lambda_{ijk} . t_{ijk}}{\sum_j \sum_k \lambda_{irs} . t_{irs}} \right)^{n_{ijk}}$$

The total event count of individual *i* (Δ_i) for the observation period is the sum of the events in each interval:

$$\Delta_i = \sum_j \sum_k \lambda_{irs} . e_{irs}$$

$$l_i = \prod_{jk} \left(\frac{\lambda_{ijk} . t_{ijk}}{\Delta_i} \right)^{n_{ijk}}$$

The conditional probability of 0 events in an interval simplifies to 1, because any value raised to the power $n_{ijk} = 0$ is 1. Therefore, only intervals containing events contribute to the likelihood. For this reason, only cases need to be included, as any individual with no event in any interval will not contribute to the group likelihood.

For example, consider hypothetical individual 1 observed for 1 year between ages 7000 days and 7365 days. Age intervals are divided into 10-year blocks from age 3650 to 7299 days (j = 0) and from 7300 days to 10950 days (j = 1). Exposure status has 2 levels, unexposed (k = 0) and exposed (k = 1). The post-exposure risk period is 30 days and individual 1 is exposed on day 101 of the observation period, at age 7101 days. They have an event at age 7115 days.

Interval	**Strata**	**Duration**	**Events**
1	J = 0, k = 0	100	0
2	J = 0, k = 1	30	1
3	J = 0, k = 0	169	0
4	J = 1, k = 0	66	0

The conditional likelihood, l_1, is modelled as:

$$l_1 = \left(\frac{100 \lambda_{100}}{\Delta_i} \right)^0 \text{ x } \left(\frac{30 \lambda_{101}}{\Delta_i} \right)^1 \text{ x } \left(\frac{169 \lambda_{100}}{\Delta_i} \right)^0 \text{ x } \left(\frac{66 \lambda_{110}}{\Delta_i} \right)^0$$

All intervals without events have conditional probabilities of 1 (because $x^0=1$). Therefore, only intervals with events (n > 0) contribute to the likelihood numerator, whereas all intervals contribute to the denominator.

$$\Delta_i=100\,\lambda_{100}+30\,\lambda_{101}+169\,\lambda_{100}+66\,\lambda_{110}$$

$$l_1=1\,x\left(\frac{30\,\lambda_{101}}{\Delta_i}\right)^1 x\,1\,x\,1\,x\,1$$

$$l_1=\frac{30\,\lambda_{101}}{\left(100\,\lambda_{100}+30\,\lambda_{101}+169\,\lambda_{100}+66\,\lambda_{110}\right)}$$

λ_{ijk} depends on the baseline incidence rate (ϕ_i, which is equivalent to λ_{i00}) and the effect of time-variant factors (exposure and age). Let $e^{\alpha j}$ represent the factor by which baseline incidence rate is altered by age from baseline (j = 0) to age j = 1 …. j = r. Let $e^{\beta k}$ represent the factor by which incidence rate in absence of exposure (k = 0) is altered by exposure (k = 1).

$\lambda_{ijk} = \phi_i e^{\alpha j}.e^{\beta k} = \phi_i e^{(\alpha j + \beta k)}$

We can show that the value of β associated with exposure is the natural log of the incidence rate ratio (IRR).

IRR = change in λ_{ijk} from baseline (β = 0) associated with exposure (β = 1):

$$\text{IRR} = \frac{\lambda_{i01}}{\lambda_{i00}}$$

$$\text{IRR} = \frac{\phi_i e_i^{\beta 1}}{\phi_i e_i^{\beta 0}}$$

$$\text{IRR} = \frac{e_i^{\beta 1}}{e_i^{\beta 0}}$$

$\beta_0 = 0$

Therefore, $e_i^{\beta 0}= 1$

$\text{IRR} = e_i^{\beta 1}$

Log(IRR) = β_1

We can substitute these time-variant factors into the likelihood:

$$l_i = \prod_{jk} ¿¿$$

In the example of individual 1 above, *j* has 2 levels (0, 1) and *k* has 2 levels (0, 1).

$$l_1 = \frac{30.\phi_1 e^{\alpha 0+\beta 1}}{\left(100.\phi_1 e^{\alpha 0+\beta 0}+30.\phi_1 e^{\alpha 0+\beta 1}+169.\phi_1 e^{\alpha 0+\beta 0}+66.\phi_1 e^{\alpha 1+\beta 0}\right)}$$

At baseline, α and β have no effect, i.e., α_0 and $\beta_0 = 0$

$$l_1 = \frac{30.\phi_1 e^{\beta 1}}{\left(100.\phi_1 e^{0}+30.\phi_1 e^{\beta 1}+169.\phi_1 e^{0}+66.\phi_1 e^{\alpha 1}\right)}$$

The individual's baseline rate cancels out:

$$l_1 = \frac{30.e^{\beta 1}}{\left(100.e^{0}+30.e^{\beta 1}+169.e^{0}+66.e^{\alpha 1}\right)}$$

$$¿ \frac{30.e^{\beta 1}}{\left(100.e^{0}+30.e^{\beta 1}+169.e^{0}+66.e^{\alpha 1}\right)}$$

$$¿ \frac{30.e^{\beta 1}}{\left(269+30.e^{\beta 1}+66.e^{\alpha 1}\right)}$$

$$¿ \frac{30.e^{\beta 1}}{\Delta_1}$$

Thus, the individual's likelihood contribution is reduced to the effects of age and exposure in this model. Other models may include different or additional time-variant factors.

The likelihood of the event distribution across all cases combined (group likelihood, l_N) is the product of all individual likelihoods and is expressed as:

$$l_N = \prod_{1}^{N} \prod_{jk} \left(\frac{\lambda_{ijk} . e_{ijk}}{\sum_{j} \sum_{k} \lambda_{irs} . e_{irs}} \right)^{nijk}$$

To simplify the calculation, log likelihoods are calculated:

$$\log l_N = \prod_{1}^{N} \prod_{jk} n_{ijk} \log \left(\frac{\lambda_{ijk} . e_{ijk}}{\sum_{j} \sum_{k} \lambda_{irs} . e_{irs}} \right)$$

$$= \prod_{1}^{N} \prod_{jk} n_{ijk} \log \left(\frac{\phi_i e^{\alpha j + \beta k} . e_{ijk}}{\sum_{1}^{J} \sum_{1}^{K} \phi_i e^{\alpha r + \beta s} . e_{irs}} \right)$$

SCCS uses conditional logistic regression to calculate maximum likelihood estimates of β (and α) to ensure their effects model the observed event distribution most accurately. Intuitively, an increase in the risk of an event during an exposure period will lead to more events occurring during exposed periods, meaning more of the numerators are defined by e^{β}. If more of the numerators contain e^{β}, maximising the likelihood will increase the estimate of e^{β}. Conversely, if exposure reduces the risk of an event, fewer of the numerators will contain an e^{β} term and maximising the likelihood will reduce the estimate of e^{β}.

Significance of the models was assessed with the Wald test.

One of the key assumptions underlying the SCCS is that events arise independently. This cannot be assumed in AICS and particularly not in MOGAD, when the occurrence of a first attack increases the probability of a future relapse. This can be overcome by limiting the analysis to the first event (230,258). This is possible if events are rare in the population, because for rare events the probability of more than one event approaches zero and the probability density is indistinguishable from non-recurrent events (230,257,259). As the event of interest was *onset attack* of MOGAD, restricting the analysis to first events was not a limitation.

Appendix 18

Edwards' test of seasonality

In his original description (411), Edwards represents a full cycle (in this case, a year) as the rim of a circle divided into sectors (in this case, corresponding to months), which are weighted according to the number of events that occur during those periods.

According to the Null hypothesis of a uniform distribution, the centre of gravity will lie at the centre of the circle. Sinusoidal variation in event frequency will shift the centre of gravity and deviations from uniformity are detected as peaks or troughs in the sine wave of the cycle. The fit of the data to the sine wave is evaluated with a χ^2 goodness of fit test.

Modification of the test statistic by Roger permits analysis of groups as small as 20 (412,413).

Appendix 19

Figure 56 and legend

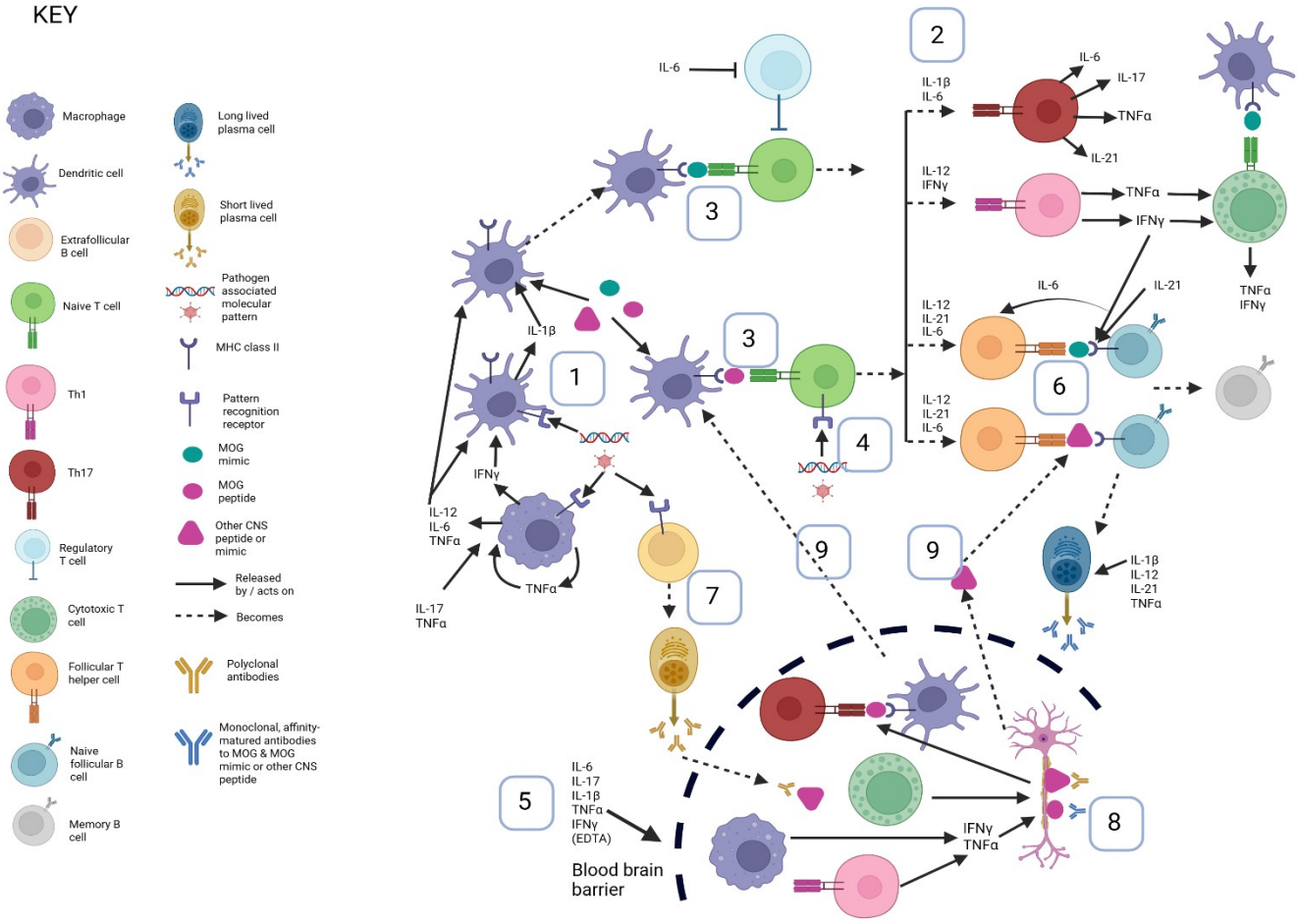

Individuals with compatible HLA genotypes and compatible germline-encoded T cell receptors capable of binding MOG (or another, unidentified CNS peptide responsible for seronegative AICS) are exposed to viral DNA and adenoviral capsid peptides in ChAdOx1S, leading to activation of PRRs on cells of the innate immune system, including macrophages and dendritic cells (process 1). Binding of PRRs stimulates these cells to produce TNFα, IFNγ, IL-1β, IL-6 and IL-12, which are common to both MOGAD and the post-ChAdOx1S inflammatory landscape. These

cytokines collectively drive differentiation of naive T cells to a Th1 (via TNFα, IFNγ, IL-12) and Th17 (via IL-1β, IL-6) phenotype and promote differentiation and activation of follicular T helper cells (TfH; IL-6, IL-12) (process 2).

These T cell responses may be antigen-specific if the receptors encounter cognate antigens within the vaccine (process 3), which is possible due to the heavy contamination of ChAdOx1S by human proteins (271,298). Cognate antigen in the vaccine may be CNS peptides, including MOG, alternative CNS antigen (resulting in epitope spread or B cell costimulation) or mimics (like neurofilament medium chain) (355).

Polyclonal bystander T cell responses are also likely in the presence of PAMPs and pro-inflammatory cytokines, switching low-affinity autoreactive T cells from a tolerogenic to an activated state without the requirement for a new cognate antigen of higher affinity (process 4) (225,309). In this case, anergic or ignorant T cells may be non-specifically activated.

Whether the initial T cell response is antigen-specific or polyclonal, activated T cells then home to the site of cognate antigen expression, i.e., the CNS. Cytokines produced in the periphery during the initial inflammatory reaction (e.g., IFNγ, TNFα, IL-1β, IL-6 and IL-17) increase expression of cell surface adhesion molecules and disrupt tight junctions, leading to lymphocyte diapedesis and entry to the CNS (360) (process 5). EDTA in ChAdOx1S may also increase BBB permeability (361). Once within the CNS parenchyma, Th1 and Th17 cells are capable of releasing cytokines and chemokines that lead to further recruitment of NK cells, macrophages, lymphocytes and dendritic cells (338,360). In this way, CNS inflammation is maintained by positive feedback loops between cells of the innate and adaptive immune systems. For example, IFNγ, TNFα and IL-17 released by cytotoxic T cells, Th1 and Th17 cells stimulate macrophages and microglia to release IL-1β, IL-6 and IL-12, leading to T cell activation and differentiation (308,414).

TfH cells and dendritic cells are important in generating an affinity-matured, class-switched antibody response in the germinal centres, which is usually considered necessary for high affinity IgG1 responses, such as those seen in MOGAD. IL-1β and IFNγ promote dendritic cell differentiation and antigen presentation to T and B cells (336,415,416) (process 3). TNFα, IL-1β, IL-6, IL-12 and IL-21 from macrophages and T cells promote TfH cell differentiation, enhancing antigen presentation to and co-stimulation of B cells (process 6). If self-reactive B cells encounter human CNS antigen or mimic from the vaccine, either in solution or in the context of APCs, the B cell receptor bound to antigen is internalised and linear epitopes are presented by complementary MHC class II molecules on the B cell surface. Interaction with T helper cells (particularly TfH cells) with cognate receptors leads to co-stimulation. Activated B cells migrate to the follicle and form germinal centres characterised by proliferation, class switching, somatic hypermutation and affinity maturation. These cells give rise to long-lived plasma cells, producing high affinity antibodies to the (auto) antigen (368,417,418). In the first instance, the target may be MOG or alternative CNS antigen, as cryptic antigen exposure, epitope spreading and B cell co-capture could broaden the response to include MOG or other targets.

In addition to germinal centre reactions, extrafollicular polyclonal B cell activation by vaccine content via toll-like receptors (TLRs) could stimulate plasma cell differentiation and autoantibody release (process 7). This process is enhanced by some of the cytokines that characterise the ChAdOx1S response, such as TNFα, IL-1β and IL-12.

Plasma cells, high-affinity and low affinity antibodies are able to breach the BBB due to cytokine-induced changes in its structure (process 5). High-affinity antibodies to MOG or other CNS antigen are capable of inducing antibody-dependent cellular cytotoxicity and complement-dependent cytotoxicity, leading to tissue damage and potentially cryptic antigen exposure (process 8). These mechanisms have been shown to contribute to pathology in MOGAD (419–421). Low affinity antibodies

from short-lived extrafollicular plasma cells may be capable of binding CNS proteins to trigger antibody-dependent cellular toxicity. Additionally, low-affinity antibodies could bind CNS antigen (MOG or alternative) to form immune complexes that are subsequently taken up by follicular dendritic cells via Fc receptors. This permits efficient follicular dendritic cell presentation of autoantigen to B cells to bridge the extrafollicular and germinal centre B cell responses (368), generating affinity-matured B cell responses potentially including MOG IgG1 (process 9).

In addition to cellular damage by antibody binding, cytotoxic T cells with receptors capable of binding MOG peptides and/or other CNS peptides are re-activated by cognate epitopes in the CNS, damaging cells with perforins and granzymes, cytokines and Fas ligand binding. Release of cytokines such as IFNγ and TNFα by T helper cells, macrophages, microglia and dendritic cells can cause direct neuronal and glial damage (336). Release of reactive oxygen species and toxic enzymes by macrophages and microglia may also contribute to CNS damage (process 8). This may expose cryptic antigens and or trigger B cell co-capture. Either means can result in epitope spreading. In this way, even if MOG or antigens targeted in seronegative AICS were not present in the vaccine and were not the primary target, CNS damage and exposure of new antigens to dendritic cells and lymphocytes could result in antigen-specific diseases (process 9).

Index of supplementary figures

Supplementary figure 54 Scatter plot of Stroop interference scores in paediatric- and adult-onset AQP4+ NMOSD

Index of supplementary tables